Hybrid techniques for state estimation : event-triggered sampling and performance improvement

Elena Petri

UNIVERSITÉ DE LORRAINE

École doctorale IAEM Lorraine

Hybrid techniques for state estimation: event-triggered sampling and performance improvement

THÈSE

présentée et soutenue publiquement le 4 octobre 2023

pour l'obtention du

Doctorat de l'Université de Lorraine

(Spécialité : Automatique, Traitement du Signal et des Images, Génie Informatique)

par

Elena Petri

Composition du jury

Président :	Luca Zaccarian	LAAS, CNRS, Toulouse, France DISI, Università degli Studi di Trento, Italy
Rapporteurs :	Antoine Girard	L2S, Centrale Supélec, CNRS, Gif-sur-Yvette, France
	Gildas Besançon	Grenoble INP, GIPSA-lab, France
Examinateurs :	Pauline Bernard	CAS, Mines Paris, Université PSL, France
	Luca Zaccarian	LAAS, CNRS, Toulouse, France DISI, Università degli Studi di Trento, Italy
	Dragan Nešić	University of Melbourne, Australia
	Daniele Astolfi	Université de Lyon 1, CNRS, LAGEPP, France
Encadrant :	Romain Postoyan	Université de Lorraine, CNRS, CRAN, France

Centre de Recherche en Automatique de Nancy (CRAN) - UMR 7039

Mis en page avec la classe thesul.

To my brother Davide

Acknowledgments

These three years of PhD have been at the same time amazing and challenging both from a personal and professional perspective. I am sure that without the support of the great people around me, I would not have been able to be here writing this thesis. Therefore, I would like to express my deepest gratitude to all of them.

First, I am extremely grateful to my PhD supervisors Romain, Dragan and Daniele for their invaluable guidance, support and patience during the whole PhD. Their feedbacks and advice allowed me understanding, deepening, and refining my research, and the results presented in this thesis would have been impossible without their mentorship and supervision. I am always impressed by their immense knowledge, and I feel honored to have had the opportunity to learn from them and to work under their guidance. In addition, I am thankful for the great opportunity I had to spend three months in Australia. Moreover, they are not only great professionals, but also wonderful people willing to help me even when facing difficult events of life. In particular, I will never forget what Romain did for me in a hard time, and I have no word to express how grateful I am.

I would also like to thank all the members of the jury Antoine Girard, Gildas Besançon, Pauline Bernard and Luca Zaccarian for having accepted to act as reviewers and examiners of this thesis.

I am also grateful to Maurice, Vincent, Thomas, and Stéphane, who contributed to the research results presented in this thesis. Their insightful comments and suggestions significantly improved the quality of the papers.

I wish also to acknowledge the members of the CRAN laboratory, and in particular, my fellow PhD students. They are not only colleagues but, most importantly, good friends with whom I shared great leisure moments, but also arduous and challenging days. With them, I am also thankful to all my friends in Nancy for the wonderful times we had together.

I cannot forget my italian friends, with whom I grew up and shared a lot of unforgettable moments. Despite the long distance, I have always felt their friendship and closeness, especially during the hardest and painful times.

Last but not least, I wish to express my deepest gratitude to my parents for their support during my whole life, for believing in me and for continuously encouraging me.

Abstract

State estimation of dynamical systems is a central theme in control theory, whereby an observer is designed to estimate the unmeasured system states by exploiting the knowledge of the system mathematical model and input and output measurements. Even though many techniques are available in the literature for the observer design of continuous-time linear and nonlinear systems, there are still many major open problems that need to be investigated. Among these challenging questions, there is the implementation of the observer in case of communication constrains between the system plant and the observer itself, which occurs when communications take place via digital networks. Another important largely open problem is the tuning of the observer gain to obtain good estimation performance. The objective of this thesis is to propose solutions for these two questions by exploiting hybrid techniques, that rely on models exhibiting both continuous-time evolution and discrete-time jumps.

In the first part of this document, we consider the scenario where a system transmits its measurements to an observer via a digital network. In this context, we design both the observer and a communication scheme to decide when the former needs to receive the measured information. A crucial question is when a transmission needs to occur over the communication network to obtain accurate state estimates, while only sporadically using the communication channel. For this purpose, we present a (hybrid) event-triggered observer design. We follow an emulation-based approach in the sense that our starting point is an observer that satisfies a robust stability property of the estimation error in absence of the network. We then take the communication channel into account and we design a dynamic triggering rule, implemented by a smart sensor, to decide when a transmission needs to be triggered. The proposed triggering rule does not require the sensor to have significant computation capabilities, but only to be able to run a scalar filter, which is a distinguishing aspect when compared to most of the works in the literature. The results are first presented for unperturbed linear time-invariant systems and are then generalized by considering perturbed nonlinear systems and a decentralized setting.

The second problem addressed in this thesis is the crucial question of tuning the observer. Indeed, we aim to design the observer to obtain a fast convergence speed, which is essential to quickly reconstruct the desired unmeasured state variables, and good accuracy in presence of measurement

noise, which is inevitable in practice. Unfortunately, there is almost always a trade-off between these properties, which complicates the observer tuning. To address this arduous problem, we use hybrid techniques to improve the estimation performance of a given robust nominal observer designed for a general nonlinear continuous-time system. We present for this purpose a novel hybrid multi-observer, which consists of the nominal one and additional dynamical systems that differ from the nominal observer only in their output injection gains, that are collectively referred to as modes. The gains of these additional modes can be freely selected, as no convergence property is required for these modes, to (heuristically) exhibit advantageous features such as fast convergence or great robustness with respect to measurement noise. We run all modes in parallel and we design a switching criterion, based on monitoring variables, that selects one mode at any time instant by evaluating their performance. Moreover, the hybrid multi-observer scheme is applied in simulation for the state estimation of an electrochemical lithium-ion battery with standard model and parameter values, for which good estimation performance is essential.

Résumé

L'estimation de l'état des systèmes dynamiques est un thème central de l'automatique, où un observateur est conçu pour estimer les états non mesurés en exploitant la connaissance du modèle mathématique du système et les mesures d'entrée et de sortie. Bien que de nombreuses techniques soient disponibles dans la littérature pour concevoir des observateurs pour les systèmes linéaires et non linéaires à temps continu, il reste encore de nombreux problèmes ouverts. Parmi ces défis, on soulignera la question de la conception de l'observateur en présence de contraintes de communication entre le système et l'observateur. Un autre exemple est celui du réglage des gains des observateurs afin d'obtenir de bonnes performances d'estimation en termes de rapidité de convergence et de robustesse. L'objectif de cette thèse est de proposer des solutions pour ces deux questions. Pour ce faire, des techniques hybrides, qui sont basées sur des modèles qui présentent à la fois une évolution en temps continu et des sauts en temps discret, sont proposées.

Dans la première partie de cette thèse, nous considérons le scénario dans lequel un système transmet ses mesures à un observateur via un réseau numérique. Dans ce contexte, nous concevons à la fois l'observateur et un système de communication pour décider quand l'observateur doit recevoir les données mesurées par les capteurs. Une question cruciale est de savoir quand une transmission doit avoir lieu sur le réseau de communication pour obtenir des estimations d'état précises, tout en n'utilisant le canal de communication que de manière sporadique. À cette fin, nous présentons une conception d'observateur événementiel (hybride). Nous suivons une approche basée sur l'émulation dans le sens où notre point de départ est un observateur qui satisfait une propriété de stabilité robuste de l'erreur d'estimation en l'absence de réseau. Ensuite, nous considérons le canal de communication et concevons une loi de transmission dynamique, mise en œuvre par un capteur intelligent, pour décider quand une transmission doit être activée. Cette loi de transmission n'exige pas que le capteur ait des capacités de calcul importantes, mais seulement qu'il soit capable d'exécuter un filtre scalaire, ce qui la distingue de la plupart des travaux dans la littérature. Les résultats sont d'abord présentés pour des systèmes linéaires invariants dans le temps, puis généralisés en considérant des systèmes non linéaires perturbés et un cadre décentralisé.

Le deuxième problème abordé dans cette thèse est la question du réglage de l'observateur. Nous souhaitons concevoir l'observateur de manière à obtenir une vitesse de convergence rapide, ce qui

est essentiel pour reconstruire rapidement les variables d'état non mesurées, et une bonne précision en présence de bruit de mesure et de perturbations sur le système, ce qui est inévitable dans la pratique. Malheureusement, il existe presque toujours un compromis entre ces propriétés. Pour lever ce paradoxe nous utilisons des techniques hybrides afin d'améliorer la performance d'estimation d'un observateur nominal robuste conçu pour un système général non linéaire à temps continu. Nous présentons à cette fin un nouveau multi-observateur hybride, qui se compose de l'observateur nominal et de systèmes dynamiques supplémentaires qui ne diffèrent de l'observateur nominal que par leurs gains d'injection de sortie, collectivement appelés modes. Les gains de ces modes supplémentaires peuvent être choisis librement, car aucune propriété de convergence n'est exigée. Nous exécutons tous les modes en parallèle et nous concevons un critère qui sélectionne un mode à tout moment en fonction de ses performances. Par ailleurs, le schéma hybride multi-observateurs est appliqué en simulation pour l'estimation de l'état d'une batterie lithium-ion à partir d'un modèle électrochimique, pour laquelle une bonne performance d'estimation est essentielle.

Contents

List of Figures

List of Tables

Notation

$\mathbb{R}$	set of the real numbers
$\mathbb{R}_{\geqslant 0}$	set of the non-negative real numbers
$\mathbb{R}_{>0}$	set of the strictly positive real numbers
$\mathbb{Z}_{\geqslant 0}$	set of the non-negative integers
$\mathbb{Z}_{>0}$	set of the strictly positive integers
$\mathbb{R}^n$	n-dimensional Euclidean space with $n \in \mathbb{Z}_{>0}$
$\in$	belongs to
$\varnothing$	empty set
$\subset$	proper subset
$\subseteq$	subset
$x^\top$	transpose of a vector $x \in \mathbb{R}^n$ with $n \in \mathbb{Z}_{>0}$
$\lvert x \rvert$	Euclidean norm of a vector $x \in \mathbb{R}^n$ with $n \in \mathbb{Z}_{>0}$
I_n	identity matrix of dimension $n \times n$ with $n \in \mathbb{Z}_{>0}$
$O_{n\times m}$	null matrix of dimension $n \times m$ with $n, m \in \mathbb{Z}_{>0}$
$\lVert A \rVert$	2-induced norm of a matrix $A \in \mathbb{R}^{n\times m}$, with $n, m \in \mathbb{Z}_{>0}$
$A^\top$	transpose of a matrix $A \in \mathbb{R}^{n\times m}$ with $n, m \in \mathbb{Z}_{>0}$
$\mathrm{diag}(x_1, \ldots, x_n)$	Diagonal matrix of dimension $\mathbb{R}^{n\times n}$ with $n \in \mathbb{Z}_{>0}$, whose diagonal elements are $x_1, \ldots, x_n \in \mathbb{R}$
$\lambda_{\max}(P)$	maximum eigenvalue of a real, symmetric matrix P

$\lambda_{\min}(P)$	minimum eigenvalue of a real, symmetric matrix P
$\mathbb{S}^n_{>0}$	set of real, symmetric, positive definite matrices of dimension n
$\mathbb{S}^n_{\geqslant 0}$	set of real, symmetric, positive semidefinite matrices of dimension n
$T_{\mathscr{C}}(x)$	tangent cone to the set $\mathscr{C}$, with $\mathscr{C} \subseteq \mathbb{R}^n$, at a point $x \in \mathbb{R}^n$. It is the set of all vectors $v \in \mathbb{R}^n$ for which there exist $x_i \in \mathscr{C}$, $\tau_i > 0$, for any $i \in \mathbb{Z}_{\geqslant 0}$, with $x_i \to x$, $\tau_i \to 0$, as $i \to \infty$ and $v = \lim_{i\to\infty} \frac{x_i - x}{\tau_i}$
$U^\circ(x;v)$	Clarke generalized directional derivative of a Lipschitz function U at x in the direction v, i.e., $U^\circ(x;v) := \limsup_{h\to 0^+, y\to x} \frac{U(y+hv)-U(y)}{h}$
$\|v\|_{[t_1,t_2]}$	essential supremum in the interval $[t_1,t_2]$ of a signal $v : \mathbb{R}_{\geqslant 0} \to \mathbb{R}^{n_v}$ with $n_v \in \mathbb{Z}_{>0}$, and $t_1, t_2 \in \mathbb{R}_{\geqslant 0} \cup \{\infty\}$ with $t_1 \leqslant t_2$, i.e., $\|v\|_{[t_1,t_2]} := \operatorname{ess\,sup}_{t\in[t_1,t_2]} \lvert v(t)\rvert$
$\operatorname{dom} f$	domain of a function $f : \mathscr{S}_1 \to \mathscr{S}_2$ with sets $\mathscr{S}_1$, $\mathscr{S}_2$, i.e., $\operatorname{dom} f := \{z \in \mathscr{S}_1 : f(z) \neq \varnothing\}$
$\mathscr{K}$	class of functions $\alpha : \mathbb{R}_{\geqslant 0} \to \mathbb{R}_{\geqslant 0}$ that are continuous, $\alpha(0) = 0$ and strictly increasing
$\mathscr{K}_\infty$	class of functions $\alpha : \mathbb{R}_{\geqslant 0} \to \mathbb{R}_{\geqslant 0}$ that are continuous, $\alpha(0) = 0$, strictly increasing and $\lim_{r\to+\infty} \alpha(r) = +\infty$
$\mathscr{KL}$	class of functions $\beta : \mathbb{R}_{\geqslant 0} \times \mathbb{R}_{\geqslant 0} \to \mathbb{R}_{\geqslant 0}$ that are nondecreasing in their first argument, nonincreasing in their second argument, $\lim_{r\to 0^+} \beta(r,s) = 0$ for each $s \in \mathbb{R}_{\geqslant 0}$ and $\lim_{s\to+\infty} \beta(r,s) = 0$ for each $r \in \mathbb{R}_{\geqslant 0}$
$\mathscr{L}_{\mathscr{U}}$	set of all functions from $\mathbb{R}_{\geqslant 0}$ to $\mathscr{U}$, with $\mathscr{U} \subseteq \mathbb{R}^n$, $n \in \mathbb{Z}_{>0}$, that are Lebesgue measurable and locally essentially bounded
O	a function $f : \mathbb{R}_{\geqslant 0} \to \mathbb{R}_{\geqslant 0}$ is said to be a "big O" of a function $g : \mathbb{R}_{\geqslant 0} \to \mathbb{R}_{\geqslant 0}$, at infinity, which we write $f(x) = O(g(x))$ as $x \to \infty$, when there exist $c \in \mathbb{R}_{>0}$ and $x_0 \in \mathbb{R}_{\geqslant 0}$ such that $\lvert f(x)\rvert \leqslant c\lvert g(x)\rvert$ for all $x \geqslant x_0$
$\delta_{i,j}$	Kronecker delta, i.e., given $i, j \in \mathbb{Z}_{>0}$, $\delta_{i,j} = \begin{cases} 0 & \text{if } i \neq j \\ 1 & \text{if } i = j \end{cases}$

Acronyms

GAS	Global Asymptotic Stability
ISS	Input-to-State Stability
IOSS	Input/Output-to-State Stability
ETM	Event-Triggering Mechanism
MIET	Minimum Inter-Event Time
IIET	Individual Inter-Event Time
LMI	Linear Matrices Inequalities
EKF	Extended Kalman Filter
KKL	Kazantzis-Kravaris-Luenberger
VC	Viability Condition
MAE	Mean Absolute Error
RMSE	Root Mean Square Error
SOC	State Of Charge
PHEV	Plug-in Hybrid Electric Vehicle
BMS	Battery Management System
SPM	Single Particle Model
OCV	Open Circuit Voltage

Chapter 1

Introduction

This chapter provides an informal introduction to the state estimation problem in control engineering and on hybrid dynamical systems, which are the two pillars of the thesis. A more formal treatment is provided in Chapter 2. Then, the motivation for the accomplished work and a summary of the proposed contributions are given together with the associated scientific outcomes.

1.1 State estimation

Dynamical system models are mathematical objects used to describe how systems evolve over time. In particular, a dynamical system can be used to model a range of engineering or natural systems, such as electronic circuits, mechanical structures, thermodynamic systems, biological systems and so on. These models are typically represented by a set of differential equations (in this case we talk of *continuous-time dynamical systems*), or difference equations (in this case we talk of *discrete-time dynamical systems*), that describe the evolution of the so-called *state variables*, which often describe physical quantities. In general, these mathematical models depend on some external signals, called *system inputs*, that influence the evolution of the system state. In addition, sensors can be used to measure a (nonlinear) combination of the system states, called *output measurements*. The mathematical model of the output measurement is given by a static map.

The knowledge of the internal state of a dynamical system is essential in many engineering applications. Indeed, it is very useful, for example, to build controllers, that are algorithms used to generate input signals to control the evolution of the system states. In addition, the knowledge of

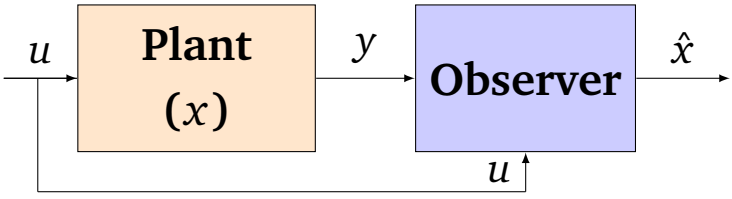

FIGURE 1.1 – Block diagram representing the state estimation problem.

the system state may be crucial to obtain real-time information for monitoring or for decision-making, see e.g. [1,2] and references therein. One way to obtain this information is to directly measure these variables by placing some sensors on the physical system. Unfortunately, not all state variables can be directly measured through sensors due to technological obstacles, like the state of charge of a battery in e.g., [3] or ammonium, nitrate and nitrite concentrations in activated sludge processes in e.g., [4]. Moreover, in many applications we have limits on the number and the type of sensors we can use for cost reasons. As a result, the internal state of a dynamical system, which we denote by x, needs to be estimated from the knowledge of the system mathematical model, called *system plant*, and the available measurements, such as the system input u and output y. This is done by designing an estimation algorithm, which takes the form of a dynamical system, called *observer*, whose output is an estimate of the system state, and is denoted by $\hat{x}$, see Figure 1.1. Note that, since this dynamical system depends on the available measurements, it is not always possible to design an observer to estimate the plant state. Indeed, such estimation algorithm is relevant only if the measurements contain enough information to reconstruct uniquely the system state. This essential property is called *detectability*, see e.g., [5]. When the system is detectable, the objective is to design this dynamical system to ensure that the estimation error, which corresponds to the difference between the unknown system state and the state estimate generated by the observer, and thus gives an indication of the estimation quality, converges to the origin as time grows. This implies that, the state estimate produced by the observer coincides, after a finite or infinite amount of time, with the unknown system state and thus, the observer correctly estimates the plant state.

As mentioned before, the design of this estimation algorithm is based on a mathematical model of the system dynamics, which virtually always exhibits some uncertainties or is affected by unknown disturbances. In addition, the output measurements collected through sensors are typically affected by measurement noise. All these exogenous inputs are usually unknown, and thus cannot be used for the observer design, which therefore needs to be *robust* to these perturbations in the sense that disturbances and measurement noise do not significantly affect the observer state estimate. In particular, in this case, the observer design has the goal to guarantee that the estimation error converges to a neighborhood of the origin, whose "size" depends on the norm of these perturbations. Indeed, note that due to the disturbances and measurement noise, it is not possible to obtain an exact state estimate in general, but it is desired to generate an estimate with guarantees of not being too far from the real system state. In particular, to be an observer, an estimation algorithm needs to ensure that the state estimation error, denoted by $e := x - \hat{x}$, is

— **stable** in the sense that the estimation error trajectory remains small if the initial error is small,

— **converging to (a neighborhood of) the origin** as the time grows,

— **robust to disturbances and measurement noise**.

One property that embeds all these desired characteristics of the state estimation error behaviour is the *input-to-state stability property* of the estimation error with respect to disturbances and measurement noise, see e.g. [6, 7] as well as Chapter 2.2.2 for more details.

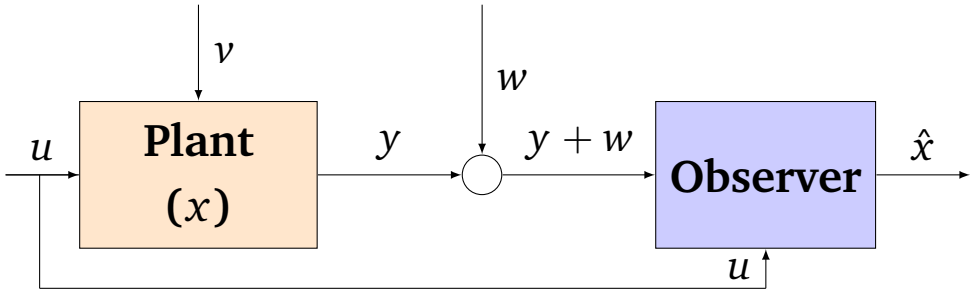

FIGURE 1.2 – Block diagram representing the state estimation problem in presence of disturbances and measurement noise.

When considering these perturbations, denoted by v for the disturbances affecting the plant dynamics and by w for the measurement noise, the state estimation problem can be summarized with the block diagram in Figure 1.2. Note that, in Figure 1.2 we show the common case where the perturbation w represents an additive measurement noise. However, we can use the notation w to refer to any kind of perturbation affecting the system output y.

In this thesis we focus on finite-dimensional continuous-time systems of the form

$$\begin{aligned} \dot{x} &= f_p(x,u,v) \\ y &= h(x,w), \end{aligned} \tag{1.1}$$

where $x \in \mathbb{R}^{n_x}$ is the system state, that is unknown and needs to be estimated, $u \in \mathbb{R}^{n_u}$ is the measured input, $y \in \mathbb{R}^{n_y}$ is the output measured by sensors, $v \in \mathbb{R}^{n_v}$ is an unmeasured disturbance input and $w \in \mathbb{R}^{n_w}$ is an unknown measurement noise, with $n_x, n_y \in \mathbb{Z}_{>0}$, and $n_u,\ n_v,\ n_w \in \mathbb{Z}_{\geqslant 0}$. The class of continuous-time observers for system (1.1) investigated in this thesis has the form

$$\begin{aligned} \dot{z} &= f_o(z,u,y,\hat{y}), \\ \hat{x} &= \psi(z) \\ \hat{y} &= h(\hat{x},0), \end{aligned} \tag{1.2}$$

where $z \in \mathbb{R}^{n_z}$ is the observer state, with $n_z \geqslant n_x$, $\hat{x} \in \mathbb{R}^{n_x}$ is the state estimate and $\hat{y}$ is the output estimate. Note that, in this thesis we consider observers whose state dimension is at least as big as the system state, namely $n_z \geqslant n_x$. More details and insights on systems (1.1) and (1.2) are provided in Chapter 2.2.1.

Designing observers in the form (1.2) to estimate the state of system (1.1) with the desired stability, convergence and robustness properties is an important research topic in control engineering, see e.g., [5,8] for surveys on the topic. In particular, depending on the dynamical system structure, different design techniques can be adopted. The starting point of most of the results in this thesis is the knowledge of an input-to-state stable observer. This implies that its estimation error is stable and converging to a neighborhood of the origin, whose size depends on the norm of the perturbations.

As shown in e.g., [5, 9], many observer design techniques are available in the literature satisfying this property for linear and nonlinear dynamical systems. However, various major methodological problems remain open. In particular, observer (1.2) requires the knowledge of the output measurements continuously. However, this is not always the case in practical applications, where the output data may be sporadically communicated from the plant to the observer via a digital network, when considering the setting where the system sensors and the observer are not co-located. Several works have addressed this challenge in the literature, see e.g., [10–30], but much more needs to be done, as we will explain later in Section 1.3.1, as well as in Chapters 3 and 4. On the other hand, even if the observer has access to the output measurement continuously, the input-to-state stability property guarantees a robust stability property of the estimation error, but it is not always satisfactory regarding the performance in terms of speed of convergence and size of ultimate bound due to disturbances and measurement noise. This poses the question of the tuning of nonlinear observers to ensure robust convergence property as well as satisfactory performances. Some techniques are obviously available in the literature for this purpose, but not for general nonlinear systems, as far as we know. More details on the literature are provided in Section 1.3.2 in the following, as well as in Chapter 5. In this thesis we focus on these two open questions and we propose solutions by exploiting hybrid techniques, that is, systems that exhibit both continuous and discrete-time dynamics.

1.2 Hybrid dynamical systems

In classical control theory, it is common to model dynamical systems either using differential equations (or inclusions), thus obtaining *continuous-time dynamical systems*, or difference equations (or inclusions), thus obtaining *discrete-time dynamical systems*. However, many physical systems exhibit a combination of continuous-time evolution and discrete-time updates, such as mechanical systems, which evolve in the physical continuous-time world, but are controlled by a digital computer, or mechanical systems experiencing impacts, as for the classical bouncing ball example in [31]. Other examples of systems presenting both continuous and discrete-time dynamics are biological systems able to produce synchronized behaviors, that imply that their continuous-time dynamics is affected by discrete-time resets, like the flashing fireflies example in [31, Chapter 1]. Another example is electrical circuits with switches, where the activation of a switch can be modeled as instantaneous resets of the variables, which are evolving continuously, as the DC/AC inverter in [32, Example 1.1] or the power control with a thyristor in [31, Example 1.3]. To model the rich behaviour of these systems, purely continuous-time models or discrete-time ones are not enough. As a result, to obtain a more comprehensive representation of real-world phenomena, a well-known combination of continuous-time and discrete-time behaviours are the so-called *hybrid dynamical systems*, or simply *hybrid systems*, which are therefore described by both differential equations (or inclusions) and difference equations (or inclusions). Various modeling frameworks are available for hybrid dynamical systems, see e.g., [31, 33–36]. In this thesis we adopt the formalism presented in [31] to model hybrid dynamical systems. In particular, we consider the extension proposed in [37] (inspired by [38]), which allows to include continuous-time inputs in the hybrid model. These inputs are denoted by u

and can be used to represent known inputs, such as control inputs, but also unknown disturbances and measurement noise. In this framework, given two sets $\mathscr{C}, \mathscr{D} \subseteq \mathbb{R}^{n_x} \times \mathbb{R}^{n_u}$, with $n_x \in \mathbb{Z}_{>0}$ and $n_u \in \mathbb{Z}_{\geqslant 0}$, and two set-valued maps $F : \mathbb{R}^{n_x} \times \mathbb{R}^{n_u} \rightrightarrows \mathbb{R}^{n_x}$ and $G : \mathbb{R}^{n_x} \times \mathbb{R}^{n_u} \rightrightarrows \mathbb{R}^{n_x}$, the dynamics of the hybrid state $x \in \mathbb{R}^{n_x}$ is described by

$$\mathscr{H} : \begin{cases} \dot{x} & \in & F(x,u), & (x,u) \in \mathscr{C}, \\ x^+ & \in & G(x,u), & (x,u) \in \mathscr{D}. \end{cases} \tag{1.3}$$

Equation (1.3) means that the hybrid state $x \in \mathbb{R}^{n_x}$ can evolve according to both continuous-time and discrete-time dynamics, possibly alternating these behaviours depending on which region of the state space the pair (x,u) lies. When the state x and the input u are in the flow set $\mathscr{C}$, then the hybrid state x evolves in continuous-time according to the flow map F. Similarly, when the state x and the input u are in the jump set $\mathscr{D}$, then the system state is updated according to the jump map G. In addition, when the state and input pair lies both in the flow and jump sets, namely $(x,u) \in \mathscr{C} \cap \mathscr{D}$, if the continuous-time evolution would keep the state and input pair in the set $\mathscr{C}$, then the hybrid state evolves according either to the differential inclusion or according to the difference inclusion in (1.3). As a result, equation (1.3) describes a system dynamics that is richer than only either differential equations (or inclusions) or difference equations (or inclusions).

Hybrid techniques have been proved to be very powerful to design controllers. For instance, controllers are typically implemented by digital hardware and computers, but are used to control physical plants, which are naturally described by continuous-time models, thereby leading to hybrid dynamical systems. Moreover, the richer behaviour given by the mix between continuous-time and discrete-time dynamics have been exploited in different control contexts, see e.g. [32] and references therein, where hybrid tools have demonstrated their relevance and strength to overcome limitations of purely continuous-time or discrete-time controllers and thus they allowed to solve problems which are unsolvable by using only classical frameworks. Similarly, it should be possible to exploit the power of hybrid tools in the context of state estimation, but this has been undoubtedly less explored in the literature. In this case we talk about *hybrid observer* design, which therefore consists in designing estimation algorithms described by both continuous and discrete-time dynamics. Note that we can design an hybrid observer also to estimate the state of a continuous-time dynamical system in case the system structure, the estimation objective or the observer design approach leads to hybrid modelling. In particular, we can classify hybrid observers into three main groups, as summarized next.

— **Hybrid system plant.** As previously mentioned, many physical and engineering systems present an hybrid behaviour and thus are well described using hybrid system models. In this case, to estimate the hybrid state, an observer exhibiting both continuous and discrete-time dynamics, i.e., a hybrid observer, should be designed, see e.g., [39, 40].

— **Hybrid connection between the plant and the observer.** Even if the system plant is described by continuous-time dynamics, and thus its state can be estimated using a continuous-time observer, due to the setting, hybrid modelling can arise. For instance, in many applications, the system and the observer have not the same physical location and the output measurements

are transmitted from the plant to the observer via a digital network. Therefore, the observer receives the output data only at some discrete-time instants, and thus, the overall system can be describe as a hybrid system, see e.g., [12, 41].

— **Estimation performance.** Hybrid techniques can be used in estimation also for performance purposes. For example, even if the system has a continuous-time dynamics, and the setting allows to design a continuous-time observer to estimate the plant state, discrete-time dynamics can be introduced in the observer design to order to exploit the power of hybrid tools and the richer hybrid dynamics to improve the estimation performance, see e.g., [42, 43].

The results presented in this thesis fall into the second and third categories. In particular, we consider continuous-time systems for which we want to estimate the plant state and hybrid techniques arise because of the considered setting or for performance improvement purposes. In the next section, we explain in more details the two case studies considered in this manuscript.

1.3 Motivation and contributions

In this thesis we aim to show the efficiency of hybrid techniques to solve two important state estimation problems, namely the event-triggered estimation and observer performance improvement for nonlinear continuous-time systems. In this section, we present and motivate the two research problems we investigate in this work in more details and we explain the contributions of the thesis.

1.3.1 Event-triggered estimation

Motivation

As mentioned before, in many applications the system and the observer are not co-located and, thus, the output measurements are transmitted from the plant to the observer through a digital network. As a result, the observer does not have access to the measured output continuously, but only at some sampling, equivalently transmission, instants, see Figure 1.3, where we denote by $\bar{y}$ and $\bar{w}$ the sampled versions of the measured output and the measurement noise, respectively. In this setting, hybrid systems naturally arise since the system and the observer evolve in continuous-time, while each output transmission over the network can be modeled as a discrete-time event. The general nonlinear observer (1.2), for which various design techniques from the literature may be adopted to obtain a convergence property of the estimation error, assumes the knowledge of the whole continuous-time measured output. The policy chosen to trigger a transmission over the network has an impact on the convergence speed, the robustness of the estimation as well as on the amount of communications. Three main approaches have been proposed in the literature to generate the transmissions instants. The first one, called *time-triggered strategy*, see, e.g., [11, 12, 44–46], consists in trigger a new transmission based on the amount of time elapsed since the last communication. A classical simple example of the time-triggered strategy is periodic sampling, where the time distance between two consecutive transmissions is constant. A potential drawback of the time-triggered paradigm is that it may generate more transmissions than actually needed to perform the estimation, which thus results in a waste of resources usage. Indeed, in the case the output remains approximately constant,

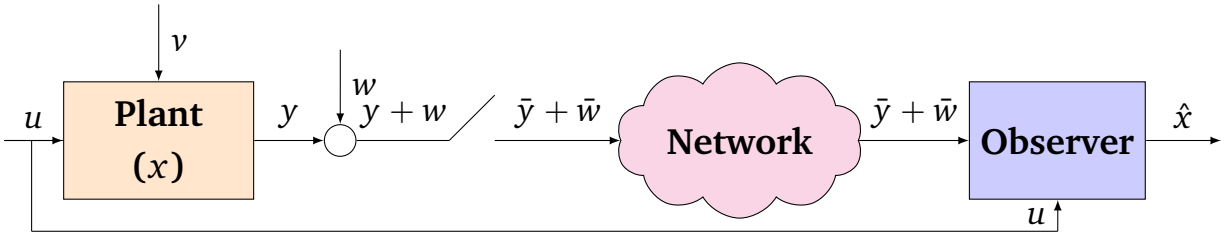

FIGURE 1.3 – Block diagram representing the state estimation problem when the communications between plant and observer take place via a digital network.

it is not needed to trigger a new transmission and thus send a new output measurement to the observer, since it already has an output data which is almost the same. On the other hand, when the output changes rapidly, the observer needs the measured information more frequently. Therefore, approaches that are not based on time, but on the need for a new output transmissions have been envisioned in the literature. In particular, by designing an observer able to predict when it needs a new data, *self-triggering strategies*, see e.g., [47, 48], have been proposed, where the estimation algorithm requests a new transmission when it needs it. This communication strategy is very useful in applications where the system output cannot be monitored continuously, since it is measured only at some discrete-time instants. However, the self-triggering strategy often requires many transmissions. Moreover, it does not monitor the system output, and thus, it is typically slower to detect fast changes on the measurements or perturbations on the measured data due to noise. Therefore, when the measured output is monitored continuously and the objective consists of deciding when a transmission needs to be triggered over the network, the information given by output measurements can be exploited to generate the transmission instants. In this context, an alternative powerful approach to generate the transmission instants is the *event-triggered strategy*, see e.g., [15–30]. In this case, an event-based triggering rule monitors the plant measurement and/or the observer state and decides when an output transmission needs to be triggered in order to reduce the number of transmissions over the network, while still ensuring good estimation performance. In this context, the majority of the event-triggered estimation works in the literature propose a triggering rule that depends on the observer state estimate and, therefore, requires the implementation of a local copy of the estimator in the sensor, see e.g., [15–21]. A possible drawback of this approach is that the sensor is required to have enough computation capabilities, which is not always the case in practice, especially for large scale systems or highly nonlinear dynamics. To overcome this drawback, a solution consists in designing an event-based triggering rule that only relies on the sensor output measurements. Solutions following this approach have been proposed in the literature, see e.g., [22–29], where the triggering strategy is only based on a static condition involving the measured output and its past transmitted value(s). However, such static triggering rules may generate a lot of transmissions. Therefore, with the aim of reducing the amount of transmissions over the network, without requiring significant computation capability on the sensor, in this thesis we propose a dynamic event-triggered approach based only on the measured output and the last transmitted output value.

Contributions

The objective of the first part of this thesis is to design a new dynamic event-triggering rule to decide when an output data needs to be transmitted from the plant to the observer via a digital network, in order to reduce the number of transmissions, while still ensuring good estimation performance. In particular, the triggering rule we design depends only on the current output measurement and the last transmitted output value. Therefore it does not rely on a copy of the observer, that might be computational prohibitive for the sensor. Instead, inspired by dynamic triggering rules used in the event-triggered control literature [49–52], we introduce an additional scalar variable that helps to reduce the number of communications over the network and keeps the required calculation simple.

The results are first presented for unperturbed linear time-invariant systems and are then generalized by considering general perturbed nonlinear systems and a decentralized setting, where the sensors are grouped in N nodes and each node decides when its measured data is transmitted to the observer independently from the others. In both cases, we have modeled the overall system as a hybrid system, where a jump corresponds to an output transmission, and we establish a stability property for the estimation error. Moreover, we prove the existence of a minimum positive time between any two transmissions of each sensor node, which is essential for practical implementation since modern digital hardware cannot implement infinitely fast samplings. We also guarantee the absence of sampling when the output remains in a small neighborhood of a constant and therefore its information is not needed to the observer to obtain a good estimation, which is an advantage against time-triggered strategies. In addition, we show how the presented results can be further extended to the case where the output measurement are affected by additive measurement noise and to the case where the plant input is transmitted as well over a digital network, and thus the observer has access also to the input only at some discrete-time instants, which may be different to the output transmission instants. Finally, the effectiveness of the proposed technique is shown in numerical examples.

1.3.2 Improving estimation performance

Motivation

The main objective when designing an observer to estimate a dynamical system state is to have guarantees that the state estimation error converges to the origin (or its neighborhood) as the time grows. As we previously mentioned, many techniques are available in the literature for linear and nonlinear systems to ensure this property, see [5,8]. However, when designing an observer we would also like to ensure good estimation performance in the sense that we desire the following properties.

— **Fast speed of convergence** so that the observer is able to rapidly generate a good state estimate and thus quickly know the desired unmeasured variables.

— **Robustness to disturbances and measurement noise** in the sense that the estimate is accurate even in presence of model uncertainties and it is not too sensitive to measurement noise, which is inevitable in practice.

— **Global domain of attraction** to guarantee the convergence property independently on the observer initialization and thus on the initial estimation error, which is unknown since the initial state is unknown.

Ideally we would like to design an observer that satisfies all these properties. Unfortunately, this is very hard, if not impossible, since fundamental limitations arise, see [53] in the context of linear systems. Indeed, there is typically a trade-off between these properties, which makes the observer tuning very challenging. Many observer design techniques in the literature consist in designing the observer dynamics by using a copy of the plant and then adding a correction term, often denoted as the output injection term. It depends on a gain (linear or nonlinear) that multiplies the output estimation error, namely, the difference between the measured output and the estimated output. The question on how to tune this gain to obtain good estimation performance is extremely hard. Indeed, typically, observers with "small" gains in their output injection terms produce an estimation robust to measurement noise, but the convergence speed is very slow. On the contrary, an observer with a "large" value usually has a fast convergence, but is more sensitive to noise.

Note that optimal estimation schemes have been presented in the literature, but only in specific contexts, like for example the well-known Kalman filter [54] for linear systems affected by additive Gaussian perturbations impacting the dynamics and the output measurements. In addition, optimal and suboptimal moving horizon estimation schemes, see e.g., [55–58] were proposed for discrete-time systems, which however is an iterative estimation approach that therefore may be computational demanding. In particular, it consists in optimizing a finite horizon cost, over a moving interval, using a fixed number of past measurements and the system model.

For general nonlinear systems and perturbations, designing an optimal observer is very hard, as this requires solving challenging partial differential equations [59]. Therefore, alternatively, we can focus on design techniques to improve the estimation performance of a given observer. To the best of the authors' knowledge, solutions in this direction concentrate on specific classes of systems, see e.g. [60–62] for linear systems or e.g., [63–70] in the context of high-gain observers, or focus only on one of the specific desired properties described above, like the robustness to measurement noise in e.g., [9, 71]. In addition, switching, adaptive estimation or gain-scheduling strategies have been studied in the literature for estimation, see e.g., [67, 72–74]. The main limitation of these works is that they consider specific classes of systems or observers. For general continuous-time nonlinear systems, a solution to improve the estimation performance is presented in [43], where the authors proposed to switch between a local and a global observer to take the best of both of them. Indeed, a local observer typically can be tuned to have good robustness to measurement noise and disturbances, but its domain of attraction may be very small. On the other hand, the global observer guarantees a global domain of attraction and often a fast convergence, but it is sensitive to noise. Unfortunately, the technique presented in [43] is not easy to implement since the knowledge of various properties of the observers is required.

An additional difficulty in tuning the observer gain to obtain good performances with robust stability guarantees arises from the fact that it is not easy to prove the convergence property of the

estimation error for all possible converging gains. Indeed, in practice, there may exist some choices of the observer gains that produce convergent estimation errors, possibly with good transient, steady state or overall performance, but unfortunately, we cannot ensure any stability guarantee for these choices of gains. Hence, to have a way to exploit such gains in the observer design would be very useful to possibly improve performance of observers with guaranteed convergence.

In this context, we feel that there is the need for estimation schemes for general deterministic nonlinear systems that ensure a robust stability property of the estimation error and guarantee good estimation performance. In this work we propose a solution based on a multi-observer and the use of hybrid techniques.

Contributions

Focusing on the challenging question related to the estimation performance of observers, in this thesis, we present a new general and flexible hybrid multi-observer scheme to improve the estimation performance of a given robust nominal observer designed for a general nonlinear continuous-time system. In particular, the nominal observer is assumed to be such that the associated estimation error system satisfies an input-to-state stability property with respect to measurement noise and disturbances. As mentioned before, a broad range of nonlinear observers in the literature satisfy this property, see [5, 9] and references therein. The multi-observer is then constructed by adding additional dynamical systems in parallel to the nominal observer, which are collectively referred to as modes. These additional modes have same structure as the nominal one, but with different gains, that can be arbitrarily selected. Indeed, we do not require any stability property for these systems. Consequently, the freedom and flexibility we introduce in the number of additional modes and in their gains can be used to address a range of very different design trade-offs between robustness and convergence speed. Moreover, the freedom in the choice of the gains may results in converging modes for which we may not have any stability guarantee. Inspired by supervisory control and estimation techniques, see e.g., [75–79], we run all the modes in parallel and we evaluate their estimation performance in terms of quadratic costs using monitoring variables. Based on these variables, we design a switching rule that selects the "best" mode at any time instant. The modes that are not selected at a switching instant are either unchanged or their state estimates, as well as their monitoring variables, are reset to the ones of the selected mode. Note that the overall system is an hybrid system. Indeed, the nonlinear system, all the modes of the multi-observer and the monitoring variables evolve in continuous-time, while the switching of the selected mode can be model as a discrete-time jump.

We prove that the proposed hybrid estimation scheme satisfies an input-to-state stability property with respect to disturbance and measurement noise. Moreover, the performance of the hybrid multi-observer scheme are at least as good as the performance of the nominal observer and, under some conditions, we show that the propose technique strictly improves the estimation performance. Finally, we illustrate the effectiveness of the proposed hybrid multi-observer approach in numerical examples. In addition, the presented estimation technique is applied, in simulation, to improve the estimation performance of an observer designed following a polytopic-based approach, for the state estimation of an electrochemical lithium-ion battery with standard model and parameter values, for

which estimation performance are extremely important.

1.4 Outline of the thesis

The remaining of the thesis is organized as follows.

— In **Chapter 2** we present some preliminaries that are helpful to understand the rest of the thesis. In particular, we first recall some mathematical concepts. After that, the class of nonlinear continuous-time observers considered in this thesis is introduced, together with examples and stability properties. In this chapter, we also introduce the formalism of hybrid dynamical systems we adopt in this thesis, presenting useful definitions, concepts and properties.

— In Part I (**Chapters 3 and 4**) the event-triggered estimation problem is presented, where we propose a new dynamic triggering rule, implemented by a smart sensor, to decide when an output transmission over the digital network needs to be triggered. The proposed triggering rule does not rely on a copy of the observer in the sensor, which is therefore not required to have significant computation capabilities. The results are first presented for unperturbed linear time-invariant systems in Chapter 3, and are then extended to general perturbed nonlinear systems and a decentralized scenario in Chapter 4.

— In Part II (**Chapters 5 and 6**) the performance of a given robust nominal nonlinear observer are improved by using hybrid techniques. In particular, a novel hybrid multi-observer is presented in Chapter 5. It is composed by the nominal one and additional dynamical systems, that differs from the nominal one only in their output injection gains. The estimation performance improvement is obtain by switching between the modes of the multi-observer. In Chapter 6 the approach is applied, in simulations, for the state estimation of an electrochemical lithium-ion battery.

— **Chapter 7** concludes the thesis by summarizing the main results described in this document and by presenting possible future research directions.

1.5 Publications

In this section we provide a list summarizing the publications that arose from this thesis, detailed by categories.

1.5.1 Journal papers

1. E. Petri, R. Postoyan, D. Astolfi, D. Nešić, and W. P. M. H. Heemels: *Decentralized event-triggered estimation of nonlinear systems*, Automatica, to appear. [80]

1.5.2 Submitted papers

1. E. Petri, R. Postoyan, D. Astolfi, D. Nešić, and V. Andrieu: *Hybrid multi-observer for improving estimation performance*, submitted to IEEE Transaction of Automatic Control. [81]

1.5.3 Conference papers

1. E. Petri, T. Reynaudo, R. Postoyan, D. Astolfi, D. Nešić, and S. Raël: *State estimation of an electrochemical lithium-ion battery model: improved observer performance by hybrid redesign*, European Control Conference, Bucharest, Romania, pp. 2151-2156, 2023. [82]
2. E. Petri, R. Postoyan, D. Astolfi, D. Nešić, and V. Andrieu: *Towards improving the estimation performance of a given nonlinear observer: a multi-observer approach*, IEEE Conference on Decision and Control, Cancún, Mexico, pp. 583–590, 2022. [83]
3. E. Petri, R. Postoyan, D. Astolfi, D. Nešić, and W. P. M. H. Heemels: *Event-triggered observer design for linear systems*, IEEE Conference on Decision and Control, Austin, USA, pp. 546-551, 2021. [84]

1.5.4 Conference extended abstracts

1. E. Petri, R. Postoyan, D. Astolfi, D. Nešić, and W. P. M. H. Heemels: *Event-triggered observer design of nonlinear systems with multiple sensor nodes*, International Symposium on Mathematical Theory of Networks and Systems (MTNS), Bayreuth, Germany, 2022.

1.6 Seminars and invited talks

During the three years of this thesis, the obtained results have been presented in different conferences, as detailed above, and several seminars and invited talks, which are now summarized.

1. Institute of Automatic Control, Leibniz University Hannover, *Hybrid multi-observer for improving estimation performance*. Hannover, Germany. 22 June 2023.
2. CRAN, Université de Lorraine, *Hybrid multi-observer for improving estimation performance*. Nancy, France. 4 May 2023.
3. Australian National University, *Hybrid techniques for state estimation: event-triggered observer design and observer performance improvement*. Canberra, Australia. 21 October 2022.
4. University of Sydney, *Hybrid techniques for state estimation: event-triggered observer design and observer performance improvement*. Sydney, Australia. 18 October 2022.
5. University of Melbourne, *Hybrid techniques for state estimation: event-triggered observer design and observer performance improvement*. Melbourne, Australia. 20 September 2022.
6. ANR HANDY workshop, *Towards improving the estimation performance of a given nonlinear observer: a multi-observer approach*. Toulouse, France. 21 June 2022.
7. Université Côte d'Azur, *Hybrid techniques for state estimation: event-triggered observer design and observer performance improvement*. Online. 2 June 2022.
8. SAGIP - GT VS-CPS / SDH. *Towards improving the estimation performance of a given nonlinear observer: a multi-observer approach*. Biarritz, France. 24 May 2022.
9. GT SYNOBS. *Towards improving the estimation performance of a given nonlinear observer: a multi-observer approach*. Paris, France. 21 April 2022.

10. LAGEPP, Université Lyon 1. *Event-triggered observer design for linear systems*. Online. 13 July 2021.
11. ANR HANDY meeting. *Event-triggered observer design for linear systems*. Online. 5 July.2021.
12. SAGIP - GT SYNOBS. *Event-triggered observer design for linear systems*. Online. 1 July 2021.

Chapter 2

Preliminaries

Contents

In this chapter we present preliminaries, which are useful for the rest of the thesis. In Section 2.1 we recall some mathematical definitions, in Section 2.2 we introduce the class of nonlinear observers considered in this thesis and in Section 2.3 we present the hybrid dynamical systems framework we will use to model the overall systems. Finally, Section 2.4 concludes the chapter.

2.1 Mathematical definitions

In this section we recall some mathematical definitions that are used in the next chapters. The material is borrowed from [31, 32, 85].

Functions regularity

A function $f : X \subseteq \mathbb{R}^n \to Y \subseteq \mathbb{R}^m$, with $n, m \in \mathbb{Z}_{>0}$, is said to be

— *continuous at* $x \in X$ if for each $\varepsilon > 0$ there exists $\delta > 0$ (possibly depending on x and ε) such that $|f(x') - f(x)| \leqslant \varepsilon$ for all $x' \in X$ satisfying $0 \leqslant |x' - x| \leqslant \delta$. Equivalently f is said to be *continuous at* $x \in X$ if for each sequence $x_i \in X$ converging to x, $\lim_{i\to\infty} f(x_i) = f(x)$,

— *continuous* if is continuous at every point $x \in X$,

— *uniformly continuous* if for each $\varepsilon > 0$ there exists $\delta > 0$ such that $|f(x') - f(x)| \leqslant \varepsilon$ for all $x, x' \in X$ satisfying $0 \leqslant |x' - x| \leqslant \delta$,

— *Lipschitz* if there exists a constant $M \in \mathbb{R}_{>0}$ such that $|f(x) - f(z)| \leqslant M|x - z|$ for any $x, z \in X$,

— *locally Lipschitz*, if for every $x \in X$ there exists a neighborhood $\mathcal{V} \subset X$ of x and a constant $M \in \mathbb{R}_{>0}$ such that, for any $z, z' \in \mathcal{V}$, $|f(z) - f(z')| \leqslant M|z - z'|$,

— *continuously differentiable* if it is continuous and its derivative exists and is itself a continuous function.

A function $f : X \subseteq \mathbb{R}^n \to Y \subseteq \mathbb{R}^n$ with $n \in \mathbb{Z}_{>0}$, is said to be *invertible* if there exists a function $g : Y \subseteq \mathbb{R}^n \to X \subseteq \mathbb{R}^n$ such that $g(f(x)) = x$ for all $x \in X$ and $f(g(y)) = y$ for all $y \in Y$. The function g is called the *inverse function* of the function f and is denoted f^{-1}. A function $f : X \subseteq \mathbb{R}^n \to Y \subseteq \mathbb{R}^m$, with $n, m \in \mathbb{Z}_{>0}$ admits a *right inverse*, denoted f^{-R}, if $f(f^{-R}(y)) = y$ for all $y \in Y$.

A function $f : \mathbb{R} \to \mathbb{R}$ is said to be

— *piecewise continuous* if for any given interval $[a, b]$, with $a < b \in \mathbb{R}$, there exist a finite number of points $a \leqslant x_0 < x_1 < x_2 < \cdots < x_{k-1} < x_k \leqslant b$, with $k \in \mathbb{Z}_{\geqslant 0}$ such that f is continuous on (x_{i-1}, x_i) for any $i \in \{1, \ldots, k\}$ and its one-sided limits exist as finite numbers,

— *piecewise continuously differentiable* if f is continuous and for any given interval $[a, b]$, with $a < b \in \mathbb{R}$, there exist a finite number of points $a \leqslant x_0 < x_1 < x_2 < \cdots < x_{k-1} < x_k \leqslant b$, with $k \in \mathbb{Z}_{\geqslant 0}$ such that f is continuously differentiable on (x_{i-1}, x_i) for any $i \in \{1, \ldots, k\}$ and the one-sided limits $\lim_{s\to x_{i-1}^+} f'(s)$ and $\lim_{s\to x_i^-} f'(s)$ exist for any $i \in \{1, \ldots, k\}$, where $f'(s)$ denotes the derivative of the function f in $s \in \mathbb{R}$, which is defined as $f'(s) := \lim_{x\to s}(f(x) - f(s))/(x - s)$.

A function $f : [a, b] \subset \mathbb{R} \to Y \subseteq \mathbb{R}^n$, with $n \in \mathbb{Z}_{>0}$, is said to be *absolutely continuous* if for each $\varepsilon > 0$ there exists $\delta > 0$ such that for each countable collection of disjoint subintervals $[a_i, b_i]$ of $[a, b]$ such that $\sum_i (b_i - a_i) \leqslant \delta$, we have that $\sum_i |f(b_i) - f(a_i)| \leqslant \varepsilon$.

Towards Lyapunov functions

The stability analysis we will present in this thesis rely on the study of Lyapunov functions, see e.g., [85, Chapter 4]. For a function to be a Lyapunov function candidate, and thus, a function that may be used to prove stability properties of a dynamical system, it generally needs to be positive definite and radially unbounded with respect to the considered attractor, as defined next. In addition, we define also positive semi-definite functions. A function $f : \mathbb{R}^n \to \mathbb{R}_{\geqslant 0}$, with $n \in \mathbb{Z}_{>0}$, is said to be

— *positive definite* with respect to the set $\mathscr{A} \subseteq \mathbb{R}^n$ if $f(x) = 0$ for any $x \in \mathscr{A}$ and $f(x) > 0$ for all $x \in \mathbb{R}^n \backslash \mathscr{A}$,

— *positive semi-definite* with respect to the set $\mathscr{A} \subseteq \mathbb{R}^n$ if $f(x) = 0$ for any $x \in \mathscr{A}$ and $f(x) \geqslant 0$ for all $x \in \mathbb{R}^n \backslash \mathscr{A}$,

— *radially unbounded* (with respect to set $\mathscr{A}$) if $\lim_{|x|_{\mathscr{A}} \to +\infty} f(x) = +\infty$.

Conversely, a function $f : \mathbb{R}^n \to \mathbb{R}_{\leqslant 0}$, with $n \in \mathbb{Z}_{>0}$, is said to be negative (semi-)definite with respect to the set $\mathscr{A}$ when $-f$ is positive (semi-)definite.

As previously mentioned, the stability analyses we will present in this thesis rely on Lyapunov functions. In particular, in the setting of differential equations used to describe the dynamics of continuous-time systems, i.e., $\dot{x} = f(x)$, where $x \in \mathbb{R}^n$ is the system state, to guarantee a stability property using Lyapunov tools, we need to evaluate the behaviour of the Lyapunov function candidate $V : \mathbb{R}^n \to \mathbb{R}_{\geqslant 0}$ along the solution to the differential equation. In particular, when the Lyapunov function V is continuously differentiable, we need to evaluate

$$\frac{\partial V(x(t))}{\partial t} = \frac{\partial V(x(t))}{\partial x}\frac{\partial x(t)}{\partial t} = \frac{\partial V(x(t))}{\partial x} f(x(t)) = \langle \nabla V(x(t)), f(x(t)) \rangle, \tag{2.1}$$

for a given solution x to the considered system and time $t \in \mathbb{R}_{\geqslant 0}$. $\nabla V(x)$ denotes the gradient of V, which is defined below. From (2.1), we see that the quantity that matters is $\langle \nabla V(x), f(x) \rangle$, which is algebraic when $x \in \mathbb{R}^n$. Hence, we can analyze the behaviour of the Lyapunov function along solutions only using vectors, and thus an algebraic expression, which therefore does not require the knowledge of the solution of the dynamical system at all time $t \in \mathbb{R}_{\geqslant 0}$.

Definition 2.1. *Given a continuously differentiable function $V : \mathbb{R}^n \to \mathbb{R}_{\geqslant 0}$, with $n \in \mathbb{Z}_{>0}$ and any vector $x := (x_1, \ldots, x_n) \in \mathbb{R}^n$, where $x_i \in \mathbb{R}$, for all $i \in \{1, \ldots, n\}$. The* gradient *of V at x is defined as*

$$\nabla V(x) := \left(\frac{\partial V(x)}{\partial x_1}, \ldots, \frac{\partial V(x)}{\partial x_n} \right) \in \mathbb{R}^n, \tag{2.2}$$

where $\dfrac{\partial V(x)}{\partial x_i}$ denotes the partial derivative of the function V with respect to x_i at a point $x \in \mathbb{R}^n$, for all $i \in \{1, \ldots, n\}$. □

Definition 2.1 requires that the function V is continuously differentiable. Unfortunately, not always the Lyapunov functions used to study the stability properties of a dynamical system have this

property. For example, the Lyapunov functions we construct in Part II of this thesis are not continuously differentiable, but only locally Lipschitz and thus differentiable almost everywhere by Rademacher's theorem [86]. In this case, to study the differential property of the function V we use the notion of *Clarke's generalized directional derivative* [86], as defined next.

Definition 2.2. *Consider a locally Lipschitz function* $V : \mathbb{R}^n \to \mathbb{R}_{\geqslant 0}$, *with* $n \in \mathbb{Z}_{>0}$. *The* Clarke's generalized directional derivative of V at a point $x \in \mathbb{R}^n$ in the direction $v \in \mathbb{R}^n$, *denoted* $V^\circ(x;v)$, *is defined as*

$$V^\circ(x;v) := \limsup_{h \to 0^+, y \to x} \frac{V(y+hv) - V(y)}{h}. \tag{2.3}$$

□

Comparison functions

To characterize the stability properties of nonlinear systems and to describe the system trajectory behaviours, comparison functions are very useful. We recall the definitions of class $\mathcal{K}$, class $\mathcal{K}_\infty$ and class $\mathcal{KL}$ functions, taken from [85, Section 4.4]. A function $\alpha : \mathbb{R}_{\geqslant 0} \to \mathbb{R}_{\geqslant 0}$ is a

— *class* $\mathcal{K}$ function, denoted $\alpha \in \mathcal{K}$, if it is continuous, strictly increasing, and $\alpha(0) = 0$,

— *class* $\mathcal{K}_\infty$ function, denoted $\alpha \in \mathcal{K}_\infty$, if $\alpha \in \mathcal{K}$ and it is unbounded, i.e., $\lim_{r \to +\infty} \alpha(r) = +\infty$.

A function $\beta : \mathbb{R}_{\geqslant 0} \times \mathbb{R}_{\geqslant 0} \to \mathbb{R}_{\geqslant 0}$ is a *class* $\mathcal{KL}$ function, denoted $\beta \in \mathcal{KL}$, if it is nondecreasing in its first argument, nonincreasing in its second argument, i.e., $\lim_{r \to 0^+} \beta(r,s) = 0$ for each $s \in \mathbb{R}_{\geqslant 0}$, and $\lim_{s \to +\infty} \beta(r,s) = 0$ for each $r \in \mathbb{R}_{\geqslant 0}$.

Signals properties

In this thesis, we consider input signals $u \in \mathcal{U} \subseteq \mathbb{R}^n$, with $n \in \mathbb{Z}_{>0}$ that are Lebesgue measurable and locally essentially bounded and with $\mathcal{L}_\mathcal{U}$ we denote the set of all these functions. The definitions are now recalled.

— A set $\mathcal{S} \subset \mathbb{R}$ is said to be *Lebesgue measurable* if it has positive *Lebesgue measure* $\mu(\mathcal{S})$, which is defined as $\mu(\mathcal{S}) = \sum_k (b_k - a_k)$, where (a_k, b_k) are all the disjoint open interval in $\mathcal{S}$. Then, the function $u : \mathcal{S} \to \mathbb{R}^n$ is said to be a *Lebesgue measurable function* if for every open set $\mathcal{U} \subset \mathbb{R}^n$, the set $\{r \in \mathcal{S} : u(r) \in \mathcal{U}\}$ is Lebesgue measurable.

— A function $u : \mathcal{T} \to \mathcal{U} \subseteq \mathbb{R}^n$, with $\mathcal{T} \subseteq \mathbb{R}_{\geqslant 0}$, $n \in \mathbb{Z}_{>0}$ is said to be *locally bounded* at $t \in \mathcal{T}$ if there exists a neighborhood Δ of t such that the set $u(\Delta \cap \mathcal{T})$ is bounded. The function u is said to be *locally bounded* if it is locally bounded at all $t \in \mathcal{T}$. Given a set $\mathcal{T}' \subset \mathcal{T}$, the function u is said to be bounded on $\mathcal{T}'$ if the set $u(\mathcal{T}')$ is bounded.

— A function $u : \mathcal{T} \to \mathcal{U} \subseteq \mathbb{R}^n$, with $\mathcal{T} \subseteq \mathbb{R}_{\geqslant 0}$, $n \in \mathbb{Z}_{>0}$ is said to be *locally essentially bounded* if for any $t \in \mathcal{T}$ there exists an open neighborhood $\tilde{\Delta}$ of t such that u is bounded almost everywhere on $\tilde{\Delta}$; i.e., there exists $c \geqslant 0$ such that $|u(t)| \leqslant c$ for almost all $t \in \tilde{\Delta} \cap \mathcal{T}$. By almost all, we mean everywhere in the considered set except on a set of Lebesgue measure zero.

Tangent cone

We finally define next the *tangent cone* to a set $\mathscr{C} \subset \mathbb{R}^n$, with $n \in \mathbb{Z}_{>0}$ at a point $x \in \mathbb{R}^{n_x}$.

Definition 2.3. *Given a set $\mathscr{C} \subseteq \mathbb{R}^n$, with $n \in \mathbb{Z}_{>0}$, the tangent cone to the set $\mathscr{C}$ at a point $x \in \mathbb{R}^n$, denoted $T_{\mathscr{C}}$, is the set of all vectors $v \in \mathbb{R}^n$ for which there exist sequences $x_i \in \mathscr{C}$, $\tau_i > 0$, for any $i \in \mathbb{Z}_{\geqslant 0}$, with $x_i \to x$, $\tau_i \to 0$ as $i \to \infty$ and $v = \lim_{i \to \infty} \frac{x_i - x}{\tau_i}$.* □

In this section we have recalled some mathematical definitions useful for this thesis. We are now ready to present the class of nonlinear continuous-time observers we focus on in this thesis.

2.2 Observers for continuous-time systems

In this section we describe the class of observers for continuous-time dynamical systems that are considered in this thesis. As explained in the introduction, an observer is designed to estimate the system state based on the knowledge of the system model, the input and the measured output. First, in Section 2.2.1, we provide the definition of an observer we adopt for a general nonlinear system and, in Section 2.2.2, we define the input-to-state stability property of the state estimation error system and we recall the Lyapunov conditions used to guarantee this property. The satisfaction of this property is the starting point for most of the results we will present in this thesis. In Section 2.2.3, some specific classes of observers we will consider in the numerical examples in the thesis are described. Finally, in Section 2.2.4, we define a useful input/output-to-state stability property and we provide its Lyapunov characterization.

2.2.1 Observer definition

In this thesis we focus on the following class of continuous-time nonlinear systems

$$\begin{aligned} \dot{x} &= f_p(x, u, v) \\ y &= h(x, w), \end{aligned} \tag{2.4}$$

where $x \in \mathbb{R}^{n_x}$ is the system state, $u \in \mathbb{R}^{n_u}$ is the measured input, $y \in \mathbb{R}^{n_y}$ is the output measured by sensors, $v \in \mathbb{R}^{n_v}$ is an unmeasured disturbance input and $w \in \mathbb{R}^{n_w}$ is the measurement noise, with $n_x, n_y \in \mathbb{Z}_{>0}$, and $n_u,\ n_v,\ n_w \in \mathbb{Z}_{\geqslant 0}$. The inputs u, v and w to (2.4) are such that $u \in \mathscr{L}_{\mathscr{U}}$, $v \in \mathscr{L}_{\mathscr{V}}$ and $w \in \mathscr{L}_{\mathscr{W}}$ for some sets $\mathscr{U} \subseteq \mathbb{R}^{n_u}$, $\mathscr{V} \subseteq \mathbb{R}^{n_v}$ and $\mathscr{W} \subseteq \mathbb{R}^{n_w}$. The vector field $f_p : \mathbb{R}^{n_x} \times \mathbb{R}^{n_u} \times \mathbb{R}^{n_v} \to \mathbb{R}^{n_x}$ is locally Lipschitz in its first argument and continuous in the others and $h : \mathbb{R}^{n_x} \times \mathbb{R}^{n_w} \to \mathbb{R}^{n_y}$ is continuously differentiable in x and continuous in w. Equation (2.4) is called *system plant equation* and describes the dynamics of the state variable x. Indeed $\dot{x}$ denotes the derivative of x with respect to the continuous-time t, i.e., $\dot{x} = \frac{dx}{dt}$. By solving the differential equation (2.4) we can therefore obtain an expression of the trajectory of the system state at every time $t \in \mathbb{R}_{\geqslant 0}$. Indeed, given any initial condition $x(0) = x_0 \in \mathbb{R}^{n_x}$ and any inputs $u \in \mathscr{L}_{\mathscr{U}}$, $v \in \mathscr{L}_{\mathscr{V}}$, which are functions of the time t, by a solution to (2.4), we mean an absolutely continuous function x satisfying

$$x(t) = x_0 + \int_0^t f_p(x(s), u(s), v(s))ds. \tag{2.5}$$

The second equation in (2.4) is the *output equation*, which is a static map that describes the relationship between the output y, which can be directly measured, and the internal state of the system x.

The objective of an observer for system (2.4) is to asymptotically reconstruct x given f, h, u and y. The class of continuous-time observers for system (2.4) considered in this thesis has the form

$$\begin{aligned} \dot{z} &= f_o(z, u, y, \hat{y}), \\ \hat{x} &= \psi(z) \\ \hat{y} &= h(\hat{x}, 0), \end{aligned} \tag{2.6}$$

where $z \in \mathbb{R}^{n_z}$ is the observer state, with $n_z \geqslant n_x$, $\hat{x} \in \mathbb{R}^{n_x}$ is the state estimate, $\hat{y}$ is the output estimate. The vector field $f_o : \mathbb{R}^{n_z} \times \mathbb{R}^{n_u} \times \mathbb{R}^{n_y} \times \mathbb{R}^{n_y} \to \mathbb{R}^{n_z}$ is continuous, and $\psi : \mathbb{R}^{n_z} \to \mathbb{R}^{n_x}$ admits a right inverse ψ^{-R} of ψ, i.e., $x = \psi(\psi^{-R}(x))$ for any $x \in \mathbb{R}^{n_x}$. Often $z = \hat{x}$, but this does not necessarily have to be the case. Note that these class of systems and observers cover many design techniques in the literature, see e.g., [5] for a survey on observers designs for nonlinear systems. Even if the class of observers considered in this thesis covers a wide range of observer design techniques in the literature, other estimations schemes, e.g, moving horizon estimation, see e.g., [55–58] for discrete-time systems, sliding-mode observers, see e.g., [87], finite-time converging observers, see e.g., [88] or interval observers, see e.g., [89, 90], exist and are not covered by the results in this thesis.

The dynamics of the observer (2.6) depends on the system input u and output y of system (2.4), which are known and on the observer state estimate z and its output estimate $\hat{y}$. Moreover, the observer dynamics is described by the function f_o, which needs to be designed and typically is related to the knowledge of the system model f_p in (2.4). Indeed, for example, when the observer has the same dimension as the system, i.e., $n_z = n_x$, the function f_o may be designed as a copy of the plant dynamics f_p plus an output injection correction term that depends on the output estimation error, see Section 2.2.3 for examples. As we have previously explained, observer (2.6) is a dynamical system that is used to estimate the system state x starting from the knowledge of the system model (2.4) and input u and output y measurements. As a consequence, such estimation scheme exists only if the measurements contain enough information to reconstruct uniquely the system state. This property, which is necessary to design the observer, is called *detectability*. In particular, for different classes of dynamical systems, there exist different detectability/observability conditions, which lead to different observer design techniques. An interested reader is referred to [5] for an overview of observer designs and detectability notions for nonlinear continuous-time systems. In this thesis we always assume that the considered system (2.4) is detectable and thus, we can design observer (2.6) to estimate its state.

Note that, in (2.6) we consider observers whose state dimension is at least as large as the system state, namely $n_z \geqslant n_x$. When the measured output corresponds to one or more system states, it is possible to design an observer to estimate only the unmeasured states. In this case, the observer may have a smaller dimension than the system, namely $n_z < n_x$, and we talk about *reduced order observers*, see e.g., [91–93]. A potential drawback of this approach is that the state estimate depends

directly on the output measurement often affected by noise, which is not filtered through the observer dynamics.

We now described the properties that system (2.6) needs to satisfied to be considered and observer for system (2.4). System (2.6) is

— an *asymptotic observer* for system (2.4) if, in absence of disturbances and measurement noise, i.e., $v(t) = 0$ and $w(t) = 0$, for all $t \in \mathbb{R}_{\geqslant 0}$, for any input $u \in \mathscr{L}_{\mathscr{U}}$ and any initial condition $x(0) \in \mathbb{R}^{n_x}$ and $z(0) \in \mathbb{R}^{n_z}$ for systems (2.4) and (2.6) respectively, we have that the solution $z(\cdot)$ is defined for all positive times and

$$\lim_{t \to +\infty} |x(t) - \hat{x}(t)| = 0. \tag{2.7}$$

Note that (2.7) implicitly implies that the solutions x and $\hat{x}$ to systems (2.4) and (2.6) are defined for all positive times. This comment applies to all statements in this section.

— an *uniformly asymptotically stable observer* for system (2.4) if there exists $\beta \in \mathscr{KL}$ such that, in absence of disturbances and measurement noise, i.e., $v(t) = 0$ and $w(t) = 0$, for all $t \in \mathbb{R}_{\geqslant 0}$, for any input $u \in \mathscr{L}_{\mathscr{U}}$ and any initial condition $x(0) \in \mathbb{R}^{n_x}$ and $z(0) \in \mathbb{R}^{n_z}$ for systems (2.4) and (2.6) respectively, we have

$$|x(t) - \hat{x}(t)| \leqslant \beta(|\psi^{-R}(x(0)) - z(0)|, t). \tag{2.8}$$

Moreover, the observer is said to be *uniformly exponentially stable* if $\beta(s,t) = cse^{-\lambda t}$, for some real numbers $c \geqslant 1$ and $\lambda > 0$.

Note that, in addition to the attractivity property in (2.7), (2.8) requires also the stability of the estimation error in the sense that, for any $\varepsilon > 0$, there exists $\delta > 0$ such that

$$|\psi^{-R}(x(0)) - z(0)| \leqslant \delta \quad \text{implies} \quad |x(t) - \hat{x}(t)| \leqslant \varepsilon \quad \text{for all } t \in \mathbb{R}_{\geqslant 0}. \tag{2.9}$$

In other words, (2.9) implies that the estimation error remains small during transient if the initial error is small. In addition, property (2.8), conversely to (2.7), requires also that the stability and the attactivity properties of observer (2.6) are uniform for any possible initial conditions $x(0) \in \mathbb{R}^{n_x}$ and $z(0) \in \mathbb{R}^{n_z}$ for systems (2.4) and (2.6), respectively.

— a *robust observer* for system (2.4) with respect to measurement noise and disturbances if there exists $\rho \in \mathscr{K}_\infty$ such that, for any $x(0) \in \mathbb{R}^{n_x}$ and $z(0) \in \mathbb{R}^{n_z}$ and any input $u \in \mathscr{L}_{\mathscr{U}}$, disturbance input $v \in \mathscr{L}_{\mathscr{V}}$ and measurement noise $w \in \mathscr{L}_{\mathscr{W}}$,

$$\limsup_{t \to +\infty} |x(t) - \hat{x}(t)| \leqslant \rho(\limsup_{t \to +\infty} |(v(t), w(t))|). \tag{2.10}$$

When designing observer (2.6) to estimate the state of system (2.4) in presence of disturbances and measurement noise, we desire both the uniform asymptotic stability property of the estimation error in absence of measurement noise and disturbance, as in (2.8), and the robustness property with

respect to disturbances and measurement noise, as in (2.10). These two properties together ensure that the estimation error converges to a neighborhood of the origin, whose size depends on the norm of the disturbances and of the measurement noise. Moreover, it is stable, as defined in (2.9), and uniform with respect the initial conditions $x(0) \in \mathbb{R}^{n_x}$ and $z(0) \in \mathbb{R}^{n_z}$. A general stability property that incorporates these two desired properties is the *input-to-state stability property* of the estimation error with respect to disturbances and measurement noise, see e.g., [6, 7, 9]. This property is the starting point for the results we will present in this thesis and is defined in the next section, together with its Lyapunov characterization.

2.2.2 Input-to-state stability property

In this section we define the input-to-state stability property [6] for the class of nonlinear observers (2.6) considered in this thesis and the corresponding Lyapunov characterization.

Definition 2.4. *Observer* (2.6) *is an input-to-state stable observer for system* (2.4) *if there exist* $\beta \in \mathcal{KL}$ *and* $\gamma \in \mathcal{K}_\infty$ *such that, for any input* $u \in \mathcal{L}_{\mathcal{U}}$*, any disturbance* $v \in \mathcal{L}_{\mathcal{V}}$ *and any measurement noise* $w \in \mathcal{L}_{\mathcal{W}}$*, for any initial condition* $x(0) \in \mathbb{R}^{n_x}$ *and* $z(0) \in \mathbb{R}^{n_z}$ *for systems* (2.4) *and* (2.6)*, respectively, the corresponding solutions* $x(t)$ *and* $z(t)$ *satisfy, for all* $t \geqslant 0$*,*

$$|\hat{x}(t) - x(t)| \leqslant \beta(|\psi^{-R}(x(0)) - z(0)|, t) + \gamma(\|v\|_{[0,t]} + \|w\|_{[0,t]}). \tag{2.11}$$

□

Definition 2.4 implies that when observer (2.6) is an input-to-state stable observer for system (2.4) then for any initial condition $x(0) \in \mathbb{R}^{n_x}$, $z(0) \in \mathbb{R}^{n_z}$ and for any $u \in \mathcal{L}_{\mathcal{U}}$, any disturbance $v \in \mathcal{L}_{\mathcal{V}}$ and any measurement noise $w \in \mathcal{L}_{\mathcal{W}}$, the corresponding estimation error solution $x(t) - \hat{x}(t)$ converges to a neighborhood of the origin, whose size depends on the disturbance v and the measurement noise w as the time t goes to infinity. In addition, in absence of noise and disturbance, namely $v(t) = 0$, $w(t) = 0$ for all $t \geqslant 0$, then observer (2.6) is a (global) asymptotic observer for system (2.4) in the sense that, for any initial condition $x(0) \in \mathbb{R}^{n_x}$, $z(0) \in \mathbb{R}^{n_z}$ and any $u \in \mathcal{L}_{\mathcal{U}}$, the corresponding solution to (2.4) and (2.6) satisfies $x(t) - \hat{x}(t) \to 0$ as $t \to +\infty$, where we recall that $\hat{x}(t) = \psi(z(t))$.

The input-to-state stability property [6] is verified by various observer design techniques in the literature, see e.g., [5, 7, 9] for more details, as well as Section 2.2.3.

To prove that observer (2.6) is an input-to-state stable observer for system (2.4) with respect to disturbance v and measurement noise w, the next Lyapunov characterization is typically used.

Proposition 2.1. *Consider system* (2.4) *and observer* (2.6)*. Suppose there exist* $\underline{\alpha}$*,* $\overline{\alpha}$*,* α*,* γ_v*,* $\gamma_w \in \mathcal{K}_\infty$*,* $V : \mathbb{R}^{n_x} \times \mathbb{R}^{n_z} \to \mathbb{R}_{\geqslant 0}$ *continuously differentiable, such that for all* $x \in \mathbb{R}^{n_x}$*,* $z \in \mathbb{R}^{n_z}$*,* $u \in \mathcal{U}$*,* $v \in \mathcal{V}$*,* $w \in \mathcal{W}$*,* $\hat{y} \in \mathbb{R}^{n_y}$*,*

$$\underline{\alpha}(|x - \psi(z)|) \leqslant V(x,z) \leqslant \overline{\alpha}(|\psi^{-R}(x) - z|) \tag{2.12}$$

$$\left\langle \nabla V(x,z), (f_p(x,u,v), f_o(z,u,y,\hat{y})) \right\rangle \leqslant -\alpha(V(x,z)) + \gamma_v(|v|) + \gamma_w(|w|). \tag{2.13}$$

Then, observer (2.6) *is an input-to-state stable observer for system* (2.4) *with respect to disturbance v and measurement noise w in the sense of Definition 2.4.* □

The proof of this proposition follows similar lines as in [6] and is therefore omitted.

The starting point to the main results in this thesis is the existence of an observer that satisfies an input-to-state stability property in the sense of Definition 2.4. This property will be therefore assumed to hold. In the numerical examples where we will show the efficiency of the proposed approaches, we thus first need to design an observer satisfying an input-to-state stability property, and then we can apply the proposed techniques. In this case, we typically consider a special class of the general class of observers in (2.6). In particular, in all the numerical examples considered in this thesis, the observer state has the same dimension as the system state, namely $n_z = n_x$ and $z = \hat{x} \in \mathbb{R}^{n_x}$ in (2.6). Moreover, the function f_o in (2.6) we will design in all the examples consists in a copy of the system model, i.e., f_p in (2.4), and an output-injection correction term. Therefore, for design purposes in the numerical examples in this thesis we consider the following class of nonlinear observers, which is a subclass of the nonlinear observers in (2.6),

$$\begin{aligned} \dot{\hat{x}} &= f_p(\hat{x}, u, 0) + L(y - \hat{y}) \\ \hat{y} &= h(\hat{x}, 0), \end{aligned} \tag{2.14}$$

where f_p and h comes from the system model (2.4) and $L \in \mathbb{R}^{n_x \times n_y}$ is the observer gain.

Note that, when considering observers (2.14) to estimate the state of system (2.4), instead of (2.6), the Lyapunov conditions in Proposition 2.1 can be simplified, as described in the next corollary.

Corollary 2.1. *Consider system* (2.4) *and observer* (2.14). *Suppose there exist* $\underline{\alpha}$, $\overline{\alpha}$, α, γ_v, $\gamma_w \in \mathcal{K}_\infty$, $L : \mathbb{R}_{\geqslant 0} \to \mathbb{R}^{n_x \times n_y}$, $V : \mathbb{R}^{n_x} \to \mathbb{R}_{\geqslant 0}$ *continuously differentiable, such that for all* $x \in \mathbb{R}^{n_x}$, $\hat{x} \in \mathbb{R}^{n_x}$, $u \in \mathcal{U}$, $v \in \mathcal{V}$, $w \in \mathcal{W}$,

$$\underline{\alpha}(|x - \hat{x}|) \leqslant V(x - \hat{x}) \leqslant \overline{\alpha}(|x - \hat{x}|) \tag{2.15}$$

$$\left\langle \nabla V(x - \hat{x}), (f_p(x, u, v) - f_p(\hat{x}, u, 0) - L(y - \hat{y})) \right\rangle \leqslant -\alpha(V(x - \hat{x})) + \gamma_v(|v|) + \gamma_w(|w|). \tag{2.16}$$

Then, observer (2.14) *is an input-to-state stable observer for system* (2.4) *with respect to disturbance v and measurement noise w in the sense of Definition 2.4.* □

Examples of observer designs modelled in the form (2.14) are given in the next section. In particular, the observer design techniques described in the next section are used in the thesis to show the efficiency of the proposed techniques in numerical examples.

2.2.3 Observer examples

This section focuses on some specific observer design techniques in the literature, which are implemented in numerical examples in the thesis. In particular, we consider the Luenberger observer for linear time-invariant systems, the high-gain observer, observer design based on a polytopic approach and the extended Kalman filter.

Luenberger observer

In this section we recall the Luenberger observer design for linear time-invariant systems [94]. Consider a linear time-invariant system

$$\begin{aligned} \dot{x} &= Ax + Bu + v \\ y &= Cx + Du + w, \end{aligned} \tag{2.17}$$

where $x \in \mathbb{R}^{n_x}$ is the state, $u \in \mathbb{R}^{n_u}$ is a known input, $y \in \mathbb{R}^{n_y}$ is the measured output, $v \in \mathbb{R}^{n_x}$ is an unknown disturbance input, and $w \in \mathbb{R}^{n_y}$ is the unknown measurement noise, with n_x, $n_y \in \mathbb{Z}_{>0}$ and $n_u \in \mathbb{Z}_{\geqslant 0}$. In this case, the detectability of system (2.17) is equivalent to the fact that there exists $L \in \mathbb{R}^{n_x \times n_y}$ such that the matrix $A - LC$ is Hurwitz, which means that all its eigenvalues have negative real part. In addition, if the eigenvalues of $A - LC$ can be arbitrarily assigned using the gain L, then the pair (A, C) is observable and the gain L can be used to obtain an arbitrarily fast speed of exponential convergence of the estimation error to the origin. Note that, if the pair (A, C) is observable it is also detectable, but the opposite is not necessarily true. When the pair (A, C) is detectable, to estimate the system state, we can thus design a Luenberger observer [94], described by

$$\begin{aligned} \dot{\hat{x}} &= A\hat{x} + Bu + L(y - \hat{y}) \\ \hat{y} &= C\hat{x} + Du, \end{aligned} \tag{2.18}$$

where $\hat{x} \in \mathbb{R}^{n_x}$ is the state estimate, $\hat{y} \in \mathbb{R}^{n_y}$ is the output estimate and $L \in \mathbb{R}^{n_x \times n_y}$ is the output-injection gain that is designed such that the matrix $A - LC$ is Hurwitz, as explained above. In absence of disturbance and measurement noise, i.e., $v(t) = 0$ and $w(t) = 0$ for all $t \in \mathbb{R}_{\geqslant 0}$, observer (2.18) guarantees that we can exponentially reconstruct the state x of the plant, implying that $\lim_{t \to +\infty} (x(t) - \hat{x}(t)) = 0$ for any initial condition to (2.17) and (2.18) and any input u. To see this, we define the estimation error $e := x - \hat{x}$ and we evaluate its dynamics, from (2.17) and (2.18), which is given by

$$\dot{e} = (A - LC)e, \tag{2.19}$$

Solving the differential equation (2.19), we obtain, for any $e_0 = e(0) \in \mathbb{R}^{n_x}$, for all $t \in \mathbb{R}_{\geqslant 0}$,

$$e(t) = e^{(A-LC)t} e_0, \tag{2.20}$$

which, since $A - LC$ is Hurwitz, implies that the estimation error exponentially converges to the origin as the time goes to infinity. In addition, in presence of disturbance v and measurement noise w, by defining the Lyapunov function $V(e) := e^\top P e$, where $P \in \mathbb{R}^{n_x \times n_x}$ is a positive definite matrix given by $P(A - LC) + (A - LC)^\top P = -Q$ for some $Q \in \mathbb{R}^{n_x \times n_x}$ positive definite, the Lyapunov conditions in Corollary 2.1 are satisfied, as stated in the next proposition.

Proposition 2.2. *Consider system* (2.17) *and observer* (2.18)*, where $L \in \mathbb{R}^{n_x \times n_y}$ is designed such that $A - LC$ is Hurwitz. Then, there exist $\underline{a}, \overline{a}, a, \gamma_v, \gamma_w > 0$ such that $V(e) = e^\top P e$ satisfies the following*

properties, for all $e = x - \hat{x} \in \mathbb{R}^{n_x}$, $v \in \mathbb{R}^{n_x}$ *and* $w \in \mathbb{R}^{n_y}$,

$$\underline{a}|e|^2 \leqslant V(e) \leqslant \overline{a}|e|^2 \tag{2.21}$$

$$\langle \nabla V(e), (A-LC)e + v - Lw) \rangle \leqslant -aV(e) + \gamma_v|v|^2 + \gamma_w|w|^2. \tag{2.22}$$

□

Proof. Consider system (2.17) and observer (2.18). Using the definition $e = x - \hat{x}$, we obtain,

$$\dot{e} = \dot{x} - \dot{\hat{x}} = (A-LC)e + v - Lw. \tag{2.23}$$

Pick any $Q \in \mathbb{R}^{n_x \times n_x}$ positive definite and consider the Lyapunov function $V(e) := e^\top Pe$, where $P \in \mathbb{R}^{n_x \times n_x}$ is a symmetric positive definite matrix given by $P(A-LC) + (A-LC)^\top P = -Q$. Note that since $A - LC$ is Hurwitz, in view of e.g., [85, Theorem 4.6], matrix P exists and is unique. Since $P \in \mathbb{R}^{n_x \times n_x}$ is a symmetric positive definite matrix, we have

$$\lambda_{\min}(P)|e|^2 \leqslant V(e) \leqslant \lambda_{\max}(P)|e|^2. \tag{2.24}$$

This proves (2.21) with $\underline{a} := \lambda_{\min}(P) > 0$ and $\overline{a} := \lambda_{\max}(P) > 0$. We now prove (2.22). Let $x, e, v \in \mathbb{R}^{n_x}$ and $w \in \mathbb{R}^{n_y}$. From the definition of V and (2.23), we obtain

$$\begin{aligned} &\langle \nabla V(e), (A-LC)e + v - Lw) \rangle \\ &\quad = e^\top (A-LC)^\top Pe + v^\top Pe - w^\top L^\top Pe + e^\top P(A-LC)e + e^\top Pv - e^\top PLe \\ &\quad = e^\top ((A-LC)^\top P + P(A-LC))e + 2v^\top Pe - 2w^\top L^\top Pe. \end{aligned} \tag{2.25}$$

Using $P(A-LC) + (A-LC)^\top P = -Q$, we obtain

$$\langle \nabla V(e), (A-LC)e + v - Lw) \rangle = -e^\top Qe + 2v^\top Pe - 2w^\top L^\top Pe. \tag{2.26}$$

Since $Q \in \mathbb{R}^{n_x \times n_x}$ is a symmetric positive definite matrix, we have

$$\lambda_{\min}(Q)|e|^2 \leqslant e^\top Qe \leqslant \lambda_{\max}(Q)|e|^2. \tag{2.27}$$

Pick any $c_v, c_w \in \mathbb{R}_{>0}$ such that $\lambda_{\min}(Q) - c_v - c_w > 0$, then, using (2.27), and the Young's inequality, from (2.26), we have

$$\begin{aligned}\langle \nabla V(e), (A-LC)e + v - Lw)\rangle &\leqslant -\lambda_{\min}(Q)|e|^2 + 2|v^\top Pe| + 2|w^\top L^\top Pe| \\ &\leqslant -\lambda_{\min}(Q)|e|^2 + 2\|P\|\,|v|^2|e|^2 + 2\left\|L^\top P\right\||w||e| \\ &\leqslant -\lambda_{\min}(Q)|e|^2 + \frac{\|P\|^2}{c_v}|v|^2 + c_v|e|^2 + \frac{\left\|L^\top P\right\|^2}{c_w}|w|^2 + c_w|e|^2 \\ &\leqslant -(\lambda_{\min}(Q)|e|^2 - c_v - c_w)|e|^2 + \frac{\|P\|^2}{c_v}|v|^2 + \frac{\left\|L^\top P\right\|^2}{c_w}|w|^2.\end{aligned} \tag{2.28}$$

Using (2.24), we obtain

$$\langle \nabla V(e), (A-LC)e + v - Lw)\rangle \leqslant -\frac{\lambda_{\min}(Q)|e|^2 - c_v - c_w}{\lambda_{\max}(P)}V(e) + \frac{\|P\|^2}{c_v}|v|^2 + \frac{\left\|L^\top P\right\|^2}{c_w}|w|^2, \tag{2.29}$$

which concludes the proof of Proposition 2.2, with $a := \dfrac{\lambda_{\min}(Q)|e|^2 - c_v - c_w}{\lambda_{\max}(P)} > 0$, $\gamma_v := \dfrac{\|P\|^2}{c_v} > 0$ and $\gamma_w := \dfrac{\left\|L^\top P\right\|^2}{c_w} > 0$. ■

From Proposition 2.2 we have that the Lyapunov conditions in Corollary 2.1 are satisifed and thus the estimation error system satisfies an input-to-state stability property with respect to the disturbance v and the measurement noise w, as defined in Definition 2.4.

We consider this observer design technique in numerical examples in Chapters 3 and 5.

High-gain observer

In this section we describe the high-gain observer design for systems in the *canonical observability form*. The material is borrowed from [63]. Consider a nonlinear system in the following form

$$\begin{aligned}\dot{x} &= Ax + B\varphi(x) + v \\ y &= Cx + w,\end{aligned} \tag{2.30}$$

where $x \in \mathbb{R}^{n_x}$ is the state, $y \in \mathbb{R}$ is the measured output $v \in \mathbb{R}^{n_x}$ is an unknown distrurbance and $w \in \mathbb{R}$ is the unknown measurement noise, with $n_x \in \mathbb{Z}_{>0}$. The nonlinear function φ in is a Lipschitz function, namely there exists $K > 0$ such that for any $x, x' \in \mathbb{R}^{n_x}$,

$$|\varphi(x) - \varphi(x')| \leqslant K|x - x'|. \tag{2.31}$$

The matrices $A \in \mathbb{R}^{n_x \times n_x}$, $B \in \mathbb{R}^{n_x \times 1}$ and $C \in \mathbb{R}^{n_x \times 1}$ are given by

$$A = \begin{bmatrix} 0_{(n_x-1)\times 1} & I_{n_x-1} \\ 0 & 0_{1\times(n_x-1)} \end{bmatrix},\ B = \begin{bmatrix} 0_{(n_x-1)\times 1} \\ 1 \end{bmatrix},\ C = \begin{bmatrix} 1 & 0_{1\times(n_x-1)}. \end{bmatrix} \tag{2.32}$$

Note that the pair (A, C) is observable.

For this class of nonlinear systems, to estimate the system state, we can design a high-gain observer of the form

$$\begin{aligned}\dot{\hat{x}} &= A\hat{x} + B\varphi(\hat{x}) + D(\ell)L(y - \hat{y})\\ \hat{y} &= C\hat{x},\end{aligned} \tag{2.33}$$

where $\hat{x} \in \mathbb{R}^{n_x}$ is the observer state estimate and $\hat{y} \in \mathbb{R}$ is the output estimate. The matrices $D(\ell) \in \mathbb{R}^{n_x \times n_x}$ and $L \in \mathbb{R}^{n_x \times 1}$ are given by

$$D(\ell) = \operatorname{diag}(\ell, \dots, \ell^{n_x}), \quad L = (l_1, \dots, l_{n_x})^\top, \tag{2.34}$$

where $l_1, \dots, l_{n_x}$ are chosen such that the matrix $A - LC$ is Hurwitz and ℓ is the high-gain design parameter, which needs to be taken sufficiently large, in the sense that $\ell \geqslant \ell^\star$, with $\ell^\star \geqslant 1$. This will be clarified in the next next proposition, where we show that observer (2.33) is input-to-state stable observer for system (2.30) in the sense that the Lyapunov conditions in Corollary 2.1 are satisfied.

Proposition 2.3. *Consider system* (2.30) *and observer* (2.33)*, where $L \in \mathbb{R}^{n_x \times 1}$ is designed such that $A - LC$ is Hurwitz. Then, there exist $\underline{\alpha}, \overline{\alpha}, \alpha, \gamma_v, \gamma_w \in \mathscr{K}_\infty$, $\ell^\star \geqslant 1$ and a continuously differentiable function $V : \mathbb{R}^{n_x} \to \mathbb{R}_{\geqslant 0}$ such that, for any $\ell > \ell^\star$ and for all $e := x - \hat{x} \in \mathbb{R}^{n_x}$, $v \in \mathbb{R}^{n_x}$ and $w \in \mathbb{R}$,*

$$\underline{\alpha}(|e|) \leqslant V(e) \leqslant \overline{\alpha}(|e|) \tag{2.35}$$

$$\big\langle \nabla V(e), (A - D(\ell)LC)e + B(\varphi(x) - \varphi(\hat{x})) + v - D(\ell)Lw \big\rangle \leqslant -\alpha(V(e)) + \gamma_v(|v|) + \gamma_w(|w|). \tag{2.36}$$

□

Proof. Consider system (2.30) and observer (2.33). Pick any $c_v, c_w \in \mathbb{R}_{>0}$, $Q \in \mathbb{R}^{n_x \times n_x}$ symmetric positive definite. Select $L \in \mathbb{R}^{n_x \times 1}$ such that $A - LC$ is Hurwitz. Pick $\ell, \ell^\star \geqslant 1$ such that $\ell > \ell^\star$ and $a := \ell^\star \lambda_{\min}(Q) + 2\ell^\star \left\| PD(\ell^\star)^{-1} B \right\| K + c_v^2 + c_w^2 > 0$, where $P \in \mathbb{R}^{n_x \times n_x}$ is a symmetric positive definite matrix given solution to $(A - LC)^\top P + P(A - LC) = -Q$ and K comes from (2.31). Note it is always possible to select $\ell^\star$ big enough such that this condition is satisfied. Denote $x := (x_1, \dots, x_{n_x}) \in \mathbb{R}^{n_x}$, $\hat{x} := (\hat{x}_1, \dots, \hat{x}_{n_x}) \in \mathbb{R}^{n_x}$, with $x_i, \hat{x}_i \in R$, $i \in \{1, \dots, n_x\}$. The proof relies on following change of coordinates

$$z := \begin{bmatrix} x_1 - \hat{x}_1 \\ \dfrac{x_2 - \hat{x}_2}{\ell} \\ \vdots \\ \dfrac{x_{n_x} - \hat{x}_{n_x}}{\ell^{n_x - 1}} \end{bmatrix} \in \mathbb{R}^{n_x}, \tag{2.37}$$

which therefore implies $e = \frac{D(\ell)}{\ell} z$ and $\hat{x} = x - \frac{D(\ell)}{\ell} z$. Using (2.30) and (2.33), we have

$$\begin{aligned}\dot{z} &= \ell D(\ell)^{-1}\dot{e} \\ &= \ell D(\ell)^{-1}(Ax + B\varphi(x) + v - A\hat{x} - B\varphi(\hat{x}) - D(\ell)L(Cx + w - C\hat{x})) \\ &= \ell D(\ell)^{-1}(A - D(\ell)LC)(x - \hat{x}) + \ell D(\ell)^{-1}B(\varphi(x) - \varphi(\hat{x})) + \ell D(\ell)^{-1}v - \ell Lw.\end{aligned} \tag{2.38}$$

Using $\hat{x} = x - \frac{D(\ell)}{\ell} z$, from (2.38) we obtain

$$\dot{z} = \ell D(\ell)^{-1}(A - D(\ell)LC)\frac{D(\ell)}{\ell} z + \ell D(\ell)^{-1}B\left(\varphi(x) - \varphi\left(x - \frac{D(\ell)}{\ell} z\right)\right) + \ell D(\ell)^{-1}v - \ell Lw. \tag{2.39}$$

From the definitions of A, C and $D(\ell)$ we have that $D(\ell)^{-1}AD(\ell) = \ell A$ and $CD(\ell) = \ell C$. Therefore, (2.39) becomes

$$\dot{z} = \ell(A - LC)z + \ell D(\ell)^{-1}B\left(\varphi(x) - \varphi\left(x - \frac{D(\ell)}{\ell} z\right)\right) + \ell D(\ell)^{-1}v - \ell Lw. \tag{2.40}$$

Let $U := z^\top P z$, with $P \in \mathbb{R}^{n_x \times n_x}$ defined at the begining of the proof. Since P is positive definite we have

$$\lambda_{\min}(P)|z|^2 \leqslant U(z) \leqslant \lambda_{\max}(P)|z|^2. \tag{2.41}$$

From the U definition and $e = \frac{D(\ell)}{\ell} z$, we define $V(e) := U(\ell D(\ell)^{-1}e) = \ell^2 e^\top D(\ell)^{-1}PD(\ell)^{-1}e$, and, from (2.41), we obtain

$$\lambda_{\min}(P)|\ell D(\ell)^{-1}e|^2 \leqslant V(e) \leqslant \lambda_{\max}(P)|\ell D(\ell)^{-1}e|^2, \tag{2.42}$$

which corresponds to (2.35) with $\underline{\alpha}(s) := \lambda_{\min}(P)|\ell D(\ell)^{-1}|^2 s^2$ and $\overline{\alpha}(s) := \lambda_{\max}(P)|\ell D(\ell)^{-1}|^2 s^2$, for all $s \in \mathbb{R}_{\geqslant 0}$. We now focus on the proof of (2.36). From (2.40) and the U definition we have,

for all $z \in \mathbb{R}^{n_x}$, $v \in \mathbb{R}^{n_x}$ and $w \in \mathbb{R}$,

$$\begin{aligned}
&\left\langle \nabla U(z), \ell(A-LC)z + \ell D(\ell)^{-1}B\left(\varphi(x) - \varphi\left(x - \frac{D(\ell)}{\ell}z\right)\right) + \ell D(\ell)^{-1}v - \ell L w \right\rangle \\
&\leqslant \ell z^\top (A-LC)^\top P z + \ell \left(\varphi(x) - \varphi\left(x - \frac{D(\ell)}{\ell}z\right)\right)^\top B^\top D(\ell)^{-\top} P z + \ell v^\top D(\ell)^{-\top} P z - \ell w^\top L P z \\
&\quad + \ell z^\top P(A-LC)z + \ell z^\top P D(\ell)^{-1} B\left(\varphi(x) - \varphi\left(x - \frac{D(\ell)}{\ell}z\right)\right) + \ell z^\top P D(\ell)^{-1} v - \ell z^\top P L w \\
&= \ell z^\top [(A-LC)^\top P + P(A-LC)]z + 2\ell z^\top P D(\ell)^{-1} B\left(\varphi(x) - \varphi\left(x - \frac{D(\ell)}{\ell}z\right)\right) \\
&\quad + 2\ell z^\top P D(\ell)^{-1} v - 2\ell z^\top P L w \\
&\leqslant -\ell z^\top Q z + 2\ell z^\top \left\| P D(\ell)^{-1} B \right\| \left| \varphi(x) - \varphi\left(x - \frac{D(\ell)}{\ell}z\right)\right| + 2\ell \left\| P D(\ell)^{-1} \right\| |v||z| + 2\ell \|PL\| |w||z|.
\end{aligned} \tag{2.43}$$

Using (2.41), the Lipschitz property of the function φ and the Young's inequality, from (2.43) we obtain

$$\begin{aligned}
&\left\langle \nabla U(z), \ell(A-LC)z + \ell D(\ell)^{-1}B\left(\varphi(x) - \varphi\left(x - \frac{D(\ell)}{\ell}z\right)\right) + \ell D(\ell)^{-1}v - \ell L w \right\rangle \\
&\leqslant -(\ell \lambda_{\min}(Q) + 2\ell \left\| P D(\ell)^{-1} B \right\| K + c_v^2 + c_w^2)|z|^2 + \frac{\ell^2}{c_v^2}\left\| P D(\ell)^{-1} \right\|^2 |v|^2 + \frac{\ell^2}{c_w^2}\|PL\|^2 |w|^2 \\
&= -a|z|^2 + \frac{\ell^2}{c_v^2}\left\| P D(\ell)^{-1} \right\|^2 |v|^2 + \frac{\ell^2}{c_w^2}\|PL\|^2 |w|^2 \\
&\leqslant -\frac{a}{\lambda_{\max}(P)}|z|^2 + \frac{\ell^2}{c_v^2}\left\| P D(\ell)^{-1} \right\|^2 |v|^2 + \frac{\ell^2}{c_w^2}\|PL\|^2 |w|^2,
\end{aligned} \tag{2.44}$$

where we recall that $a = \ell^\star \lambda_{\min}(Q) + 2\ell^\star \left\| P D(\ell^\star)^{-1} B \right\| K + c_v^2 + c_w^2 > 0$ and $\ell > \ell^\star$. Using $e = \frac{D(\ell)}{\ell} z$, we go back in the original coordinates, and from (2.44), we obtain (2.36), which concludes the proof. Note that, following similar lines, we could have directly prove Proposition 2.3 without the change of coordinates and using $V(e) = \ell^2 e^\top D(\ell)^{-1} P D(\ell)^{-1} e$, for all $e \in \mathbb{R}^{n_x}$. ■

Proposition 2.3 shows that the high-gain observer (2.33) satisfies the Lyapunov conditions in Corollary 2.1, when the high-gain design parameter $\ell > 0$ is big enough and the matrix $L \in \mathbb{R}^{n_x \times 1}$ is designed such that $A - LC$ is Hurwitz. In this case, in view of Corollary 2.1, the high-gain observer (2.33) is an input-to-state stable observer for system (2.30) in the sense of Definition 2.4. In addition, as explained in [63] the estimation error $e := x - \hat{x} \in \mathbb{R}^{n_x}$, originating from (2.30) and (2.33) exponentially converges to a neighborhood of the origin, whose size depends on the measurement noise w, namely, for all possible initial conditions $x(0) \in \mathbb{R}^{n_x}$, as long as $x(t) \in \mathscr{X}$, for all $t \geqslant 0$,

$$|x(t) - \hat{x}(t)| \leqslant \alpha \ell^{n_x - 1} e^{-\beta \ell t} |x(0) - \hat{x}(0)| + \gamma_v \|v\|_{[0,t]} + \gamma_w \ell^{n_x - 1} \|w\|_{[0,t]}, \tag{2.45}$$

where α, β, γ_v and γ_w are positive constants. From (2.45) we note that the high-gain design pa-

rameter ℓ impacts both the speed of convergence, and the ultimate-bound of the estimation error due to the noise. Indeed, the bigger is ℓ, the faster is the observer convergence, but the larger is the ultimate bound due to the noise. In addition, the high-gain design parameter ℓ has an impact also on the transient behaviour, which presents an overshoot, whose amplitude depends on ℓ. This phenomenon, typical for high-gain observers, is known as *peaking phenomenon*.

We design a high-gain observer in a numerical example in Chapter 5.

Polytopic-based observer

In this section we describe polytopic-based observer design. This approach is useful to estimate the system state of a nonlinear system when the system nonlinearities lie on polytopes. In particular, for this class of nonlinear systems, the problem is solved using a collection of linear systems that can over approximate the behaviour of the nonlinear system and the observer design results in LMI-based conditions. In some numerical examples considered in this thesis, we design a polytopic-based observer to estimate a nonlinear system state where the system nonlinearities are either in the dynamic state equation or in the static output map. In the first case, the observer design is inspired by [95], while in the second case follows similar lines as in [96,97]. In this section we describe the polytopic-based observer design in a more general case, where both the state dynamics and the output map may present nonlinearities that lie on polytopes.

Consider a nonlinear system in the following form

$$\begin{aligned} \dot{x} &= Ax + Bu + Gg(x) + v \\ y &= Cx + Du + Hh(x) + w, \end{aligned} \tag{2.46}$$

where $x \in \mathbb{R}^{n_x}$ is the state, $u \in \mathbb{R}^{n_u}$ is a known input, $y \in \mathbb{R}^{n_y}$ is the measured output, $v \in \mathscr{V} \subseteq \mathbb{R}^{n_x}$ is an unknown disturbance input, and $w \in \mathscr{W} \subseteq \mathbb{R}^{n_y}$ is the unknown measurement noise, with n_x, $n_y \in \mathbb{Z}_{>0}$ and $n_u \in \mathbb{Z}_{\geqslant 0}$. The matrices $A \in \mathbb{R}^{n_x \times n_x}$, $B \in \mathbb{R}^{n_x \times n_u}$, $C \in \mathbb{R}^{n_y \times n_x}$, $D \in \mathbb{R}^{n_y \times n_u}$, $G \in \mathbb{R}^{n_x \times 1}$ and $H \in \mathbb{R}^{n_y \times 1}$ are known matrices and the nonlinear functions $g : \mathbb{R}^{n_x} \to \mathbb{R}$ and $h : \mathbb{R}^{n_x} \to \mathbb{R}$ are continuously differentiable functions such that, for all $x, x' \in \mathbb{R}^{n_x}$, there exist $\tilde{G}_1, \ldots, \tilde{G}_{2^{n_x}} \in \mathbb{R}^{1 \times \mathbb{R}^{n_x}}$ and $\tilde{H}_1, \ldots, \tilde{H}_{2^{n_x}} \in \mathbb{R}^{1 \times \mathbb{R}^{n_x}}$ such that

$$g(x) - g(x') = \tilde{G}(x, x')(x - x') \quad \forall x, x' \in \mathbb{R}^{n_x} \tag{2.47}$$

and

$$h(x) - h(x') = \tilde{H}(x, x')(x - x') \quad \forall x, x' \in \mathbb{R}^{n_x}, \tag{2.48}$$

where, for $i \in \{1, \ldots, 2^{n_x}\}$,

$$\tilde{G}(x, x') := \sum_{i=1}^{2^{n_x}} \lambda_{g,i}(x, x')\tilde{G}_i \quad \text{with } \lambda_{g,i}(x, x') \in [0, 1] \text{ and } \sum_{i=1}^{2^{n_x}} \lambda_{g,i}(x, x') = 1 \tag{2.49}$$

and for $j \in \{1, \dots, 2^{n_x}\}$,

$$\tilde{H}(x, x') := \sum_{j=1}^{2^{n_x}} \lambda_{h,j}(x, x') \tilde{H}_j \quad \text{with } \lambda_{h,j}(x, x') \in [0, 1] \text{ and } \sum_{j=1}^{2^{n_x}} \lambda_{h,j}(x, x') = 1. \tag{2.50}$$

Equations (2.47) and (2.49) means that the function $\tilde{G}$ lies in a polytope with vertices $\tilde{G}_i$, $i \in \{1, \dots, 2^{n_x}\}$. This property is satisfied for instance when the continuously differentiable function g can be written as $g(x) = \sum_{k=1}^{n_x} g_k(x_k)$, with $\underline{g}_k \leqslant \dfrac{\partial g_k(x_k)}{\partial x_k} \leqslant \overline{g}_k$ for almost all $x_k \in \mathbb{R}$, with $\underline{g}_k, \overline{g}_k \in \mathbb{R}$. From this, we can define the matrices $\tilde{G}_i$, $i \in \{1, \dots, 2^{n_x}\}$, as all the possible combinations of $\underline{g}_k, \overline{g}_k$, for all the g_ks. Similar comments apply to the function h and the respective equations (2.48) and (2.50).

An observer to estimate the state of system (2.46), where the nonlinear functions g and h satisfy the properties described in equations (2.47)-(2.50), has the following form

$$\begin{aligned} \dot{\hat{x}} &= A\hat{x} + Bu + Gg(\hat{x}) + L(y - \hat{y}) \\ \hat{y} &= C\hat{x} + Du + Hh(\hat{x}), \end{aligned} \tag{2.51}$$

where $\hat{x} \in \mathbb{R}^{n_x}$ is the observer state estimate, $\hat{y} \in \mathbb{R}^{n_y}$ is the output estimate and $L \in \mathbb{R}^{n_x \times n_y}$ is the observer gain, which is obtained by solving some linear matrices inequalities (LMI) as described in the next proposition.

Proposition 2.4. *Consider system* (2.46) *and observer* (2.51) *and define the estimation error* $e := x - \hat{x} \in \mathbb{R}^{n_x}$. *If there exist* $L \in \mathbb{R}^{n_x \times n_y}$, α, μ_v *and* $\mu_w \in \mathbb{R}_{>0}$ *and* $P \in \mathbb{R}^{n_x \times n_x}$ *symmetric positive definite such that*

$$\begin{pmatrix} \mathscr{K}_{i,j} + \alpha P & P & -PL \\ P & -\mu_v I_{n_x} & 0 \\ -L^\top P & 0 & -\mu_w I_{n_y} \end{pmatrix} \leqslant 0, \tag{2.52}$$

with $\mathscr{K}_{i,j} := (A + G\tilde{G}_i - LC - LH\tilde{H}_j)^\top P + P(A + G\tilde{G}_i - LC - LH\tilde{H}_j)$ *for all* $i, j \in \{1, \dots, 2^{n_x}\}$. *Then,* $V : e \to e^\top Pe$ *satisfies, for any* $e \in \mathbb{R}^{n_x}$, $v \in \mathscr{V}$ *and* $w \in \mathscr{W}$,

$$\lambda_{min}(P)|e|^2 \leqslant V(e) \leqslant \lambda_{max}(P)|e|^2, \tag{2.53}$$

$$\left\langle \nabla V(e), (A + G\tilde{G}(x, \hat{x}) - LC - LH\tilde{H}(x, \hat{x}))e + v - Lw \right\rangle \leqslant -\alpha V(e) + \mu_v |v|^2 + \mu_w |w|^2. \tag{2.54}$$

□

Proof. Let $x, \hat{x} \in \mathbb{R}^{n_x}$ and recall the definition of the estimation error $e = x - \hat{x} \in \mathbb{R}^{n_x}$. Let $V(e) = e^\top Pe$. Since P is symmetric positive definite, (2.53) follows from the definition of V.

Let $v \in \mathscr{V}$, $w \in \mathscr{W}$. From (2.46) and (2.51), and using $e = x - \hat{x}$, we have

$$\begin{aligned}\dot{e} &= Ax + Gg(x) + v - A\hat{x} - Gg(\hat{x}) - L(y - \hat{y}) \\ &= Ax + Gg(x) + v - A\hat{x} - Gg(\hat{x}) - L(Cx + Hh(x) + w - C\hat{x} - Hh(\hat{x})) \\ &= (A - LC)e + G(g(x) - g(\hat{x})) + v - LH(h(x) - h(\hat{x})) - Lw.\end{aligned} \tag{2.55}$$

Using (2.47) and (2.48), from (2.55), we obtain

$$\dot{e} = (A + G\tilde{G}(x,\hat{x}) - LC - LH\tilde{H}(x,\hat{x}))e + v - Lw. \tag{2.56}$$

As $V(e) = e^\top Pe$, from (2.56), (2.49) and (2.50), we have

$$\begin{aligned}&\left\langle \nabla V(e), (A + G\tilde{G}(x,\hat{x}) - LC - LH\tilde{H}(x,\hat{x}))e + v - Lw \right\rangle \\ &\quad = e^\top (A + G\tilde{G}(x,\hat{x}) - LC - LH\tilde{H}(x,\hat{x}))^\top Pe + v^\top Pe + w^\top L^\top Pe \\ &\qquad + e^\top P(A + G\tilde{G}(x,\hat{x}) - LC - LH\tilde{H}(x,\hat{x}))e + e^\top Pv + e^\top PLw \\ &\quad = \sum_{i=1}^{2^{n_x}} \lambda_{g,i}(x,\hat{x}) \sum_{j=1}^{2^{n_x}} \lambda_{h,j}(x,\hat{x}) \Big[e^\top \big((A + GG_i - LC - LHH_j)^\top P + P(A + GG_i - LC - LHH_j) \big) e \\ &\qquad + v^\top Pe + e^\top Pv - w^\top L^\top Pe - e^\top PLw \Big].\end{aligned} \tag{2.57}$$

Defining $\chi := (e, v, w)$, using $\mathscr{K}_{i,j} := (A + G\tilde{G}_i - LC - LH\tilde{H}_j)^\top P + P(A + G\tilde{G}_i - LC - LH\tilde{H}_j)$ for all $i, j \in \{1, \ldots, 2^{n_x}\}$, (2.57) becomes

$$\begin{aligned}&\left\langle \nabla V(e), (A + G\tilde{G}(x,\hat{x}) - LC - LH\tilde{H}(x,\hat{x}))e + v - Lw \right\rangle \\ &\qquad = \sum_{i=1}^{2^{n_x}} \lambda_{g,i}(x,\hat{x}) \sum_{j=1}^{2^{n_x}} \lambda_{h,j}(x,\hat{x}) \chi^\top \begin{pmatrix} \mathscr{K}_{i,j} & P & -PL \\ P & 0 & 0 \\ -L^\top P & 0 & 0 \end{pmatrix} \chi.\end{aligned} \tag{2.58}$$

Using $\sum_{i=1}^{2^{n_x}} \lambda_{g,i}(x,\hat{x}) = 1$, $\sum_{j=1}^{2^{n_x}} \lambda_{h,j}(x,\hat{x}) = 1$ and (2.52) for all $i \in \{1, \ldots, 2^{n_x}\}$, $j \in \{1, \ldots, 2^{n_x}\}$, we

obtain

$$\begin{aligned}
&\left\langle \nabla V(e), (A + G\tilde{G}(x,\hat{x}) - LC - LH\tilde{H}(x,\hat{x}))e + v - Lw \right\rangle \\
&\quad \leqslant \sum_{i=1}^{2^{n_x}} \lambda_{g,i}(x,\hat{x}) \sum_{j=1}^{2^{n_x}} \lambda_{h,j}(x,\hat{x}) \chi^\top \begin{pmatrix} -\alpha P & 0 & 0 \\ 0 & +\mu_v I_{n_v} & 0 \\ 0 & 0 & +\mu_w I_{n_w} \end{pmatrix} \chi \\
&\quad = \chi^\top \begin{pmatrix} -\alpha P & 0 & 0 \\ 0 & +\mu_v I_{n_v} & 0 \\ 0 & 0 & +\mu_w I_{n_w} \end{pmatrix} \chi \\
&\quad = -\alpha e^\top P e + \mu_v v^\top I_{n_v} v + \mu_w w^\top I_{n_w} w \\
&\quad = -\alpha V(e) + \mu_v |v|^2 + \mu_w |w|^2.
\end{aligned} \tag{2.59}$$

This concludes the proof. ■

Proposition 2.4 provides conditions to design the gain L of observer (2.51) to guarantee the existence of a Lyapunov function V that satisfies (2.53) and (2.54), and thus, from Corollary 2.1, it guarantees an input-to-state stability property of the estimation error with respect to the disturbance v and the measurement noise w. Note that, it is not always possible to solve linear matrices inequalities. As a result, only when we have a solution to the linear matrices inequalities we obtain the gain L that guarantees the input-to-state stability property. In addition, note that (2.52) is not linear, indeed, two unknown matrices $P \in \mathbb{R}^{n_x \times n_x}$ and $L \in \mathbb{R}^{n_x \times n_y}$ are multiplied both in the definition of $\mathscr{K}_{i,j}$, for all $i, j \in \{1, \ldots, 2^{n_x}\}$ and in equation (2.52). Thus, we need to define $W = PL \in \mathbb{R}^{n_x \times n_y}$ and solve a linear matrix inequality where the unknown terms are α, μ_v and $\mu_w \in \mathbb{R}_{>0}$ and $P \in \mathbb{R}^{n_x \times n_x}$ and $W \in \mathbb{R}^{n_x \times n_y}$ and, then obtain the gain $L \in \mathbb{R}^{n_x \times n_y}$ by using $L = P^{-1}W$.

Polytopic-based observers are considered in numerical examples in Chapters 4, 5 and 6.

Extended Kalman filter

The last observer we present is the extended Kalman filter, see e.g., [98–100]. Consider a nonlinear system

$$\begin{aligned}
\dot{x} &= f(x,u) \\
y &= h(x),
\end{aligned} \tag{2.60}$$

where $x \in \mathbb{R}^{n_x}$ is the state, $u \in \mathbb{R}^{n_u}$ is the input and $y \in \mathbb{R}^{n_y}$ is the measured output. The nonlinear functions $f(x,u)$ and $h(x)$ are continuously differentiable for all $x \in \mathbb{R}^{n_x}$. The input u is a continuous signal.

To estimate the state of system (2.60) we can design an extended Kalman filter (EKF), which is described by

$$\begin{aligned}
\dot{\hat{x}} &= f(\hat{x},u) + L(y - \hat{y}) \\
\hat{y} &= h(\hat{x}),
\end{aligned} \tag{2.61}$$

where $\hat{x} \in \mathbb{R}^{n_x}$ is the state estimate, $y \in \mathbb{R}^{n_y}$ is the output estimate and $L \in \mathbb{R}^{n_x \times n_y}$ is the extended Kalman filter gain, which needs to be designed.

The extended Kalman filter design is based on the linearization of the system dynamics along the

system trajectories. Therefore, we define

$$\begin{aligned} A(\hat{x},u) &= \frac{\partial f(\hat{x},u)}{\partial x} \\ C(\hat{x},u) &= \frac{\partial h(\hat{x})}{\partial x}. \end{aligned} \tag{2.62}$$

These time-varying matrices, which correspond to the linearization of the nonlinear maps along the trajectory $\hat{x}(\cdot)$, are used to define the following Riccati differential equation

$$\dot{P} = (A + \alpha_{\text{EKF}} I_{n_x}) P (A^\top + \alpha_{\text{EKF}} I_{n_x}) - P C^\top R_{\text{EKF}}^{-1} C P + Q_{\text{EKF}}, \tag{2.63}$$

where $R_{\text{EKF}} \in \mathcal{S}_{>0}^{n_y}$, $Q_{\text{EKF}} \in \mathcal{S}_{>0}^{n_x}$ and $\alpha_{\text{EKF}} \in \mathbb{R}_{\geqslant 0}$ are design matrices and parameter, for all $t \in \mathbb{R}_{\geqslant 0}$. Then, the extended Kalman filter gain $L(t)$ in (2.61) is given by, for all $t \in \mathbb{R}_{\geqslant 0}$,

$$L = P C^\top R_{\text{EKF}}^{-1}. \tag{2.64}$$

Conditions to guarantee the local convergence of the state estimation error generated by the extended Kalman filter can be found in e.g., [98–100]. In particular, it is proved that, under some conditions, see e.g., [98, Assumptions 1, 2 and 3], the estimation error $e = x - \hat{x}$ exponentially converges when the initial estimation error is small enough, i.e., there exist $b, c, \theta \in \mathbb{R}_{>0}$ such that observer (2.61) for system (2.60), with gain (2.64), satisfies, $|x(0) - \hat{x}(0)| \in \mathbb{B}$, where $\mathbb{B} := \{x \in \mathbb{R}^{n_x} : |x| \leqslant b\}$,

$$|x(t) - \hat{x}(t)| \leqslant c e^{-\theta t} |x(0) - \hat{x}(0)|, \tag{2.65}$$

for all $t \in \mathbb{R}_{\geqslant 0}$, where $\theta > \alpha$. In this thesis, this design is considered in a numerical example in Chapter 5, where we do not require any stability property of the corresponding estimation error [1]. For this reason, we do not provide details on the required assumptions that need to hold to obtain the stability property. Note that (2.65) guarantees a local convergence of the estimation error. Indeed, it holds only if the initial error is small enough. In addition, the extended Kalman filter does not satisfy globally the Lyapunov conditions in Proposition 2.1, and thus it is not a global input-to-state stable observer.

2.2.4 Input/output-to-state stability property

In Section 2.2.2, we have described the important input-to-state stability property for the class of nonlinear observers we consider in this thesis. This property guarantees that the estimation error solution converges to a neighborhood of the origin. A different stability property, namely the input/output-to-state stability property for the nonlinear system (2.4), and its Lyapunov characterization are presented in this section. Moreover, when this property is satisfied for the state estimation error system, we can define an input/output-to-state stable observer, together with its Lyapunov characterization, which will play a key role in Chapter 5. The material presented in this section is

1. The reason why we consider an observer design technique without requiring a stability property of the estimation error will be clarified in Chapter 5.

inspired by [101, 102].

Definition 2.5. *System* (2.4) *is input/output-to-state stable if there exist* $\beta \in \mathcal{KL}$ *and* $\gamma_u, \gamma_v, \gamma_y \in \mathcal{K}_\infty$ *such that, for any input* $u \in \mathcal{L}_{\mathcal{U}}$*, any disturbance* $v \in \mathcal{L}_{\mathcal{V}}$ *and any measurement noise* $w \in \mathcal{L}_{\mathcal{W}}$*, for any initial condition* $x(0) \in \mathbb{R}^{n_x}$*, the corresponding solution* x *satisfies, for all* $t \geqslant 0$*,*

$$|x(t)| \leqslant \beta(|x(0)|, t) + \gamma_u(\|u\|_{[0,t]}) + \gamma_v(\|v\|_{[0,t]}) + \gamma_y(\|y\|_{[0,t]}). \tag{2.66}$$

□

Roughly speaking, when system (2.4) is input/output-to-state stable, it implies that no matter what is the initial state, if the control input u, disturbance input v and the output y, which depends also on the measurement noise w, are small, then the state x must eventually be small. As shown in [101, 102], to prove that system (2.4) is input/output-to-state stable, Lyapunov conditions can be used, as stated in the next proposition.

Proposition 2.5. *Consider system* (2.4)*. Suppose there exist* $\underline{\alpha}$*,* $\overline{\alpha}$*,* α*,* γ_u*,* γ_v*,* $\gamma_y \in \mathcal{K}_\infty$*,* $V : \mathbb{R}^{n_x} \to \mathbb{R}_{\geqslant 0}$ *continuously differentiable, such that for all* $x \in \mathbb{R}^{n_x}$*,* $u \in \mathcal{U}$*,* $v \in \mathcal{V}$*,* $y \in \mathbb{R}^{n_y}$*,*

$$\underline{\alpha}(|x|) \leqslant V(x) \leqslant \overline{\alpha}(|x|) \tag{2.67}$$

$$\big\langle \nabla V(x), f_p(x,u,v) \big\rangle \leqslant -\alpha(V(x)) + \gamma_u(|u|) + \gamma_v(|v|) + \gamma_y(|y|). \tag{2.68}$$

Then, system (2.4) *is input/output-to-state stable with respect to input* u*, disturbance* v *and the output* y *in the sense of Definition 2.5.* □

The proof of Proposition 2.5 follows similar steps as in [101, 102] and is therefore omitted.

In this thesis, we will use the notion of input/output-to-state stability presented in Definition 2.5 for the state estimation error system generated from system (2.4) and observer (2.6). In this case, we talk about input/output-to-state stable observer, where the inputs are the disturbance v and the measurement noise w, and the output is the output estimation error, as defined next.

Definition 2.6. *Observer* (2.6) *is an input/output-to-state stable observer for system* (2.4) *if there exist* $\beta \in \mathcal{KL}$ *and* $\gamma_1, \gamma_2 \in \mathcal{K}_\infty$ *such that, for any input* $u \in \mathcal{L}_{\mathcal{U}}$*, any disturbance* $v \in \mathcal{L}_{\mathcal{V}}$ *and any measurement noise* $w \in \mathcal{L}_{\mathcal{W}}$*, for any initial condition* $x(0) \in \mathbb{R}^{n_x}$ *and* $z(0) \in \mathbb{R}^{n_z}$ *for systems* (2.4) *and* (2.6)*, respectively, the corresponding solutions* x *and* z *satisfy, for all* $t \geqslant 0$*,*

$$|x(t) - \hat{x}(t)| \leqslant \beta(|\psi^{-R}(x(0)) - z(0)|, t) + \gamma_1(\|v\|_{[0,t]} + \|w\|_{[0,t]}) + \gamma_2(\|y - \hat{y}\|_{[0,t]}). \tag{2.69}$$

□

The input/output-to-state stability property in (2.69) does not imply a convergence property of the estimation error. Indeed, the term $\gamma_2(\|y - \hat{y}\|_{[0,t]})$ may grow as the time goes to infinity and, in that case, the estimation error $|x(t) - \hat{x}(t)|$ is not guaranteed to converge to a neighborhood of

the origin. As a result, the input/output-to-state stability property is weaker than the input-to-state stability property for observer (2.6), described in Definition 2.4. However, it can be useful because it is linked with the concept of *detectability*. Indeed, from Definition 2.6 we notice that, if the system and observer output trajectories are indistinguishable, i.e., $y(t) = \hat{y}(t)$ for all $t \in \mathbb{R}_{\geqslant 0}$, then their states ($x(t)$ and $\hat{x}(t)$) must converge to each other, up to an ultimate bound that depends on the disturbance v and the measurement noise w. Note that the concept of input/output-to-state stable observer and its link with the concept of detectability is associated to the notion of *incremental input/output-to-state stability* defined in [102, Definition 20].

Similarly to the input-to-state stability property described in Section 2.2.2, in the next proposition we provide a Lyapunov characterization of the input/output-to-state stability property of the estimation error system.

Proposition 2.6. *Consider system* (2.4) *and observer* (2.6). *Suppose there exist* $\underline{\alpha}$, $\overline{\alpha}$, α, γ_v, γ_w, $\gamma_y \in \mathcal{K}_\infty$, $V : \mathbb{R}^{n_x} \times \mathbb{R}^{n_z} \to \mathbb{R}_{\geqslant 0}$ *continuously differentiable, such that for all* $x \in \mathbb{R}^{n_x}$, $z \in \mathbb{R}^{n_z}$, $u \in \mathcal{U}$, $v \in \mathcal{V}$, $w \in \mathcal{W}$, $\hat{y} \in \mathbb{R}^{n_y}$,

$$\underline{\alpha}(|x - \psi(z)|) \leqslant V(x,z) \leqslant \overline{\alpha}(|\psi^{-R}(x) - z|) \tag{2.70}$$

$$\left\langle \nabla V(x,z), (f_p(x,u,v), f_o(z,u,y,\hat{y})) \right\rangle \leqslant -\alpha(V(x,z)) + \gamma_v(|v|) + \gamma_w(|w|) + \gamma_y(|y - \hat{y}|). \tag{2.71}$$

Then, observer (2.6) *is an input/output-to-state stable observer for system* (2.4) *with respect to disturbance* v, *measurement noise* w *and the output estimation error* $y - \hat{y}$ *in the sense of Definition 2.6.* □

The proof of Proposition 2.6 follows similar lines as in [101, 102] and is therefore omitted.

As previously mentioned when comparing Definitions 2.4 and 2.6, the major difference between (2.13) and (2.71) is the term $\gamma_y(|y - \hat{y}|)$ in (2.71), which may have a destabilizing effect and may thus prevent the estimation error system to exhibit input-to-state stability property.

2.3 Hybrid dynamical systems

In the previous section, the class of continuous-time nonlinear observers we consider in this thesis have been introduced, together with the corresponding input-to-state stability property. Starting from this stability property, as explained in the introduction, the purpose of this thesis is to propose solutions to two state estimation problems, namely event-triggered estimation and observer performance improvement, by using hybrid techniques. In this section some preliminaries on the hybrid dynamical systems framework introduced in [31] are given. In particular, in this manuscript we consider the class of hybrid dynamical system with continuous-time inputs presented in [37], which is an alternative to the hybrid systems with hybrid inputs in [38], and is an extension of the hybrid system (without inputs) framework in [31]. In Section 2.3.1, we recall the hybrid system model and the notion of solution for this system is given in Section 2.3.2. In Section 2.3.3, we present a proposition, taken from [37, Proposition 6], that is used in the thesis to prove existence and completeness of maximal solutions of the considered hybrid systems. In the same section we also provide an additional result, which is an adaptation to [103, Lemma 5] in the context of hybrid systems with inputs.

The Zeno phenomenon is described in Section 2.3.4, together with the definition of dwell-time and average dwell-time for a solution to an hybrid system. Finally, a stability property for the considered hybrid system is given in Section 2.3.5, together with its Lyapunov characterization.

2.3.1 Hybrid systems with continuous-time inputs

In this section we present the modelling framework of an hybrid system with continuous-time inputs [31,37], namely

$$\mathcal{H} : \begin{cases} \dot{x} &= F(x,u), & (x,u) \in \mathcal{C}, \\ x^+ &\in G(x,u), & (x,u) \in \mathcal{D}, \end{cases} \tag{2.72}$$

where $x \in \mathbb{R}^{n_x}$ is the state and $u \in \mathbb{R}^{n_u}$ is the input, that can represent known inputs, but also unknown disturbances and/or measurement noise. As shown in (2.72), the system state of an hybrid dynamical system can have both continuous-time and discrete-time dynamics. In particular, when the system state x and the input u are in the *flow set* $\mathcal{C} \subseteq \mathbb{R}^{n_x} \times \mathbb{R}^{n_u}$, then, the state x evolves according to the ordinary differential equation in (2.72), if the continuous-time evolution keeps the state and input pair in the flow set $\mathcal{C}$. On the other hand, when the system state x and the input u are in the *jump set* $\mathcal{D} \subseteq \mathbb{R}^{n_x} \times \mathbb{R}^{n_u}$, then the state x exhibits jumps according to the difference inclusion in (2.72). Note that in (2.72) only the jump map G is a set-valued map. To be more general, we could have defined also the flow map F as a set-valued map, see [37, equation (1)], however, all the hybrid systems in this thesis have a single-valued flow map and thus we consider only single-valued flow map in (2.72). Moreover, the sets $\mathcal{C}$ and $\mathcal{D}$ may overlap, partially or totally. In this case, when the system state x and the input u are in the intersection of the flow and jump sets, namely $(x,u) \in \mathcal{C} \cap \mathcal{D}$, then, the hybrid state evolves according either to difference inclusion or according to the ordinary differential equation in (2.72). This last option is possible only if the continuous-time flow keeps the state and input pair in the set $\mathcal{C}$. As a result, different hybrid solutions can be generated.

In this thesis, we consider inputs u for system (2.72) such that $u \in \mathcal{L}_{\mathcal{U}}$, namely, for a given set $\mathcal{U} \subseteq \mathbb{R}^{n_u}$, $\mathcal{L}_{\mathcal{U}}$ is the set of all functions from $\mathbb{R}_{\geqslant 0}$ to $\mathcal{U}$ that are Lebesgue measurable and locally essentially bounded. We also concentrate on the case where the sets $\mathcal{C}$, $\mathcal{D}$ and $\mathcal{U}$ in (2.72) are closed. This corresponds to [37, Standing Assumption], which is needed to define the solution for system (2.72). The sets $\mathcal{C}$ and $\mathcal{D}$ we will design in this thesis do not always depend both on the state $x \in \mathbb{R}^{n_x}$ and the input $u \in \mathcal{U}$, but, in some cases, we will design $\mathcal{C} \subseteq \mathbb{R}^{n_x}$ and $\mathcal{D} \subseteq \mathbb{R}^{n_x}$. Note that this is a special case of the general formulation in (2.72), and all the definitions and results in this chapters apply *mutatis mutandi*.

Since an hybrid system exhibits both continuous-time and discrete-time dynamics, it is not straightforward to define a solution. In the next section we introduce the notion of solution, taken from [37], along with the required concepts needed to define it.

2.3.2 Solution concept

In this section we define the notion of solution to system (2.72). The material is borrowed from [31,37].

We start by introducing the concept of *hybrid time domain* given in [31, Definition 2.3]. Solutions

to continuous-time systems are parameterized by the continuous-time $t \in \mathbb{R}_{\geqslant 0}$. On the other hand, solutions to discrete-time systems are defined using the discrete-time $j \in \mathbb{Z}_{\geqslant 0}$, which represents the number of jumps or discrete steps. As a result, since an hybrid system is a combination of a continuous-time system and a discrete-time one, it is natural to define its solution on a domain that depends both on the continuous-time $t \in \mathbb{R}_{\geqslant 0}$, which accounts the time elapsed, and on the discrete-time $j \in \mathbb{Z}_{\geqslant 0}$, which counts the number of jumps that have occurred. However, only certain subsets of $\mathbb{R}_{\geqslant 0} \times \mathbb{Z}_{\geqslant 0}$, namely the *hybrid time domains*, are needed to characterize the evolution of an hybrid system.

Definition 2.7. *A set $E \subset \mathbb{R}_{\geqslant 0} \times \mathbb{Z}_{\geqslant 0}$ is a* compact hybrid time domain *if*

$$E = \bigcup_{j=0}^{J-1} ([t_j, t_{j+1}], j) \tag{2.73}$$

for some finite sequence of times $0 = t_0 \leqslant t_1 \leqslant \cdots \leqslant t_J$. It is a hybrid time domain *if for all $(T, J) \in E$, $E \cap ([0, T] \times \{0, \ldots, J\})$ is a compact hybrid domain.* □

Definition 2.7 means that the set E is a *hybrid time domain* if it is a union of a finite or infinite sequence of intervals $[t_j, t_{j+1}] \times \{j\}$ with the last one, if it exists, of the form $[t_j, T)$, with T finite or $T = \infty$. In addition, each element $(t, j) \in E$ represents the elapsed hybrid time, which therefore implies that there is a natural way of ordering the hybrid times, i.e., given $(t, j), (t', j') \in E$, $(t, j) \leqslant (t', j')$ implies that either $t < t'$ or $t = t'$ and $j \leqslant j'$.

Given a hybrid time domain E, we define

— $\sup_t E := \sup\{t \in \mathbb{R}_{\geqslant 0} : \exists j \in \mathbb{Z}_{\geqslant 0}$ such that $(t, j) \in E\}$,

— $\sup_j E := \sup\{j \in \mathbb{Z}_{\geqslant 0} : \exists t \in \mathbb{R}_{\geqslant 0}$ such that $(t, j) \in E\}$,

— $\sup E := (\sup_t E, \sup_j E)$,

— $\text{length}(E) := \sup_t E + \sup_j E$.

We now define the concept of *hybrid arc*, which comes from [31, Definition 2.4].

Definition 2.8. *A hybrid signal $x : \text{dom } x \to \mathbb{R}^{n_x}$ is called a hybrid arc if $x(\cdot, j)$ is locally absolutely continuous for each j.* □

We can now define the concept of solution for the hybrid system with input (2.72), which is taken from [37, Defintion 4].

Definition 2.9. *A hybrid arc x is a* solution *to $\mathscr{H}$ for a given input $u \in \mathscr{L}_{\mathscr{U}}$, if*

— ***(Flow condition)*** *for all $j \in \mathbb{N}$ such that $I^j := \{t \mid (t, j) \in \text{dom } x\}$ has nonempty interior, $\dot{x}(t, j) \in F(x(t, j), u(t))$ and $(x(t, j), u(t, j)) \in \mathscr{C}$ for almost all $t \in I^j$;*

— ***(Jump condition)*** *for all $(t, j) \in \text{dom } x$ such that $(t, j + 1) \in \text{dom } x$, $(x(t, j), u(t, j)) \in \mathscr{D}$ and $x(t, j + 1) \in G(x(t, j), u(t))$.*

□

Observe that in equation (2.72) we used the notation x^+ to denote $x(t, j+1)$, for some $t \in \mathbb{R}_{\geqslant 0}$, $j \in \mathbb{Z}_{>0}$. In the remaining of the thesis, both notations will be used to denote a jump (or discrete update) of the hybrid state x.

In the next definition we characterize some properties of solutions to system (2.72). This definition is inspired by [37, Defintion 5] and [31, Definition 2.5].

Definition 2.10. *A solution x to $\mathscr{H}$ for a given input $u \in \mathscr{L}_{\mathscr{U}}$ is*

- nontrivial *if $\operatorname{dom} x$ contains at least two points,*
- maximal, *if there does not exist another solution $\tilde{x}$ to $\mathscr{H}$ for the same input u such that $\operatorname{dom} x$ is a proper subset of $\operatorname{dom} \tilde{x}$ and $x(t, j) = \tilde{x}(t, j)$ for all $(t, j) \in \operatorname{dom} x$,*
- complete *if is maximal and $\operatorname{dom} x$ is unbounded, i.e., $\operatorname{length}(\operatorname{dom} x) = \infty$,*
- t-complete *if is complete and $\sup_t \operatorname{dom} x = \infty$,*
- Zeno *if it is complete and $\sup_t \operatorname{dom} x < \infty$,*
- eventually discrete *if $T = \sup_t \operatorname{dom} x < \infty$ and $\operatorname{dom} x \cap (\{T\} \times \mathbb{Z}_{\geqslant 0})$ contains at least two points,*
- discrete *if nontrivial and $\operatorname{dom} x \subset (\{0\} \times \mathbb{Z}_{\geqslant 0})$,*
- eventually continuous *if $J = \sup_j \operatorname{dom} x < \infty$ and $\operatorname{dom} x \cap (\mathbb{R}_{\geqslant 0} \times \{J\})$ contains at least two points,*
- continuous *if nontrivial and $\operatorname{dom} x \subset (\mathbb{R}_{\geqslant 0} \times \{0\})$.*

□

2.3.3 Existence and completeness of solutions

In the previous section we have defined the notion of solution for the hybrid system with continuous-time inputs (2.72). In this section we present the conditions for the existence of maximal complete solutions to system (2.72). After that, we provide an additional result, which is an adaptation of [103, Lemma 5] in the context of hybrid systems with continuous-time inputs.

The next proposition is copied from [37, Proposition 6], which is an extension of the results in [31, Proposition 2.10] for systems with inputs. We will refer to this proposition in the thesis to prove the completeness of maximal solutions of the considered hybrid systems.

Proposition 2.7. *Consider system* (2.72). *There exists a nontrivial solution x to* (2.72) *for input $u \in \mathscr{L}_{\mathscr{U}}$ with $\xi := x(0,0) \in \mathbb{R}^{n_x}$ if and only if $\xi \in \mathscr{D}$ or*

(VC): there exists $\varepsilon > 0$ and an absolutely continuous function $z : [0, \varepsilon] \to \mathbb{R}^{n_x}$ such that $z(0) = \xi$, $\dot{z}(t) \in F(z(t), u(t)) \in \mathscr{C}$ for all $t \in (0, \varepsilon)$.

If the viability condition (VC) holds for all $\xi \in \mathscr{C}$ with $\xi \notin \mathscr{D}$, then, for all $u \in \mathscr{L}_{\mathscr{U}}$ every maximal solution x satisfies exactly one of the following properties:

(a) x is complete;

(b) x *is* not complete and "ends with flows"*: dom* x *is bounded and the interval* $I^J := \{t : (t,J) \in dom\, x\}$ *with* $J = \sup_j dom\, x$ *is open to the right, and does not exist an absolutely continuous function* $z : I^J \to \mathbb{R}^{n_x}$ *satisfying* $\dot{z}(t) \in F(z(t),u(t))$ *for almost all* $t \in I^J$ *and* $z(t) \notin \mathscr{C}$ *for all* $t \in intI^J$*, and such that* $z(t) = x(t,J)$ *for all* $t \in I^J$*;*

(c) x *is* not complete and "ends with a jump"*: dom* x *is bounded with* $(T,J) := \sup dom\, x \in dom\, x$*,* $I^J = T, x(T,J) \notin \mathscr{D}$ *and* $x(T,J) \notin \mathscr{C}$*.*

□

The first part of Proposition 2.7 presents the conditions to prove the existence of a nontrivial solution starting from ξ. Therefore it provides conditions to guarantee that the domain of the solution contains at least two points. This occurs if the initial condition ξ is in the jump set $\mathscr{D}$, and thus, a jump can occur, or if the solution can flow at least for an arbitrarly small amount of time ε. The second part of Proposition 2.7 describes the possible behaviours of the maximal solutions, that are, solutions whose domains cannot be further extended. In particular, this proposition is useful to prove that all maximal solutions to a hybrid system are complete, which means that their domains are unbounded, and thus they do not cease to exist. To this end, it is necessary to prove that items (b) and (c) cannot occur for the specific hybrid system in consideration. In particular, item (b) considers the case where the domain of a solution is bounded and ends with flow, in the sense that, there exists a time $t \in I^J$, where J is the discrete-time supremum of the domain of the solution, such that the solution is in the border of the flow set $\mathscr{C}$ and it is not in the jump set $\mathscr{D}$, and the flow map is pointing outside the flow set. As a result, the hybrid solution can neither flow or jump, and thus it is not complete since its domain is bounded. One the other hand, item (c) considers the case where there exists a solution whose domain is bounded and ends with a jump. This occurs when the hybrid solution jumps outside $\mathscr{C} \cup \mathscr{D}$, and thus it can neither flow or jump.

We now provide an additional result, which is an adaptation of [103, Lemma 5] to hybrid system with continuous-time inputs (2.72). The next Lemma is needed to prove the results in Chapter 5.

Lemma 2.1. *Consider system* (2.72) *with* $\mathscr{C}$ *closed. For any solution* q *with input* $u \in \mathscr{L}_{\mathscr{U}}$*, for any* $(t,j) \in dom\, q$ *with* $I^j := \{t : (t,j) \in dom\, q\}$ *non-empty,* $\frac{d}{dt}q(t,j) \in \{F(q(t,j),u(t))\} \cap T_{\mathscr{C}}(q(t,j))$ *holds for almost all* $t \in I^j$*.*

Proof. The proof follows similar lines as [103, proof of Lemma 5]. Let q be solution to (2.72) for input $u \in \mathscr{L}_{\mathscr{U}}$ and let $j \in \mathbb{Z}_{\geqslant 0}$ be such that $(t,j) \in \mathrm{dom}\, q$ and I^j is non-empty. Then, since q is a solution to (2.72) and the flow set $\mathscr{C}$ is closed, for all $t \in \mathrm{int}\, I^j$, $q(t,j) \in \mathscr{C}$. From [37, Definition 4], $\dfrac{d}{dt}q(t,j)$ exists and belongs to $\{F(q(t,j),u(t))\}$ for almost all $t \in I^j$. Hence, for almost all $t \in I^j$, for any sequence $\{\tau_i\}_{i \in \mathbb{Z}_{>0}}$ with $\tau_i > 0$, $\tau_i \to 0$ as $i \to \infty$, and $t + \tau_i \in I^j$,

$$\frac{d}{dt}q(t,j) = \lim_{i \to \infty} \frac{q(t+\tau_i,j) - q(t,j)}{\tau_i}. \tag{2.74}$$

From the Definition 2.3 and since $q(t+\tau_i) \in \mathscr{C}$ for any $i \in \mathbb{Z}_{>0}$ (as $t+\tau_i \in I^j$),

$$\lim_{i\to\infty} \frac{q(t+\tau_i, j) - q(t,j)}{\tau_i} \in T_{\mathscr{C}}(q(t,j)). \tag{2.75}$$

Hence, we have proved that

$$\frac{d}{dt}q(t,j) \in \{F(q(t,j),u(t))\} \cap T_{\mathscr{C}}(q(t,j)) \tag{2.76}$$

for all $j \in \mathbb{Z}_{\geqslant 0}$ and almost all $t \in I^j$. ■

2.3.4 Zeno phenomenon and dwell-time

As explained in Definition 2.10, a solution x to a hybrid dynamical system can be Zeno. This occurs when it is complete and $\sup_t \operatorname{dom} x < +\infty$, namely, when the continuous-time part of the hybrid time domain of the solution is finite. Note that this does not imply that the solution is discrete or eventually discrete. Indeed, the case where a solution exhibits an infinite number of jumps and, as j grows, the continuous-time interval between jumps is converges to zero, but it is not zero, and thus $\sup_t \operatorname{dom} x = \bar{t} < +\infty$, is a Zeno solution, which is not eventually discrete. Roughly speaking, a solution to an hybrid system is a Zeno solution when, after a certain hybrid time, either there is no continuous-time between any two consecutive jumps (eventually discrete case), or this continuous-time interval between two jumps is vanishing as j goes to $+\infty$. Zeno solutions that are not eventually discrete can be referred as *genuinely Zeno*, while complete and eventually discrete solutions can be denoted as *instantaneously Zeno*.

When designing a hybrid system, it is common to wish to exclude this possible Zeno behaviour, and thus design the hybrid system in such a way that none of its solutions is a Zeno solution. Indeed, it is often desired that the continuous-time evolution of the solutions is not bounded for physical implementation. In the thesis we will prove that the Zeno phenomenon is excluded for the two considered problems and we will explain why this is important for these specific estimation scenarios.

One option to rule out the Zeno phenomenon is to design an hybrid system for which any possible solution has a *dwell-time* or, at least, an *average dwell-time*, as defined next.

Definition 2.11. *A solution x to $\mathscr{H}$ for a given input $u \in \mathscr{L}_{\mathscr{U}}$ has a*

- dwell-time τ*, if, for any $(t,i),(s,j) \in \operatorname{dom} x$ with $t+s \leqslant i+j$, we have $j - i \leqslant \dfrac{s-t}{\tau} + 1$.*
- average dwell-time $\tau^\star$ *if, there exists $N_0 \in \mathbb{Z}_{>0}$ such that for any $(t',i'),(s',j') \in \operatorname{dom} x$, we have $j' - i' \leqslant \dfrac{s'-t'}{\tau^\star} + N_0$.*

In other words, given a solution x to $\mathscr{H}$ for a given input $u \in \mathscr{L}_{\mathscr{U}}$, we can define the jump times as $0 = t_0 \leqslant t_1 \leqslant \cdots \leqslant t_{j+1} = t$ satisfy $\operatorname{dom} q \cap ([0,t] \times \{0,1,\ldots,j\}) = \bigcup_{i=0}^{j} [t_i, t_{i+1}] \times \{i\}$. Then, Definition 2.11 implies that, if a solution x to an hybrid system has a dwell-time τ, then, $t_{i+1} - t_i \geqslant \tau$ for all $i \in \{1,2,\ldots,j\}$. Similarly, if $t_{i+1} - t_i \geqslant \tau$ holds only on average (not necessary

for all $i \in \{1,2,\dots,j\}$), namely, $t_{i+N_0} - t_i \geqslant \tau^\star N_0$ for all $i \in \{1,2,\dots,j-N_0\}$, then the solution x has an average dwell-time. Note that, the average dwell-time is a weaker property than the dwell-time, indeed a solution to a hybrid system that has a dwell-time property, guarantees also an average dwell-time property, where $N_0 = 1$, but the opposite is not necessary true. However, the average dwell-time property is enough to guarantee that the Zeno phenomenon is ruled out. Indeed, if a solution has an average dwell-time $\tau^\star$, then, it cannot produce an infinite number of jumps in a finite continuous-time interval.

2.3.5 Stability property

Stability properties are fundamental properties of dynamical systems, since they provide information about the solution behaviours and they guarantee that the trajectories converge to a specific attractor and do not diverge. In particular, as we have seen in Section 2.2.2, in an estimation problem, stability guarantees are useful to prove that the estimation error, namely the difference between the real state and the state estimate produced by the observer, is converging to the origin, or at least to its neighborhood.

In this section we formalize the stability property we will ensure for the hybrid systems in this thesis. In particular, we first define a global two-measure flow input-to-state stability property for system (2.72) and provide a Lyapunov characterization, which is useful to prove the property. After that, we consider a parameterized version of system (2.72) and we describe the concept of global practical two-measure flow input-to-state stability property, together with its Lyapunov characterization. More general stability definitions exist in the literature, but we focus only on a general enough definition to embed the stability results we will prove in the next chapters. The material in this section is inspired by [31, 104–106].

Definition 2.12. *System* (2.72) *is* uniformly globally two-measure flow input-to-state stable [2] *if there exist* $\beta \in \mathcal{KL}$, $\gamma \in \mathcal{K}_\infty$ *and two continuous functions* $\omega_i : \mathbb{R}^{n_x} \to \mathbb{R}_{\geqslant 0}$, $i \in \{1,2\}$, *such that, for any input* $u \in \mathcal{L}_{\mathcal{U}}$, *any corresponding solution* x *to* (2.72), *for all* $(t,j) \in \operatorname{dom} x$, *satisfies*

$$\omega_1(x(t,j)) \leqslant \beta(\omega_2(x(0,0)),t) + \gamma(\|u\|_{[0,t]}). \tag{2.77}$$

In addition, in case (2.77) *is satisfied with* $\omega_1(x) = \omega_2(x) = |x|_{\mathcal{A}}$, *for all* $x \in \mathbb{R}^{n_x}$, *where* $\mathcal{A} \subseteq \mathbb{R}^{n_x}$ *is a given closed set and* $|x|_{\mathcal{A}}$ *denotes the distance of* x *to the set* $\mathcal{A}$, *then, the set* $\mathcal{A}$ *is said to be* uniformly globally flow input-to-state stable. *Moreover, if* $u(t) = 0$ *for all* $t \in \mathbb{R}_{\geqslant 0}$, *then the set* $\mathcal{A}$ *is said to be* uniformly globally flow asymptotically stable *and if, in addition,* $\beta \in \mathcal{KL}$ *is exponential, then the set* $\mathcal{A}$ *is* uniformly globally flow exponentially stable. □

The next Lyapunov theorem can be used to establish the stability property stated in Definition 2.12.

2. To be precise, the property described in Definition 2.12 is a global two-measure flow pre-input-to-state stability property since (2.77) only holds on the solution domain, which may be bounded. However, we will not specify this in the stability properties we will prove in this thesis.

Theorem 2.1. *Consider system* (2.72). *Suppose there exists a Lyapunov function* $U : \mathbb{R}^{n_x} \to \mathbb{R}_{\geqslant 0}$ *continuously differentiable on an open set containing* $\mathscr{C}$, *and there exist* $\underline{\alpha}_U$, $\overline{\alpha}_U$, α_U, $\gamma_U \in \mathscr{K}_\infty$, *and two continuous functions* $\omega_i : \mathbb{R}^{n_x} \to \mathbb{R}_{\geqslant 0}$, $i \in \{1,2\}$ *such that the following properties hold.*

(i) For any $x \in \mathscr{C} \cup \mathscr{D}$,

$$\underline{\alpha}_U(\omega_1(x)) \leqslant U(q) \leqslant \overline{\alpha}_U(\omega_2(x)). \tag{2.78}$$

(ii) For any $x \in \mathscr{C}$ *and any* $u \in \mathscr{U}$,

$$\langle \nabla U(x), F(x,u) \rangle \leqslant -\alpha_U(U(x)) + \gamma_U(|u|). \tag{2.79}$$

(iii) For any $x \in \mathscr{D}$ *and any* $u \in \mathscr{U}$,

$$U(G(x,u)) \leqslant U(x). \tag{2.80}$$

Then, system (2.72) *is* uniformly globally two-measure flow input-to-state stable *in the sense of Definition 2.12.* □

The proof of Theorem 2.1 follows similar lines as in [31, 104] and is therefore omitted. Note that, Theorem 2.1 requires the existence of a continuously differentiable Lyapunov function U on an open set containing $\mathscr{C}$. However, in case the considered Lyapunov function candidate is not continuously differentiable, but only locally Lipschitz, the Clarke's generalized derivative, presented in Definition 2.2, can be used instead of the gradient in item *(ii)* and the results of Theorem 2.1 hold *mutatis mutandi*.

In the event-triggered part of this thesis (Chapters 3 and 4), due to the proposed event-triggering rule, the considered hybrid system is a parameterized hybrid system, where a design parameter $\varepsilon \in \mathbb{R}_{>0}$ influences the flow and jump sets. In general, in a parameterized hybrid system with continuous-time inputs, not only the sets, but also the flow and jump maps may depend on the design parameter $\varepsilon \in \mathbb{R}_{>0}$, as described next.

$$\mathscr{H} : \begin{cases} \dot{x} &= F_\varepsilon(x,u), & (x,u) \in \mathscr{C}_\varepsilon, \\ x^+ &\in G_\varepsilon(x,u), & (x,u) \in \mathscr{D}_\varepsilon. \end{cases} \tag{2.81}$$

In this case, the notion of stability depends also on the design parameter $\varepsilon \in \mathbb{R}_{>0}$ and the stability concept in Definition 2.12 can be generalized by a uniform global practical two-measure stability property, which is now defined.

Definition 2.13. *System* (2.81) *is* uniformly globally practically two-measure flow input-to-state stable *if there exist* $\beta \in \mathscr{KL}$, $\gamma_1, \gamma_2 \in \mathscr{K}_\infty$ *and two continuous functions* $\omega_i : \mathbb{R}^{n_x} \to \mathbb{R}_{\geqslant 0}$, $i \in \{1,2\}$, *such that, for any* $\upsilon > 0$ *there exists* $\varepsilon^\star \in \mathbb{R}_{>0}$ *such that, for all* $\varepsilon \in [0, \varepsilon^\star)$ *and any input* $u \in \mathscr{L}_\mathscr{U}$, *any corresponding solution* x *to* (2.81), *for all* $(t,j) \in \operatorname{dom} x$, *satisfies*

$$\omega_1(x(t,j)) \leqslant \beta(\omega_2(x(0,0)), t) + \gamma_1(\upsilon) + \gamma_2(\|u\|_{[0,t]}). \tag{2.82}$$

In addition, if (2.82) *is satisfied with* $\omega_1(x) = \omega_2(x) = |x|_{\mathscr{A}}$*, for all* $x \in \mathbb{R}^{n_x}$*, where* $\mathscr{A} \subseteq \mathbb{R}^{n_x}$ *is a given closed set, then, the set* $\mathscr{A}$ *is said to be* uniformly globally practically flow input-to-state stable. *Moreover, if* $u(t) = 0$ *for all* $t \in \mathbb{R}_{\geqslant 0}$*, then the set* $\mathscr{A}$ *is said to be* uniformly globally practically flow asymptotically stable *and if, in addition,* $\beta \in \mathscr{KL}$ *is exponential, then the set* $\mathscr{A}$ *is* uniformly globally practically flow exponentially stable. □

Similar to Theorem 2.1, Lyapunov conditions can be used to prove a global practical two-measure flow input-to-state stability property for system (2.81), as stated in the next theorem.

Theorem 2.2. *Consider system* (2.81). *Suppose there exists a Lyapunov function* $U : \mathbb{R}^{n_x} \to \mathbb{R}_{\geqslant 0}$ *continuously differentiable on an open set containing* $\mathscr{C}_\varepsilon$*, and there exist* $\underline{\alpha}_U$*,* $\overline{\alpha}_U$*,* α_U*,* $\gamma_U \in \mathscr{K}_\infty$*, and two continuous functions* $\omega_i : \mathbb{R}^{n_x} \to \mathbb{R}_{\geqslant 0}$*,* $i \in \{1,2\}$ *such that for any* $\upsilon > 0$ *there exist* $\varepsilon^\star \in \mathbb{R}_{>0}$ *such that, for all* $\varepsilon \in [0, \varepsilon^\star)$ *the following properties hold.*

(i) For any $x \in \mathscr{C}_\varepsilon \cup \mathscr{D}_\varepsilon$*,*

$$\underline{\alpha}_U(\omega_1(x)) \leqslant U(q) \leqslant \overline{\alpha}_U(\omega_2(x)). \tag{2.83}$$

(ii) For any $x \in \mathscr{C}_\varepsilon$ *and any* $u \in \mathscr{U}$*,*

$$\langle \nabla U(x), F_\varepsilon(x,u) \rangle \leqslant -\alpha_U(U(x)) + \upsilon + \gamma_U(|u|). \tag{2.84}$$

(iii) For any $x \in \mathscr{D}_\varepsilon$ *and any* $u \in \mathscr{U}$*,*

$$U(G_\varepsilon(x,u)) \leqslant U(x). \tag{2.85}$$

Then, system (2.81) *is* uniformly globally practically two-measure flow input-to-state stable *in the sense of Definition 2.13.* □

The proof of Theorem 2.2 can be obtained following similar steps as in [31,104] and thus we omit it. Note that, similar to Theorem 2.1, if the Lyapunov function candidate U is not continuosly differentiable in an open set containing $\mathscr{C}_\varepsilon$ we can we the Clarke's generalized derivative (see Definition 2.2) and the result presented in this theorem still holds.

2.4 Conclusions

In this chapter we have presented some preliminaries, which are used in the remaining of the thesis. In particular, first some mathematical definitions were given. After that, we have described the class of systems and observers considered in this thesis, together with the input-to-state stability property definition and Lyapunov characterization. We have also shown some examples of observer design techniques that will be considered in this manuscript. Finally, we have presented the hybrid system with continuous-time inputs framework we will use in this thesis, together with the needed notions of solutions, dwell-time and stability properties.

The concepts provided in this chapter form the basis and the starting point for the results we will present in the next chapters.

First part

Event-triggered estimation

Chapter 3

Event-triggered estimation of linear systems

Contents

Abstract - *We present an event-triggered observer design for linear time-invariant systems, where the measured output is sent to the observer only when a triggering condition is satisfied. We proceed by emulation and we first construct a continuous-time Luenberger observer. We then propose a dynamic rule to trigger transmissions, which only depends on the plant output and an auxiliary scalar state variable. The overall system is modeled as a hybrid system, for which a jump corresponds to an output transmission. We show that the proposed event-triggered observer guarantees global practical asymptotic stability for the estimation error dynamics. Moreover, under mild boundedness conditions on the plant state and its input, we prove that there exists a uniform strictly positive minimum inter-event time between any two consecutive transmissions, guaranteeing that the system does not exhibit Zeno solutions. Finally, the proposed approach is applied to a numerical case study of a lithium-ion battery, described by an electrical circuit equivalent model.*

The results of this chapter are based on [84], which is a preliminary version of [80], that considers a more general setting and will be presented in the next chapter.

3.1 Introduction

While digital networks exhibit a range of benefits for control applications in terms of ease of installation, maintenance and reduced weight and volume, they also require adapted control theoretical tools to cope with the induced communication constraints (e.g., sampling, delays, packet drops, scheduling, quantization), see e.g., [107, 108]. In this chapter, we concentrate on the state estimation of linear time-invariant systems over a digital channel and we focus on the effect of sampling. In particular, we consider state estimation where the plant is linear and communicates its measured output over a digital network to a remote observer, whose goal is to estimate the plant state. The transmission policy then has an impact on the convergence speed, the robustness of the estimator, as well as on the amount of communication resources required. An option is to generate the transmission instants based on time, in which case we talk of time-triggered strategies for which various results are available in the literature, see, e.g., [11, 12, 44–46]. However, this paradigm may generate (significantly) more transmissions over the network than necessary to fulfill the estimation task, thereby leading to a waste of the network resources. As a potential and promising solution, one can use event-triggered transmissions to overcome this drawback, see e.g., [109] and the references therein. In this case, an event-based triggering rule monitors the plant measurement and/or the observer state and decides when an output transmission is needed. In this way, it is possible to reduce the number of transmissions over the network, while still ensuring good estimation performance.

Various event-triggered techniques are available in the literature for estimation, see, e.g., [15–30]. Numerous papers propose to implement a copy of the observer within the sensor and then use its information to define the transmission instants, see e.g., [15–21]. A possible drawback with this technique is that it may require significant computation capabilities on the sensors, which may be unavailable, especially in the case of large-scale systems, or highly nonlinear dynamics. An alternative is offered by self-triggering policies, see e.g., [47, 48], where the observer requests a new output measurement when it needs it to perform the estimation. In this case, the plant output is not continuously monitored. Moreover, self-triggering rules typically generate more transmissions than event-triggered ones. Another solution is to follow an event-triggered strategy, which is only based on a static condition involving the measured output and its past transmitted value(s) see, e.g., [22–29]. Consequently, it is not necessary to implement a copy of the observer in the sensors and thus the sensors are not required to have significant computation capabilities. However, such static triggering rules may generate a lot of transmissions.

In this chapter, we adopt a dynamic event-triggered approach based only on the measured output and the last transmitted output value. This strategy keeps monitoring the plant output, and thereby may lead to less transmissions compared to a self-triggering approach. Moreover, it does not require a copy of the observer, which simplifies the implementation and requires less computation capability on the sensor. In particular, we present an event-triggered observer for deterministic linear time-invariant continuous-time systems, where the main novelty is the design of a new triggering rule, which involves an auxiliary scalar variable, that has several benefits as explained in the sequel. Our design consists in following an emulation-based approach in the sense that we first design a Luen-

berger observer for the continuous-time plant ignoring the packet based nature of communication network. Secondly, we take into account the latter and develop a triggering rule to approximately preserve the original properties of the observer. As already stated, we desire the triggering rule not to rely on a copy of the observer, which might be computational prohibitive. Instead, we only require the sensors to have enough computation resources to run a simple scalar linear filter. To be precise, the proposed policy is inspired by dynamic triggering rules used in the event-triggered control literature [49–52] and in [48], where self-triggered interval observers are designed. In particular, our strategy consists in filtering an absolute threshold strategy, as opposed to the relative threshold technique as done in the context of control in [49–51]. Indeed, the latter cannot be implemented for estimation, as we recall in Section 3.3.1, which motivates our choice. Also, we cover the absolute threshold strategy considered in [26–28] as a special case. Compared to [22–25], we do not consider a stochastic setting and discrete-time plants, but deterministic continuous-time systems, which raise the issue of potential Zeno phenomena. The triggering rule presented in this work aims to reduce the number of transmissions over the digital network, while still guaranteeing good estimation performance. We guarantee the existence of a strictly positive bound on the inter-event times as well as the absence of sampling when the output remains in a small neighborhood of a constant and therefore its information is not needed to the observer to obtain a good estimation, which is an advantage against time-triggered strategies. We show on an example that the addition of the scalar auxiliary variable can significantly reduce the number of transmissions compared to an absolute threshold rule, thereby providing a strong motivation for its use.

To analyze the proposed event-triggered observer, the overall plant-observer interconnection is modeled as a hybrid system using the formalism of [31], where a jump corresponds to an output transmission. We show that the estimation error system satisfies a global practical stability property. The latter is not asymptotic in general mostly because we do not implement a copy of the observer in the triggering mechanism. Moreover, the existence of a strictly positive minimum inter-event time is ensured under mild boundedness conditions on the plant state and its input. Finally, we apply the proposed approach in a numerical case study of a lithium-ion battery as mentioned above, for which the number of transmissions can be significantly reduced compared to an absolute threshold strategy, while still ensuring good estimation performance. Various event-triggered observer-based control strategies are available in the literature, such as e.g., [50, 110–112]. Nevertheless, these do not cover event-triggered estimation as a particular case, as significant technical difficulties arise, in particular in ruling out Zeno phenomenon, when the plant state is not required to converge towards a given attractor.

The chapter is organized as follows. The model and the problem statement are presented in Section 3.2. The proposed triggering rule is given in Section 3.3, where we model the system as a hybrid system. In Section 3.4, we analyze the obtained estimation error as well as the inter-event times. The numerical case study is reported in Section 3.5. Finally, Section 3.6 concludes the chapter.

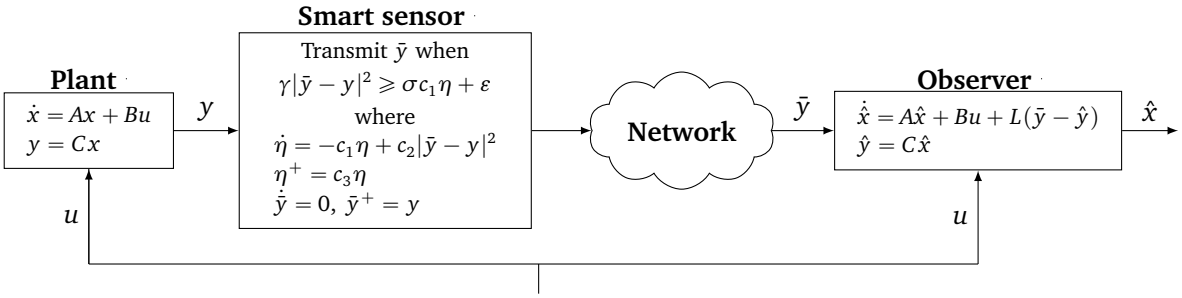

FIGURE 3.1 – Block diagram representing the system architecture.

3.2 Problem statement

Consider the linear system

$$\begin{aligned} \dot{x} &= Ax + Bu \\ y &= Cx, \end{aligned} \tag{3.1}$$

where $x \in \mathbb{R}^{n_x}$ is the state, $u \in \mathbb{R}^{n_u}$ is a known input, and $y \in \mathbb{R}^{n_y}$ is the measured output with n_x, $n_y \in \mathbb{Z}_{>0}$ and $n_u \in \mathbb{Z}_{\geqslant 0}$. The input u in (3.1) is such that $u \in \mathscr{L}_{\mathscr{U}}$ for some set $\mathscr{U} \subseteq \mathbb{R}^{n_u}$. The pair (A, C) is assumed to be detectable. Hence, by letting $L \in \mathbb{R}^{n_x \times n_y}$ be any matrix such that $A - LC$ is Hurwitz, we can design a Luenberger observer [113] of the form

$$\begin{aligned} \dot{\hat{x}} &= A\hat{x} + Bu + L(y - \hat{y}) \\ \hat{y} &= C\hat{x}, \end{aligned} \tag{3.2}$$

where $\hat{x} \in \mathbb{R}^{n_x}$ is the state estimate. Observer (3.2), when it has access to input u and measured output y continuously, guarantees that we are able to asymptotically reconstruct the state x of the plant, implying that $\lim_{t\to\infty}(x(t) - \hat{x}(t)) = 0$ for any initial condition to (3.1) and (3.2) and any input u. In this work, we investigate the scenario where the plant measurement y is transmitted to observer (3.2) via a digital channel, see Figure 3.1, and therefore only samples of y are available to the observer. Moreover, since the output is sent via a packet-based network, we want to sporadically transmit it, while still achieving good estimation properties. Therefore, our goal is to design a triggering rule to decide when y needs to be transmitted to observer (3.2), with the mentioned properties. We assume for this purpose that the sensor is “smart" in the sense that it can run a local one-dimensional dynamical system. We also adopt the following assumption.

Assumption 3.1. *The observer has access to the input u continuously.* □

Assumption 3.1 is a reasonable assumption in many control applications, such as, for example, when the control input is generated on the observer side. This assumption is relaxed in Section 4.6.3 in the next chapter, where a more general setting is considered.

In this setting, the observer does not know y but only its sampled version $\bar{y}$, which is generated with a zero-order-hold device between two successive transmission instants, i.e., in terms of the

hybrid systems notation of Chapter 2,

$$\dot{\bar{y}} = 0 \tag{3.3}$$

and, when a transmission occurs the output is sampled, considering an ideal sampler,

$$\bar{y}^+ = y. \tag{3.4}$$

The observer equations in (3.2) are then modified to become

$$\begin{aligned} \dot{\hat{x}} &= A\hat{x} + Bu + L(\bar{y} - \hat{y}) \\ \hat{y} &= C\hat{x}. \end{aligned} \tag{3.5}$$

Defining the sampling-induced error $e := \bar{y} - y$, we obtain

$$\dot{\hat{x}} = A\hat{x} + Bu + L(y - \hat{y} + e). \tag{3.6}$$

The sampling-induced error e dynamics between two successive transmission instants is, in view of (3.1) and (3.3),

$$\dot{e} = \dot{\bar{y}} - \dot{y} = -\dot{y} = -C\dot{x} = -CAx - CBu, \tag{3.7}$$

and, at each transmission instant we have

$$e^+ = 0, \tag{3.8}$$

in view of (3.4). Let $\xi := x - \hat{x} \in \mathbb{R}^{n_x}$ be the state estimation error. Its dynamics is, between two successive transmission instants, in view of (3.1) and (3.6),

$$\dot{\xi} = (A - LC)\xi - Le \tag{3.9}$$

and, at each transmission instant,

$$\xi^+ = \xi. \tag{3.10}$$

Our objective is to define a triggering rule, which ensures global practical asymptotic stability of estimation error dynamics and guarantees the existence of a positive minimum inter-event time between two consecutive transmissions.

Remark 3.1. *When the system output is of the form $y = Cx + Du + d$, where d is measured or is a known constant, we can generate a new output $z = Cx$ by using the knowledge of d, the measured output y and the input u, which is available thanks to Assumption 3.1. The system then becomes of the form of* (3.1) *again. We will exploit this observation in the example of Section 3.5.* □

3.3 Triggering rule and hybrid model

3.3.1 Relative threshold is not suitable for estimation

We first note that the general event-triggered control solutions for stabilization may not be (directly) used for the estimation problem at hand. We illustrate this with the relative threshold technique developed for control in [51] to define the triggering rule. To see this, note that since $A-LC$ is Hurwitz, we can define,

$$V(\xi) := \xi^\top P \xi, \quad \forall \xi \in \mathbb{R}^{n_x}, \tag{3.11}$$

where $P \in \mathbb{R}^{n_x \times n_x}$ is symmetric, positive definite and verifies $(A-LC)^\top P + P(A-LC) = -Q$ for some $Q \in \mathbb{R}^{n_x \times n_x}$ symmetric and positive definite. Then, for any $\xi \in \mathbb{R}^{n_x}$ and $e \in \mathbb{R}^{n_y}$,

$$\langle \nabla V(\xi), (A-LC)\xi - Le \rangle \leqslant -\alpha V(\xi) + \gamma |e|^2, \tag{3.12}$$

where $\alpha := \dfrac{\lambda_{\min}(Q)}{\lambda_{\max}(P)}(1-c) > 0$, $\gamma := \dfrac{\|PL\|^2}{c\lambda_{\min}(Q)} > 0$ and $c \in (0,1)$ a design parameter. We might then be tempted, in line with the design philosophy of [51], to define the triggering rule as

$$\gamma |e|^2 \leqslant \varsigma \alpha V(\xi), \tag{3.13}$$

with $\varsigma \in (0,1)$, which implies

$$\langle \nabla V(\xi), (A-LC)\xi - Le \rangle \leqslant -(1-\varsigma)\alpha V(\xi) \tag{3.14}$$

and thus that V strictly decreases along the solutions to (3.9). However, (3.13) cannot be implemented because the estimation error ξ is not available for the triggering rule, as it depends on the unknown state x and on the state estimate $\hat{x}$.

3.3.2 Dynamic triggering rule

To overcome the issue presented in Section 3.3.1, we introduce a scalar auxiliary variable η, whose equations during flows and jumps are

$$\begin{aligned} \dot{\eta} &= -c_1 \eta + c_2 |e|^2, \\ \eta^+ &= c_3 \eta, \end{aligned} \tag{3.15}$$

where $c_1 > 0$, $c_2 \geqslant 0$ and $c_3 \in [0,1]$ are design parameters, that will be selected later according to Theorem 3.1.

Remark 3.2. *The choice of the dynamics* (3.15) *is inspired by norm-estimators [101]. Indeed, if* c_1 *and* c_2 *are selected such that* $c_1 = \alpha$ *and* $c_2 = \gamma$, η *in* (3.15) *is a norm-estimator, according to [101, Definition 2.4], but this particular choice of* c_1 *and* c_2 *is not necessary for the proposed triggering rule.* □

By collecting all the equations, we obtain the hybrid model

$$\left.\begin{aligned}\dot{x} &= Ax + Bu\\ \dot{\xi} &= (A - LC)\xi - Le\\ \dot{e} &= -CAx - CBu\\ \dot{\eta} &= -c_1\eta + c_2|e|^2\end{aligned}\right\} \quad (x,\xi,e,\eta) \in \mathscr{C}, \tag{3.16a}$$

$$\left.\begin{aligned}x^+ &= x\\ \xi^+ &= \xi\\ e^+ &= 0\\ \eta^+ &= c_3\eta\end{aligned}\right\} \quad (x,\xi,e,\eta) \in \mathscr{D}, \tag{3.16b}$$

for which a jump corresponds to a transmission of the current value of y to the observer. The triggering rule is implemented through the flow and jump sets, $\mathscr{C}$ and $\mathscr{D}$, which are defined as

$$\mathscr{C} := \left\{q \in \mathbb{R}^{n_q} : \gamma|e|^2 \leqslant \sigma c_1\eta + \varepsilon, \eta \geqslant 0\right\} \tag{3.17a}$$

$$\mathscr{D} := \left\{q \in \mathbb{R}^{n_q} : \gamma|e|^2 \geqslant \sigma c_1\eta + \varepsilon, \eta \geqslant 0\right\}, \tag{3.17b}$$

where q is the overall state, defined as $q := (x,\xi,e,\eta) \in \mathbb{R}^{n_q} = \mathbb{R}^{n_x} \times \mathbb{R}^{n_x} \times \mathbb{R}^{n_y} \times \mathbb{R}$, with $n_q := 2n_x + n_y + 1$. Constant γ in (3.17) comes from (3.12), $\sigma \geqslant 0$ is a design parameter and ε is a strictly positive constant needed to avoid the Zeno phenomenon [3]. Indeed, we will prove in the sequel that there exists a minimum inter-event time between two consecutive jumps under mild extra conditions whenever $\varepsilon > 0$. Sets $\mathscr{C}$ and $\mathscr{D}$ in (3.17a)-(3.17b) essentially mean that a transmission is triggered whenever $\gamma|e|^2 \geqslant \sigma c_1\eta + \varepsilon$, see Figure 3.1. The condition that $\eta \geqslant 0$ in (3.17) never generates a transmission as it is always true whenever η is initialized with a non-negative value. It is thus only specified in (3.17) to emphasize that η only takes non-negative values. It is worth noting that, when $\sigma = 0$, the triggering rule proposed in (3.17) corresponds to an absolute threshold triggering rule, as in, e.g., [26–28].

For the sake of convenience we write system (3.16)-(3.17) as

$$\begin{aligned}\dot{q} &= F(q,u), \quad q \in \mathscr{C}\\ q^+ &= G(q), \quad\;\; q \in \mathscr{D}.\end{aligned} \tag{3.18}$$

We are ready to proceed with the analysis of system (3.18).

3. A definition of the Zeno phenomenon is given in Section 2.3.4.

3.4 Main result

3.4.1 Stability

The next theorem explains how to select the design parameters c_1, c_2, c_3 and σ in (3.18) in order to guarantee that the observer (3.2) is able to globally practically estimate the state x of system (3.1) in the configuration explained in Section 3.2, in which the measured outputs are not available at all times but only when the triggering rule enables transmissions.

Theorem 3.1 (Global practical stability property)**.** *Consider system* (3.18)*, for any* $\bar{\alpha} \in (0, \alpha]$*, where* α *comes from* (3.12)*, and any* $\nu > 0$*, select* c_1*,* c_2*,* c_3*,* σ *and* ε *as follows.*

(i) $c_2 \in [0, c_2^\star]$ *and* $\sigma \in [0, \sigma^\star]$*, where* $c_2^\star \geqslant 0$ *and* $\sigma^\star > 0$ *are such that* $\sigma^\star c_2^\star < \gamma$*, where* γ *comes from* (3.12)*.*

(ii) $c_1 \geqslant c_1^\star$*, where* $c_1^\star > 0$ *is such that* $c_1^\star > \bar{\alpha}\Big(1 - \dfrac{\sigma^\star c_2^\star}{\gamma}\Big)^{-1}$*.*

(iii) $c_3 \in [0, 1]$*.*

(iv) $\varepsilon \in (0, \varepsilon^\star]$*, where* $\varepsilon^\star = \nu\bar{\alpha}\gamma(\gamma + c_2^\star d)^{-1}$ *with* $d := \sigma^\star\Big(1 - \dfrac{\sigma^\star c_2^\star}{\gamma} - \dfrac{\bar{\alpha}}{c_1^\star}\Big)^{-1} > 0$*.*

Then, for any input $u \in \mathscr{L}_{\mathscr{U}}$*, any solution* q *satisfies, for all* $(t, j) \in \operatorname{dom} q$*,*

$$V(\xi(t,j)) + d\eta(t,j) \leqslant e^{-\bar{\alpha}t}(V(\xi(0,0)) + d\eta(0,0)) + \nu, \tag{3.19}$$

with V *defined in* (3.11)*.* □

Proof. Let all conditions of Theorem 3.1 hold. We consider the Lyapunov function candidate

$$U(q) = V(\xi) + d\eta, \tag{3.20}$$

for any $q \in \mathbb{R}^{n_q}$, where V is defined in (3.11) and d is defined in item (*iv*) of Theorem 3.1; note that $d > 0$ in view of items (*i*) and (*ii*) of Theorem 3.1.

We first show that the function U is positive definite and radially unbounded, i.e., there exist $\underline{\alpha}_U, \overline{\alpha}_U \in \mathscr{K}_\infty$ such that

$$\underline{\alpha}_U(|(\xi,\eta)|) \leqslant U(q) \leqslant \overline{\alpha}_U(|(\xi,\eta)|), \tag{3.21}$$

for any $q \in \mathbb{R}^{n_q}$. For this purpose, recall that $V(\xi) = \xi^\top P \xi$ with P is symmetric and positive definite, which implies

$$\lambda_{\min}(P)|\xi|^2 \leqslant V(\xi) \leqslant \lambda_{\max}(P)|\xi|^2. \tag{3.22}$$

As a result, using the definition of U and recalling that $d > 0$ and $\eta \geqslant 0$, we obtain

$$\lambda_{\min}(P)|\xi|^2 + d\eta \leqslant U(q) \leqslant \lambda_{\max}(P)|\xi|^2 + d\eta. \tag{3.23}$$

We first prove the upper-bound in (3.21). Since $|\xi| \leqslant |(\xi,\eta)|$ and $\eta \leqslant |(\xi,\eta)|$, we have

$$\begin{aligned} U(q) &\leqslant \lambda_{\max}(P)|\xi|^2 + d\eta \\ &\leqslant \lambda_{\max}(P)|(\xi,\eta)|^2 + d|(\xi,\eta)| \\ &=: \overline{\alpha}_U(|(\xi,\eta)|), \end{aligned} \tag{3.24}$$

where $\overline{\alpha}_U(s) := \lambda_{\max}(P)s^2 + ds$, for all $s \geqslant 0$. On the other hand, by applying [114, Lemma 4], and recalling that $|\xi| + \eta \geqslant |(\xi,\eta)|$, we have

$$\begin{aligned} U(q) &\geqslant \lambda_{\min}(P)|\xi|^2 + d\eta \\ &\geqslant \underline{\alpha}_U(|\xi| + \eta) \\ &=: \underline{\alpha}_U(|(\xi,\eta)|), \end{aligned} \tag{3.25}$$

where $\underline{\alpha}_U(s) := \min\left(\frac{\lambda_{\min}(P)|s|^2}{2}, \frac{ds}{2}\right)$, for all $s \geqslant 0$.

Let $q \in \mathscr{C}$ and $u \in \mathscr{U}$, in view of (3.12) and (3.16),

$$\begin{aligned} \langle \nabla U(q), F(q,u)\rangle &= \langle \nabla V(\xi), (A-LC)\xi - Le\rangle + d(-c_1\eta + c_2|e|^2) \\ &\leqslant -\alpha V(\xi) + \gamma|e|^2 + d(-c_1\eta + c_2|e|^2) \\ &= -\alpha V(\xi) - c_1 d\eta + (\gamma + c_2 d)|e|^2. \end{aligned} \tag{3.26}$$

Since $q \in \mathscr{C}$, we have $\gamma|e|^2 \leqslant \sigma c_1\eta + \varepsilon$, which is equivalent to $|e|^2 \leqslant \frac{\sigma c_1}{\gamma}\eta + \frac{\varepsilon}{\gamma}$ as $\gamma > 0$. Hence, the next inequalities hold

$$\begin{aligned} \langle \nabla U(q), F(q,u)\rangle &\leqslant -\alpha V(\xi) - c_1 d\eta + (\gamma + c_2 d)\left(\frac{\sigma c_1}{\gamma}\eta + \frac{\varepsilon}{\gamma}\right) \\ &= -\alpha V(\xi) - c_1 d\eta + (\gamma + c_2 d)\frac{\sigma c_1}{\gamma}\eta + \frac{1}{\gamma}(\gamma + c_2 d)\varepsilon \\ &= -\alpha V(\xi) - c_1\left(1 - \frac{\sigma}{d} - \frac{\sigma}{\gamma}c_2\right)d\eta + \frac{1}{\gamma}(\gamma + c_2 d)\varepsilon \\ &\leqslant -\min\left\{\alpha, c_1\left(1 - \frac{\sigma}{d} - \frac{\sigma}{\gamma}c_2\right)\right\}U(z) + \frac{1}{\gamma}(\gamma + c_2 d)\varepsilon. \end{aligned} \tag{3.27}$$

Due to the choice of parameters c_1, c_2 and σ, we have that (3.27) implies

$$\langle \nabla U(q), F(q,u)\rangle \leqslant -\bar{\alpha}U(q) + \frac{1}{\gamma}(\gamma + c_2 d)\varepsilon. \tag{3.28}$$

Indeed, when $\min\left\{\alpha, c_1\left(1 - \frac{\sigma}{d} - \frac{\sigma}{\gamma}c_2\right)\right\} = \alpha$, then $-\min\left\{\alpha, c_1\left(1 - \frac{\sigma}{d} - \frac{\sigma}{\gamma}c_2\right)\right\} = -\alpha \leqslant -\bar{\alpha}$. Conversely, when $\min\left\{\alpha, c_1\left(1 - \frac{\sigma}{d} - \frac{\sigma}{\gamma}c_2\right)\right\} = c_1\left(1 - \frac{\sigma}{d} - \frac{\sigma}{\gamma}c_2\right)$, which is strictly positive due

to the definition of d in item (*iv*) of Theorem 3.1, σ and c_2, we have

$$\begin{aligned} -c_1\Big(1-\frac{\sigma}{d}-\frac{\sigma}{\gamma}c_2\Big) &\leqslant -c_1^\star\Big(1-\frac{\sigma}{d}-\frac{\sigma}{\gamma}c_2\Big) \\ &\leqslant -c_1^\star\Big(1-\frac{\sigma^\star}{d}-\frac{\sigma^\star}{\gamma}c_2^\star\Big) \end{aligned} \tag{3.29}$$

and since $d=\sigma^\star\Big(1-\dfrac{\sigma^\star c_2^\star}{\gamma}-\dfrac{\bar\alpha}{c_1^\star}\Big)^{-1}$, we obtain

$$-c_1\Big(1-\frac{\sigma}{d}-\frac{\sigma}{\gamma}c_2\Big) \leqslant -c_1^\star\Big(1-\frac{\sigma^\star}{d}-\frac{\sigma^\star}{\gamma}c_2^\star\Big) = -\bar\alpha. \tag{3.30}$$

Hence, (3.28) holds and since $\varepsilon \leqslant \varepsilon^\star = \nu\bar\alpha\gamma(\gamma+c_2^\star d)^{-1}$ and $c_2 \leqslant c_2^\star$,

$$\begin{aligned} \langle \nabla U(q), F(q,u)\rangle &\leqslant -\bar\alpha U(q) + \frac{1}{\gamma}(\gamma + c_2 d)\varepsilon \\ &\leqslant -\bar\alpha U(q) + \frac{1}{\gamma}(\gamma + c_2^\star d)\varepsilon^\star \\ &= -\bar\alpha U(q) + \bar\alpha\,\nu. \end{aligned} \tag{3.31}$$

Let q in $\mathscr{D}$, in view of (3.16) and since $c_3 \in [0,1]$,

$$U(G(q)) = V(\xi) + dc_3\eta \leqslant V(\xi) + d\eta = U(q). \tag{3.32}$$

We now follow similar steps as in [31, proof of Theorem 3.18] to show that (3.19) holds. Let $u \in \mathscr{L}_{\mathscr{U}}$ and q be a solution to system (3.18). Pick any $(t,j) \in \operatorname{dom} q$ and let $0 = t_0 \leqslant t_1 \leqslant \cdots \leqslant t_{j+1} = t$ satisfy $\operatorname{dom} q \cap ([0,t]\times\{0,1,\ldots,j\}) = \bigcup_{i=0}^{j}[t_i, t_{i+1}]\times\{i\}$. For each $i \in \{0,\ldots,j\}$ and almost all $s \in [t_i, t_{i+1}]$, $q(s,i) \in \mathscr{C}$. Then, (3.31) implies that, for each $i \in \{0,\ldots,j\}$ and for almost all $s \in [t_i, t_{i+1}]$,

$$\frac{d}{ds}U(q(s,i)) \leqslant -\bar\alpha U(q(s,i)) + \bar\alpha\,\nu. \tag{3.33}$$

Applying the comparison principle [85, Lemma 3.4], we obtain, for all $(s,i) \in \operatorname{dom} q$,

$$\begin{aligned} U(q(s,i)) &\leqslant e^{-\bar\alpha(s-t_i)}U(q(t_i,i)) + \bar\alpha\,\nu\int_{t_i}^{s} e^{-\bar\alpha(s-\tau)}d\tau \\ &= e^{-\bar\alpha(s-t_i)}U(q(t_i,i)) + \bar\alpha\,\nu\frac{1}{\bar\alpha}[1-e^{-\bar\alpha(s-t_i)}]. \end{aligned} \tag{3.34}$$

Thus,

$$U(q(t_{i+1},i)) \leqslant e^{-\bar\alpha(t_{i+1}-t_i)}U(q(t_i,i)) + \nu - \nu e^{-\bar\alpha(t_{i+1}-t_i)} \tag{3.35}$$

for all $i \in \{0,\dots,j\}$. Similarly, for each $i \in \{1,\dots,j\}$, $q(t_i, i-1) \in \mathscr{D}$. From (3.32), we obtain

$$U(q(t_i,i)) - U(q(t_i,i-1)) \leqslant 0 \quad \forall i \in \{1,\dots,j\}. \tag{3.36}$$

From (3.34), (3.35) and (3.36), we can deduce that for any $(t,j) \in \operatorname{dom} q$,

$$\begin{aligned} U(q(t,j)) &\leqslant e^{-\bar{\alpha}t} U(q(0,0)) + \nu - \nu e^{-\bar{\alpha}t} \\ &\leqslant e^{-\bar{\alpha}t} U(q(0,0)) + \nu. \end{aligned} \tag{3.37}$$

On the other hand, from (3.20), we have

$$\begin{aligned} U(q(t,j)) &\leqslant e^{-\bar{\alpha}t} U(q(0,0)) + \nu \\ &= e^{-\bar{\alpha}t} [V(\xi(0,0)) + d\eta(0,0))] + \nu, \end{aligned} \tag{3.38}$$

which concludes the proof as $U(q(t,j)) = V(\xi(t,j)) + d\eta(t,j)$. ■

It is important to note that, in absence of a digital network between the plant and the observer (i.e., when $e = 0$), we have from (3.12) that for any solution ξ to $\dot{\xi} = (A - LC)\xi$,

$$V(\xi(t)) \leqslant e^{-\alpha t} V(\xi(0)) \tag{3.39}$$

for all $t \geqslant 0$. In view of (3.19), and as $d > 0$, for any solution q to (3.18) with input $u \in \mathscr{L}_{\mathscr{U}}$, since η takes non-negative values in view of (3.17a)-(3.17b),

$$V(\xi(t,j)) \leqslant e^{-\bar{\alpha}t} (V(\xi(0,0)) + d\eta(0,0)) + \nu. \tag{3.40}$$

Hence, we guarantee a convergence rate $\bar{\alpha} \in (0, \alpha]$ of V along the ξ-component of the solution to (3.18), which can be equal to α. We also have ν in (3.19), which is an ultimate bound of the estimation error, that is tuneable and can thus be made arbitrarily small (by selecting ε small mainly) irrespective of the chosen convergence rate at the price of more frequent transmissions in general. Property (3.19) also ensures that the auxiliary variable η is bounded and converges to a neighborhood of the origin.

In Theorem 3.1, we first fix a convergence rate $\bar{\alpha}$ and a guaranteed ultimate bound ν for $V(\xi) + d\eta$, and then we explain how to select the design parameters to accomplish this. It is worth noting that the conditions of Theorem 3.1 can be always ensured. Indeed, we just have to select $\sigma^\star$ and $c_2^\star$ sufficiently small such that $\sigma^\star c_2^\star < \gamma$, which is always possible, and all the other parameters can be always selected such that items (ii)-(iv) of Theorem 3.1 are verified as well. Another way to use the result of Theorem 3.1 is to select σ and c_2 such that $\sigma c_2 < \gamma$ holds. Then, by selecting $c_3 \in [0,1]$ and any strictly positive value for c_1 and ε, (3.19) holds for some strictly positive $\bar{\alpha}$ and ν. This is how we select parameters in the example in Section 3.5.

3.4.2 Properties of the inter-event times

In this section we provide properties of the inter-event times. In particular, we first show the existence of a strictly positive minimum inter-event time between two consecutive transmissions under mild boundedness conditions on plant (3.1). This corresponds to the existence of a dwell-time for the solutions to (3.18), as defined in [31] and recalled in Section 2.3.4, see, e.g., [115], [103]. From the definitions of $\mathscr{C}$ and $\mathscr{D}$ in (3.17a) and (3.17b), the inter-event time is lower bounded by the time that it takes for $|e|^2$ to grow from 0, that is the $|e|^2$ value after a jump according to (3.16), to $\frac{\varepsilon}{\gamma}$. A proof that this time is bounded from below by a positive constant can be obtained by establishing that the time-derivative of $|e|^2$ is bounded. For this purpose, recalling that, from (3.16) we have $\dot{e} = -CAx - CBu$, we define the following set

$$\mathscr{S}_\rho = \{(q,u) \in \mathbb{R}^{n_q} \times \mathscr{U} : |CAx + CBu| \leqslant \rho\}, \tag{3.41}$$

where ρ is an arbitrarily large positive constant. We restrict the flow and the jump sets of system (3.18) so that

$$\begin{aligned} \dot{q} &= F(q,u), \quad (q,u) \in \mathscr{C}_\rho := (\mathscr{C} \times \mathscr{U}) \cap \mathscr{S}_\rho \\ q^+ &= G(q), \qquad (q,u) \in \mathscr{D}_\rho := (\mathscr{D} \times \mathscr{U}) \cap \mathscr{S}_\rho. \end{aligned} \tag{3.42}$$

By doing so, we therefore only consider solutions to (3.18) such that the derivative of e is bounded. Hence, (3.19) still applies. Note that (3.41) is verified for all hybrid times when the state x and the input u are known to lie in a compact set for all positive times and the constant ρ is selected sufficiently large for instance. It is important to notice that the constraint (3.41) does not need to be implemented in the triggering rule: it is only used here for analysis purposes.

In the next theorem we prove that there exists a positive minimum inter-event time between any two consecutive transmissions for solutions to system (3.42).

Theorem 3.2 (Minimum inter-event time)**.** *Consider system* (3.42)*, then for any input $u \in \mathscr{L}_\mathscr{U}$, any solution q has a dwell-time $\tau := \frac{1}{2\rho}\sqrt{\frac{\varepsilon}{\gamma}}$, i.e., for any $(s,i),(t,j) \in \operatorname{dom} q$ with $s + i \leqslant t + j$, we have $j - i \leqslant \frac{t-s}{\tau} + 1$.* □

Proof. Let $u \in \mathscr{L}_\mathscr{U}$ and q be a solution to system (3.42). Pick any $(t,j) \in \operatorname{dom} q$ and let $0 = t_0 \leqslant t_1 \leqslant \cdots \leqslant t_{j+1} = t$ satisfy $\operatorname{dom} q \cap ([0,t] \times \{0,1,\ldots,j\}) = \bigcup_{i=0}^{j} [t_i, t_{i+1}] \times \{i\}$. For each $i \in$

$\{0,\dots,j\}$ and almost all $s \in [t_i, t_{i+1}]$, $(q(s,i),u(s,i)) \in \mathscr{C}_\rho$. Then, from (3.16) for all $s \in [t_i, t_{i+1}]$,

$$\begin{aligned}\frac{d}{ds}|e|^2 &= \frac{d}{ds}(e^\top e)\\ &= (\dot{e}^\top e + e^\top \dot{e})\\ &= (-CAx - CBu)^\top e + e^\top(-CAx - CBu)\\ &= -2e^\top(CAx + CBu)\\ &\leqslant 2|e||CAx + CBu|.\end{aligned} \tag{3.43}$$

Since $(q(s,i),u(s,i)) \in \mathscr{C}_\rho = (\mathscr{C} \times \mathscr{U}) \cap \mathscr{S}_\rho$, in view of (3.41),

$$\frac{d}{ds}|e|^2 \leqslant 2|e|\rho. \tag{3.44}$$

Let $t_i' := \inf\left\{t \geqslant t_i : |e(t,i)| = \sqrt{\frac{\varepsilon}{\gamma}}\right\}$, hence $t_i' \leqslant t_{i+1}$ in view of (3.17b). For almost all $s \in [t_i, t_i']$, from (3.44), we have

$$\frac{d}{ds}|e|^2 \leqslant 2\sqrt{\frac{\varepsilon}{\gamma}}\rho. \tag{3.45}$$

Integrating this equation and applying the comparison principle [85, Lemma 3.4], we obtain, for all $s \in [t_i, t_i']$

$$|e(s,i)|^2 \leqslant |e(t_i,i)|^2 + 2\sqrt{\frac{\varepsilon}{\gamma}}\rho(s - t_i). \tag{3.46}$$

Moreover, since $e(t_i,i) = 0$, we obtain

$$|e(s,i)|^2 \leqslant 2\sqrt{\frac{\varepsilon}{\gamma}}\rho(s - t_i) \quad \forall s \in [t_i, t_i']. \tag{3.47}$$

In view of (3.47), $s \mapsto 2\sqrt{\frac{\varepsilon}{\gamma}}\rho(s - t_i)$ upper bounds $s \mapsto |e(s,i)|^2$ on $[t_i, t_i']$. Hence, the time it takes for $s \mapsto 2\sqrt{\frac{\varepsilon}{\gamma}}\rho(s - t_i)$ to grow from 0 to $\frac{\varepsilon}{\gamma}$ is a lower bound on $t_i' - t_i \leqslant t_{i+1} - t_i$. Therefore, the solution q with input u has a dwell-time $\tau = \frac{1}{2\rho}\sqrt{\frac{\varepsilon}{\gamma}}$. ■

From Theorem 3.2, we see that the guaranteed minimum inter-event time τ grows when ρ decreases or when ε increases, which corresponds to an increase of the ultimate bound ν, as shown in Theorem 3.1. Note that, because of (3.19), the η and the ξ components of the solutions to system (3.42) cannot blow up in finite continuous time. In addition, if the constraint on the state x and the input u in (3.41) is satisfied for all continuous time $t \geqslant 0$, then we can ensure the t-completeness of maximal solutions to system (3.42), see [31, Definition 2.5]. As the conditions on x and u are assumptions on the original system (3.1), and not part of our design, we can indeed establish that t-completeness of maximal solutions to (3.42) is guaranteed, under appropriate assumptions on the initial states of η and ξ, and thus a positive lower bounded on the inter-event times is guaranteed.

Although this already sketches the main arguments, a complete and formal proof will be given in Chapter 4, where a more general setting is considered.

An additional feature of the proposed triggering rule is that it stops transmitting when the sampling-induced error $|e|$ becomes small enough, as formalized in the next lemma.

Lemma 3.1 (Stop transmissions)**.** *Consider system* (3.18)*, given a solution q with input $u \in \mathscr{L}_{\mathscr{U}}$, if there exists $(t,j) \in \operatorname{dom} q$ such that $|e(t',j')| < \sqrt{\frac{\varepsilon}{\gamma}}$ for all $(t',j') \in \operatorname{dom} q$ with $t'+j' \geqslant t+j$, then* $\sup_j \operatorname{dom} q = j' < \infty$. □

Proof. The condition $|e(t',j')| < \sqrt{\frac{\varepsilon}{\gamma}}$ for all $(t',j') \in \operatorname{dom} q$ with $t'+j' \geqslant t+j$ implies $\gamma|e(t',j')|^2 < \gamma\frac{\varepsilon}{\gamma} \leqslant \sigma c_1 \eta + \varepsilon$ for all $(t',j') \geqslant (t,j)$. Thus, the triggering condition is never triggered after (t,j), hence no jumps occur after (t,j) and $j' = j$ consequently. Therefore $\sup_j \operatorname{dom} q = j' < \infty$, which concludes the proof. ■

The condition on $|e|$ in Lemma 3.1 occurs when the plant output y remains for all positive times in a small neighborhood of a constant for instance. Indeed, when the output to plant (3.1) satisfies $|y(t) - y^\star| < \frac{1}{2}\sqrt{\frac{\varepsilon}{\gamma}}$ for all $t \geqslant T$ for some $T \geqslant 0$ and some constant $y^\star \in \mathbb{R}^{n_y}$, we have for any solution q to system (3.42) with input $u \in \mathscr{L}_{\mathscr{U}}$, for any $(t_j, j), (t,j) \in \operatorname{dom} q$ with $(t_j, j-1) \in \operatorname{dom} q$ and $t_j \geqslant T$, $t \geqslant t_j$ and $|e(t,j)| = |y(t_j,j) - y(t,j)| = |y(t_j,j) - y^\star + y^\star - y(t,j)| \leqslant |y(t_j,j) - y^\star| + |y^\star - y(t,j)| < 2\frac{1}{2}\sqrt{\frac{\varepsilon}{\gamma}}$ and the condition of Lemma 3.1 holds. Moreover, it automatically starts transmitting again if that condition is no longer verified. This is a clear advantage over time-triggered strategies, where the measured output is always transmitted, which may be important in practical applications. The above condition of y of Lemma 3.1 is verified, for example, when the plant is asymptotically stable and the input u is constant, see also the example in the next section. Note that Lemma 3.1 applies to system (3.18), and not only to system (3.42).

3.5 Numerical case study

We apply the proposed event-triggered observer to a lithium-ion battery example [116]. This can be relevant when the battery management system is not co-located with the battery and communicates with it via a digital network. The considered electrical equivalent circuit of the battery cell is shown in Figure 3.2. From the circuit, the following system model is derived

$$\begin{aligned} \dot{U}_{RC} &= -\frac{1}{\tau}U_{RC} + \frac{1}{C}i_{bat} \\ \dot{SOC} &= -\frac{1}{Q}i_{bat} \\ V_{bat} &= -U_{RC} + \alpha_f SOC + \beta_f - R_{int} i_{bat}. \end{aligned} \tag{3.48}$$

The states $U_{RC} \in \mathbb{R}$ and $SOC \in \mathbb{R}$ are the voltage on the RC circuit and the battery state of charge, respectively. The input $i_{bat} \in \mathbb{R}$ is the battery current and the output $V_{bat} \in \mathbb{R}$ is the battery voltage.

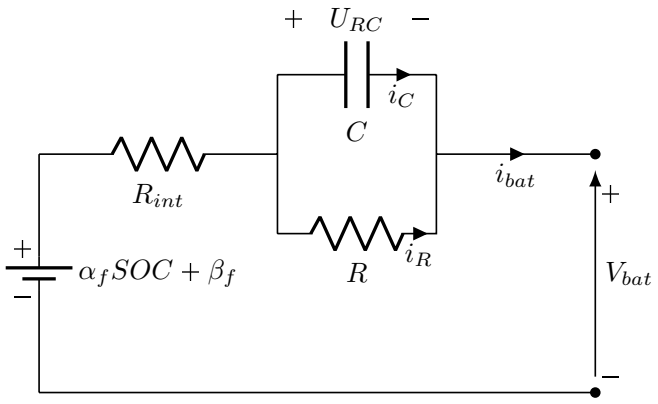

FIGURE 3.2 – Equivalent electrical circuit of a single battery cell.

Considering the temperature to be constant and equal to 25 °C, the following values are taken $\tau = 7$ s, $C = 2.33 \cdot 10^4$ F, $Q = 25$ Ah, $R_{int} = 4$ mΩ, $\alpha_f = 0.6$ and $\beta_f = 3.4$, which have been derived from experimental data. We design observer (3.2) with $L = [0.64, 2.33]$. As a result, (3.12) holds with $P = \begin{bmatrix} 1.57 \cdot 10^4 & -3.39 \cdot 10^3 \\ -3.39 \cdot 10^3 & 1.29 \cdot 10^3 \end{bmatrix}$, $Q = \begin{bmatrix} 100 & 0 \\ 0 & 1000 \end{bmatrix}$, $\alpha = 0.003$ and $\gamma = 1.104 \cdot 10^5$.

From (3.48), we see that the system output has a feedthrough term, indeed, the output equation has the following structure $y = Cx + Du + \beta_f$. However, since the observer has access to the input $u = i_{bat}$ continuously thanks to Assumption 3.1 and β_f is known, we can rewrite the output equation as $z = Cx$, as explained in Remark 3.1.

We have first simulated the event-triggered observer with $\sigma = 500$, $c_1 = 1$, $c_2 = 50$, $c_3 = 1$, $\varepsilon = 1$. With this choice of parameters, the condition $\sigma c_2 < \gamma$ is satisfied. The input is given by a plug-in hybrid electric vehicle (PHEV) current profile, shown in Figure 3.3, for which the solutions to (3.48) remains in a compact set, so that $|CAx + CBu| \leqslant \rho$ for ρ large enough along the solutions like in (3.41) and Theorem 3.2 applies. Figure 3.3 also provides the plots of the corresponding output, state estimation error and inter-transmission times obtained with the following initial conditions: $U_{RC}(0,0) = 1$ V, $SOC(0,0) = 100\%$, $\xi_{U_{RC}}(0,0) = 0$ V, $\xi_{SOC}(0,0) = 75\%$, $e(0,0) = 0$ and $\eta(0,0) = 10^6$. The minimum-inter event time seen in simulation is 0.227 s. It is clear that both state estimation errors practically converge to zero. Moreover, the proposed scheme stops the transmissions whenever voltage V_{bat} tends to a constant, like in $[720\,\text{s}, 900\,\text{s}]$ and $[1260\,\text{s}, 1500\,\text{s}]$, where the inter-transmission time keeps growing, which is again a clear advantage over time-triggered policies. Indeed, when the input $i_{bat} = 0$, the output V_{bat} tends to constant and no data are transmitted, as explained in Lemma 3.1. Moreover, the transmissions start again when the input becomes different from 0.

We have also analyzed the impact of the design parameters, in particular we focus on the effect of σ, c_1 and ε. For this purpose, we have simulated the corresponding system (3.18) with different

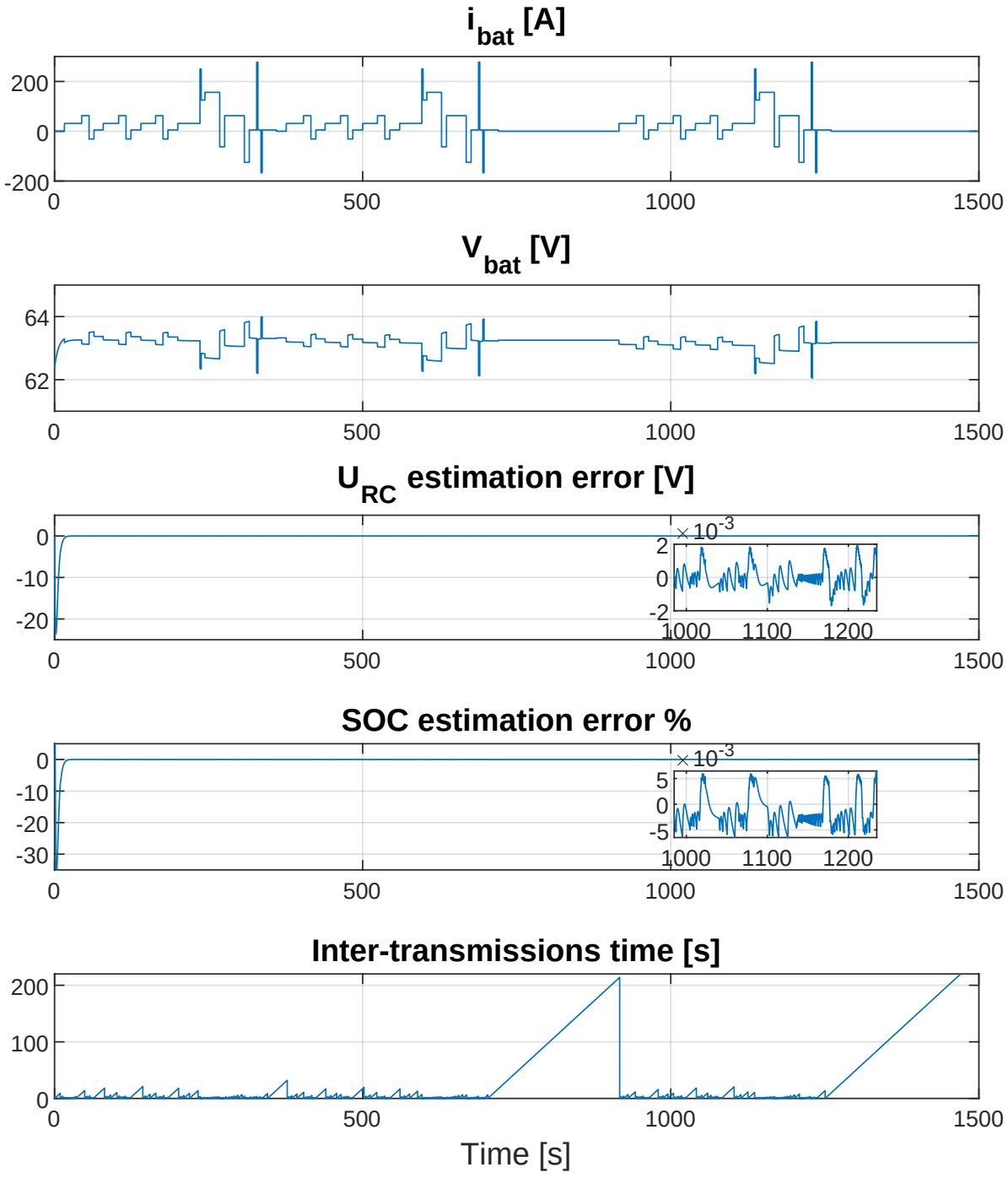

FIGURE 3.3 – Input i_{bat}, output V_{bat}, state estimation error $\xi_{U_{RC}}$ and ξ_{SOC}, and inter-transmissions time, with $\sigma = 500$, $c_1 = 1$, $c_2 = 50$, $c_3 = 1$, $\varepsilon = 1$.

TABLE 3.1 – Average number of transmissions in the time interval $[0\,\text{s}, 1500\,\text{s}]$, maximum absolute value of the state estimation errors $|\xi_{U_{RC}}(t,j)|$ and $|\xi_{SOC}(t,j)|$ for $t \in [1000\,\text{s}, 1500\,\text{s}]$ with different choices for σ, c_1, ε.

σ	c_1	ε	Transmissions	$\lvert\xi_{U_{RC}}\rvert$ [V]	$\lvert\xi_{SOC}\rvert$%
500	1	1	390	0.0019	0.0074
500	1	0.1	1301	0.0006	0.0025
500	1	10	102	0.0067	0.0251
500	1	100	19	0.0163	0.0754
500	0.01	1	10	0.0171	0.0653
500	0.1	1	340	0.0019	0.0069
500	10	1	681	0.0021	0.0077
1000	1	1	364	0.0021	0.0082
0	1	1	886	0.0018	0.0069

parameters configurations and 100 different initial conditions each time, which were selected randomly in the interval $(0,3)V$ for $U_{RC}(0,0)$ and $\xi_{U_{RC}}(0,0)$ and in the interval $(0,100)\%$ for $SOC(0,0)$ and $\xi_{SOC}(0,0)$. The scalar variable η and the sampling induced error were always initialized as $\eta(0,0) = 10^6$ and $e(0,0) = 0$. For each choice of parameters, we have evaluated how many transmissions occur in the time interval $[0\,\text{s}, 1500\,\text{s}]$ on average as well the maximum absolute value of the state estimation errors $|\xi_{U_{RC}}(t,j)|$ and $|\xi_{SOC}(t,j)|$ with $t \in [1000\,\text{s}, 1500\,\text{s}]$ averaged over all simulations. The data collected are shown in Table 3.1.

Table 3.1 shows that, in all considered configurations, the estimation error is small. Moreover, the data suggest that there is a trade-off between the number of transmissions and the estimation accuracy, as already indicated in Section 3.4. In particular, when ε is small, we have more transmissions, but the error is smaller. Conversely, when ε is large, the number of transmissions is reduced, but the estimation error increases, even if it is still reasonably small in view of the application. Moreover, Table 3.1 shows that the larger c_1, the higher the number of transmissions required, without a big impact on the accuracy of the estimation error, except from the case when $c_1 = 0.01$ which produces only 10 transmissions, but the estimation error is higher. Furthermore, there is a trade-off also on the choice of σ. Indeed, the larger σ, the smaller the number of transmissions, but the larger the error. It is important to note that the last parameters choice in Table 3.1, with $\sigma = 0$, corresponds to an absolute threshold triggering rule and leads to many transmissions.

3.6 Conclusions

We have presented an event-triggered observer design for linear time-invariant systems. In order to reduce the number of transmissions over a network while still ensuring good estimation performance, we have proposed a dynamic triggering rule, implemented by a smart sensor, which decides when the measured output needs to be transmitted to the observer. Compared with other works in the literature, we do not need a copy of the observer in the sensor, but only a first order filter of the sampling-induced error, which may allow to significantly reduce the number of transmissions compared to an absolute threshold policy, while being easily implementable.We have modeled the system as a hybrid system and we have shown that the estimation error system satisfies a global practical stability property. Moreover, under mild boundeness conditions on the plant state and its input, we have proved that the system does not exhibit the Zeno phenomenon and even has a positive lower bound on the inter-event times.

In the next chapter, we extend the results to general nonlinear systems assuming the estimation error system satisfies an input-to-state stability property [4]. We will also consider a decentralized scenario, with N independent sensor nodes.

4. The definition of input-to-state stability property for observers and some examples are given in Chapter 2.

Chapter 4

Decentralized event-triggered estimation of nonlinear systems

Contents

The results of this chapter are based on [80], whose preliminary version [84] was presented in Chapter 3.

Abstract - *This chapter generalizes the results presented in Chapter 3 for unperturbed linear time-invariant systems. In particular, we investigate the scenario where a perturbed nonlinear system transmits its output measurements to a remote observer via a packet-based communication network. The sensors are grouped into N nodes and each of these nodes decides when its measured data is transmitted over the network independently. The objective is to design both the observer and the local transmission policies in order to obtain accurate state estimates, while only sporadically using the communication network. In particular, given a general nonlinear observer designed in continuous-time satisfying an input-to-state stability property, we explain how to systematically design a dynamic event-triggering rule for each sensor node that avoids the use of a copy of the observer, thereby keeping local calculation simple. We prove the practical convergence property of the estimation error to the origin and we show that there exists a uniform strictly positive minimum inter-event time for each local triggering rule under mild conditions on the plant. The efficiency of the proposed techniques is illustrated on a numerical case study of a flexible joint robotic arm.*

4.1 Introduction

As explained in Chapter 3, when the system and the observer are not co-located, the output measurements, obtained through a sensor, may need to be transmitted to the observer via a digital network. In this case, the transmission policy has an impact on the convergence speed, robustness of the estimator, as well as on the amount of communication resources required. In this chapter we generalize the previous results, where a centralized event-triggered observer was designed for unperturbed linear time-invariant systems. In particular, as before, we adopt a dynamic event-triggered approach based only on the measured output and the last transmitted output value, which does not require a copy of the observer in the sensor and we design a triggering rule that involves an auxiliary scalar variable. Compared to the results presented in Chapter 3, we now consider general, perturbed nonlinear systems contrary to the vast majority of event-triggered estimation works in the literature, which concentrates on specific classes of systems, see e.g., [16–30]. In addition, the triggering strategies are now decentralized. Indeed, we consider the scenario with N sensor nodes, where each node decides independently when to transmit its local data to the observer via a digital network. Consequently, each sensor node has its own triggering rule.

As in Chapter 3 we follow an emulation-based approach in the sense that in the first step the observer is designed ignoring the effects of the communication network. In particular, we assume that an observer has been synthesized in continuous-time in such a way that it satisfies an input-to-state stability property, in the sense of Definition 2.4. It was also shown in Chapter 2 that numerous observers design techniques of the literature satisfy this stability property, see e.g., [7, 9] and the references therein. In the second step, we take the network into account and propose a new hybrid model using the formalism of [31]. We then design a dynamic triggering rule for each sensor node to approximately preserve the original properties of the observer. In particular, we ensure that the estimation error system satisfies a global practical stability property and we show that, in some particular cases, it is possible to recover the same decay rate for the Lyapunov function along solutions as

in the absence of the communication network, similarly to the linear time-invariant case presented in Chapter 3. Note that, we do not guarantee an asymptotic stability property, but a practical one in general, which is a consequence of the absence of a copy of the observer in the triggering mechanism as we explain later (see Remark 4.2). As for the linear time-invariant case, we design dynamic triggering rules in the sense that they involve a local scalar auxiliary variable, which essentially filters an absolute threshold type condition, see e.g., [26–29]. Our design of the triggering rules rely on very mild knowledge of the observer properties; only some qualitative knowledge is needed on the gains appearing in the input-to-state stability dissipativity property, which is assumed to hold for the state estimation error system, as will be explained in more detail below.

The closest work is [30] where a similar triggering rule is presented, but only for polynomial systems and for a centralized approach (one communication sensor node only). In contrary, our results essentially only rely on an input-to-state stability assumption of the estimation error system, which is commonly satisfied [9]. Moreover we consider the more challenging case of a decentralized set-up, we provide in-depth characterizations of the domains of the solutions and we provide various extensions for scenarios where the outputs are affected by additive noise, and where the plant input is also transmitted to the observer over the network (see Section 4.6).

The remainder of the chapter is organized as follows. The problem setting, the assumption on the observer and the problem statement are presented in Section 4.2. The proposed triggering rule and the overall hybrid system model are given in Section 4.3. In Section 4.4 we analyze the stability properties of the proposed event-triggered observer. In Section 4.5 we derive various properties of the solutions domains (completeness of maximal solutions and the existence of a minimum time between any two transmissions of each sensor node). Some generalizations and extensions are presented in Section 4.6 and a numerical case study on a flexible joint robotic arm is reported in Section 4.7. Finally, Section 4.8 concludes the chapter.

4.2 Problem statement

4.2.1 Setting

Consider the nonlinear system

$$\begin{aligned} \dot{x} &= f_p(x,u,v) \\ y &= h(x), \end{aligned} \tag{4.1}$$

where $x \in \mathbb{R}^{n_x}$ is the state to be estimated by the observer, $u \in \mathbb{R}^{n_u}$ is the measured input, $y \in \mathbb{R}^{n_y}$ is the output measured by sensors, and $v \in \mathbb{R}^{n_v}$ is an unmeasured disturbance input, with $n_x, n_y \in \mathbb{Z}_{>0}$, and $n_u, n_v \in \mathbb{Z}_{\geqslant 0}$. The inputs u and v to (4.1) are such that $u \in \mathscr{L}_{\mathscr{U}}$ and $v \in \mathscr{L}_{\mathscr{V}}$ for some sets $\mathscr{U} \subseteq \mathbb{R}^{n_u}$ and $\mathscr{V} \subseteq \mathbb{R}^{n_v}$. The vector field $f_p : \mathbb{R}^{n_x} \times \mathbb{R}^{n_u} \times \mathbb{R}^{n_v} \to \mathbb{R}^{n_x}$ is locally Lipschitz in its first argument and continuous in the others and $h : \mathbb{R}^{n_x} \to \mathbb{R}^{n_y}$ is continuously differentiable.

We consider the scenario where the measured output is transmitted sporadically to the observer via a digital network, see Figure 4.1. As a result, only sampled versions of the outputs are available to the observer. We follow an emulation-based design in the sense that a continuous-time observer

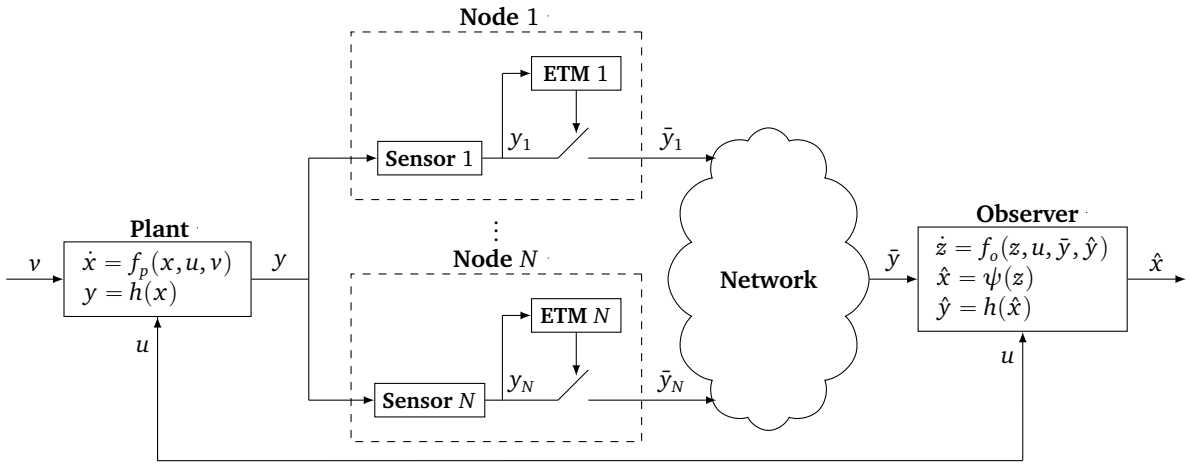

FIGURE 4.1 – Block diagram representing the system architecture (ETM: Event-Triggering Mechanism).

for system (4.1) is first designed ignoring the communication network. Afterwards, we will consider the network and design a triggering rule to decide when the output data need to be transmitted to the observer in order to approximately preserve its original properties. In particular, we assume the availability of a continuous-time observer for system (4.1) of the form

$$\begin{aligned} \dot{z} &= f_o(z,u,y,\hat{y}), \\ \hat{x} &= \psi(z) \\ \hat{y} &= h(\hat{x}), \end{aligned} \tag{4.2}$$

where $z \in \mathbb{R}^{n_z}$ is the observer state, with $n_z \geqslant n_x$, $\hat{x} \in \mathbb{R}^{n_x}$ is the state estimate, $\hat{y}$ is the output estimate. The vector field $f_o : \mathbb{R}^{n_z} \times \mathbb{R}^{n_u} \times \mathbb{R}^{n_y} \times \mathbb{R}^{n_y} \to \mathbb{R}^{n_z}$ is continuous, and $\psi : \mathbb{R}^{n_z} \to \mathbb{R}^{n_x}$ admits a right inverse ψ^{-R} of ψ, i.e., $x = \psi(\psi^{-R}(x))$ for any $x \in \mathbb{R}^{n_x}$. Often $z = \hat{x}$, but this does not necessary have to be the case, like in Kalman filters, which involve extra variables that can be stacked in vector z. Observer (4.2) has a general structure and can be designed using several observer design procedures, including Luenberger-like observers and Kalman filters, see e.g., [9, 12], [7, Section IV] and the references therein. The precise assumption we make on observer (4.2) is stated later in this section. For simplicity, we do not consider in this work the case of reduced-order observers (see e.g., [91]), but we believe that similar derivations could be developed in this scenario. We also adopt the following assumption.

Assumption 4.1. *The plant and the observer have access to the input u at any time instant.* □

Assumption 4.1 is reasonable in many control applications such as, for example, when the control input is jointly communicated to the observer and the plant, or when the input is generated at the observer node, which is collocated with the plant actuator node. It is worth noting that, when the plant and/or the observer do not know the input u, meaning that Assumption 4.1 is not satisfied, the

input u can be included in the unknown disturbance input v in (4.1) and the results presented in the sequel apply, as long as Assumption 4.2 presented later holds. Furthermore, in the case where the input u is transmitted from the plant to the observer via a digital network, we explain in Section 4.6.3 how to define a triggering rule for u so that the forthcoming results hold *mutatis mutandis*.

We investigate the scenario where the output measurements of system (4.1) are transmitted to observer (4.2) via a digital channel, as depicted in Figure 4.1. In particular, we consider the setup where the sensors are grouped into N nodes, where $N \in \{1,\dots,n_y\}$ and we write, after re-ordering (if necessary), $y = (y_1,\dots,y_N) = (h_1(x),\dots,h_N(x))$ with $y_i \in \mathbb{R}^{n_{y_i}}$, $n_{y_i} \in \{1,\dots,n_y\}$ and $n_{y_1}+\dots+n_{y_N} = n_y$. Each sensor node decides when its output measurement needs to be transmitted to the observer over the network, independently of the other sensor nodes. Hence, several nodes are allowed to communicate at the same time instant. Note that this is not a strong assumption. Indeed, in practice, the sensors may use different channels to communicate over the network. On the other hand, if two or more sensors transmit their output data on the same channel at the same time instant, there could be some interference in the communication. These interferences can be modeled as additive measurement noise and we explain in Section 4.6.2 how the proposed approach can be modified to account for measurement noise.

Considering a decentralized setup allows to cover the case where the sensors are spatially distributed, such as, for example, in the case of large-scale systems where different sensors are not collocated and transmit their data independently. Moreover, compared to a centralized scenario, with the considered setup, only the sensor (or sensors) that needs to communicate transmits its data over the network, instead of the full plant output vector. As a result, the data packet size transmitted over the network can be reduced. Note that, the considered decentralized setup covers also the case with only one sensor node when $N = 1$, for which the results presented afterwards are new as well. In particular, the setting presented in Chapter 3 is a special case of the setup considered in this chapter, where system (4.1) was a linear time-invariant system not affected by external disturbances ($v = 0$), observer (4.2) was a linear Luenberger observer and the whole output y was communicated to the observer when a transmission is triggered, i.e., $N = 1$.

In the setting where the output measurement of system (4.1) are transmitted sporadically to observer (4.2) via a digital network, the observer does not know y, but its networked version $\bar{y} := (\bar{y}_1,\dots,\bar{y}_N) \in \mathbb{R}^{n_y}$. Each $\bar{y}_i \in \mathbb{R}^{n_{y_i}}$, with $i \in \{1,\dots,N\}$, is generated with a zero-order-hold device between two successive transmission instants, i.e., in terms of the hybrid systems notation in Chapter 2,

$$\dot{\bar{y}}_i = 0 \tag{4.3}$$

and, when a transmission of node i occurs the corresponding output y_i is transmitted, considering an ideal sampler, hence

$$\bar{y}_i^+ = y_i, \tag{4.4}$$

otherwise, when another node generates a transmission the last received value is kept constant, i.e.

$$\bar{y}_i^+ = \bar{y}_i. \tag{4.5}$$

It is worth noting that the zero-order-hold is just a choice we make to generate the output sampled version $\bar{y}_i$ for all $i \in \{1,\dots,N\}$ between transmission times. Other options are for example the first-order-hold and the model-based holding function [117].

Since the output y is transmitted over the network, observer (4.2) does not have access to the exact measurement output y, but only to its networked version $\bar{y}$. As a result, the observer equations in (4.2) become

$$\begin{aligned} \dot{z} &= f_o(z,u,\bar{y},\hat{y}), \\ \hat{x} &= \psi(z) \\ \hat{y} &= h(\hat{x}). \end{aligned} \tag{4.6}$$

We define the network-induced error for each sensor node $e_i := \bar{y}_i - y_i \in \mathbb{R}^{n_{y_i}}$, with $i \in \{1,\dots,N\}$, and the concatenated vector $e := (e_1,\dots,e_N) = \bar{y} - y \in \mathbb{R}^{n_y}$. We obtain, in view of (4.1) and (4.6),

$$\dot{z} = f_o(z,u,y+e,\hat{y}) = f_o(z,u,h(x)+e,h(\psi(z))). \tag{4.7}$$

The dynamics of variable e_i, for $i \in \{1,\dots,N\}$, between two successive transmission instants is, in view of (4.1) and (4.3) and since h_i is (continuously) differentiable,

$$\dot{e}_i = \dot{\bar{y}}_i - \dot{y}_i = -\frac{\partial h_i(x)}{\partial x} f_p(x,u,v) =: g_i(x,u,v). \tag{4.8}$$

Furthermore, at each transmission instant of the i-th sensor node, we have

$$e_i^+ = 0, \tag{4.9}$$

in view of (4.4), while, for $j \in \{1,\dots,N\}$ with $j \neq i$,

$$e_j^+ = e_j. \tag{4.10}$$

4.2.2 Assumption on the observer

Inspired by [9], we require observer (4.2) to satisfy the following input-to-state stability property, as defined in Chapter 2.

Assumption 4.2. *There exist $\underline{\alpha}$, $\overline{\alpha}$, α, $\gamma_1,\dots,\gamma_N, \theta \in \mathcal{K}_\infty$, $V : \mathbb{R}^{n_x} \times \mathbb{R}^{n_z} \to \mathbb{R}_{\geqslant 0}$ continuously differentiable, such that for all $x \in \mathbb{R}^{n_x}$, $z \in \mathbb{R}^{n_z}$, $u \in \mathcal{U}$, $v \in \mathcal{V}$, $e \in \mathbb{R}^{n_y}$, $\hat{y} \in \mathbb{R}^{n_y}$,*

$$\underline{\alpha}(|x-\psi(z)|) \leqslant V(x,z) \leqslant \overline{\alpha}(|\psi^{-R}(x)-z|) \tag{4.11}$$

$$\left\langle \nabla V(x,z), (f_p(x,u,v), f_o(z,u,y+e,\hat{y})) \right\rangle \leqslant -\alpha(V(x,z)) + \sum_{i=1}^{N} \gamma_i(|e_i|) + \theta(|v|). \tag{4.12}$$

□

Assumption 4.2 implies that (4.2) is a global asymptotic observer when $v = 0$ for system (4.1) in the sense that (4.11) and (4.12) guarantee that, in this case, for any initial condition $x(0) \in \mathbb{R}^{n_x}$, $z(0) \in \mathbb{R}^{n_z}$ and any input $(u, v) \in \mathscr{L}_{\mathscr{U}} \times \{0\}$, the corresponding (maximal) solution x and z to (4.1) and (4.2), if complete [5], satisfies $x(t) - \hat{x}(t) \to 0$ as $t \to +\infty$, where $\hat{x}(t) = \psi(z(t))$. More precisely, Assumption 4.2 implies that the estimation error system $x - \hat{x}$ satisfies an input-to-state stability property [6] with respect to both the network-induced errors e_i, which act as additive measurement noises in (4.12), and to the unknown disturbance input v. In other words, there exist $\beta \in \mathscr{KL}$ and $\gamma \in \mathscr{K}_\infty$ such that, for any input $u \in \mathscr{L}_{\mathscr{U}}$ and any disturbance $v \in \mathscr{L}_{\mathscr{V}}$ the corresponding solutions x and z to (4.1) and (4.2) respectively, for all $t \geqslant 0$ satisfy

$$|\hat{x}(t) - x(t)| \leqslant \beta(|\psi^{-R}(x(0)) - z(0)|, t) + \gamma(\sum_{i=1}^{N} \|e_i\|_{[0,t]} + \|v\|_{[0,t]}). \tag{4.13}$$

Hence, Assumption 4.2 is a robustness property of the observer with respect to measurement noise and disturbance, which is independent of the network.

In view of [9, Section VI], the class of observers in (4.2) satisfying Assumption 4.2 cover various observer designs in the literature, including Luenberger observers for linear systems, various observers for systems with globally Lipschitz vector fields, observers for input affine systems and extended Kalman filters, see [5] and references therein. See [7] for further results on input-to-state stability properties for observers. More details on input-to-state stability property for nonlinear observer are given in Chapter 2. It is important to notice that for the design of the triggering rule, that will be presented in Section 4.3, $\alpha \in \mathscr{K}_\infty$ and the Lyapunov function V in Assumption 4.2 are not needed to be known. Indeed, only γ_i is needed and, in addition, we have a lot of freedom regarding the definition of γ_i, as explained later in Remark 4.1. Note that we work, for simplicity, with global assumption (see Assumption 4.2) but all the analysis could be done in a more local setting (i.e. semi-global, or regional).

4.2.3 Problem formulation

Our goal is to design the local triggering rules to decide when each node i needs to transmit its data to observer (4.2), while approximately preserving the properties of observer (4.2) in the absence of the network as stated in Assumption 4.2. We assume for this purpose that the N sensors are sufficiently "smart" so that they have enough computation capabilities to run a local *scalar* filter, as detailed in the next section.

4.3 Design of the triggering rules

In the proposed architecture, each sensor node $i \in \{1, \dots, N\}$ has access to its local output measurement y_i and its last transmitted output value $\bar{y}_i$. We also introduce a set of local scalar variables $\eta_i \in \mathbb{R}_{\geqslant 0}$, with $i \in \{1, \dots, N\}$. The η_i-dynamics is, between two successive transmissions of any node

5. Completeness of maximal solution will be ensured in Section 4.5.1

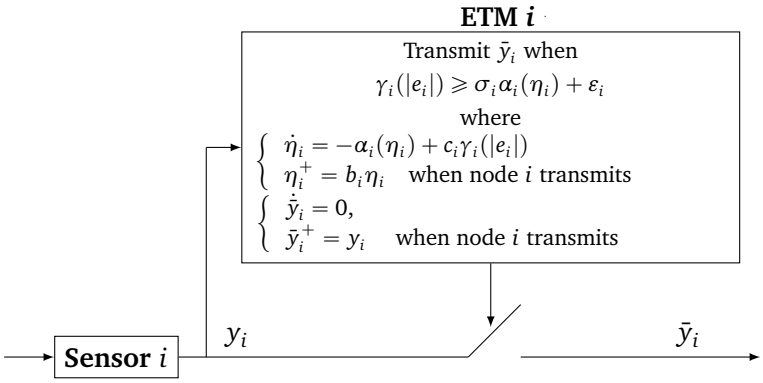

FIGURE 4.2 – Event triggering mechanism (ETM) of node i, $i \in \{1,\dots,N\}$.

and at each transmission of node i, respectively, given by

$$\begin{aligned} \dot{\eta}_i &= -\alpha_i(\eta_i) + c_i \gamma_i(|e_i|) =: \ell_i(\eta_i, e_i) \\ \eta_i^+ &= b_i \eta_i \\ \eta_j^+ &= \eta_j, \qquad j \in \{1,\dots,N\} \text{ with } j \neq i, \end{aligned} \tag{4.14}$$

where $\gamma_i \in \mathscr{K}_\infty$ comes from Assumption 4.2, while $\alpha_i \in \mathscr{K}_\infty$, $c_i \geqslant 0$, $b_i \in [0,1]$ are design functions and parameters. In particular, equation (4.14) means that when node i transmits, with $i \in \{1,\dots,N\}$, the corresponding η_i is updated according to $\eta_i^+ = b_i \eta_i$, while the auxiliary scalar variables η_j, with $j \in \{1,\dots,N\}$, $j \neq i$, associated to the other sensors are not updated. The auxiliary scalar variable η_i is used to define the triggering instants for sensor node i. Indeed, sensor i, with $i \in \{1,\dots,N\}$, transmits its output measurement only when the condition

$$\gamma_i(|e_i|) \geqslant \sigma_i \alpha_i(\eta_i) + \varepsilon_i \tag{4.15}$$

is satisfied, where $\sigma_i \geqslant 0$ and $\varepsilon_i > 0$ are additional design parameters, as summarized in Figure 4.2.

The variables η_i in (4.14), for $i \in \{1,\dots,N\}$, and the triggering rule in (4.15) are inspired by the dynamic event-triggered mechanism in [49] in the context of control. The proposed triggering rule is a filtered version of the absolute threshold triggering rule in e.g., [26–29], which we recover by letting $\sigma_i = 0$ for all $i \in \{1,\dots,N\}$ in (4.15). This dynamic rule is generally able to reduce the number of transmissions over the network, as illustrated on an example in Section 4.7.

The design functions and parameters α_i, c_i, b_i, σ_i and ε_i in (4.14) and (4.15) can be selected differently for different $i \in \{1,\dots,N\}$. We can therefore design them to trigger more often the transmissions of more relevant output data and less frequently the ones whose information is less important. This is an advantage of the decentralized setup compared to the case with only one sensor node, where the whole output is transmitted at every triggering instant.

Note that the parameter ε_i is essential to avoid the Zeno phenomena. Indeed, we will show in Section 4.5.2, under mild extra conditions, that there exists a strictly positive minimum time between

any two transmissions of the same sensor node, which vanishes when $\varepsilon_i = 0$.

Remark 4.1. *To design the triggering mechanism it is not necessary to know $\alpha \in \mathscr{K}_\infty$ and the Lyapunov function V in Assumption 4.2 in view of* (4.14)-(4.15)*: only γ_i is needed, and, as a result, there is a lot of freedom regarding the definition of γ_i. Indeed, if Assumption 4.2 is satisfied with some $\gamma_1, \ldots, \gamma_N \in \mathscr{K}_\infty$, then Assumption 4.2 holds with any $\tilde{\gamma}_1, \ldots, \tilde{\gamma}_N \in \mathscr{K}_\infty$ verifying $\gamma_i(r) = O(\tilde{\gamma}_i(r))$ as $r \to +\infty$ with a different V and a different α in view of Lemma A.1 in the appendix. This implies for instance that, when Assumption 4.2 holds with γ_i quadratic for all $i \in \{1, \ldots, N\}$, the γ_i's can be replaced by any quadratic function in* (4.14)-(4.15)*. We will exploit this property in the example in Section 4.7. Note that, in this case, the proposed technique will not necessary approximately preserve the input-to-state stability property of observer* (4.2)*, but it still ensures a desirable input-to-state stability property.* □

We write $\eta := (\eta_1, \ldots, \eta_N) \in \mathbb{R}^N_{\geqslant 0}$ and we define the overall state as $q := (x, z, e, \eta) \in \mathscr{Q} := \mathbb{R}^{n_x} \times \mathbb{R}^{n_z} \times \mathbb{R}^{n_y} \times \mathbb{R}^N_{\geqslant 0}$ and the overall input $w := (u, v) \in \mathscr{W} := \mathscr{U} \times \mathscr{V}$. We obtain the hybrid model

$$\begin{cases} \dot{q} = F(q, w), & q \in \mathscr{C} \\ q^+ \in G(q), & q \in \mathscr{D}. \end{cases} \tag{4.16}$$

where the flow map F is defined as, for any $q \in \mathscr{C}$ and any $w \in \mathscr{W}$,

$$F(q, w) := \big(f_p(x, w), f_o(z, u, h(x), h(\psi(z))), g(x, w), \ell(\eta, e)\big), \tag{4.17}$$

where $g(x, w) := (g_1(x, w), \ldots, g_N(x, w))$ with g_i in (4.8) and $\ell(\eta, e) := (\ell_1(\eta_1, e_1), \ldots, \ell_N(\eta_N, e_N))$ with ℓ_i in (4.14). The flow set $\mathscr{C}$ is defined as

$$\mathscr{C} := \bigcap_{i=1}^{N} \mathscr{C}_i \tag{4.18a}$$

with

$$\mathscr{C}_i := \{q \in \mathscr{Q} : \gamma_i(|e_i|) \leqslant \sigma_i \alpha_i(\eta_i) + \varepsilon_i\}, \tag{4.18b}$$

for any $i \in \{1, \ldots, N\}$. On the other hand, the jump set $\mathscr{D}$ is defined as

$$\mathscr{D} := \bigcup_{i=1}^{N} \mathscr{D}_i \tag{4.19a}$$

with

$$\mathscr{D}_i := \{q \in \mathscr{Q} : \gamma_i(|e_i|) \geqslant \sigma_i \alpha_i(\eta_i) + \varepsilon_i\}, \tag{4.19b}$$

for any $i \in \{1, \ldots, N\}$. Sets $\mathscr{C}$ and $\mathscr{D}$ in (4.18)-(4.19) are such that a transmission is triggered whenever one of the conditions $\gamma_i(|e_i|) \geqslant \sigma_i \alpha_i(\eta_i) + \varepsilon_i$ is satisfied by at least one sensor node, as illustrated in Figure 4.2. These conditions may be verified simultaneously by different sensor nodes. In this case, several jumps may occur immediately one after the other, with no flow in between.

The set-valued jump map G in (4.16) is defined as, for any $q \in \mathscr{D}$,

$$G(q) := \bigcup_{i=1}^{N} G_i(q), \tag{4.20a}$$

with

$$G_i(q) := \begin{cases} \begin{pmatrix} x \\ z \\ \Lambda_i e \\ (b_i(I_N - \Gamma_i) + \Gamma_i)\eta \end{pmatrix} & q \in \mathscr{D}_i \\ \varnothing & q \notin \mathscr{D}_i, \end{cases} \tag{4.20b}$$

where Λ_i is the block diagonal matrix of dimension n_y with N blocks, where the i-th block is $0_{n_{y_i} \times n_{y_i}}$, while all the other blocks are $I_{n_{y_j}}$, for all $i \in \{1, \dots, N\}$, $j \in \{1, \dots, N\}$, with $j \neq i$. Moreover, Γ_i is the diagonal matrix of dimension N with all elements on the diagonal being equal to 1 except for the i-th element, which is 0, for $i \in \{1, \dots, N\}$. The set $\mathscr{D}_i$ corresponds to the region of the state space where a triggering of node i is allowed. Indeed, a jump in (4.16) corresponds to a transmission of one current output y_i to the observer. In this case $x^+ = x$, $z^+ = z$, $e_i^+ = 0$, $e_j^+ = e_j$, $\eta_i^+ = b_i \eta_i$ and $\eta_j^+ = \eta_j$ for $j \in \{1, \dots, N\}$ with $j \neq i$. The empty set in (4.20b) essentially means that we consider the jump map G_i only when its argument is in the jump set $\mathscr{D}_i$. Indeed, in our setting, each sensor performs its output transmission, according to G_i, independently of the other sensors and the transmission does not affect the other sensor nodes. However, this notation is useful because we also have to define $G_i(q)$ when $q \notin \mathscr{D}_i$ in view of the definition of the jump set $\mathscr{D}$ in (4.19a)-(4.19b). Note also that the empty set in (4.20b) guarantees that the jump map G in (4.20a) is outer semicontinuous and locally bounded relative to the jump set $\mathscr{D}$, which is necessary to satisfy the hybrid basic conditions [31, Assumption 6.5].

We are ready to proceed with the design of α_i, σ_i, c_i, ε_i, b_i in (4.14)-(4.15) and the stability analysis of system (4.16).

4.4 Stability guarantees

The objective of this section is to prove that the proposed event-triggered observer satisfies a uniform global practical stability property, as defined below.

Definition 4.1. *Observer* (4.6) *is uniform globally practically stable for system* (4.1)*, if there exist* $\beta^\star \in \mathscr{KL}$ *and* $\gamma^\star \in \mathscr{K}_\infty$ *such that, for any* $\upsilon > 0$ *there exist non-empty sets of values for parameters* σ_i*,* c_i*,* ε_i *and* b_i *such that for any input* $w \in \mathscr{L}_\mathscr{W}$*, any corresponding solution* q *to* (4.16)-(4.20)*, for all* $(t, j) \in \operatorname{dom} q$*, satisfies*

$$|x(t,j) - \hat{x}(t,j)| \leqslant \beta^\star(|(\psi^{-R}(x(0,0)) - z(0,0), \eta(0,0))|, t) + \gamma^\star(\upsilon + \theta(\|v\|_{[0,t]})), \tag{4.21}$$

where $\theta \in \mathscr{K}_\infty$ *comes from Assumption 4.2.* □

For this purpose, we first present Lyapunov properties in Sections 4.4.1, then we derive stability

guarantees in Section 4.4.2. Finally, in Section 4.4.3 we show how to tune the design parameters, in the special case where Assumption 4.2 holds with a linear $\alpha \in \mathcal{K}_\infty$, to obtain the same decay rate of the Lyapunov function along solutions in absence of network.

4.4.1 Lyapunov stability analysis

In the next theorem we prove a Lyapunov stability property for the overall system (4.16). In particular, we define a Lyapunov function, which depends on the additional scalar variables η_i, $i \in \{1,\dots,N\}$ and on the Lyapunov function V from Assumption 4.2, which guarantees the input-to-state stability property of the observer in absence of network. Moreover, we show how to tune the design parameters to guarantee that this new Lyapunov function is positive definite and radially unbounded, decreases along solutions during flows (up to a ultimate bound) and does not increase at jumps, which implies that a uniform practical stability property of the estimation error is satisfied. In addition, the choice of the design parameters impacts the size of the ultimate bound of the convergence. In particular, we can tune the parameters to have υ, which is the adjustable parameter of the uniform practical stability property, arbitrarily small. However, typically, the smaller we choose υ, the higher is the number of transmissions triggered over the network.

Theorem 4.1 (Lyapunov stability property)**.** *Suppose Assumptions 4.1-4.2 hold and consider the hybrid model* (4.16)-(4.20)*. For any $\upsilon > 0$, select $\sigma_i^\star > 0$, $c_i^\star \geqslant 0$ such that $\sigma_i^\star c_i^\star < 1$ and $d_i > d_i^\star$ where $d_i^\star := \dfrac{\sigma_i^\star}{1-\sigma_i^\star c_i^\star} > 0$ and select $\varepsilon_i^\star > 0$ such that $\sum_{i=1}^{N}(1+d_i c_i^\star)\varepsilon_i^\star \leqslant \upsilon$, for all $i \in \{1,\dots,N\}$. Define*

$$U(q) := V(x,z) + \sum_{i=1}^{N} d_i \eta_i, \tag{4.22}$$

for any $q \in \mathcal{Q}$. Then, there exist $\underline{\alpha}_U$, $\overline{\alpha}_U \in \mathcal{K}_\infty$ such that for any $\alpha_i \in \mathcal{K}_\infty$ in (4.14)*, $\sigma_i \in [0,\sigma_i^\star]$, $c_i \in [0,c_i^\star]$, $\varepsilon_i \in (0,\varepsilon_i^\star]$ and $b_i \in [0,1]$, for all $i \in \{1,\dots,N\}$, the following properties hold.*

(i) For any $q \in \mathcal{Q}$,

$$\underline{\alpha}_U(|(x-\psi(z),\eta)|) \leqslant U(q) \leqslant \overline{\alpha}_U(|(\psi^{-R}(x)-z,\eta)|). \tag{4.23}$$

(ii) For any $q \in \mathcal{C}$ and any $w \in \mathcal{W}$,

$$\langle \nabla U(q), F(q,w)\rangle \leqslant -\alpha(V(x,z)) - \sum_{i=1}^{N} \delta_i \alpha_i(\eta_i) + \upsilon + \theta(|v|), \tag{4.24}$$

where $\alpha, \theta \in \mathcal{K}_\infty$ come from Assumption 4.2, and $\delta_i := d_i - \sigma_i^\star(1+d_i c_i^\star) > 0$.

(iii) For any $q \in \mathcal{D}$, for any $\mathfrak{g} \in G(q)$,

$$U(\mathfrak{g}) \leqslant U(q). \tag{4.25}$$

□

Proof. Let all conditions of Theorem 4.1 hold. We prove the three items of Theorem 4.1 separately.

Proof of item (i). Let $q \in \mathscr{Q}$. From (4.11) and (4.22), we have

$$\underline{\alpha}(|x-\psi(z)|)+\sum_{i=1}^{N} d_i\eta_i \leqslant U(q) \leqslant \overline{\alpha}(|\psi^{-R}(x)-z|)+\sum_{i=1}^{N} d_i\eta_i. \tag{4.26}$$

We first show the upper-bound in (4.23). Since $|\psi^{-R}(x)-z| \leqslant |(\psi^{-R}(x)-z,\eta)|$ and $\eta_i \leqslant |(\psi^{-R}(x)-z,\eta))|$, we have

$$\begin{aligned} U(q) &\leqslant \overline{\alpha}(|\psi^{-R}(x)-z|)+\sum_{i=1}^{N} d_i\eta_i \\ &\leqslant \overline{\alpha}(|(\psi^{-R}(x)-z,\eta)|)+\sum_{i=1}^{N} d_i|(\psi^{-R}(x)-z,\eta)| \\ &=: \overline{\alpha}_U(|(\psi^{-R}(x)-z,\eta)|), \end{aligned} \tag{4.27}$$

where $\overline{\alpha}_U(s)=\overline{\alpha}(s)+\sum\limits_{i=1}^{N} d_i s$ for any $s \geqslant 0$. On the other hand, we have

$$U(q) \geqslant \underline{\alpha}(|x-\psi(z)|)+\sum_{i=1}^{N} d_i\eta_i. \tag{4.28}$$

We obtain, by applying [114, Lemma 4],

$$U(q) \geqslant \underline{\alpha}_U\left(|x-\psi(z)|+\sum_{i=1}^{N}\eta_i\right), \tag{4.29}$$

where $\underline{\alpha}_U(s) := \min\left\{\underline{\alpha}\left(\frac{s}{N+1}\right), d_1\frac{s}{N+1},\ldots,d_N\frac{s}{N+1}\right\}$. Moreover, since $|x-\psi(z)|+\sum\limits_{i=1}^{N}\eta_i \geqslant |(x-\psi(z),\eta)|$,

$$U(q) \geqslant \underline{\alpha}_U(|(x-\psi(z),\eta)|). \tag{4.30}$$

This completes the proof of item (i) of Theorem 4.1.

Proof of item (ii). Let $q \in \mathscr{C}$ and $w \in \mathscr{W}$. In view of (4.12), (4.14) and (4.22),

$$\begin{aligned} \langle \nabla U(q), F(q,w)\rangle &\leqslant -\alpha(V(x,z))+\sum_{i=1}^{N}\gamma_i(|e_i|)+\theta(|v|)+\sum_{i=1}^{N} d_i(-\alpha_i(\eta_i)+c_i\gamma_i(|e_i|)) \\ &= -\alpha(V(x,z))-\sum_{i=1}^{N} d_i\alpha_i(\eta_i)+\sum_{i=1}^{N}(1+d_ic_i)\gamma_i(|e_i|)+\theta(|v|). \end{aligned} \tag{4.31}$$

Since $q \in \mathscr{C}$, we have from (4.18b) that $\gamma_i(|e_i|) \leqslant \sigma_i\alpha_i(\eta_i)+\varepsilon_i$ for all $i \in \{1,\ldots,N\}$. Hence, the

next inequality holds

$$\begin{aligned}\langle \nabla U(q), F(q,w)\rangle &\leqslant -\alpha(V(x,z)) - \sum_{i=1}^{N} d_i\alpha_i(\eta_i) + \sum_{i=1}^{N}(1+d_ic_i)(\sigma_i\alpha_i(\eta_i)+\varepsilon_i) + \theta(|v|)\\ &= -\alpha(V(x,z)) - \sum_{i=1}^{N}(d_i-\sigma_i(1+d_ic_i))\alpha_i(\eta_i) + \sum_{i=1}^{N}(1+d_ic_i)\varepsilon_i + \theta(|v|).\end{aligned} \tag{4.32}$$

Due to the conditions $\sigma_i \in [0,\sigma_i^\star], c_i \in [0,c_i^\star]$ and $\varepsilon_i \in (0,\varepsilon_i^\star]$ in Theorem 4.1,

$$\langle \nabla U(q), F(q,w)\rangle \leqslant -\alpha(V(x,z)) - \sum_{i=1}^{N}(d_i-\sigma_i^\star(1+d_ic_i^\star))\alpha_i(\eta_i) + \sum_{i=1}^{N}(1+d_ic_i^\star)\varepsilon_i^\star + \theta(|v|). \tag{4.33}$$

Using the definitions of δ_i in item (ii) of Theorem 4.1 and the fact that $\upsilon \geqslant \sum_{i=1}^{N}(1+d_ic_i^\star)\varepsilon_i^\star$, we obtain

$$\langle \nabla U(q), F(q,w)\rangle \leqslant -\alpha(V(x,z)) - \sum_{i=1}^{N}\delta_i\alpha_i(\eta_i) + \upsilon + \theta(|v|), \tag{4.34}$$

where δ_i is strictly positive for any $i \in \{1,\dots,N\}$ as $d_i > d_i^\star$ and $\sigma_i^\star c_i^\star < 1$. The proof of item *(ii)* is complete.

Proof of item (iii). Let $q \in \mathscr{D}$, in view of (4.14) and (4.20b) and since $b_i \in [0,1]$ for all $i \in \{1,\dots,N\}$, for any $\mathfrak{g} \in G(q)$, there exists $k \in \{1,\dots,N\}$ such that $\mathfrak{g} \in G_k(q)$, hence

$$\begin{aligned}U(\mathfrak{g}) &= V(x,z) + \sum_{\substack{i=1\\ i\neq k}}^{N} d_i\eta_i + d_kb_k\eta_k\\ &\leqslant V(x,z) + \sum_{i=1}^{N} d_i\eta_i\\ &= U(q),\end{aligned} \tag{4.35}$$

which concludes the proof of item *(iii)*. ■

Theorem 4.1 shows the existence of a Lyapunov function U for system (4.16)-(4.20), which guarantees a uniform practical stability property, where the adjustable parameter is υ. The conditions of Theorem 4.1 can always be ensured. Indeed, we just need to select $\sigma_i^\star$ and $c_i^\star$ such that $\sigma_i^\star c_i^\star < 1$, for all $i \in \{1,\dots,N\}$, which is always possible and then all the other parameters can be selected such that conditions in Theorem 4.1 hold. Moreover, as already mentioned υ in (4.24) can be taken arbitrary small. However, typically the smaller υ is selected, the higher the number of transmissions required. In Theorem 4.1, we first fix υ and then we present how to select the design parameters in order to obtain the Lyapunov properties in (4.23)-(4.25). An alternative approach is to select σ_i and c_i such that $\sigma_ic_i < 1$ for all $i \in \{1,\dots,N\}$, and then, by simply selecting $b_i \in [0,1]$, and any positive value for ε_i, any $\alpha_i \in \mathscr{K}_\infty$, for all $i \in \{1,\dots,N\}$, (4.23)-(4.25) hold for some strictly positive υ. The selection of the design parameters in the example in Section 4.7 is done exploiting this second

strategy.

Item (*ii*) of Theorem 4.1 guarantees that the Lyapunov function U decreases along solutions to system (4.16)-(4.20) during flows with a decay rate that depends on the functions $\alpha \in \mathcal{K}_\infty$ and $\alpha_i \in \mathcal{K}_\infty$, $i \in \{1,\dots,N\}$, and that, in general, is different from the decay rate $\alpha \in \mathcal{K}_\infty$ of the Lyapunov function V along the solutions to (4.1) and (4.2) in absence of network, as detailed in Assumption 4.2. We can ensure any decay rate $\alpha_U \in \mathcal{K}_\infty$ such that $\alpha_U \leqslant \alpha$ on flows for the Lyapunov function U along the solutions to (4.16)-(4.20) on any given compact set by suitably selecting α_i in (4.14), for all $i \in \{1,\dots,N\}$. The result is global in some special cases, like when $\alpha \in \mathcal{K}_\infty$ is subadditive, i.e. $\alpha(s_1)+\alpha(s_2) \geqslant \alpha(s_1+s_2)$, for all $s_1, s_2 \geqslant 0$, or when $\alpha \in \mathcal{K}_\infty$ is uniformly continuous. We formalize this in the next proposition.

Proposition 4.1 (Decay rate of the Lyapunov function)**.** *Consider system* (4.16)-(4.20) *and suppose Assumptions 4.1-4.2 hold. For any $\alpha_U \in \mathcal{K}_\infty$ such that $\alpha_U \leqslant \alpha$, any compact set $\mathcal{M} \subset \mathcal{Q}$ and any $\upsilon > 0$, select σ_i, c_i, ε_i, d_i, b_i and δ_i as in Theorem 4.1 for all $i \in \{1,\dots,N\}$ and define $\overline{d} := \max\{d_1,\dots,d_N\}$. Select $\alpha_i \in \mathcal{K}_\infty$ such that $\min\left\{\delta_1\alpha_1\left(\frac{s}{\overline{d}N}\right),\dots,\delta_N\alpha_N\left(\frac{s}{\overline{d}N}\right)\right\} \geqslant \psi_{\mathcal{M}}(s)$ for all $s \geqslant 0$, where $\psi_{\mathcal{M}} \in \mathcal{K}_\infty$ is the modulus of continuity of the function α_U in the compact set $\mathcal{M}$. Then, for any $q \in \mathcal{C} \cap \mathcal{M}$ and any $w \in \mathcal{W}$,*

$$\langle \nabla U(q), F(q,w)\rangle \leqslant -\alpha_U(U(q)) + \upsilon + \theta(|v|), \tag{4.36}$$

with U defined in (4.22) *and $\theta \in \mathcal{K}_\infty$ comes from Assumption 4.2. Moreover,* (4.36) *holds globally, i.e., for any $q \in \mathcal{C}$ and $w \in \mathcal{W}$, when $\alpha \in \mathcal{K}_\infty$ is uniformly continuous or when $\alpha \in \mathcal{K}_\infty$ is subadditive, i.e. $\alpha(s_1)+\alpha(s_2) \geqslant \alpha(s_1+s_2)$, for all $s_1, s_2 \geqslant 0$ and $\alpha_i \in \mathcal{K}_\infty$ with $i \in \{1,\dots,N\}$ are selected such that $\alpha_i\left(\frac{s}{\overline{d}N}\right) \geqslant \frac{\alpha(s)}{\delta_i}$ for all $s \geqslant 0$.* □

Proof. We first show that we can ensure any decay rate α_U on flows for U along solutions to (4.16)-(4.20) with $\alpha_U \in \mathcal{K}_\infty$ and $\alpha_U \leqslant \alpha$ on any given compact set by suitably selecting α_i in (4.14), for all $i \in \{1,\dots,N\}$.

Let $\mathcal{M} \subset \mathcal{Q}$ be a compact set, $q \in \mathcal{C} \cap \mathcal{M}$ and $w \in \mathcal{W}$, from (4.24) and by using [114, Lemma 4] we obtain

$$\langle \nabla U(q), F(q,w)\rangle \leqslant -\alpha(V(x,z)) - \alpha_\eta\Big(\sum_{i=1}^{N} d_i\eta_i\Big) + \upsilon + \theta(|v|), \tag{4.37}$$

where $\alpha_\eta(s) := \min\left\{\delta_1\alpha_1\left(\frac{s}{\overline{d}N}\right),\dots,\delta_N\alpha_N\left(\frac{s}{\overline{d}N}\right)\right\} \in \mathcal{K}_\infty$, with $\overline{d} := \max\{d_1,\dots,d_N\}$. Take any $\alpha_U \in \mathcal{K}_\infty$ such that $\alpha_U \leqslant \alpha$ on $\mathcal{M}$. From the Heine-Canton theorem, we have that α_U is uniformly continuous on $\mathcal{M}$. Applying [118, Proposition A.2.1] we have that, for all $q \in \mathcal{M}$,

$$\alpha_U\Big(V(x,z)+\sum_{i=1}^{N} d_i\eta_i\Big) - \alpha_U\Big(V(x,z)\Big) \leqslant \psi_{\mathcal{M}}\Big(\sum_{i=1}^{N} d_i\eta_i\Big), \tag{4.38}$$

where $\psi_{\mathscr{M}} \in \mathscr{K}_\infty$ is the modulus of continuity of α_U. Selecting $\alpha_i \in \mathscr{K}_\infty$, $i \in \{1,\dots,N\}$ such that, for all $s \geqslant 0$, $\alpha_\eta(s) = \min\left\{\delta_1\alpha_1\left(\frac{s}{\overline{d}N}\right),\dots,\delta_N\alpha_N\left(\frac{s}{\overline{d}N}\right)\right\} \geqslant \psi_{\mathscr{M}}(s)$, we obtain from (4.37),

$$\begin{aligned}\langle \nabla U(q), F(q,w)\rangle &\leqslant -\alpha(V(x,z)) - \alpha_\eta\Big(\sum_{i=1}^N d_i\eta_i\Big) + \upsilon + \theta(|v|)\\ &\leqslant -\alpha(V(x,z)) - \alpha_U\Big(V(x,z) + \sum_{i=1}^N d_i\eta_i\Big) + \alpha_U(V(x,z)) + \upsilon + \theta(|v|),\end{aligned} \tag{4.39}$$

and since $\alpha_U \leqslant \alpha$,

$$\begin{aligned}\langle \nabla U(q), F(q,w)\rangle &\leqslant -\alpha_U\Big(V(x,z) + \sum_{i=1}^N d_i\eta_i\Big) + \upsilon + \theta(|v|)\\ &= -\alpha_U(U(q)) + \upsilon + \theta(|v|).\end{aligned} \tag{4.40}$$

Moreover, when $\alpha \in \mathscr{K}_\infty$ is uniformly continuous the result is global for all $\alpha_U \in \mathscr{K}_\infty$ such that $\alpha_U \leqslant \alpha$ and α_U uniformly continuous. This comes directly from the first part of this proof.

We now prove the last part of the proposition, in particular we prove that (4.36) holds globally when $\alpha \in \mathscr{K}_\infty$ is subadditive, i.e. $\alpha(s_1) + \alpha(s_2) \geqslant \alpha(s_1+s_2)$, for all $s_1, s_2 \geqslant 0$ and $\alpha_i \in \mathscr{K}_\infty$ with $i \in \{1,\dots,N\}$ are selected such that $\alpha_i\left(\frac{s}{\overline{d}N}\right) \geqslant \frac{\alpha(s)}{\delta_i}$ for all $s \geqslant 0$. From (4.37) we have

$$\begin{aligned}\langle \nabla U(q), F(q,w)\rangle &\leqslant -\alpha(V(x,z)) - \alpha_\eta\Big(\sum_{i=1}^N d_i\eta_i\Big) + \upsilon + \theta(|v|)\\ &\leqslant -\alpha(V(x,z)) - \alpha\Big(\sum_{i=1}^N d_i\eta_i\Big) + \upsilon + \theta(|v|),\end{aligned} \tag{4.41}$$

where the last inequality comes from $\alpha_\eta(s) = \min\left\{\delta_1\alpha_1\left(\frac{s}{\overline{d}N}\right),\dots,\alpha_N\left(\frac{s}{\overline{d}N}\right)\right\} \geqslant \alpha(s)$, for all $s \geqslant 0$. Since α is subadditive, we obtain

$$\begin{aligned}\langle \nabla U(q), F(q,w)\rangle &\leqslant -\alpha\Big(V(x,z) + \sum_{i=1}^N d_i\eta_i\Big) + \upsilon + \theta(|v|)\\ &= -\alpha(U(q)) + \upsilon + \theta(|v|)\end{aligned} \tag{4.42}$$

and since $\alpha_U \leqslant \alpha$,

$$\langle \nabla U(q), F(q,w)\rangle \leqslant -\alpha_U(U(q)) + \upsilon + \theta(|v|). \tag{4.43}$$

■

Proposition 4.1 shows that, in some cases, it is possible to recover the same decay rate α of the Lyapunov function in absence of network. We will further explore the special case when Assumption 4.2 holds with a linear $\alpha \in \mathscr{K}_\infty$ in Theorem 4.2 in Section 4.4.3.

4.4.2 Stability property of the estimation error

Based on Theorem 4.1, we prove that the event-triggered observer satisfies a global practical stability property of the estimation error $|x-\hat{x}|$. In particular, starting from the Lyapunov properties proved in the previous section, in the next proposition we characterize the behaviour of the system trajectories and we show that the estimation error and the variables η_i, $i \in \{1,\dots,N\}$, converge to a neighborhood of the origin, whose size depends on the adjustable parameter υ and the disturbance v.

Proposition 4.2 (Global practical stability property)**.** *Consider system* (4.16)-(4.20) *and suppose Assumptions 4.1-4.2 hold. For any $\upsilon > 0$, select α_i, σ_i, c_i, ε_i, d_i and b_i as in Theorem 4.1 for all $i \in \{1,\dots,N\}$. Then there exist $\beta^\star \in \mathcal{KL}$ and $\gamma^\star \in \mathcal{K}_\infty$, all independent of υ, such that, for any input $w \in \mathcal{L}_\mathcal{W}$, any solution q satisfies for all $(t,j) \in \operatorname{dom} q$,*

$$|(x(t,j)-\hat{x}(t,j),\eta(t,j))| \leqslant \beta^\star(|(\psi^{-R}(x(0,0))-z(0,0),\eta(0,0))|,t)+\gamma^\star(\upsilon+\theta(\|v\|_{[0,t]})), \quad (4.44)$$

with $\theta \in \mathcal{K}_\infty$ from Assumption 4.2. □

Proof. Consider the Lyapunov function U defined in (4.22). From item *(ii)* of Theorem 4.1 and [114, Lemma 4], we derive that for any $q \in \mathcal{C}$ and $w \in \mathcal{W}$,

$$\langle \nabla U(q), F(q,w)\rangle \leqslant -\alpha_U(U(q))+\upsilon+\theta(|v|), \quad (4.45)$$

where $\alpha_U(s) := \min\left\{\alpha\left(\frac{s}{2}\right), \alpha_\eta\left(\frac{s}{2}\right)\right\}$ and $\alpha_\eta(s) := \min\left\{\delta_1\alpha_1\left(\frac{s}{\bar{d}N}\right),\dots,\delta_N\alpha_N\left(\frac{s}{\bar{d}N}\right)\right\}$, with $\bar{d} := \max\{d_1,\dots,d_N\}$. Hence, given $\zeta \in (0,1)$, when $\upsilon+\theta(|v|) \leqslant (1-\zeta)\alpha_U(U(q))$,

$$\langle \nabla U(q), F(q,w)\rangle \leqslant -\zeta\alpha_U(U(q)). \quad (4.46)$$

We then follow similar steps as in [31, proof of Theorem 3.18]. Let $w \in \mathcal{L}_\mathcal{W}$ and q be a solution to system (4.16)-(4.20). Pick any $(t,j) \in \operatorname{dom} q$ and let $0 = t_0 \leqslant t_1 \leqslant \cdots \leqslant t_{j+1} = t$ satisfy $\operatorname{dom} q \cap ([0,t]\times\{0,1,\dots,j\}) = \bigcup_{k=0}^{j}[t_k,t_{k+1}]\times\{k\}$. For each $k \in \{0,\dots,j\}$ and almost all $s \in [t_k,t_{k+1}]$, $q(s,k) \in \mathcal{C}$. In view of (4.46), applying [119, pages 19-21], there exists $\beta_U \in \mathcal{KL}, \gamma_U \in \mathcal{K}_\infty$ such that

$$U(q(s,k)) \leqslant \beta_U(U(q(t_k,k)),s-t_k)+\gamma_U(\upsilon+\theta(\|v\|_{[t_k,s]})) \quad (4.47)$$

for all $s \in [t_k,t_{k+1}]$, for all $k \in \{0,\dots,j\}$. Consequently, we have, for any $k \in \{0,\dots,j\}$,

$$U(q(t_{k+1},k)) \leqslant \beta_U((U(q(t_k,k)),t_{k+1}-t_k)+\gamma_U(\upsilon+\theta(\|v\|_{[0,t_{k+1}]})) \quad (4.48)$$

On the other hand, from item *(iii)* of Theorem 4.1, for each $k \in \{1,\dots,j\}$,

$$U(q(t_k,k))-U(q(t_k,k-1)) \leqslant 0 \quad \forall k \in \{1,\dots,j\}. \quad (4.49)$$

From (4.48) and (4.49), we deduce that for any $(t,j) \in \operatorname{dom} q$,

$$U(q(t,j)) \leqslant \beta_U(U(q(0,0)),t) + \gamma_U(\upsilon + \theta(\|v\|_{[0,t]})). \tag{4.50}$$

Using the U definition in (4.22), we obtain

$$\begin{aligned} V(x(t,j),z(t,j)) + \sum_{i=1}^{N} d_i \eta_i(t,j) \leqslant & \beta_U(V(x(0,0),z(0,0)) + \sum_{i=1}^{N} d_i \eta_i(0,0), t) \\ & + \gamma_U(\upsilon + \theta(\|v\|_{[0,t]})). \end{aligned} \tag{4.51}$$

Using (4.23), from (4.51) we have, for all $(t,j) \in \operatorname{dom} q$,

$$\begin{aligned} \underline{\alpha}_U(|(x(t,j) - \hat{x}(t,j), \eta(t,j))|) \leqslant & \beta_U(V(x(0,0),z(0,0)) + \sum_{i=1}^{N} d_i \eta_i(0,0), t) \\ & + \gamma_U(\upsilon + \theta(\|v\|_{[0,t]})), \end{aligned} \tag{4.52}$$

recalling that $\hat{x} = \psi(z)$ from (3). Consequently,

$$\begin{aligned} |(x(t,j) - \hat{x}(t,j), \eta(t,j))| \leqslant & \underline{\alpha}_U^{-1}(\beta_U(V(x(0,0),z(0,0)) + \sum_{i=1}^{N} d_i \eta_i(0,0), t)) \\ & + \underline{\alpha}_U^{-1}(\gamma_U(\upsilon + \theta(\|v\|_{[0,t]}))), \end{aligned} \tag{4.53}$$

for all $(t,j) \in \operatorname{dom} q$. Moreover, from (4.23), we have

$$\begin{aligned} U(q(0,0)) &= V(x(0,0),z(0,0)) + \sum_{i=1}^{N} d_i \eta_i(0,0) \\ &\leqslant \overline{\alpha}_U(|(\psi^{-R}(x(0,0)) - z(0,0), \eta(0,0))|). \end{aligned} \tag{4.54}$$

Thus, from (4.53) and (4.54) we obtain

$$\begin{aligned} |(x(t,j) - \hat{x}(t,j), \eta(t,j))| &\leqslant \underline{\alpha}_U^{-1}(\beta_U(\overline{\alpha}_U(|(\psi^{-R}(x(0,0)) - z(0,0), \eta(0,0))|), t)) \\ &\quad + \underline{\alpha}_U^{-1}(\gamma_U(\upsilon + \theta(\|v\|_{[0,t]}))) \\ &= \beta^\star(|(\psi^{-R}(x(0,0)) - z(0,0), \eta(0,0))|), t)) + \gamma^\star(\upsilon + \theta(\|v\|_{[0,t]}))), \end{aligned} \tag{4.55}$$

where $\beta^\star(s,t) := \underline{\alpha}_U^{-1}(\beta_U(\overline{\alpha}_U(s),t) \in \mathscr{KL}$ and $\gamma^\star(s) := \underline{\alpha}_U^{-1}(\gamma_U(s))$ for all $s,t \geqslant 0$. This concludes the proof. ■

Proposition 4.2 guarantees that the estimation error $x - \hat{x}$ satisfies a uniform global practical stability property. Moreover, (4.44) also ensures that the η_i components, with $i \in \{1,\ldots,N\}$, are bounded and converge to a neighborhood of the origin. Note that for general nonlinear systems it is difficult to analyze the impact of the parameters on $\beta^\star$ and $\gamma^\star$ in (4.44). However, this can be done in some specific cases, as we will show in Theorem 4.2 in the case when Assumption 4.2 is

satisfied with a linear $\alpha \in \mathscr{K}_\infty$ as well as in the context of linear time-invariant systems in absence of disturbance, presented in Chapter 3.

Remark 4.2. *To ensure an asymptotic stability property for the estimation error system, in the sense that* (4.21) *holds with* $\upsilon = 0$*, as opposed to a practical one as in Proposition 4.2, we argue that a different set-up would be needed, which would require to implement a copy of the observer at each node. Indeed, a typical way to ensure an asymptotic stability property for the estimation error system when emulating an observer of the form of* (4.2) *is not to only hold the plant output* y *as we do in* (4.7) *but the output estimation error* $\bar{y} - y$ *see e.g., [12, 41, 120]. In this case, the network-induced error associated to node* i *becomes* $(\bar{y}_i - \hat{\bar{y}}_i) - (y_i - \hat{y}_i)$*. Hence, for the local triggering rule* i *to evaluate this network-induced error, it would need to know* $\hat{y}_i$*, which can only be done by implementing a local copy of the observer at node* i *to generate* $\hat{y}_i$*. Because our goal is precisely not to rely on a copy of the observer at each node, as explained in the introduction, the triggering rules we present do not rely on* $\hat{y}_i$*, but only on* y_i *(and* η_i*), which leads to a practical stability property.* □

As mentioned before, we do not need to know $\alpha \in \mathscr{K}_\infty$ and V to design the triggering conditions such that the results in Theorem 4.1 and in Proposition 4.2 hold. However, the knowledge of $\alpha \in \mathscr{K}_\infty$ is useful when we want to recover the decay rate $\alpha \in \mathscr{K}_\infty$ of the Lyapunov function along solutions in absence of network, as formalized in the next section for the case where Assumption 4.2 holds with α linear.

4.4.3 Decay rate of the Lyapunov function

In the next theorem we show that, when Assumption 4.2 holds with a linear $\alpha \in \mathscr{K}_\infty$, it is possible to recover the same decay rate α of the Lyapunov function along solutions in absence of network. In particular, following similar lines as in Theorem 4.1 and in Proposition 4.2 we first prove the Lyapunov properties, and then we evaluate the behaviour of the Lyapunov function along solutions. We also show how to tune the design parameters in order to recover the decay rate of the Lyapunov function along the system trajectories that we would have in absence of communication network.

Theorem 4.2 (Global practical stability property with the recovering of the decay rate of the Lyapunov function)**.** *Consider system* (4.16)-(4.20) *and suppose Assumption 4.1 holds and Assumption 4.2 is satisfied with* $\alpha(s) = as$*, for any* $s \geqslant 0$ *with* $a > 0$*. For any* $a_U \in (0, a]$ *and* $\mu > 0$ *select* α_i*,* c_i*,* σ_i*,* ε_i *and* b_i *as follows for all* $i \in \{1, \dots, N\}$*.*

(i) $c_i \in [0, c_i^\star]$ *and* $\sigma_i \in [0, \sigma_i^\star]$*, where* $c_i^\star \geqslant 0$ *and* $\sigma_i^\star > 0$ *are such that* $\sigma_i^\star c_i^\star < 1$*, for all* $i \in \{1, \dots, N\}$*.*

(ii) $\alpha_i(s) = a_i s$ *for any* $s \geqslant 0$ *with* $a_i \geqslant a_i^\star$ *and* $a_i^\star > 0$ *such that* $a_i^\star > \dfrac{a_U}{1 - \sigma_i^\star c_i^\star}$*, for all* $i \in \{1, \dots, N\}$*.*

(iii) $b_i \in [0, 1]$*, for all* $i \in \{1, \dots, N\}$*.*

(iv) $\varepsilon_i \in (0, \varepsilon_i^\star]$ *for all* $i \in \{1, \dots, N\}$ *and* $\varepsilon_1^\star + \dots + \varepsilon_N^\star \leqslant \dfrac{a_U \mu}{1 + \varsigma}$ *with* $\varsigma := \max\{d_1 c_1^\star, \dots, d_N c_N^\star\}$*, where* $d_i := \sigma_i^\star \left(1 - \sigma_i^\star c_i^\star - \dfrac{a_U}{a_i^\star}\right)^{-1} > 0$*, for all* $i \in \{1, \dots, N\}$*.*

Then, for U defined in (4.22) *with d_i selected as in item (iv), which satisfies the condition stated in Theorem 4.1, for all $i \in \{1,\dots,N\}$, for any solution q with input $w \in \mathscr{L}_{\mathscr{W}}$ and any $(t,j) \in \operatorname{dom} q$,* $V(x(t,j),z(t,j)) + \sum_{i=1}^{N} d_i\eta_i(t,j) \leqslant e^{-a_U t}(V(x(0,0),z(0,0)) + \sum_{i=1}^{N} d_i\eta_i(0,0)) + \mu + \frac{1}{a_U}\theta(\|v\|_{[0,t]})$. □

Theorem 4.2 guarantees that it is always possible to recover the same decay rate of the Lyapunov function along solutions in absence of network when the observer satisfies Assumption 4.2 with α linear. In particular, with Theorem 4.2 we guarantee, in presence of network, a convergence rate $a_U \in (0,a]$ for $U(q) = V(x,z) + \sum_{i=1}^{N} d_i\eta_i$ along solutions to (4.16)-(4.20), which can therefore be equal to the decay rate a of V in absence of network.

It is important to notice that many observers in the literature satisfy Assumption 4.2 with a linear α, see [9]. Moreover, it is always possible to ensure the conditions in Theorem 4.2, like in Theorem 4.1. Indeed, selecting $\sigma_i^\star$ and $c_i^\star$ such that $\sigma_i^\star c_i^\star < 1$ for all $i \in \{1,\dots,N\}$, which is always possible, we have that all the other parameters can be always chosen such that items *(ii)-(iv)* of Theorem 4.2 are satisfied.

Proof. Let all conditions of Theorem 4.2 hold and consider the Lyapunov function U defined in (4.22) with d_i satisfying item (*iv*) of Theorem 4.2. Note that d_i satisfies the condition $d_i > d_i^\star$ in Theorem 4.1. As $\alpha(s) = as$ and $\alpha_i(s) = a_i s$ for any $s \geqslant 0$, for all $i \in \{1,\dots N\}$, by following the steps of the proof of Theorem 4.1, we derive that for any $q \in \mathscr{C}$ and $w \in \mathscr{W}$,

$$\langle \nabla U(q), F(q,w)\rangle \leqslant -aV(x,z) - \sum_{i=1}^{N} \delta_i a_i \eta_i + \sum_{i=1}^{N}(1 + d_i c_i^\star)\varepsilon_i^\star + \theta(|v|). \tag{4.56}$$

Defining $a_\eta := \min\left\{\frac{\delta_1 a_1}{d_1},\dots,\frac{\delta_N a_N}{d_N}\right\} > 0$, we obtain

$$\begin{aligned}
\langle \nabla U(q), F(q,w)\rangle &\leqslant -aV(x,z) - a_\eta \sum_{i=1}^{N} d_i\eta_i + \sum_{i=1}^{N}(1 + d_i c_i^\star)\varepsilon_i^\star + \theta(|v|)\\
&\leqslant -\min\{a,a_\eta\}(V(x,z) + \sum_{i=1}^{N} d_i\eta_i) + \sum_{i=1}^{N}(1 + d_i c_i^\star)\varepsilon_i^\star + \theta(|v|)\\
&= -\min\{a,a_\eta\}U(q) + \sum_{i=1}^{N}(1 + d_i c_i^\star)\varepsilon_i^\star + \theta(|v|)\\
&\leqslant -a_U U(q) + \sum_{i=1}^{N}(1 + d_i c_i^\star)\varepsilon_i^\star + \theta(|v|),
\end{aligned} \tag{4.57}$$

where the last inequality comes from the choice of parameters. Indeed, when $\min\{a,a_\eta\} = a$, then $-\min\{a,a_\eta\} = -a \leqslant -a_U$. Conversely, when $\min\{a,a_\eta\} = a_\eta = \min\left\{\frac{\delta_1 a_1}{d_1},\dots,\frac{\delta_N a_N}{d_N}\right\}$,

we have from the definition of δ_i in item (*ii*) of Theorem 4.1, for all $i \in \{1,\dots,N\}$,

$$\begin{aligned} -\frac{\delta_i a_i}{d_i} &= -(d_i - \sigma_i^\star(1+d_i c_i^\star))\frac{a_i}{d_i} \\ &\leqslant -(d_i - \sigma_i^\star(1+d_i c_i^\star))\frac{a_i^\star}{d_i} \\ &= -\left(1-\sigma_i^\star\left(\frac{1}{d_i}+c_i^\star\right)\right)a_i^\star \end{aligned} \tag{4.58}$$

and since $d_i = \sigma_i^\star\big(1-\sigma_i^\star c_i^\star - \frac{a_U}{a_i^\star}\big)^{-1}$, we derive that $-\frac{\delta_i a_i}{d_i} \leqslant -a_U$. Therefore (4.57) holds and since $\sum_{i=1}^{N}\varepsilon_i^\star \leqslant \frac{a_U\mu}{1+\varsigma}$, with $\varsigma = \max\{d_1c_1^\star,\dots,d_Nc_N^\star\}$, we have

$$\begin{aligned} \langle \nabla U(q), F(q,w)\rangle &\leqslant -a_U U(q) + (1+\varsigma)\sum_{i=1}^{N}\varepsilon_i^\star + \theta(|v|) \\ &\leqslant -a_U U(q) + a_U\mu + \theta(|v|). \end{aligned} \tag{4.59}$$

Similarly to the proof of Proposition 4.2, we now follow similar steps as in [31, Proof of Theorem 3.18]. Let $w \in \mathscr{L}_{\mathscr{W}}$ and q be a solution to hybrid system (4.16). Pick any $(t,j) \in \operatorname{dom} q$ and let $0 = t_0 \leqslant t_1 \leqslant \cdots \leqslant t_{j+1} = t$ satisfy $\operatorname{dom} q \cap ([0,t]\times\{0,1,\dots,j\}) = \bigcup_{k=0}^{j}[t_k,t_{k+1}]\times\{k\}$. For each $k \in \{0,\dots,j\}$ and almost all $s \in [t_k,t_{k+1}]$, $q(s,k) \in \mathscr{C}$. Then, (4.59) implies that, for each $k \in \{0,\dots,j\}$ and for almost all $s \in [t_k,t_{k+1}]$,

$$\frac{d}{ds}U(q(s,k)) \leqslant -a_U U(q(s,k)) + a_U\mu + \theta(|v(s)|). \tag{4.60}$$

Applying the comparison principle [85, Lemma 3.4], we obtain, for all $(s,k) \in \operatorname{dom} q$,

$$\begin{aligned} U(q(s,k)) &\leqslant e^{-a_U(s-t_k)}U(q(t_k,k)) + \int_{t_k}^{s}(a_U\mu + \theta(|v(\tau)|))e^{-a_U(s-\tau)}d\tau \\ &\leqslant e^{-a_U(s-t_k)}U(q(t_k,k)) + (a_U\mu + \theta(\|v\|_{[t_k,s]}))\int_{t_k}^{s}e^{-a_U(s-\tau)}d\tau \\ &= e^{-a_U(s-t_k)}U(q(t_k,k)) + (a_U\mu + \theta(\|v\|_{[t_k,s]}))\frac{1}{a_U}(1-e^{-a_U(s-t_k)}) \\ &\leqslant e^{-a_U(s-t_k)}U(q(t_k,k)) + (a_U\mu + \theta(\|v\|_{[0,t]}))\frac{1}{a_U}(1-e^{-a_U(s-t_k)}). \end{aligned} \tag{4.61}$$

Thus,

$$U(q(t_{k+1},k)) \leqslant e^{-a_U(t_{k+1}-t_k)}U(q(t_k,k)) + \mu + \frac{\theta(\|v\|_{[0,t]})}{a_U} - \left(\mu + \frac{\theta(\|v\|_{[0,t]})}{a_U}\right)e^{-a_U(t_{k+1}-t_k)} \tag{4.62}$$

for all $k \in \{0,\dots,j\}$. Similarly, for each $k \in \{1,\dots,j\}$, $q(t_k,k-1) \in \mathscr{D}$. From (4.25) in item *(iii)* of Theorem 4.1, we obtain

$$U(q(t_k,k)) - U(q(t_k,k-1)) \leqslant 0 \quad \forall k \in \{1,\dots,j\}. \tag{4.63}$$

From (4.61), (4.62) and (4.63), we deduce that for any $(t,j) \in \operatorname{dom} q$,

$$U(q(t,j)) \leqslant e^{-a_U t} U(q(0,0)) + \mu + \frac{1}{a_U}\theta(\|v\|_{[0,t]}). \tag{4.64}$$

Finally, using (4.22), we obtain

$$V(x(t,j),z(t,j)) + \sum_{i=1}^{N} d_i \eta_i(t,j) \leqslant e^{-a_U t}\Big(V(x(0,0),z(0,0)) + \sum_{i=1}^{N} d_i \eta_i(0,0)\Big) + \mu + \frac{1}{a_U}\theta(\|v\|_{[0,t]}), \tag{4.65}$$

which concludes the proof. ■

4.5 Properties of the solution domains

We present in this section the properties of the domain of the solutions to system (4.16)-(4.20). In Section 4.5.1, we show that maximal solutions are complete, while in Section 4.5.2 we prove that the time between any two consecutive transmissions of each sensor node is lower-bounded by a uniform strictly positive constant. Finally, we show in Section 4.5.3 that the triggering condition associated to node i stops transmitting whenever the corresponding output y_i remains in a small neighborhood of a constant for all future times, with $i \in \{1,\dots,N\}$.

4.5.1 Completeness of maximal solutions

The results in Theorem 4.1, Proposition 4.2 and Theorem 4.2 are valid on the domain of the solutions, but we did not say anything yet about completeness of maximal solutions. Extra properties on the system plant and the observer are needed for this purpose. In particular, we assume that system (4.1) is forward complete and observer (4.7) has the unboundeness observability property with respect to output $\hat{x}$ [121], as formalized in the next assumption.

Assumption 4.3. *The following hold.*

(i) For any initial condition x_0 in $\mathbb{R}^{n_x}$ and any input $u \in \mathscr{L}_{\mathscr{U}}$, $v \in \mathscr{L}_{\mathscr{V}}$, the maximal solution to (4.1) *is complete.*

(ii) For any input $u \in \mathscr{L}_{\mathscr{U}}$ and $y, \hat{y}, e \in \mathscr{L}_{\mathbb{R}^{n_y}}$, any maximal solution z to system (4.7) *defined on $[0,t^\star)$ with $t^\star := \sup_t \operatorname{dom} q < \infty$ satisfies $\limsup_{t \to t^\star} |\hat{x}(t)| = \infty$.* □

Note that Assumption 4.3 is needed to prove completeness of maximal solutions, but it is not needed for the stability results in Section 4.4 to hold. We are now ready to prove the completeness of maximal solutions of system (4.16)-(4.20).

Theorem 4.3 (Completeness of maximal solutions)**.** *Under Assumptions 4.1, 4.2 and 4.3, any maximal solution to system* (4.16)-(4.20) *is complete.* □

Proof. We exploit [37, Proposition 6], which is recalled in Proposition 2.7 in Chapter 2. Let $w \in \mathscr{L}_{\mathscr{W}}$ and q be a maximal solution to (4.16)-(4.20) with w as input. We denote, for the sake of convenience, $\xi := q(0,0) \in \mathscr{Q}$. By definition of $\mathscr{C}$ and $\mathscr{D}$ in (4.18a)-(4.19b), $\xi \in \mathscr{C} \cup \mathscr{D}$. Suppose $\xi \in \mathscr{C} \backslash \mathscr{D}$, we want to prove that q is not trivial. Since F is continuous and $w \in \mathscr{L}_{\mathscr{W}}$, from [122, Proposition S1] there exist $\epsilon > 0$ and an absolutely continuous function $\mathfrak{z} : [0, \epsilon] \to \mathscr{Q}$ such that $\mathfrak{z}(0) = \xi$, $\dot{\mathfrak{z}}(t) = F(\mathfrak{z}(t), w(t))$ for almost all $t \in [0, \epsilon]$. We now write $\mathfrak{z} = (\mathfrak{z}_x, \mathfrak{z}_z, \mathfrak{z}_e, \mathfrak{z}_\eta)$ where $\mathfrak{z}_e = (\mathfrak{z}_{e_1}, \ldots, \mathfrak{z}_{e_N})$ and $\mathfrak{z}_\eta = (\mathfrak{z}_{\eta_1}, \ldots, \mathfrak{z}_{\eta_N})$. By the definition of F, $\mathfrak{z}_\eta(t) \geqslant 0$ for any $t \in [0, \epsilon]$. Moreover, since $\xi \in \mathscr{C} \backslash \mathscr{D}$, $\mathfrak{z}(0) = \xi$ and $\mathfrak{z}$ is (absolutely) continuous, there exists $\epsilon' \in (0, \epsilon]$ such that, for any $i \in \{1, \ldots, N\}$, $\gamma_i(|\mathfrak{z}_{e_i}(t)|) \leqslant \sigma_i \alpha_i(\mathfrak{z}_{\eta_i}(t)) + \varepsilon_i$ for almost all $t \in [0, \epsilon']$. Consequently, $\mathfrak{z}(t) \in \mathscr{C}$ for almost all $t \in [0, \epsilon']$. We have proved that the viability condition in Proposition 2.7 holds, which implies that q is non-trivial.

To prove that q is complete, we need to exclude items (b) and (c) in Proposition 2.7. Item (c) cannot occur because $G(\mathscr{D}) \subset \mathscr{C} \cup \mathscr{D}$ and the jump set imposes no condition on w. On the other hand, to exclude item (b), q must not blow up in finite time. Hence, each component of q must not blow up in finite time. Let $q = (x, z, e, \eta)$. By Assumption 4.3, we have that x cannot blow up in finite time. Moreover, z cannot do so as well in view of Proposition 4.2 and item (ii) of Assumption 4.3. In addition, e cannot blow up in finite time by its definition and η_i cannot in view of its dynamics (4.14) and because e_i does not, for all $i \in \{1, \ldots, N\}$. Hence, item (b) in Proposition 2.7 cannot occur. Consequently, we conclude that any maximal solution to (4.16)-(4.20) is complete. ■

4.5.2 Minimum individual inter-event time

To exclude the Zeno phenomena, in this section we guarantee the existence of a strictly positive minimum time between any two transmissions of each sensor node, which is an important requirement that is needed in practical applications. Indeed, modern digital hardware cannot implement infinitely fast sampling. For this purpose, we adopt a mild boundedness condition on plant (4.1). As this property is satisfied for each sensor node, and not for the overall system, it is an *individual inter-event time* property, as in [123, Definition 3]. Indeed, simultaneous or arbitrarily close in time transmissions performed by different sensor nodes are allowed, which cannot be avoided due to the decentralized nature of the setting, see Figure 4.1.

We define, like in [123], the set of hybrid times at which a jump occurs due to a transmission of sensor i for $i \in \{1, \ldots, N\}$, as

$$\mathscr{T}_i(q) := \{(t, j) \in \operatorname{dom} q : q(t, j) \in \mathscr{D}_i \text{ and } q(t, j+1) \in G_i(q(t, j))\}. \tag{4.66}$$

From the definition of $\mathscr{C}_i$ and $\mathscr{D}_i$ in (4.18b) and (4.19b), we see that the time between two consecutive transmissions of a specific sensor i is lower-bounded by the time it takes for $|e_i|$ to grow from 0, which is the value after a jump due to sensor i, according to (4.20b), to at least $\gamma_i^{-1}(\varepsilon_i)$. To prove that this time is lower-bounded by a strictly positive constant, we want to exploit the fact that the time derivative of e_i is bounded. For this purpose, recalling that from (4.8) we have $\dot{e}_i =$

$g_i(x,u,v) = g_i(x,w) = -\dfrac{\partial h_i(x)}{\partial x} f_p(x,w)$, we define the following set, for any given $\rho > 0$,

$$\mathcal{S}_\rho := \left\{ (q,w) \in \mathcal{Q} \times \mathcal{W} : \left| \frac{\partial h_i(x)}{\partial x} f_p(x,w) \right| \leqslant \rho, \forall i \in \{1,\dots,N\} \right\}, \tag{4.67}$$

Note that, we can take the same ρ for all $i \in \{1,\dots,N\}$. Indeed, if this is not the case and the set $\mathcal{S}_\rho$ in (4.67) is defined with arbitrarily (large) constants ρ_i, which can be different for $i \in \{1,\dots,N\}$, we can always take $\rho := \max_{i\in\{1,\dots,N\}} \rho_i$, and obtain (4.67). We now restrict the flow and jump sets in (4.18a)-(4.19b) to obtain the following hybrid system

$$\begin{aligned} \dot{q} &= F(q,w), \quad (q,w) \in \mathcal{C}_\rho := (\mathcal{C} \times \mathcal{W}) \cap \mathcal{S}_\rho \\ q^+ &\in G(q), \qquad (q,w) \in \mathcal{D}_\rho := (\mathcal{D} \times \mathcal{W}) \cap \mathcal{S}_\rho. \end{aligned} \tag{4.68}$$

With the sets $\mathcal{C}_\rho$ and $\mathcal{D}_\rho$, we essentially only consider solutions to system (4.16) such that the norm of the derivative of e_i is bounded. Hence, Theorem 4.1, Proposition 4.2 and Theorem 4.2 apply to system (4.68). It is important to notice that the constraint (4.67) does not need to be implemented in the triggering rule: it is only used here for analysis purposes. Moreover, this constraint is always verified as long as the solution to plant (4.1) evolves in a compact set, which is usually the case in practical applications.

In the next theorem we prove the existence of a strictly positive individual minimum inter-event time [123, Definition 3] between any two consecutive transmissions of any sensor node for system (4.68).

Theorem 4.4 (Minimum individual inter-event time)**.** *Consider system* (4.68) *with* $\rho > 0$ *under Assumptions 4.1-4.2. Then, for any input* $w \in \mathcal{L}_\mathcal{W}$*, any solution* q *has an individual minimum inter-event time, in the sense that for any* $i \in \{1,\dots,N\}$ *and any* $(t,j),(t',j') \in \mathcal{T}_i(q)$*,*

$$t + j < t' + j' \implies t' - t \geqslant \tau_i \tag{4.69}$$

with $\tau_i := \dfrac{\gamma_i^{-1}(\varepsilon_i)}{\rho}$*, for all* $i \in \{1,\dots,N\}$*. As a consequence, for any input* $w \in \mathcal{L}_\mathcal{W}$*, any solution* q *to* (4.68) *has an average dwell-time, in the sense that, for any* (t,j)*,* $(t',j') \in \operatorname{dom} q$ *with* $t + j \leqslant t' + j'$*,*

$$j - j' \leqslant \frac{1}{\tau}(t - t') + N \tag{4.70}$$

holds with $\tau := \dfrac{1}{N} \min\{\tau_1,\dots,\tau_N\}$. □

Proof. Let $w \in \mathcal{L}_\mathcal{W}$ and q be a solution to system (4.68). Pick any $(t,j) \in \operatorname{dom} q$ and let $0 = t_0 \leqslant t_1 \leqslant \cdots \leqslant t_{j+1} = t$ satisfy $\operatorname{dom} q \cap ([0,t] \times \{0,1,\dots,j\}) = \bigcup_{k=0}^{j} [t_k, t_{k+1}] \times \{k\}$. For each $k \in \{0,\dots,j\}$ and almost all $s \in [t_k, t_{k+1}]$, $(q(s,k), w(s,k)) \in \mathcal{C}_\rho$. Then, for almost all $s \in [t_k, t_{k+1}]$, from (4.8) and (4.68), $(q(s,k), w(s,k)) \in \mathcal{C}_\rho = (\mathcal{C} \times \mathcal{W}) \cap \mathcal{S}_\rho$ and, in view of

(4.67),

$$\frac{d}{ds}|e_i| = \left|\frac{\partial h_i(x)}{\partial x} f_p(x,w)\right| \leqslant \rho, \tag{4.71}$$

for all $i \in \{1,\dots,N\}$. Let $i \in \{1,\dots,N\}$, from (4.20b), when $(t_k,k) \notin \mathcal{T}_i(q)$, $e_i(t_{k+1},k+1) = e_i(t_k,k)$. Conversely, when $(t_k,k) \in \mathcal{T}_i(q)$, $e_i(t_{k+1},k+1) = 0$.

Let $(t_k,k) \in \mathcal{T}_i(q)$ and $t'_{k'} := \inf\{t \geqslant t_k : |e_i(t,k')| = \gamma_i^{-1}(\varepsilon_i)$ with $k' \geqslant k$ such that $(t,k') \in \operatorname{dom} q\}$. Note that $t'_{k'}$ is not necessary the next time after t_k at which sensor node i generates a transmission, and that, between t_k and $t'_{k'}$ only jumps, which are not due to sensor node i, may occur. Consider that there are $n \in \mathbb{Z}_{\geqslant 0}$ of these jumps. Note that n is finite because of (4.71) and because the sampled induced errors e_i are reset to 0 after a jump, according to (4.20b). From (4.71), we have that for all $m \in [0, n-1]$ and almost all $s \in [t_{k+m}, t_{k+m+1}]$,

$$\frac{d}{ds}|e_i(s,\cdot)| \leqslant \rho. \tag{4.72}$$

Integrating this equation and applying the comparison principle [85, Lemma 3.4], we obtain, for all $m \in [0, n-1]$ and almost all $s \in [t_{k+m}, t_{k+m+1}]$,

$$|e_i(s,k+m)| \leqslant |e_i(t_{k+m},k+m)| + \rho(s - t_{k+m}). \tag{4.73}$$

Similarly, for all $s \in [t_{k+n}, t'_k]$,

$$|e_i(s,k+n)| \leqslant |e_i(t_{k+n},k+n)| + \rho(s - t_{k+n}). \tag{4.74}$$

Moreover, recalling that when $(t_k,k) \notin \mathcal{T}_i(q)$, $e_i(t_{k+1},k+1) = e_i(t_k,k)$, we obtain that, for all $s \in [t_k, t'_k]$

$$|e_i(s,k')| \leqslant |e_i(t_k,k)| + \rho(s - t_k), \tag{4.75}$$

for $k' \in [k, k+n]$, such that $(s,k') \in \operatorname{dom} q$. Moreover, since $(t_k,k) \in \mathcal{T}_i(q)$, $e_i(t_k,k) = 0$ and (4.75) becomes

$$|e_i(s,k')| \leqslant \rho(s - t_k), \quad \forall s \in [t_k, t'_k]. \tag{4.76}$$

As a consequence, the time it takes for $s \mapsto \rho(s - t_k)$ to grow from 0 to $\gamma_i^{-1}(\varepsilon_i)$ is $\tau_i = \dfrac{\gamma_i^{-1}(\varepsilon_i)}{\rho} > 0$, and it lower-bounds $t'_k - t_k$ in view of (4.76).

Let $w \in \mathscr{L}_{\mathscr{W}}$ and q be a solution to system (4.68). Pick any $(t,j),(t',j') \in \operatorname{dom} q$ such that $t + j \leqslant t' + j'$. For any $i \in \{1,\dots,N\}$, denote with $n_i(t,t')$ the number of transmission of node i that occur between (t,j) and (t',j'). In view of the above developments, we have that $n_i(t,t') \leqslant \dfrac{t'-t}{\tau_i} + 1$. Noting that $\sum_{i=1}^{N} n_i(t,t') = j' - j$, we have $j' - j \leqslant \sum_{i=1}^{N}(\dfrac{t'-t}{\tau_i} + 1)$. Using $\tau = \dfrac{1}{N}\min\{\tau_1,\dots,\tau_N\}$ and we obtain $j' - j \leqslant \dfrac{1}{\tau}(t'-t) + N$, which concludes the proof. ■

The event-triggered observer presented in this chapter guarantees a strictly positive individual minimum inter-event time between transmissions according to Theorem 4.4. Therefore, the time

between any two consecutive transmissions of sensor i is always greater or equal than the strictly positive constant τ_i, which can be arbitrarily tuned using the design parameter ε_i. However, the larger τ_i is desired or needed for a practical application, the larger ε_i has to be chosen and consequently, υ in Theorem 4.1 increases. Note that to guarantee the individual minimum inter-transmissions time we do not need Assumption 4.3.

4.5.3 A condition for transmissions to stop

The proposed triggering rules stop the transmissions of sensor i when the sampling-induced error e_i becomes and remains small enough, with $i \in \{1,\dots,N\}$. Moreover, if the sampling-induced errors of all sensors become and remain small enough, no transmissions occurs anymore. This is formalized in the next lemma.

Lemma 4.1 (Stop transmissions)**.** *Under Assumptions 4.1-4.2, consider system* (4.16)*, given a solution q with input $w \in \mathscr{L}_{\mathscr{W}}$, if there exists $(t,j) \in \operatorname{dom} q$ such that*

$$|e_i(t',j')| < \gamma_i^{-1}(\varepsilon_i) \tag{4.77}$$

for all $(t',j') \in \operatorname{dom} q$ with $t'+j' \geqslant t+j$, $i \in \{1,\dots,N\}$, then $\sup_j \mathscr{T}_i(q) < \infty$. In addition, if (4.77) *holds for all $i \in \{1,\dots,N\}$, then $\sup_j \operatorname{dom} q < \infty$.* □

Proof. Let q be a solution to system (4.16) with input $w \in \mathscr{L}_{\mathscr{W}}$. The condition $|e_i(t',j')| < \gamma_i^{-1}(\varepsilon_i)$ for all $(t',j') \in \operatorname{dom} q$ with $t'+j' \geqslant t+j$ in (4.77) implies that

$$\gamma_i(|e_i(t',j')|) < \gamma_i(\gamma_i^{-1}(\varepsilon_i)) = \varepsilon_i \leqslant \sigma_i\alpha_i(\eta_i) + \varepsilon_i \tag{4.78}$$

for all $(t',j') \geqslant (t,j)$ with $(t',j') \in \operatorname{dom} q$. Therefore, no jumps due to sensor i occurs after (t,j). Hence,

$$\sup_j \mathscr{T}_i(q) < \infty. \tag{4.79}$$

Moreover, if the condition $|e_i(t',j')| < \gamma_i^{-1}(\varepsilon_i)$ is satisfied for all $i \in \{1,\dots,N\}$, then, from the first part of this proof we have $\sup_j \mathscr{T}_i(q) < \infty$ for all $i \in \{1,\dots,N\}$. Thus,

$$\max_{i\in\{1,\dots,N\}} \{\sup_j \mathscr{T}_i(q)\} < \infty. \tag{4.80}$$

From (4.19a), (4.19b), a jump can occur only when one or more sensors need to transmit, therefore, from (4.66),

$$\sup_j \operatorname{dom} q = \max_{i\in\{1,\dots,N\}} \{\sup_j \mathscr{T}_i(q)\} < \infty. \tag{4.81}$$

■

Condition (4.77) occurs when the output y_i, $i \in \{1,\dots,N\}$, remains in a small neighborhood of a constant for all positive times for instance. Indeed, when, for some constant $y_i^\star \in \mathbb{R}^{n_{y_i}}$, the output

y_i satisfies $|y_i(t) - y_i^\star| < \frac{1}{2}\gamma_i^{-1}(\varepsilon_i)$ for all $t \geqslant T$ for some $T \geqslant 0$, then for any solution q to (4.16) and any $(t_{j_i}, j_i), (t, j) \in \operatorname{dom} q$, with $(t_{j_i}, j_i - 1) \in \mathcal{T}_i(q)$ and $t_{j_i} \geqslant T$, $t \geqslant t_{j_i}$, $j \geqslant j_i$ and

$$\begin{aligned} |e_i(t,j)| &= |y_i(t_{j_i}, j_i) - y_i(t,j)| \\ &= |y_i(t_{j_i}, j_i) - y_i^\star + y_i^\star - y_i(t,j)| \\ &\leqslant |y_i(t_{j_i}, j_i) - y_i^\star| + |y_i^\star - y_i(t,j)| \\ &< 2\frac{1}{2}\gamma_i^{-1}(\varepsilon_i) \end{aligned} \tag{4.82}$$

and (4.77) holds. Moreover, sensor i automatically starts transmitting again if condition (4.77) is no longer satisfied. This is a clear advantage over time-triggered strategies, where output y_i is always transmitted, even if its information is not needed to perform the estimation; see Figure 3.3 in Chapter 3 for an illustration. It is worth noting that Lemma 4.1 applies to system (4.16), and not only to system (4.68). Therefore, it is not necessary restrict the flow and jump sets with the $\mathcal{S}_\rho$ set in (4.67). Moreover, as for Theorem 4.4, Assumption 4.3 is not needed for this result.

4.6 Extensions

In this section, we discuss generalizations and extensions of the results presented so far. In Section 4.6.1, we explain how the triggering condition can be generalized, while in Section 4.6.2 we discuss the modifications needed in presence of measurement noise. In Section 4.6.3 we consider the case when the input u is sampled and transmitted to the observer via a digital network and we propose a triggering condition for u, which is compatible with the previous results.

4.6.1 Generalized triggering conditions

The η_i-system and the triggering rule in (4.14) and (4.15) are special cases of a more general η_i-system and a more general triggering rule that guarantee the stability results. Indeed, we can design the auxiliary scalar variable η_i with the following dynamics instead of (4.14), for all $i \in \{1, \dots, N\}$,

$$\dot{\eta}_i := -\breve{\alpha}_i(\eta_i) + \breve{\gamma}_i(|e_i|), \tag{4.83}$$

with any $\breve{\alpha}_i \in \mathcal{K}_\infty$ and any $\breve{\gamma}_i \in \mathcal{K}_\infty$. Regarding the triggering rule, let $\mathfrak{d}_i$ be any non-decreasing continuous function from $\mathbb{R}_{\geqslant 0}$ to $\mathbb{R}_{\geqslant 0}$, which can be equal to 0 only at 0. The triggering rule in (4.15) can then be replaced by

$$\gamma_i(|e_i|) + \frac{\partial d_i(\eta_i)}{\partial \eta_i}\breve{\gamma}_i(|e_i|) \leqslant \sigma_i \frac{\partial d_i(\eta_i)}{\partial \eta_i}\breve{\alpha}_i(\eta_i) + \varepsilon_i, \tag{4.84}$$

where $d_i \in \mathcal{K}_\infty$ is defined as $d_i(s) := \int_0^s \mathfrak{d}_i(\tau)d\tau$ for all $s \geqslant 0$ and $\sigma_i \in (0,1)$ for all $i \in \{1, \dots, N\}$. We can then follow the same lines as in Sections 4.4.1-4.4.2 to obtain similar Lyapunov and stability results.

In particular, note that, generalizing the triggering rule in (4.84) implies the definition of new

flow and jump sets, denoted $\breve{\mathscr{C}}$ and $\breve{\mathscr{D}}$. Similarly, the new dynamics for the monitoring variables implies the definition of a new flow map $\breve{F}$. As a consequence, a new hybrid system is defined, for which, similar Lyapunov and stability properties can be established. Indeed, considering the Lyapunov function $\breve{U}(q) := V(x,z) + \sum_{i=1}^{N} d_i(\eta_i)$, for $q \in \mathscr{Q}$, following similar steps as in the proof of Theorem 4.1 we have that there exist $\underline{\breve{\alpha}}_U, \breve{\overline{\alpha}}_U \in \mathscr{K}_\infty$ such that, For any $q \in \mathscr{Q}$,

$$\underline{\breve{\alpha}}_U(|(x-\psi(z),\eta)|) \leqslant \breve{U}(q) \leqslant \breve{\overline{\alpha}}_U(|(\psi^{-R}(x)-z,\eta)|). \tag{4.85}$$

In addition, for any $q \in \breve{\mathscr{D}}$, for any $\mathfrak{g} \in G(q)$,

$$\breve{U}(\mathfrak{g}) \leqslant \breve{U}(q). \tag{4.86}$$

Finally, for any $q \in \breve{\mathscr{C}}$ from (4.12), (4.83) and (4.84) we obtain

$$\begin{aligned}
\left\langle \nabla \breve{U}(q), \breve{F}(q,w) \right\rangle &\leqslant -\alpha(V(x,z)) + \sum_{i=1}^{N} \gamma_i(|e_i|) + \theta(|v|) + \sum_{i=1}^{N} \frac{\partial d_i(\eta_i)}{\partial \eta_i} \left(-\breve{\alpha}_i(\eta_i) + \breve{\gamma}_i(|e_i|)\right) \\
&\leqslant -\alpha(V(x,z)) + \sum_{i=1}^{N} \left(\gamma_i(|e_i|) + \frac{\partial d_i(\eta_i)}{\partial \eta_i} \breve{\gamma}_i(|e_i|)\right) - \sum_{i=1}^{N} \frac{\partial d_i(\eta_i)}{\partial \eta_i} \breve{\alpha}_i(\eta_i) + \theta(|v|) \\
&\leqslant -\alpha(V(x,z)) + \sum_{i=1}^{N} \left(\sigma_i \frac{\partial d_i(\eta_i)}{\partial \eta_i} \breve{\alpha}_i(\eta_i) + \varepsilon_i\right) - \sum_{i=1}^{N} \frac{\partial d_i(\eta_i)}{\partial \eta_i} \breve{\alpha}_i(\eta_i) + \theta(|v|) \\
&\leqslant -\alpha(V(x,z)) - \sum_{i=1}^{N} (1-\sigma_i) \frac{\partial d_i(\eta_i)}{\partial \eta_i} \breve{\alpha}_i(\eta_i) + \sum_{i=1}^{N} \varepsilon_i + \theta(|v|).
\end{aligned} \tag{4.87}$$

Thus, we can prove Lyapunov properties similar to the ones in Theorem 4.1 and, following similar lines as in the proof of Proposition 4.2, we can obtain stability results similar to the ones in Section 4.4.2. Although this sketches the main arguments, we do not provide all the details to avoid repetitions with the previous proofs. Note that, we do not consider this more general setup in the whole chapter to not over-complicate the result and to not blur the main message of the work.

4.6.2 Additive measurement noise

In the case where the system output is affected by additive measurement noise, system (4.1) becomes

$$\begin{aligned}
\dot{x} &= f_p(x,u,v) \\
\tilde{y} &= h(x) + m,
\end{aligned} \tag{4.88}$$

with $m \in \mathscr{L}_{\mathscr{M}}$, where $\mathscr{M} := \mathscr{M}_1 \times \cdots \times \mathscr{M}_N \subseteq \mathbb{R}^{n_{y_1}} \times \cdots \times \mathbb{R}^{n_{y_N}}$. The output measured by sensor i, with $i \in \{1,\ldots,N\}$ is

$$\tilde{y}_i = y_i + m_i \tag{4.89}$$

where $m_i \in \mathscr{L}_{\mathscr{M}_i}$ is the measurement noise of sensor i. We assume that we know a bound on the $\mathscr{L}_\infty$-norm of the measurement noise. Therefore, the set $\mathscr{M}_i$ is defined as

$$\mathscr{M}_i := \{\breve{m}_i \in \mathbb{R}^{n_{y_i}} : |\breve{m}_i| \leqslant \mathfrak{m}_i\} \tag{4.90}$$

for some $\mathfrak{m}_i \in \mathbb{R}_{\geqslant 0}$. Consequently, the observer does not know the real output y_i, but its sampled noisy version, due to the network, $\tilde{\bar{y}}_i := \bar{y}_i + \bar{m}_i$, where $\bar{m}_i$ is the networked version of the measurement noise m_i, with $i \in \{1,\dots,N\}$. Due to the measurement noise, sensor i does not know the network-induced error e_i, but only $\tilde{e}_i$, which is the network-induced error of sensor i in presence of noise, which is defined following [123],

$$\begin{aligned} \tilde{e}_i &:= \tilde{\bar{y}}_i - \tilde{y}_i \\ &= \bar{y}_i + \bar{m}_i - y_i - m_i \\ &= e_i + \bar{m}_i - m_i \end{aligned} \tag{4.91}$$

for all $i \in \{1,\dots,N\}$. As a consequence, the triggering rule cannot rely on e_i, and sensor i needs to decide when the measured output $\tilde{y}_i$ has to be transmitted to the observer based on $\tilde{e}_i$. We therefore replace the dynamic of η_i in (4.14) by $\dot{\tilde{\eta}}_i = -\alpha_i(\tilde{\eta}_i) + c_i\gamma_i(|\tilde{e}_i|)$ and the triggering rule in (4.15) by $\gamma_i(|\tilde{e}_i|) \geqslant \sigma_i\alpha_i(\tilde{\eta}_i) + \varepsilon_i$, for all $i \in \{1,\dots,N\}$. We can then follow similar lines as in [123] to guarantee a practical input-to-state stability property for the estimation error system and a semi-global individual minimum inter-event time. We just need to select $\varepsilon_i > \gamma_i(2\mathfrak{m}_i)$, for all $i \in \{1,\dots,N\}$ and then all the previous results hold. Note that, since, in presence of measurement noise we have a lower-bound on ε_i, for all $i \in \{1,\dots,N\}$, we cannot select υ arbitrary small, as in Theorem 4.1.

The measurement noise can be used to model possible interference in the communication channel due to the simultaneous transmission of two or more sensor nodes. In addition, the impact of possible delays in the received measurements packets can be modeled as addictive measurement noise when the transmission delays smaller than the inter-transmission time. Indeed, denote with t_k^i, $k \in \mathbb{R}_{>0}$, the transmission instants of sensor i, with $i \in \{1,\dots,N\}$ and with $\tau_k^i \in \mathbb{R}_{>0}$ the transmission delay at time t_k^i. Under the small delay assumption, see e.g., [124], we have that the delay τ_k^i is smaller than the inter-event time $t_{k+1}^i - t_k^i$, for all $i \in \{1,\dots,N\}$, $k \in \mathbb{R}_{>0}$. Due to the delay, for all $t \in [t_k^i, t_k^i + \tau_k^i)$ the observer uses $\bar{y}_i(t_{k-1}^i)$ instead of $\bar{y}_i(t_k^i)$. When the transmission is triggered (at time t_k^i), from (4.4) and (4.15), we have

$$|\bar{y}_i(t_{k-1}^i) - y_i(t_k^i)| = |\bar{y}_i(t_{k-1}^i) - \bar{y}_i(t_k^i)| = \gamma_i^{-1}(\sigma_i\alpha_i(\eta_i(t_k^i)) + \varepsilon_i) := \Delta_k^i \in \mathbb{R}_{>0}. \tag{4.92}$$

Thus, for all $t \in [t_k^i, t_k^i + \tau_k^i)$ the observer uses $\bar{y}_i(t_k^i)$ with the error due to the delay, equal to $\bar{y}_i(t_{k-1}^i) - y_i(t_k^i)$, whose norm is smaller than Δ_k^i. As a consequence, $|\bar{y}_i(t_{k-1}^i) - y_i(t_k^i)|$ can be modeled as measurement noise with bounded norm.

4.6.3 Triggering the input u

When the input u to (4.1) is communicated to the observer over a digital network, Assumption 4.1 does not hold. Assuming that the input u is continuously differentiable, we explain how to define a

triggering rule for u in this case so that the previous results apply *mutatis mutandis*.

Let $\bar{u}$ be the networked version of u available to the observer. Between two successive transmission instants, using zero-order-hold device we have

$$\dot{\bar{u}} = 0, \tag{4.93}$$

and when the input is sent,

$$\bar{u}^+ = u. \tag{4.94}$$

We define the input network-induced error e_u as

$$e_u := \bar{u} - u, \tag{4.95}$$

whose dynamics between two successive input transmissions is, assuming u is continuously differentiable,

$$\dot{e}_u = -\dot{u} =: \nu \in \mathbb{R}^{n_u} \tag{4.96}$$

and when an input transmission occurs

$$e_u^+ = 0. \tag{4.97}$$

Consequently, the observer equations in (4.6) becomes

$$\begin{aligned} \dot{z} &= f_o(z, \bar{u}, \bar{y}, \hat{y}) = f_o(z, u + e_u, y + e, \hat{y}), \\ \hat{x} &= \psi(z) \\ \hat{y} &= h(\hat{x}). \end{aligned} \tag{4.98}$$

In this new setting, where also the input is sampled, Assumption 4.2 needs to be modified so that an input-to-state stability property holds also with respect to the input sampled-induced error e_u.

Assumption 4.4. *There exist $\underline{\alpha}$, $\overline{\alpha}$, α, $\gamma_1, \dots, \gamma_N$, θ, $\gamma_u \in \mathscr{K}_\infty$, $V : \mathbb{R}^{n_x} \times \mathbb{R}^{n_z} \to \mathbb{R}_{\geqslant 0}$ continuously differentiable, such that for all $x \in \mathbb{R}^{n_x}$, $z \in \mathbb{R}^{n_z}$, $u \in \mathbb{R}^{n_u}$, $e \in \mathbb{R}^{n_y}$, $\hat{y} \in \mathbb{R}^{n_y}$, $\nu \in \mathbb{R}^{n_\nu}$, $e_u \in \mathbb{R}^{n_u}$, (4.11) holds and*

$$\underline{\alpha}(|x - \psi(z)|) \leqslant V(x,z) \leqslant \overline{\alpha}(|\psi^{-R}(x) - z|) \tag{4.99}$$

$$\left\langle \nabla V(x,z), (f_p(x,u,\nu), f_o(z, u + e_u, y + e, \hat{y})) \right\rangle \leqslant -\alpha(V(x,z)) + \sum_{i=1}^{N} \gamma_i(|e_i|) + \theta(|\nu|) + \gamma_u(|e_u|). \tag{4.100}$$

□

For many classes of observers in the literature, if the observer is input-to-state stable with respect to ν, then it is also input-to-state stable with respect to e_u, see [9] for more details.

Based on Assumption 4.4, we can design the triggering rule for the input similarly to the triggering rule designed in (4.15) for the output y_i, with $i \in \{1, \dots, N\}$. In particular, let η_u be an auxiliary

scalar variable, whose equations during flows and jumps are, respectively,

$$\begin{aligned} \dot{\eta}_u &= -\alpha_u(\eta_u) + c_u\gamma_u(|e_u|) =: \ell_u(\eta_u, e_u) \\ \eta_u^+ &= b_u\eta_u \end{aligned} \tag{4.101}$$

where γ_u comes from Assumption 4.4 and $\alpha_u \in \mathscr{K}_\infty$, $c_u \geqslant 0$ and $b_u \in [0,1]$ are design function and parameters. An input data is transmitted to the observer when the condition

$$\gamma_u(|e_u|) \geqslant \sigma_u\alpha_u(\eta_u) + \varepsilon_u \tag{4.102}$$

is satisfied, where $\sigma_u \geqslant 0$ and $\varepsilon_u > 0$ are design parameters. As for the output triggering rule, parameter ε_u is needed to avoid the Zeno phenomena. In this new setting, all previous stability results apply similarly. Moreover, to have an individual minimum inter-event time a sufficient condition is that the input u is continuously differentiable and $|\dot{u}| \leqslant \rho_u$, where ρ_u is any positive constant. For completeness, we now present how the hybrid model is modified and we show how the statement of the main results need to be adapted when also the input is sampled and transmitted over a digital network. The proofs follow similar lines as the ones provided in the previous sections and are thus omitted.

In the setting where also the input is communicated via a digital network, following similar lines as before, we can model the overall system as a new hybrid system, whose state is defined as $\tilde{q} := (x, z, e, \eta, \eta_u, e_u) \in \tilde{\mathscr{Q}} = \mathbb{R}^{n_x} \times \mathbb{R}^{n_z} \times \mathbb{R}^{n_y} \times \mathbb{R}^N_{\geqslant 0} \times \mathbb{R}_{\geqslant 0} \times \mathbb{R}^{n_u}$. We define a new overall input for the new hybrid system as $\tilde{w} := (u, v, \nu) \in \tilde{\mathscr{W}} := \mathscr{U} \times \mathscr{U} \times \mathscr{V}$. The hybrid model (4.16) is modified and become

$$\begin{aligned} \dot{\tilde{q}} &= \tilde{F}(\tilde{q}, \tilde{w}), \qquad & \tilde{q} &\in \tilde{\mathscr{C}} \\ \tilde{q}^+ &\in \tilde{G}(\tilde{q}), & \tilde{q} &\in \tilde{\mathscr{D}}, \end{aligned} \tag{4.103}$$

where the flow map $\tilde{F}$ is defined as, for any $\tilde{q} \in \tilde{\mathscr{C}}$ and any $\tilde{w} \in \tilde{\mathscr{W}}$,

$$\tilde{F}(\tilde{q}, \tilde{w}) := \begin{cases} f_p(x, u, v) \\ f_o(z, u + e_u, h(x) + e, h(\psi(z))) \\ g(x, u, v) \\ \ell(\eta, e) \\ \ell_u(\eta_u, e_u) \\ \nu \end{cases} \tag{4.104}$$

where $f_p(x,u,v), g(x,u,v)$ and $\ell(\eta,e)$ are defined in (4.1) and (4.17), while $f_o(z, u + e_u, h(x) + e, h(\psi(z)))$, $\ell_u(\eta_u, e_u)$ and ν are defined in (4.98), (4.101) and (4.96), respectively.

The flow set $\tilde{\mathscr{C}}$ in (4.103) is defined as

$$\tilde{\mathscr{C}} := \left(\bigcap_{i=1}^{N} \mathscr{C}_i \right) \bigcap \mathscr{C}_u \tag{4.105a}$$

with $\mathscr{C}_i$ defined as

$$\mathscr{C}_i := \Big\{\tilde{q} \in \tilde{\mathscr{Q}} : \gamma_i(|e_i|) \leqslant \sigma_i \alpha_i(\eta_i) + \varepsilon_i\Big\}, \tag{4.105b}$$

for all $i \in \{1, \dots, N\}$ and $\mathscr{C}_u$ defined as

$$\mathscr{C}_u := \Big\{\tilde{q} \in \tilde{\mathscr{Q}} : \gamma_u(|e_u|) \leqslant \sigma_u \alpha_u(\eta_u) + \varepsilon_u\Big\}. \tag{4.105c}$$

The jump set $\tilde{\mathscr{D}}$ in (4.103) is defined as

$$\tilde{\mathscr{D}} := \left(\bigcup_{i=1}^{N} \mathscr{D}_i\right) \bigcup \mathscr{D}_u \tag{4.106a}$$

with

$$\mathscr{D}_i := \Big\{\tilde{q} \in \tilde{\mathscr{Q}} : \gamma_i(|e_i|) \geqslant \sigma_i \alpha_i(\eta_i) + \varepsilon_i\Big\}, \tag{4.106b}$$

for all $i \in \{1, \dots, N\}$ and

$$\mathscr{D}_u := \Big\{\tilde{q} \in \tilde{\mathscr{Q}} : \gamma_u(|e_u|) \geqslant \sigma_u \alpha_u(\eta_u) + \varepsilon_u\Big\}. \tag{4.106c}$$

The set-valued jump map $\tilde{G}$ in (4.103) is defined as, for any $\tilde{q} \in \tilde{\mathscr{D}}$,

$$\tilde{G}(\tilde{q}) := \left(\bigcup_{i=1}^{N} \tilde{G}_i(\tilde{q})\right) \bigcup \tilde{G}_u(\tilde{q}), \tag{4.107a}$$

with

$$\tilde{G}_i(\tilde{q}) := \begin{cases} \left\{\begin{array}{c} x \\ z \\ \Lambda_i e \\ (b_i(I_N - \Gamma_i) + \Gamma_i)\eta \\ \eta_u \\ e_u \end{array}\right\} & \tilde{q} \in \tilde{\mathscr{D}}_i \\ \varnothing & \tilde{q} \notin \tilde{\mathscr{D}}_i \end{cases} \text{ and } \tilde{G}_u(\tilde{q}) := \begin{cases} \left\{\begin{array}{c} x \\ z \\ e \\ \eta \\ b_u \eta_u \\ 0 \end{array}\right\} & \tilde{q} \in \tilde{\mathscr{D}}_u \\ \varnothing & \tilde{q} \notin \tilde{\mathscr{D}}_u, \end{cases} \tag{4.107b}$$

where Λ_i and Γ_i are defined in (4.20b).

Following similar lines as before, in the next theorem and proposition we adapt the stability results of Theorem 4.1 and Proposition 4.2 to the case where also the input is transmitted from the plant to the observer via a digital network.

Theorem 4.5 (Lyapunov stability property)**.** *Suppose Assumption 4.4 holds and consider system* (4.103) - (4.107). *For any* $\tilde{\upsilon} > 0$, *select* $\sigma_i^\star > 0$, $c_i^\star \geqslant 0$, $\sigma_u^\star > 0$, $c_u^\star \geqslant 0$ *such that* $\sigma_i^\star c_i^\star < 1$, $\sigma_u^\star c_u^\star < 1$ *and* $d_i > d_i^\star$ *where* $d_i^\star := \dfrac{\sigma_i^\star}{1 - \sigma_i^\star c_i^\star} > 0$, $d_u > d_u^\star$ *where* $d_u^\star := \dfrac{\sigma_u^\star}{1 - \sigma_u^\star c_u^\star} > 0$, *and select* $\varepsilon_i^\star > 0$, $\varepsilon_u^\star > 0$

such that $\sum_{i=1}^{N}(1+d_i c_i^\star)\varepsilon_i^\star + (1+d_u c_u^\star)\varepsilon_u^\star \leqslant \tilde{\upsilon}$, *for all* $i \in \{1,\dots,N\}$. *Define*

$$\tilde{U}(\tilde{q}) := V(x,z) + \sum_{i=1}^{N} d_i \eta_i + d_u \eta_u, \tag{4.108}$$

for any $\tilde{q} \in \tilde{\mathcal{Q}}$. *Then, there exist* $\underline{\tilde{\alpha}}_U, \overline{\tilde{\alpha}}_U \in \mathcal{K}_\infty$ *such that the following properties hold for any* $\alpha_i \in \mathcal{K}_\infty$ *in* (4.14), $\alpha_u \in \mathcal{K}_\infty$ *in* (4.101), $\sigma_i \in [0,\sigma_i^\star]$, $\sigma_u \in [0,\sigma_u^\star]$, $c_i \in [0,c_i^\star]$, $c_u \in [0,c_u^\star]$, $\varepsilon_i \in (0,\varepsilon_i^\star]$, $\varepsilon_u \in (0,\varepsilon_u^\star]$, $b_i \in [0,1]$ *and* $b_u \in [0,1]$, *for all* $i \in \{1,\dots,N\}$.

(i) For any $\tilde{q} \in \tilde{\mathcal{Q}}$,

$$\underline{\tilde{\alpha}}_U(|(x-\psi(z),\eta,\eta_u)|) \leqslant \tilde{U}(\tilde{q}) \leqslant \overline{\tilde{\alpha}}_U(|(\psi^{-R}(x)-z,\eta,\eta_u)|). \tag{4.109}$$

(ii) For any $\tilde{q} \in \tilde{\mathcal{C}}$ *and any* $\tilde{w} \in \tilde{\mathcal{W}}$,

$$\left\langle \nabla \tilde{U}(\tilde{q}), \tilde{F}(\tilde{q},w) \right\rangle \leqslant -\alpha(V(x,z)) - \sum_{i=1}^{N} \delta_i \alpha_i(\eta_i) - \delta_u \alpha_u(\eta_u) + \tilde{\upsilon} + \theta(|\nu|), \tag{4.110}$$

where α, $\theta \in \mathcal{K}_\infty$ *come from Assumption 4.2,* $\delta_i := d_i - \sigma_i^\star(1+d_i c_i^\star) > 0$ *and* $\delta_u := d_u - \sigma_u^\star(1+d_u c_u^\star) > 0$.

(iii) For any $\tilde{q} \in \tilde{\mathcal{D}}$, *for any* $\tilde{\mathfrak{g}} \in \tilde{G}(\tilde{q})$,

$$\tilde{U}(\tilde{\mathfrak{g}}) \leqslant \tilde{U}(\tilde{q}). \tag{4.111}$$

□

Proposition 4.3 (Global practical stability property)**.** *Consider system* (4.103) - (4.107) *and suppose Assumption 4.4 holds. For any* $\tilde{\upsilon} > 0$, *select* α_i, α_u, σ_i, σ_u, c_i, c_u, ε_i, ε_u, d_i, d_u, b_i *and* b_u *as in Theorem 4.5 for all* $i \in \{1,\dots,N\}$. *Then there exist* $\tilde{\beta}_U^\star \in \mathcal{KL}$ *and* $\tilde{\gamma}_U^\star$, *all independent of* $\tilde{\upsilon}$, *such that, for any input input* $\tilde{w} \in \mathcal{L}_{\tilde{\mathcal{W}}}$, *any solution* $\tilde{q}$ *satisfies, for all* $(t,j) \in \operatorname{dom}\tilde{q}$,

$$\begin{aligned} &|(x(t,j)-\hat{x}(t,j),\eta(t,j),\eta_u(t,j)| \\ &\qquad \leqslant \tilde{\beta}_U^\star(|(\psi^{-R}(x(0,0))-z(0,0),\eta(0,0),\eta_u(0,0)|,t) + \tilde{\gamma}_U^\star(\tilde{\upsilon}+\theta(\|\nu\|_{[0,t]})), \end{aligned} \tag{4.112}$$

with $\theta \in \mathcal{K}_\infty$ *from Assumption 4.4.* □

The proofs Theorem 4.5 and Proposition 4.3 follow similar lines as the proofs of Theorem 4.1 and Proposition 4.2, respectively. Therefore, they are omitted to avoid repetitions with the previous proofs. In the case where also the input is sampled and transmitted via a digital network, following similar steps as before, we can state and prove stability properties similar to the ones in Proposition 4.1 and Theorem 4.2. We do not write them explicitly to not be repetitive. In addition, the properties of the solution domain presented in Section 4.5 need to be modified when also the input is transmitted via a digital network. In particular, we now state the adaptation of Theorem 4.3, where the only difference is the considered input-to-state stability assumption.

Theorem 4.6 (Completeness of maximal solutions)**.** *Under Assumptions 4.3 and 4.4, any maximal solution to system* (4.103)-(4.107) *is complete.* □

The proof of Theorem 4.6 is omitted since it follows similar lines as the proof of Theorem 4.3.

In the case of triggered input, also the inter-event time properties in Section 4.5.2 need to be modified. The set $\mathcal{T}_i$, defined in (4.66), of hybrid times at which a jump occurs due to a transmission of sensor i for $i \in \{1,\dots,N\}$ is now redefined as

$$\tilde{\mathcal{T}}_i(\tilde{q}) := \{(t,j) \in \operatorname{dom}\tilde{q} : \tilde{q}(t,j) \in \tilde{\mathcal{D}}_i \text{ and } \tilde{q}(t,j+1) \in \tilde{G}_i(\tilde{q}(t,j))\}. \tag{4.113a}$$

Moreover, we need to define the set of hybrid times at which a jump corresponds to an input transmission

$$\tilde{\mathcal{T}}_u(\tilde{q}) := \{(t,j) \in \operatorname{dom}\tilde{q} : \tilde{q}(t,j) \in \tilde{\mathcal{D}}_u \text{ and } \tilde{q}(t,j+1) \in \tilde{G}_u(\tilde{q}(t,j))\}. \tag{4.113b}$$

To guarantee an individual minimum inter-transmission time, in (4.67) we have defined a set where the time derivative of the sampling induced-error for all sensor nodes is bounded. Then, we used this set to define new flow and jump sets for the hybrid system in (4.68). In case when also the input is transmitted via a digital network, we need not only that the time derivative of the sampling induced-error for all sensor nodes is bounded but also that the time derivative of the input is bounded. Therefore, we define the following set, for any given $\rho > 0$ and $\rho_u > 0$,

$$\tilde{\mathcal{S}}_\rho := \left\{(\tilde{q},\tilde{w}) \in \tilde{\mathcal{Q}} \times \tilde{\mathcal{W}} : |v| \leqslant \rho_u \text{ and } \left|\frac{\partial h_i(x)}{\partial x} f_p(x,u,v)\right| \leqslant \rho, \quad \forall i \in \{1,\dots,N\}\right\}, \tag{4.114}$$

Similarly to Section 4.5.2, we now restrict the flow and jump sets in (4.105a) - (4.106c) and we obtain the following hybrid system

$$\begin{aligned} \dot{\tilde{q}} &= \tilde{F}(\tilde{q},\tilde{w}), && (\tilde{q},\tilde{w}) \in \tilde{\mathcal{C}}' := (\tilde{\mathcal{C}} \times \tilde{\mathcal{W}}) \cap \tilde{\mathcal{S}}_\rho \\ \tilde{q}^+ &\in \tilde{G}(\tilde{q}), && (\tilde{q},\tilde{w}) \in \tilde{\mathcal{D}}' := (\tilde{\mathcal{D}} \times \tilde{\mathcal{W}}) \cap \tilde{\mathcal{S}}_\rho. \end{aligned} \tag{4.115}$$

We can now adapt the results presented in Theorem 4.4 and Lemma 4.1 for the case where also the input is triggered and transmitted via a digital network.

Theorem 4.7 (Minimum individual inter-event time)**.** *Consider system* (4.115) *with $\rho > 0$ and $\rho_u > 0$ under Assumption 4.4. Then, for any input $\tilde{w} \in \mathcal{L}_{\tilde{\mathcal{W}}}$, any solution $\tilde{q}$ has an individual minimum inter-event time, in the sense that for any $i \in \{1,\dots,N\}$ and any $(t,j),(t',j') \in \tilde{\mathcal{T}}_i(\tilde{q})$,*

$$t + j < t' + j' \implies t' - t \geqslant \tau_i \tag{4.116}$$

with $\tau_i := \dfrac{\gamma_i^{-1}(\varepsilon_i)}{\rho} > 0$, for all $i \in \{1,\dots,N\}$ and for any solution $\tilde{q}$ with input $\tilde{w} \in \mathcal{L}_{\tilde{\mathcal{W}}}$ and any $(t,j),(t'',j'') \in \tilde{\mathcal{T}}_u(\tilde{q})$

$$t + j < t'' + j'' \implies t'' - t \geqslant \tau_u \tag{4.117}$$

with $\tau_u := \dfrac{\gamma_u^{-1}(\varepsilon_u)}{\rho_u} > 0$. *As a consequence, for any input* $\tilde{w} \in \mathscr{L}_{\tilde{\mathscr{W}}}$, *any solution* $\tilde{q}$ *to* (4.115) *has an average dwell-time, in the sense that, for any* (t,j), $(t',j') \in \operatorname{dom}\tilde{q}$ *with* $t+j \leqslant t'+j'$,

$$j - j' \leqslant \frac{1}{\tilde{\tau}}(t-t') + N + 1 \tag{4.118}$$

holds with $\tilde{\tau} := \dfrac{1}{N+1}\min\{\tau_1,\dots,\tau_N,\tau_u\}$. □

Lemma 4.2 (Stop transmissions). *Consider system* (4.103) *under Assumption 4.4. Given a solution* $\tilde{q}$ *with input* $\tilde{w} \in \mathscr{L}_{\tilde{\mathscr{W}}}$, *if there exists* $(t,j) \in \operatorname{dom}\tilde{q}$, *such that*

$$|e_i(t',j')| < \gamma_i^{-1}(\varepsilon_i) \tag{4.119}$$

for all $(t',j') \in \operatorname{dom}\tilde{q}$ *with* $t'+j' \geqslant t+j$, $i \in \{1,\dots,N\}$, *then* $\sup_j \mathscr{T}_i(\tilde{q},\tilde{w}) < \infty$. *Moreover, if there exists* $(t,j) \in \operatorname{dom}\tilde{q}$, *such that*

$$|e_u(t'',j'')| < \gamma_u^{-1}(\varepsilon_u) \tag{4.120}$$

for all $(t'',j'') \in \operatorname{dom}\tilde{q}$ *with* $t''+j'' \geqslant t+j$, *then* $\sup_j \mathscr{T}_u(\tilde{q},\tilde{w}) < \infty$. *In addition, if* (4.119) *holds for all* $i \in \{1,\dots,N\}$ *and* (4.120) *holds, then* $\sup_j \operatorname{dom}\tilde{q} < \infty$. □

The proofs of Theorem 4.7 and Lemma 4.2 follow similar steps as the proofs of Theorem 4.4 and Lemma 4.1, respectively. Thus they are omitted to avoid repetitions with the previous proofs.

In this section we have generalized the previous results considering the case where the input u is communicated to the observer over a digital network. The setup can be further generalized considering multiple actuator nodes, similarly to the decentralized setting considered for the output sensor nodes. In particular, we can consider the scenario where there are N_u actuator nodes and each of them communicates its own control input u_k, $k \in \{1,\dots,N_u\}$, where $N_u \in \{1,\dots,n_u\}$, independently from the others. We do not do it explicitly since it follows similar lines as the decentralized scenario we have considered for the output sensor nodes. Moreover, providing details on this generalization would complicate the result and thus risk hiding the main contribution of the work.

4.7 Numerical case study

We design the event-triggered observer presented in this chapter to a flexible joint robotic arm [125]. Note that, we assume that the observer has access to the input continuously in this example. However, it would have been possible to consider the setting where also the input is transmitted via a digital network, as described in Section 4.6.3. For this application, our framework is relevant in scenarios where the observer is not co-located with the robotic arm and communicates with it through a digital network. In this case study, we consider two sensor nodes, but the results would also be relevant if we would have only one node. The system model is described by

$$\begin{aligned} \dot{x} &= Ax + Bu + G\sigma(Hx) + v \\ y &= Cx + m, \end{aligned} \tag{4.121a}$$

where the system state that need to be estimated is $x := (x_1, x_2, x_3, x_4)$, while the measured output y is defined as $y := (y_1, y_2) = (x_1, x_2)$. The system matrices are

$$A = \begin{bmatrix} 0 & 1 & 0 & 0 \\ -48.6 & -1.25 & 48.6 & 0 \\ 0 & 0 & 0 & 1 \\ 19.5 & 0 & -19.5 & 0 \end{bmatrix}, B = \begin{bmatrix} 0 \\ 21.6 \\ 0 \\ 0 \end{bmatrix}, G = \begin{bmatrix} 0 \\ 0 \\ 0 \\ -1 \end{bmatrix}, H^\top = \begin{bmatrix} 0 \\ 0 \\ 1 \\ 0 \end{bmatrix}, C^\top = \begin{bmatrix} 1 & 0 \\ 0 & 1 \\ 0 & 0 \\ 0 & 0 \end{bmatrix}, \tag{4.121b}$$

and $\sigma(Hx) = 3.3\sin(x_3)$ for any $x \in \mathbb{R}^4$. As in [125], we assume that the input is $u(t) = \sin(t)$ for all $t \in \mathbb{R}_{\geqslant 0}$. Moreover, we consider the disturbance input $v(t) = 0.02[0\ 1\ 0\ 1]^\top \sin(0.4t)$ for all $t \in \mathbb{R}_{\geqslant 0}$ and the measurement noise $m(t) = 0.01[0\ 1]^\top \sin(0.3t)$ for all $t \in \mathbb{R}_{\geqslant 0}$. We design a continuous-time observer

$$\begin{aligned} \dot{\hat{x}} &= A\hat{x} + Bu + G\sigma(H\hat{x}) + L(y - \hat{y}) \\ \hat{y} &= C\hat{x}, \end{aligned} \tag{4.122}$$

where $L \in \mathbb{R}^{4\times 2}$ is the observer gain that is designed following a polytopic approach [95], as described in Section 2.2.3. To do so, we solve the linear matrix inequalities $PA - WC + PG_i + G_i^\top P + A^\top P - C^\top W^\top \leqslant -Q$, $i \in \{1,2\}$, with $P \in \mathbb{R}^{4\times 4}$ symmetric positive definite and $W := PL \in \mathbb{R}^{4\times 2}$, where $G_1 := \begin{bmatrix} 0 & 0 & 0 & 0 \\ 0 & 0 & 0 & 0 \\ 0 & 0 & 0 & 0 \\ 0 & 0 & 3.3 & 0 \end{bmatrix}$, $G_2 := \begin{bmatrix} 0 & 0 & 0 & 0 \\ 0 & 0 & 0 & 0 \\ 0 & 0 & 0 & 0 \\ 0 & 0 & -3.3 & 0 \end{bmatrix}$ and $Q = I_4$. We obtain $L = \begin{bmatrix} 0.58 & -42.96 \\ -4.67 & 2.83 \\ 3.16 & 49.25 \\ 16.34 & 88.46 \end{bmatrix}$. Note that, observer (4.122) is in the form of (4.2) with $z = \hat{x}$. Defining the Lyapunov function $V(\xi) := \xi^\top P \xi$ for any $\xi \in \mathbb{R}^4$, where $\xi := x - \hat{x}$ is the state estimation error, Assumption 4.2 is satisfied with $\alpha(s) = \dfrac{\lambda_{\min}(Q) - \mathfrak{c}_v - \mathfrak{c}_1 - \mathfrak{c}_2}{\lambda_{\max}(P)} s$, $\theta(s) = \dfrac{1}{\mathfrak{c}_v}\|P\|^2 |s|^2$, $\gamma_1(s) = \dfrac{1}{\mathfrak{c}_1}\|PL_1\|^2 |s|^2$ and $\gamma_2(s) = \dfrac{1}{\mathfrak{c}_2}\|PL_2\|^2 |s|^2$, where $\mathfrak{c}_v, \mathfrak{c}_1, \mathfrak{c}_2$ are parameters chosen such that $\mathfrak{c}_v > 0, \mathfrak{c}_1 > 0, \mathfrak{c}_2 > 0$ and $\lambda_{\min}(Q) - \mathfrak{c}_v - \mathfrak{c}_1 - \mathfrak{c}_2 > 0$, while L_1 and L_2 are the first and the second column of the matrix gain L, respectively.

We have first simulated the event-triggered observer (4.16)-(4.20) with $\sigma_1 = 600$, $\sigma_2 = 800$, $c_1 = 0.001$, $c_2 = 0.001$, $b_1 = 1$, $b_2 = 1$, $\alpha_1(s) = a_1 s$, with $a_1 = 2$, $\alpha_2(s) = a_2 s$, with $a_2 = 3$, $\varepsilon_1 = 10$ and $\varepsilon_2 = 10$. With this choice of parameters the conditions $\sigma_1 c_1 < 1$ and $\sigma_2 c_2 < 1$ are satisfied and Theorems 4.1 and 4.2 apply. Moreover, the condition $\left|\dfrac{\partial h_i(x)}{\partial x} f_p(x,w)\right| \leqslant \rho$ is satisfied for $i \in \{1,2\}$, for ρ large enough and Theorem 4.4 applies. Thanks to the freedom on the choice of γ_i in Remark 4.1, we do not need to use γ_1, γ_2 coming from Assumption 4.2, as explained in Section 4.3, but we can select any γ_1, γ_2 such that $\gamma_1(s) = \mathfrak{l}_1 s^2$ and $\gamma_2(s) = \mathfrak{l}_2 s^2$, with $\mathfrak{l}_1 > 0$ and $\mathfrak{l}_2 > 0$, which are thus additional design parameters. We select $\gamma_1(s) = 5s^2$ and $\gamma_2(s) = 5s^2$.

We have considered the following initial conditions $x(0,0) = (3,2,3,-2)$, $\hat{x}(0,0) = (0,0,0,0)$, $e(0,0) = (0,0)$ and $\eta(0,0) = (10,10)$. In Figure 4.3, we provide the plots obtained for the plant states and its estimates, in Figure 4.4 the plots of the state estimation errors, whose norm is shown in Figure 4.5. In Figure 4.6 the inter-transmissions time is reported. From these figures, it is clear that

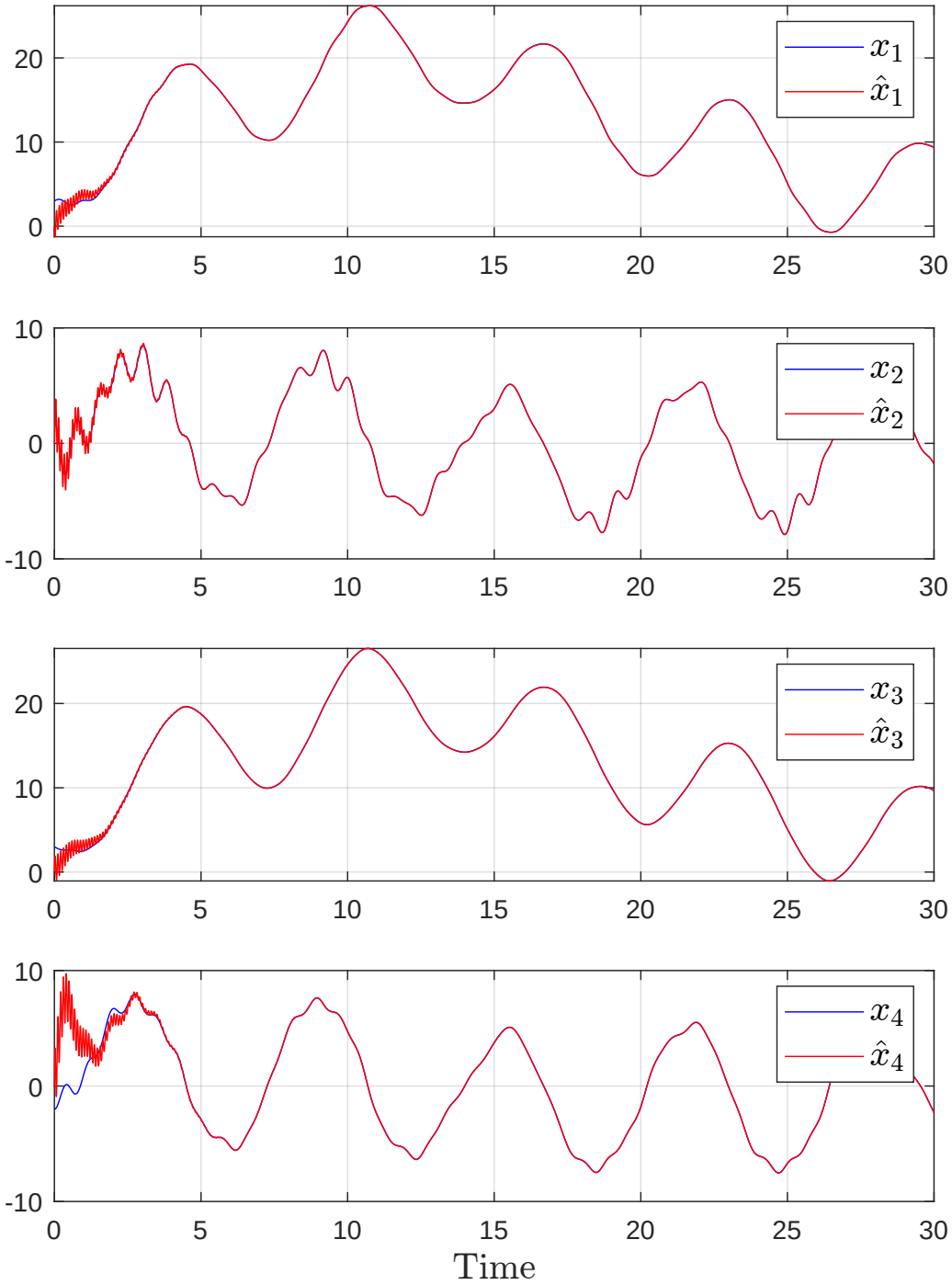

FIGURE 4.3 – State x and state estimate $\hat{x}$.

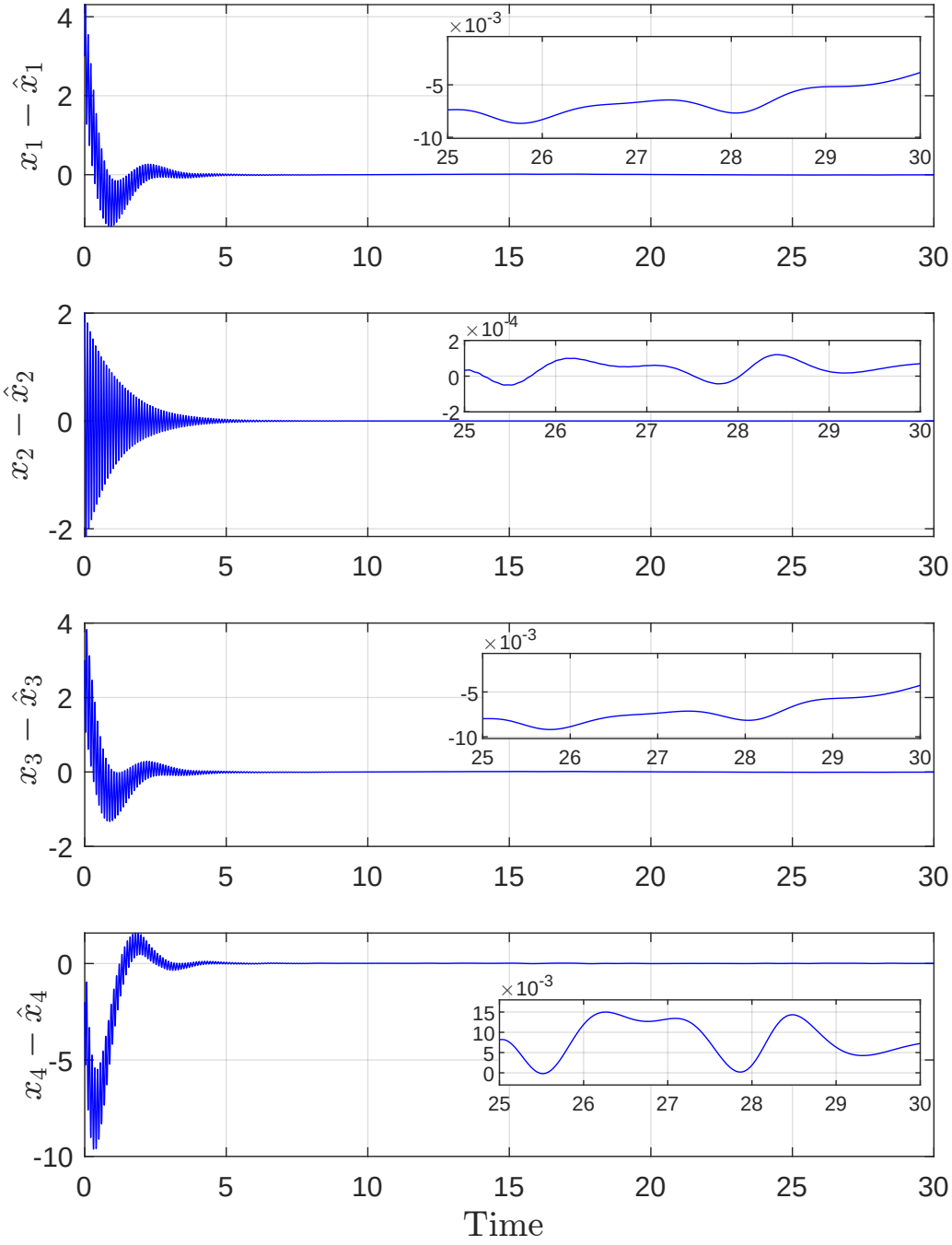

FIGURE 4.4 – State estimation errors $x_i - \hat{x}_i$, $i \in \{1, \ldots, 4\}$.

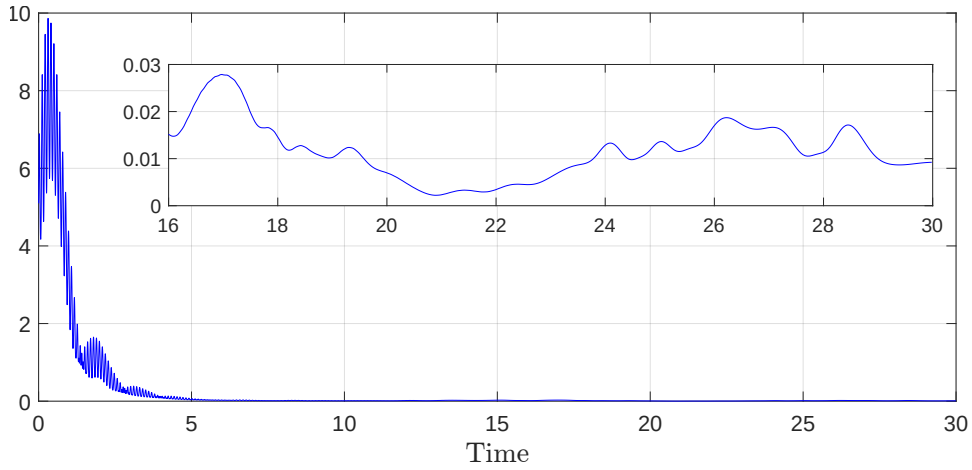

FIGURE 4.5 – Norm of the state estimation error $|\xi| := |x - \hat{x}|$.

all state estimation error practically converge. Moreover, the minimum inter-event time measured is 0.201 s for sensor 1 and 0.112 s for sensor 2.

We have also analyzed the impact of the design parameters, in particular we focus on the effect of σ_1, σ_2, ε_1, ε_2, a_1, a_2, $\mathfrak{l}_1$ and $\mathfrak{l}_2$. We have run for this purpose simulations with different parameters configurations and 100 different initial conditions for each chosen parameters configuration. In particular, $x_1(0,0)$ and $x_3(0,0)$ were selected randomly in the interval $[0,20]$, while $x_2(0,0)$ and $x_4(0,0)$ were chosen randomly in the interval $[0,10]$. The initial conditions of the observer states $\hat{x}_1(0,0), \hat{x}_2(0,0), \hat{x}_3(0,0), \hat{x}_4(0,0)$ and of the network-induced errors $e_1(0,0), e_2(0,0)$ were always selected equal to 0, while $\eta_1(0,0) = \eta_2(0,0) = 10$ in all simulations. For all the choice of parameters, we have evaluated the number of transmissions in the (continuous) time interval $[0,30]$ on average and the maximum ultimate bound on the state estimation error in the time interval $[20,30]$ averaged over all simulations. The data collected are shown in Table 4.1. The same analysis was repeated also in the case where the system is not affected by the disturbance input v and the measurement noise m. In Table 4.1 the data collected in this configuration are also reported.

Table 4.1 shows that choice of the design parameters impacts the average number of transmissions both when the system is affected by the additional disturbance input v and measurement noise m and when it is not. Moreover, data shows that the ultimate bound of the estimation error is small in all the chosen configurations and that the obtained values are not significantly affected by the choice of the parameters in presence of noise m and disturbance v, but this is no longer true when those are absent.

4.8 Conclusions

We have presented a decentralized event-triggered observer design for perturbed nonlinear systems. We have designed for this purpose new dynamic triggering rules for each sensor node to define the transmissions over the digital network. We have formally established a uniform global practical stability property for the estimation error and we guarantee the existence of a uniform, strictly posi-

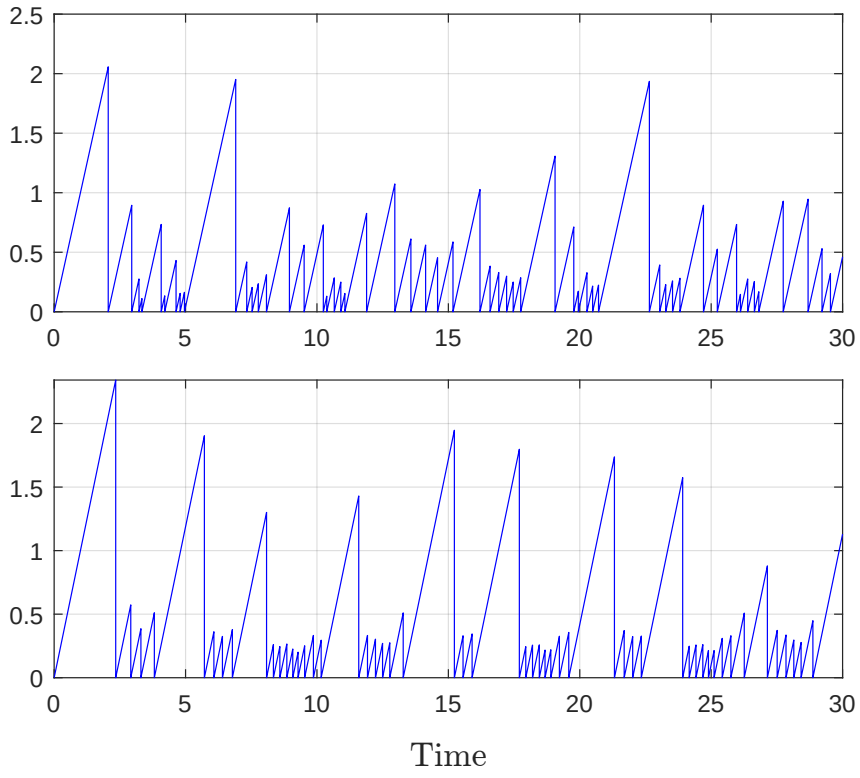

FIGURE 4.6 – Inter-transmissions times (sensor 1 top, sensor 2 bottom).

tive time between any two transmissions of each sensor node. Moreover, the proposed triggering rule does not require significant computation capability on the smart sensor, as it only needs to run a local scalar filter. We have also shown how the triggering rule can be generalized and how to cope with measurement noise and/or sampled input. Possible future research directions are discussed in Chapter 7. This chapter concludes Part I of the thesis. In the next part we present a hybrid multi-observer to improve the estimation performance.

TABLE 4.1 – Average number of transmissions in the time interval $[0, 30]$ and maximum absolute value of the state estimation error $|\xi|$ for $t \in [20, 30]$ with different choices for σ_1, σ_2, ε_1, ε_2, a_1, a_2, $\mathfrak{l}_1$ and $\mathfrak{l}_2$, both with and without disturbance input and measurement noise.

σ_1	σ_2	ε_1	ε_2	a_1	a_2	$\mathfrak{l}_1$	$\mathfrak{l}_2$	Transmissions with v and m	$\lvert\xi\rvert$ with v and m	Transmissions without v and m	$\lvert\xi\rvert$ without v and m
600	800	10	10	2	3	5	5	163	0.0236	167	$6.32 \cdot 10^{-5}$
600	800	1	1	2	3	5	5	497	0.0235	515	$2.13 \cdot 10^{-5}$
600	800	100	100	2	3	5	5	47	0.0236	49	$2.34 \cdot 10^{-4}$
600	800	1000	1000	2	3	5	5	10	0.0234	7	$2.63 \cdot 10^{-4}$
0	0	10	10	2	3	5	5	452	0.0238	474	$4.02 \cdot 10^{-5}$
300	400	10	10	2	3	5	5	221	0.0235	214	$4.98 \cdot 10^{-5}$
950	950	10	10	2	3	5	5	148	0.0236	156	$7.43 \cdot 10^{-5}$
600	800	10	10	1	1.5	5	5	126	0.0238	125	$1.14 \cdot 10^{-4}$
600	800	10	10	4	6	5	5	223	0.0235	228	$6.08 \cdot 10^{-5}$
600	800	10	10	10	10	5	5	267	0.0234	238	$4.01 \cdot 10^{-5}$
600	800	10	10	2	3	1	1	55	0.0236	52	$2.01 \cdot 10^{-4}$
600	800	10	10	2	3	10	10	256	0.0236	256	$2.54 \cdot 10^{-5}$
600	800	10	10	2	3	100	100	922	0.0236	923	$9.88 \cdot 10^{-7}$

Second part

Improving estimation performance

Chapter 5

Hybrid multi-observer for improving estimation performance

Contents

The results of this chapter are based on [81, 83].

Abstract - *Various methods are nowadays available to design observers for broad classes of systems, where the primary focus is on establishing the convergence of the estimated states. Nevertheless, the question of the tuning of the observer to achieve satisfactory estimation performance remains largely open. In this context, we present a general design framework for the online tuning of the observer gains. Our starting point is a robust nominal observer designed for a general nonlinear system, for which an input-to-state stability property can be established. Our goal is then to improve the performance of this nominal observer. We present for this purpose a new hybrid multi-observer scheme, whose great flexibility can be exploited to enforce various desirable properties, e.g., fast convergence and good sensitivity to measurement noise. We prove that an input-to-state stability property also holds for the proposed scheme and, importantly, we ensure, under some conditions, that the estimation performance in terms of a quadratic cost is (strictly) improved. We illustrate the efficiency of the approach in improving the performance of given nominal observers in three numerical examples.*

5.1 Introduction

State estimation of dynamical systems is a central theme in control theory, whereby an observer is designed to estimate the unmeasured system states exploiting the knowledge of the system model and input and output measurements. Many techniques are available in the literature for the observer design of linear and nonlinear systems, see [5] and the references therein. The vast majority of these works focuses on designing the observer so that the origin of the associated estimation error system is (robustly) asymptotically stable. A critical and largely open question is how to tune the observer to obtain desirable performance (e.g. convergence speed and overshoot in the transient response) in the presence of model uncertainties, measurement noise and disturbances.

One of the challenges in observer tuning is that there exist different trade-offs between these properties. Indeed, a standard approach to observer design consists in using a copy of the plant (in some coordinates that may be different from the original ones) and then adding a correction term, often denoted as the output injection term. This term is designed by multiplying the difference between the measured output and the estimated one by a (possibly nonlinear) gain, whose tuning produces different estimation performance. Typically, the output injection term with small gains produces an observer robust to measurement noise, but its convergence is very slow. On the contrary, an observer with a large gain usually has a fast convergence, but is more sensitive to noise. An answer to the question on how to tune the observer gain in the special context of linear systems affected by additive Gaussian noise impacting the dynamics and the output is the celebrated Kalman filter [54]. However, for general nonlinear systems and noise/disturbances, optimal observer design is notoriously hard. For instance, in the context of nonlinear systems, optimal state estimation requires solving challenging partial differential equations [59]. In this context, an alternative consists in aiming at *improving* the estimation performance of a given observer. To the best of the authors' knowledge, existing works in this direction either concentrate on specific classes of systems (see e.g., [60–62] for linear systems or e.g., [63–70] in the context of high-gain observers) or on specific pro-

perties like robustness to measurement noise (see, e.g., [9, 71]) or the reduction of the undesired effect of the peaking phenomenon (see e.g., [126] for a general approach and [64, 66, 68, 69] for specific solutions in the context of high-gain observer). An exception is [43], where two observers designed for a general nonlinear system are "united" to exploit the good properties of each. However, the design in [43] is not always easy to implement as it requires knowledge of various properties of the observers (basin of attraction, ultimate bound), which may be difficult to obtain. In addition, in [58, 127] a suboptimal moving horizon estimation scheme is proposed for general discrete-time nonlinear systems, where the performance of a given auxiliary observer is improved.

In this context, we present a flexible and general observer design methodology based on supervisory multi-observer ideas that can be used to address various trade-offs between robustness to modeling errors and measurement noise, and convergence speed. A multi-observer consists of a bank of observers that run in parallel. It has been used in the literature in a range of different contexts, including improvement of the sensitivity to measurement noise and/or reduction of the undesired overshoot during the transient (e.g., [65, 66, 128] for high-gain observer and [129] for KKL observer), joint state-parameter estimation (e.g., [75, 130–132]) or distributed observers (e.g., [133–135]). In this chapter, we propose a new problem formulation that we believe has not yet been addressed in the literature. Our starting point is the knowledge of a nominal observer, which ensures that the associated state estimation error system satisfies an input-to-state stability property with respect to measurement noise and disturbances. Various methods from the literature can be used to design the nominal observer, see [7, 9] and the references therein. Then, we construct a multi-observer, composed of the nominal observer and additional dynamical systems, all together called *modes*, that have the same structure as the nominal observer, but different gains. It is important to emphasize that the number of modes and the associated gains can be freely assigned (no specific stability/convergence property is required). Because the gains are different, each mode exhibits different properties in terms of speed of convergence and robustness to measurement noise. We run all modes in parallel and we evaluate their estimation performance in terms of a quadratic cost using monitoring variables, inspired by supervisory control and estimation techniques, see e.g., [75–79]. Based on these running costs (i.e., monitoring variables), we design a switching rule that selects, at any time instant, the mode which is providing the best performance. When a new mode is selected, the other ones may reset or not their current state estimate (and their monitoring variable) to it.

We model the overall system as a hybrid system using the formalism of [31]. We prove that the proposed hybrid estimation scheme satisfies an input-to-state stability property with respect to deterministic disturbance and measurement noise. Note that such a property is not straightforward as we do not require any convergence guarantee on the additional modes, but only for the nominal one. We also guarantee the existence of a (semiglobal uniform) average dwell-time thereby ruling out Zeno phenomenon. The performance of the proposed hybrid multi-observer in terms of the cost associated to the designed monitoring variables is guaranteed to be, at least, as good as the performance of the nominal observer by design. Moreover, we provide extra conditions under which the proposed hybrid multi-observer produces a strict performance improvement compared to the nominal one in

terms of an integral cost. The efficiency of the proposed technique is illustrated on three numerical examples. In the first one, the proposed approach is used to improve the estimation performance of a high-gain observer used to estimate the state of a Van der Pol oscillator. In the second example, the proposed hybrid multi-observer improves the estimation performance of an observer designed using a polytopic approach and used for the state estimation of a flexible joint robotic arm. In the third example, we consider an equivalent circuit model for an Li-Ion battery, whose state is estimated with an observer designed using a polytopic approach and we implement the hybrid estimation scheme to improve its performance. Another example is given in Chapter 6, where the hybrid estimation scheme is applied for the state estimation of a more advanced Li-Ion battery model, namely a single-particle electrochemical model.

The chapter is organized as follows. The problem statement is given in Section 5.2. Section 5.3 presents the hybrid estimation scheme and its stability is analyzed in Section 5.4. Section 5.5 is dedicated to the analysis of the solutions time domains. The performance improvement brought by the hybrid scheme compared to the nominal observer is established in Section 5.6. Three numerical case studies are reported in Section 5.7. Finally, Section 5.8 concludes the chapter.

5.2 Problem statement

The aim of this work is to improve the estimation performance of a given nonlinear nominal observer by exploiting a novel hybrid estimation scheme that is presented in the next section. We consider the plant model

$$\begin{aligned} \dot{x} &= f_p(x,u,v) \\ y &= h(x,w), \end{aligned} \tag{5.1}$$

where $x \in \mathbb{R}^{n_x}$ is the state to be estimated, $u \in \mathbb{R}^{n_u}$ is the measured input, $y \in \mathbb{R}^{n_y}$ is the measured output, $v \in \mathbb{R}^{n_v}$ is an unknown disturbance input and $w \in \mathbb{R}^{n_w}$ is an unknown measurement noise, with $n_x, n_y \in \mathbb{Z}_{>0}$ and $n_u, n_v, n_w \in \mathbb{Z}_{\geqslant 0}$. The input signal $u : \mathbb{R}_{\geqslant 0} \to \mathbb{R}^{n_u}$, the unknown disturbance input $v : \mathbb{R}_{\geqslant 0} \to \mathbb{R}^{n_v}$ and the measurement noise $w : \mathbb{R}_{\geqslant 0} \to \mathbb{R}^{n_w}$ are such that $u \in \mathscr{L}_{\mathscr{U}}$, $v \in \mathscr{L}_{\mathscr{V}}$ and $w \in \mathscr{L}_{\mathscr{W}}$ for closed sets $\mathscr{U} \subseteq \mathbb{R}^{n_u}$, $\mathscr{V} \subseteq \mathbb{R}^{n_v}$ and $\mathscr{W} \subseteq \mathbb{R}^{n_w}$.

We consider a so-called nominal observer for system (5.1) of the form

$$\begin{aligned} \dot{\hat{x}}_1 &= f_o(\hat{x}_1, u, L_1(y - \hat{y}_1)) \\ \hat{y}_1 &= h(\hat{x}_1, 0), \end{aligned} \tag{5.2}$$

where $\hat{x}_1 \in \mathbb{R}^{n_x}$ is the state estimate, $\hat{y}_1 \in \mathbb{R}^{n_y}$ is the output estimate and $L_1 \in \mathbb{R}^{n_{L_1} \times n_y}$ is the observer output injection gain with $n_{L_1} \in \mathbb{Z}_{>0}$. We define the estimation error as $e_1 := x - \hat{x}_1 \in \mathbb{R}^{n_x}$ and introduce a *perturbed* version of the error dynamics, following from (5.1) and (5.2), as

$$\dot{e}_1 = f_p(x,u,v) - f_o(\hat{x}_1, u, L_1(y - \hat{y}_1) + d) =: \tilde{f}(e_1, x, u, v, w, d) \tag{5.3}$$

where $d \in \mathbb{R}^{n_{L_1}}$ represents an additive perturbation on the output injection term $L_1(y - \hat{y}_1)$. We assume that observer (5.2) is designed such that system (5.3) is input-to-state stable with respect to

v, w and d, uniformly in u and x, as formalized next.

Assumption 5.1. *There exist $\underline{\alpha},\overline{\alpha},\psi_1,\psi_2 \in \mathscr{K}_\infty$, $\alpha \in \mathbb{R}_{>0}$, $\gamma \in \mathbb{R}_{\geqslant 0}$ and $V : \mathbb{R}^{n_x} \to \mathbb{R}_{\geqslant 0}$ continuously differentiable, such that for all $x \in \mathbb{R}^{n_x}$, $e_1 \in \mathbb{R}^{n_x}$, $d \in \mathbb{R}^{n_{L_1}}$, $u \in \mathscr{U}$, $v \in \mathscr{V}$, $w \in \mathscr{W}$,*

$$\underline{\alpha}(|e_1|) \leqslant V(e_1) \leqslant \overline{\alpha}(|e_1|) \tag{5.4}$$

$$\left\langle \nabla V(e_1), \tilde{f}(e_1,x,u,v,w,d) \right\rangle \leqslant -\alpha V(e_1) + \psi_1(|v|) + \psi_2(|w|) + \gamma|d|^2. \tag{5.5}$$

□

A large number of observers in the literature have the form of (5.2) and satisfy Assumption 5.1, possibly after a change of coordinates, see [7, 9, 126] and the references therein. More details on observers satisfying an input-to-state stability property are provided in Chapter 2. Assumption 5.1 implies that there exist $\beta \in \mathscr{KL}$ and $\rho \in \mathscr{K}_\infty$ such that, for any $u \in \mathscr{L}_{\mathscr{U}}$, $v \in \mathscr{L}_{\mathscr{V}}$, $w \in \mathscr{L}_{\mathscr{W}}$ and $d \in \mathscr{L}_{\mathbb{R}^{n_{L_1}}}$, any corresponding solution (x, e_1) to systems (5.1) and (5.3) verifies, for all $t \in \mathrm{dom}\,(x, e_1)$,

$$|e_1(t)| \leqslant \beta(|e_1(0)|, t) + \rho(\|v\|_{[0,t]} + \|w\|_{[0,t]} + \|d\|_{[0,t]}). \tag{5.6}$$

Inequality (5.6) provides a desirable robust stability property of the estimation error associated to observer (5.2). However, this property may not be satisfactory in terms of performance, like convergence speed and noise/disturbance rejection. To tune L_1 to obtain desirable performance properties is highly challenging in general and even impossible in some cases when the desired properties are conflicting like high convergence speed and efficient noise rejection, see e.g., [53]. To address this challenge, we propose a hybrid redesign of observer (5.2), which aims at improving its performance, in a sense made precise in the following, while preserving an input-to-state stability property for the obtained estimation error system.

Remark 5.1. *The results of the chapter apply* mutatis mutandis *to the case where Assumption 5.1 holds semiglobally or when the Lyapunov function V depends on both x and e_1, which allow to cover an even broader class of observers [5, Section V]. We do not consider these to keep the result as easy as possible and to avoid obscuring the main message of the work.* □

In the following we also need the next technical assumption on the output map h in (5.1).

Assumption 5.2. *There exist $\delta_1, \delta_2 \in \mathbb{R}_{>0}$ such that for all $x, x' \in \mathbb{R}^{n_x}$, $w, w' \in \mathscr{W}$,*

$$|h(x,w) - h(x',w')|^2 \leqslant \delta_1 V(x - x') + \delta_2 |w - w'|^2, \tag{5.7}$$

where V comes from Assumption 5.1. □

Assumption 5.2 holds in the common case where V in Assumption 5.1 is quadratic and h is globally Lipschitz. Indeed, in this case, $V(x-x') := (x-x')^\top P(x-x')$, with $P \in \mathbb{R}^{n_x \times n_x}$ symmetric, positive definite, and $|h(x,w) - h(x',w')| \leqslant K|(x-x', w-w')|$ for any $x, x' \in \mathbb{R}^{n_x}$, $w, w' \in \mathscr{W}$ and

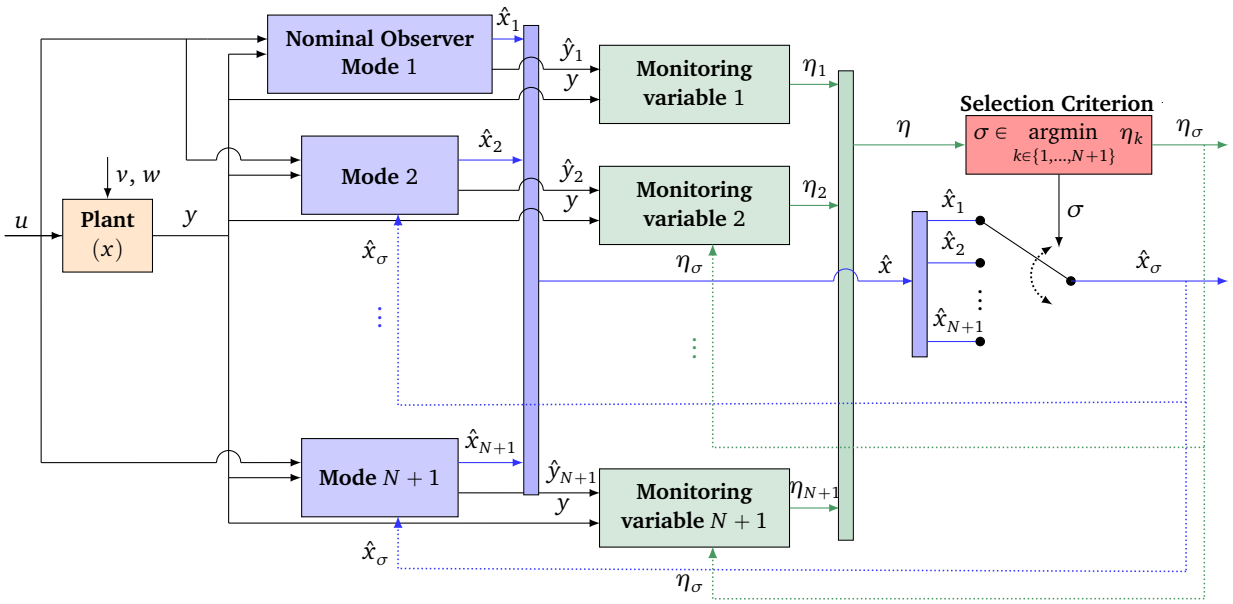

FIGURE 5.1 – Block diagram representing the system architecture with $\eta := (\eta_1, \dots \eta_{N+1})$, $\hat{x} := (\hat{x}_1, \dots, \hat{x}_{N+1})$.

some $K \in \mathbb{R}_{\geqslant 0}$, then (5.7) holds with $\delta_1 = \dfrac{K^2}{\lambda_{\min}(P)}$ and $\delta_2 = K^2$. Note that h globally Lispchitz covers the common case where $h(x,w) = Cx + Dw$ with $C \in \mathbb{R}^{n_y \times n_x}$ and $D \in \mathbb{R}^{n_y \times n_w}$.

5.3 Hybrid estimation scheme

The hybrid estimation scheme we propose consists of the following elements, see Figure 5.1:

— *nominal observer* given in (5.2);

— N additional dynamical systems of the form (5.2) but with a different output injection gain, where $N \in \mathbb{Z}_{>0}$. Each of these systems, as well as the nominal observer, is called *mode* for the sake of convenience;

— *N+1 monitoring variables* used to evaluate the performance of each mode of the multi-observer;

— *a selection criterion*, that switches between the state estimates produced by the different modes exploiting the performance knowledge given by the monitoring variables;

— *a reset rule*, that defines how the estimation scheme may be updated when the selected mode switches.

All these elements together form the hybrid multi-observer. We describe each component in the sequel.

5.3.1 Additional modes

We consider N additional dynamical systems, where the integer $N \in \mathbb{Z}_{>0}$ is arbitrarily selected by the user. These N extra systems are of the form of (5.2) but with a different output injection gain, i.e., for any $k \in \{2,\dots,N+1\}$, the k^{th} mode of the multi-observer is given by

$$\begin{aligned} \dot{\hat{x}}_k &= f_o(\hat{x}_k, u, L_k(y-\hat{y}_k)) \\ \hat{y}_k &= h(\hat{x}_k, 0), \end{aligned} \tag{5.8}$$

where $\hat{x}_k \in \mathbb{R}^{n_x}$ is the k^{th} mode state estimate, $\hat{y}_k \in \mathbb{R}^{n_y}$ is the k^{th} mode output and $L_k \in \mathbb{R}^{n_{L_1} \times n_y}$ is its gain. It is important to emphasize that we make no assumptions on the convergence properties of the solution to system (5.8) contrary to observer (5.2). There is thus full freedom for selecting the gains $L_k \in \mathbb{R}^{n_{L_1} \times n_y}$, with $k \in \{2,\dots,N+1\}$. We will elaborate more on the choice of the L_k's in Section 5.3.5.

Remark 5.2. *There is also full freedom in the choice of the initial conditions of all modes in* (5.2) *and* (5.8)*. We can therefore select all of them equal, but this is not necessary for the stability results in Section 5.4 to hold. See Remark 5.4 in the sequel for more details.* □

Remark 5.3. *The nominal observer* (5.2) *and the additional modes* (5.8) *have constant gains L_k, but it is also possible to consider time-varying gains $L_k(t)$. In this case, if all the gains are uniformly bounded, i.e. there exists $\mathscr{M} > 0$ such that $|L_k(t)| \leqslant \mathscr{M}$ for all $t \geqslant 0$ and all $k \in \{1,\dots,N+1\}$, then the results in this chapter hold* mutatis mutandis*. In the numerical example in Section 5.7.3 one of the modes is an extended Kalman filter, which thus has a time-varying gain.* □

5.3.2 Monitoring variables

Given the $N+1$ modes, our goal is now to find a way to select the "best" between them, namely the one providing a better estimate, possibly improving the estimation given by the nominal observer (5.2). Ideally, the criterion used to evaluate the performance of each mode would depend on the estimation errors $e_k = x - \hat{x}_k$, with $k \in \{1,\dots,N+1\}$. However, since the state x is unknown, e_k is unknown and any performance criterion involving e_k would not be implementable. As a consequence, as done in other contexts, see e.g., [136,137], we rely on the knowledge of the output y and the estimated outputs $\hat{y}_k$ for $k \in \{1,\dots,N+1\}$. In particular, inspired by [136], in order to evaluate the performance of each mode, we introduce the $N+1$ monitoring variables $\eta_k \in \mathbb{R}_{\geqslant 0}$ for any $k \in \{1,\dots,N+1\}$, with dynamics given by

$$\begin{aligned} \dot{\eta}_k &= -\nu\eta_k + (y-\hat{y}_k)^\top(\Lambda_1 + L_k^\top \Lambda_2 L_k)(y-\hat{y}_k) \\ &=: g(\eta_k, L_k, y, \hat{y}_k), \end{aligned} \tag{5.9}$$

with $\Lambda_1 \in \mathbb{S}^{n_y}_{\geqslant 0}$ and $\Lambda_2 \in \mathbb{S}^{n_x}_{\geqslant 0}$ with at least one of them positive definite and $\nu \in (0, \alpha]$ a design parameter, where α comes from Assumption 5.1. The term $(y-\hat{y}_k)^\top \Lambda_1 (y-\hat{y}_k)$ in (5.9) is related to the output estimation error, while $(y-\hat{y}_k)^\top L_k^\top \Lambda_2 L_k (y-\hat{y}_k)$ takes into account the correction effort

of the observer, also called latency in [136]. Note that the monitoring variable η_k in (5.9) for all $k \in \{1,\dots,N+1\}$ is implementable since we have access to the output y and all the estimated outputs $\hat{y}_k$ at all time instants. The monitoring variables η_k, with $k \in \{1,\dots,N+1\}$, provide evaluations of the performance of all the modes of the multi-observer. Indeed, by integrating (5.9) between time 0 and $t \in \mathbb{R}_{\geqslant 0}$, we obtain that for any $k \in \{1,\dots,N+1\}$, for any initial condition $\eta_k(0) \in \mathbb{R}_{\geqslant 0}$, for any $y, \hat{y}_k \in \mathscr{L}_{\mathbb{R}^{n_y}}$, and any $t \geqslant 0$,

$$\eta_k(t) = e^{-\nu t}\eta_k(0) + \int_0^t e^{-\nu(t-\tau)} \left((y(\tau)-\hat{y}_k(\tau))^\top (\Lambda_1 + L_k^\top \Lambda_2 L_k)(y(\tau)-\hat{y}_k(\tau))\right) d\tau. \tag{5.10}$$

Equation (5.10) is a finite-horizon discounted cost, which depends on the output estimation error.

5.3.3 Selection criterion

Based on the monitoring variables η_k, with $k \in \{1,\dots,N+1\}$, we define a criterion to select the state estimate to look at. We use a signal $\sigma : \mathbb{R}_{\geqslant 0} \to \{1,\dots,N+1\}$ for this purpose, and we denote the selected state estimate mode $\hat{x}_\sigma$ and the associated monitoring variable η_σ. The criterion consists in selecting the mode with the minimal monitoring variable, which implies minimizing the cost (5.10) over the modes $k \in \{1,\dots,N+1\}$. When several modes produce the same minimum monitoring variable at a given time, we select the mode, between the ones with the minimum monitoring variables, with the smaller derivative of η_k (which is given by $g(\eta_k, L_k, y, \hat{y}_k)$ from (5.9)). Moreover, if two or more modes have the same minimum monitoring variable and the same minimum derivative of the monitoring variable, then the proposed technique selects randomly one of them and this is not an issue to obtain the results in Sections 5.4, 5.5 and 5.6. Thus, we switch the selected mode only when there exists $k \in \{1,\dots,N+1\}\backslash\{\sigma\}$ such that $\eta_k \leqslant \eta_\sigma$. In that way, at the initial time $t_0 = 0$, we take

$$\sigma(0) \in \underset{k\in\Pi}{\operatorname{argmin}} \left(g(\eta_k(0), L_k, y(0), \hat{y}_k(0))\right), \tag{5.11}$$

where $\eta := \{\eta_1,\dots,\eta_{N+1}\}$ and $\Pi(\eta) := \underset{k\in\{1,\dots,N+1\}\backslash\{\sigma\}}{\operatorname{argmin}} \eta_k$, for all $\eta \in \mathbb{R}^{N+1}_{\geqslant 0}$. Then, σ is kept constant, i.e., $\dot{\sigma}(t) = 0$ for all $t \in (0, t_1)$, with

$$t_1 := \inf\{t \geqslant 0 : \exists k \in \{1,\dots,N+1\}\backslash\{\sigma(t)\} \text{ such that } \eta_k(t) \leqslant \eta_{\sigma(t)}(t)\}. \tag{5.12}$$

At time t_1, we switch the selected mode according to

$$\sigma(t_1^+) \in \underset{k\in\Pi}{\operatorname{argmin}} \left(g(\eta_k(t_1), L_k, y(t_1), \hat{y}_k(t_1))\right). \tag{5.13}$$

We repeat these steps iteratively and we denote with $t_i \in \mathbb{R}_{\geqslant 0}$, $i \in \mathbb{Z}_{>0}$ the i^{th} time when the selected mode changes (if it exists), i.e.,

$$t_i := \inf\{t \geqslant t_{i-1} : \exists k \in \{1,\dots,N+1\}\backslash\{\sigma(t)\} \text{ such that } \eta_k(t) \leqslant \eta_{\sigma(t)}(t)\}. \tag{5.14}$$

Consequently, for all $i \in \mathbb{Z}_{>0}$, $\dot{\sigma}(t) = 0$ for all $t \in (t_{i-1}, t_i)$ and

$$\sigma(t_i^+) \in \underset{k\in\Pi}{\operatorname{argmin}} \left(g(\eta_k(t_i), L_k, y(t_i), \hat{y}_k(t_i))\right), \tag{5.15}$$

where we recall that $\eta = \{\eta_1, \ldots, \eta_{N+1}\}$ and $\Pi(\eta) = \underset{k\in\{1,\ldots,N+1\}\backslash\{\sigma\}}{\operatorname{argmin}} \eta_k$, for all $\eta \in \mathbb{R}_{\geqslant 0}^{N+1}$. We also argue that, implementing (5.15) online, which requires the knowledge of the derivative of the monitoring variables, is not an issue.

Remark 5.4. *The proposed scheme works for any initial condition $\eta_k(0) \in \mathbb{R}_{\geqslant 0}$, for all $k \in \{1, \ldots, N+1\}$, which corresponds to the initial cost of each mode of the multi-observer. Consequently, the choice of $\eta_k(0)$ is an extra degree of freedom that can be used to initially penalize the modes when there is a prior knowledge of which mode should be initially selected, as done in Chapter 6 in the context of Li-Ion batteries. Conversely, in the case where there is no prior knowledge on which mode should be chosen at the beginning, all η_k, with $k \in \{1, \ldots, N+1\}$, can be initialized at the same value such that the term $e^{-\nu t}\eta_k(0)$ in (5.10) is irrelevant for the minimization.* □

Remark 5.5. *The results in Sections 5.4 and 5.5 also apply with $\sigma(t_i^+) \in \underset{k\in\{1,\ldots,N+1\}\backslash\{\sigma\}}{\operatorname{argmin}} \eta_k$ instead of* (5.15). *To select the mode with the minimum derivative of the monitoring variable, among those with the minimum η_k, allows us to prove a strict performance improvement in Section 5.6.* □

5.3.4 Reset rule

When a switching occurs, i.e., when a different mode is selected, we propose two different options to update the hybrid estimation scheme. The first one, called *without resets*, consists in only updating σ, and consequently, we only switch the state estimate we are looking at. Conversely, the second option, called *with resets*, consists in not only switching the mode that is considered, but also resetting the state estimates and the monitoring variables of all the modes $k \in \{2, \ldots, N+1\}$ to the updated $\hat{x}_\sigma$ and η_σ, respectively. The state estimate and the monitoring variable of the nominal observer (5.2), corresponding to mode 1, are never reset.

To avoid infinitely fast switching, we introduce a regularization parameter $\varepsilon \in \mathbb{R}_{>0}$. In particular, when a switch of the selected mode occurs, the value of monitoring variables η_k, with $k \in \{2, \ldots, N+1\}\backslash\{\sigma\}$, is increased by ε, both in the case without and with resets. The idea is to penalize the unselected modes and to allow the selected one to run for some amount of time before a new switch occurs. The analysis of the properties of the hybrid time domains of the overall solutions and the existence of a uniform semiglobal average dwell-time are presented Section 5.5.

We use the parameter $r \in \{0, 1\}$ to determine which option is selected, where $r = 0$ corresponds to the case without resets, while $r = 1$ corresponds to the case where the resets are implemented. When a switch of the considered mode occurs, the state estimate of the nominal observer $\hat{x}_1$ is defined as, at a switching time $t_i \in \mathbb{R}_{\geqslant 0}$,

$$\hat{x}_1(t_i^+) := \hat{x}_1(t_i) \tag{5.16a}$$

and, the state estimate $\hat{x}_k$ of the k^{th} additional mode is defined as, at a switching time $t_i \in \mathbb{R}_{\geqslant 0}$, for

all $k \in \{2,\dots,N+1\}$,

$$\begin{aligned}\hat{x}_k(t_i^+) &\in \{(1-r)\hat{x}_k(t_i) + r\hat{x}_{k^\star}(t_i) : k^\star \in \underset{j\in\Pi}{\operatorname{argmin}}\,(g(\eta_j(t_i), L_j, y(t_i), \hat{y}_j(t_i)))\} \\ &=: \hat{\ell}_k(\hat{x}(t_i), \eta(t_i), L, y(t_i), \hat{y}(t_i)),\end{aligned} \tag{5.16b}$$

where $\hat{x} := (\hat{x}_1,\dots,\hat{x}_{N+1})$, $\eta = (\eta_1,\dots,\eta_{N+1})$, $L := (L_1,\dots,L_{N+1})$ and $\hat{y} := (\hat{y}_1,\dots\hat{y}_{N+1})$. Similarly, at a switching time $t_i \in \mathbb{R}_{\geqslant 0}$, the monitoring variables are defined as,

$$\eta_1(t_i^+) := \eta_1(t_i), \tag{5.17a}$$

$$\eta_\sigma(t_i^+) := \eta_\sigma(t_i) \tag{5.17b}$$

and, for all $k \in \{2,\dots,N+1\}\backslash\{\sigma\}$,

$$\eta_k(t_i^+) = (1-r)\eta_k + r\eta_{k^\star} + \varepsilon \tag{5.17c}$$

where $\varepsilon \in \mathbb{R}_{>0}$ and $\eta_{k^\star} = \min_{j\in\{1,\dots,N+1\}\backslash\{\sigma\}} \eta_j$. Note that, if the monitoring variables of more than one mode have the same value and it is the minimum between all the η_k, with $k \in \{1,\dots,N+1\}$, then, from (5.16b), the modes may be reset with different state estimates. Merging (5.17b) and (5.17c) and using the Kronecker delta definition, we obtain, at a switching time $t_i \in \mathbb{R}_{\geqslant 0}$, for all $k \in \{2,\dots,N+1\}$,

$$\begin{aligned}\eta_k(t_i^+) &= \delta_{k,\sigma}\eta_k + (1-\delta_{k,\sigma})((1-r)\eta_k + r\eta_{k^\star} + \varepsilon) \\ &=: p_k(\eta(t_i)),\end{aligned} \tag{5.17d}$$

where $\varepsilon \in \mathbb{R}_{>0}$ and $\eta_{k^\star} = \min_{j\in\{1,\dots,N+1\}\backslash\{\sigma\}} \eta_j$.

We can already note that, with the proposed technique, $\eta_{\sigma(t)}(t) \leqslant \eta_1(t)$ for all $t \geqslant 0$, both in the case without and with resets. Therefore, the estimation performance of the proposed hybrid multi-observer is always not worse than the performance of the nominal one according to the monitoring variables that we consider. We will study the performance of the estimation scheme in more depth in Section 5.6.

5.3.5 Design guidelines

We summarize the procedure to follow to design the hybrid estimation scheme.

1. Design the nominal observer (5.2) such that Assumption 5.1 holds.
2. Select N gains $L_2,\dots,L_{N+1}$ for the N additional modes in (5.8).
3. Implement in parallel the $N+1$ modes of the multi-observer.
4. Generate the monitoring variables η_k, with $k \in \{1,\dots,N+1\}$.
5. Evaluate the signal σ.
6. Select $\varepsilon \in \mathbb{R}_{>0}$ and run the hybrid scheme without or with resets.
7. $\hat{x}_\sigma$ is the state estimate to be considered for estimation purpose.

There is a lot of flexibility in the number of additional modes N and the selection of the gains L_k, with $k \in \{2, \dots, N+1\}$. This allows to address the different trade-offs of the state estimation of nonlinear systems. Note that, all the results we will show in Sections 5.4, 5.5 and 5.6 apply with any choice of the number of the additional modes and their gains. We believe that the gains selection has to be done on a case-by-case basis since it is related to the structure of the nominal observer and it depends on the available computational capabilities. For example, when the nominal observer (5.2) is a high-gain observer, see e.g., [63, 138] or, more generally, an infinite gain margin observer [5, Section 3.4], we typically need to select a very large gain based on a conservative bound to ensure Assumption 5.1, which would result in fast convergence of the estimation error, but, unfortunately, it will be very sensitive to measurement noise. In this case, to overcome the conservatism of the theory, an option is to select the L_k gains (much) smaller than the nominal one, even though there is no convergence proof for these choices, in order to obtain a state estimate which is more robust to measurement noise. This is the approach followed in Section 5.7.1 on an example. Another possible approach is to select the additional gains L_k's considering the behavior of the nominal observer in simulation and choose them based on the properties we want to improve. For instance, similarly to the case where the nominal observer is an high-gain observer, when the convergence speed of the nominal observer is satisfactory, but its estimation error is very sensitive to noises, the gains L_k's should be selected smaller than the nominal one L_1. On the other hand, if the convergence speed of the estimation error of the nominal observer is too slow, the additional gains may be chosen bigger than L_1. This approach to select the additional gains is used Chapter 6, where the hybrid multi-observer is implemented to improve the estimation performance of a electrochemical Li-Ion battery model. In general, possible options to select the additional gains are to pick them in a neighborhood of the nominal one, or to scale the nominal gain by some factors. This gain selection will produce systems with different behaviors and switching between them should allow an improvement of the estimation performance, as illustrated on numerical examples in Section 5.7. The question of the selection of the gains goes beyond this work, as various approaches can be envisioned. For instance, one could select gains based on off-line learning techniques inspired by modern optimization/machine learning algorithms. This will be further investigated in future work. However, three possible methods for the selection of the additional gains are illustrated in Section 5.7 in numerical examples.

The results we will show in this chapter apply for any $\Lambda_1 \in \mathbb{S}^{n_y}_{\geqslant 0}$ and $\Lambda_2 \in \mathbb{S}^{n_x}_{\geqslant 0}$ with at least one of them positive definite. However, their tuning impacts when a switch of the selected mode occurs and which mode is chosen. Indeed, Λ_1 and Λ_2 are the weights of the two terms in (5.9) and thus their values reflect how much we take into account the output estimation error and the correction effort of the observer in the monitoring variables. In particular, selecting Λ_1 bigger than Λ_2 implies that we weight more the term related to the output estimation error compared to the term related to the correction effort of the observer in the design of the monitoring variables. Conversely, if Λ_1 is smaller than Λ_2, then the correction effort of the observer weight is bigger than the one of the output estimation error in the considered monitoring variables. In addition, note that, Λ_2 multiplies the mode gains L_k and thus it implicitly considers also the effect of the measurement noise in the

ultimate bound of the estimation error.

5.3.6 Filtered state estimate

The state estimate $\hat{x}_\sigma$ of the hybrid multi-observer is subject to jumps and can therefore be discontinuous, which may not be suitable in some applications. For this reason, as we will do in Chapter 6 for the state estimation of lithium-ion batteries, it is possible to add a filtered version of $\hat{x}_\sigma$, denoted $\hat{x}_f$, whose dynamics between two successive switching instants is

$$\dot{\hat{x}}_f = -\zeta \hat{x}_f + \zeta \hat{x}_\sigma, \tag{5.18}$$

where $\zeta > 0$ is an additional design parameter and, $\hat{x}_f$ does not change at switching times $t_i \in \mathbb{R}_{\geqslant 0}$, $i \in \mathbb{Z}_{>0}$, i.e.,

$$\hat{x}_f(t_i^+) = \hat{x}_f(t_i). \tag{5.19}$$

Note that, in the following we will prove the stability results for the state estimate of the hybrid multi-observer $\hat{x}_\sigma$ and we do not consider the filtered version $\hat{x}_f$. However, we can define a filtered version of the hybrid multi-observer estimation error as

$$e_f := x_f - \hat{x}_f, \tag{5.20}$$

where x_f is the filtered version of the system state x_f, whose dynamics between two transmission instants is

$$\dot{x}_f = -\zeta x_f + \zeta x, \tag{5.21}$$

where $\zeta > 0$ comes from (5.18), and at switching times $t_i \in \mathbb{R}_{\geqslant 0}$, $i \in \mathbb{Z}_{>0}$,

$$x_f(t_i^+) = x_f(t_i). \tag{5.22}$$

From (5.18), (5.20) and (5.21) we have that, the filtered estimation error dynamics between switching is given by

$$\dot{e}_f = -\zeta e_f + \zeta e_\sigma, \tag{5.23}$$

where $\zeta > 0$ comes from (5.18), and at switching times $t_i \in \mathbb{R}_{\geqslant 0}$, $i \in \mathbb{Z}_{>0}$, from (5.19), (5.20) and (5.22) we have

$$e_f(t_i^+) = e_f(t_i). \tag{5.24}$$

As a results, the filtered estimation error e_f does not change at jumps and is an input-to-state stable system in cascade with the system describing the dynamics of e_σ, see [6, Section 4]. In the following we will consider the hybrid multi-observer state estimate $\hat{x}_\sigma$ and, in Section 5.4, we will prove the stability results for the corresponding estimation error e_σ. For the reason written above, similar stability results hold *mutatis mutandis* for the filtered estimation error e_f. More details on this will be given in Theorem 6.2 in Chapter 6 on a specific example of a lithium-ion battery. Note that the parameter ζ in (6.30) impacts the frequency of the filter and thus its speed. In particular, a big

ζ produces a fast filter and, as a consequence, $\hat{x}_f$ follows $\hat{x}_\sigma$ faster, however, since $\hat{x}_\sigma$ may have discontinuities due to the switching, typically, the faster the filter is designed, the less smoother $\hat{x}_f$ will be.

5.3.7 Hybrid model

To proceed with the analysis of the hybrid estimation scheme presented so far, we model the overall system as a hybrid system of the form of [31], where a jump corresponds to a switch of the selected mode and a possible reset as explained in Section 5.3.4.

We define the overall state as $q := (x, \hat{x}_1, \dots, \hat{x}_{N+1}, \eta_1, \dots, \eta_{N+1}, \sigma) \in \mathcal{Q} := \mathbb{R}^{n_x} \times \mathbb{R}^{(N+1)n_x} \times \mathbb{R}^{N+1}_{\geqslant 0} \times \{1, \dots, N+1\}$, and, by collecting all the equations, we obtain the hybrid model

$$
\left.
\begin{aligned}
\dot{x} &= f_p(x, u, v) \\
\dot{\hat{x}}_1 &= f_o(\hat{x}_1, u, L_1(y - y_1)) \\
&\vdots \\
\dot{\hat{x}}_{N+1} &= f_o(\hat{x}_{N+1}, u, L_{N+1}(y - y_{N+1})) \\
\dot{\eta}_1 &= -\nu\eta_1 + (y - \hat{y}_1)^\top(\Lambda_1 + L_1^\top \Lambda_2 L_1)(y - \hat{y}_1) \\
&\vdots \\
\dot{\eta}_{N+1} &= -\nu\eta_{N+1} + (y - \hat{y}_{N+1})^\top(\Lambda_1 + L_{N+1}^\top \Lambda_2 L_{N+1})(y - \hat{y}_{N+1}) \\
\dot{\sigma} &= 0
\end{aligned}
\right\} \; q \in \mathscr{C},
$$

$$
\left.
\begin{aligned}
x^+ &= x \\
\hat{x}_1^+ &= \hat{x}_1 \\
\hat{x}_2^+ &\in \{(1-r)\hat{x}_2 + r\hat{x}_{k^\star} : k^\star \in \operatorname*{argmin}_{j \in \Pi} (g(\eta_j, L_j, y, \hat{y}_j)\} \\
&\vdots \\
\hat{x}_{N+1}^+ &\in \{(1-r)\hat{x}_{N+1} + r\hat{x}_{k^\star} : k^\star \in \operatorname*{argmin}_{j \in \Pi} (g(\eta_j, L_j, y, \hat{y}_j)\} \\
\eta_1^+ &= \eta_1 \\
\eta_2^+ &= \delta_{2,\sigma}\eta_2 + (1 - \delta_{2,\sigma})((1-r)\eta_2 + r\eta_{k^\star} + \varepsilon) \\
&\vdots \\
\eta_{N+1}^+ &= \delta_{N+1,\sigma}\eta_{N+1} + (1 - \delta_{N+1,\sigma})((1-r)\eta_{N+1} + r\eta_{k^\star} + \varepsilon) \\
\sigma^+ &= \operatorname*{argmin}_{k \in \Pi} g(\eta_k, L_k, y, \hat{y}_k)
\end{aligned}
\right\} \; q \in \mathscr{D},
\tag{5.25}
$$

with $\Pi(q) = \operatorname*{argmin}_{k \in \{1,\dots,N+1\} \setminus \{\sigma\}} \eta_k$ and $g(\eta_k, L_k, y, \hat{y}_k)$ defined in (5.9). In view of Section 5.3.3, the flow

and jump sets $\mathscr{C}$ and $\mathscr{D}$ in (5.25) are defined as

$$\mathscr{C} := \{q \in \mathscr{Q} : \forall k \in \{1,\dots,N+1\} \ \ \eta_k \geqslant \eta_\sigma\}, \tag{5.26}$$

$$\mathscr{D} := \{q \in \mathscr{Q} : \exists k \in \{1,\dots,N+1\}\backslash\{\sigma\} \ \ \eta_k \leqslant \eta_\sigma\}. \tag{5.27}$$

For the sake of convenience we write system (5.25) - (5.27) in the compact form

$$\begin{cases} \dot{q} = F(q,u,v,w), & q \in \mathscr{C} \\ q^+ \in G(q), & q \in \mathscr{D}, \end{cases} \tag{5.28}$$

where flow map is defined as, for any $q \in \mathscr{C}$, $u \in \mathscr{U}$, $v \in \mathscr{V}$ and $w \in \mathscr{W}$, from (5.1), (5.2), (5.8), (5.9),

$$F := (f_p, f_{o,1}, \dots, f_{o,N+1}, g_1, \dots, g_{N+1}, 0), \tag{5.29}$$

with the short notation $f_{o,k} = f_o(\hat{x}_k, u, L_k(y-y_k))$, $g_k = g(\eta_k, L_k, y, y_k)$. The jump map G in (5.28) is defined as, for any $q \in \mathscr{D}$, from (5.15)-(5.17d),

$$G := (x, \hat{x}_1, \hat{\ell}_2 \dots, \hat{\ell}_{N+1}, \eta_1, p_2, \dots, p_{N+1}, \operatorname*{argmin}_{k\in\Pi} g_k), \tag{5.30}$$

with the short notation $\hat{\ell}_k = \hat{\ell}_k(\hat{x}, \eta, L_k, y, \hat{y}_k)$ and $p_k = p_k(\eta)$, where $\Pi(q) = \operatorname*{argmin}_{k\in\{1,\dots,N+1\}\backslash\{\sigma\}} \eta_k$ for all $q \in \mathscr{D}$, $k \in \{1,\dots,N+1\}$.

5.4 Stability guarantees

The goal of this section is to prove that the proposed hybrid estimation scheme satisfies an input-to-state stability property. Even though the nominal observer satisfies an input-to-state stability property by Assumption 5.1, it is not obvious that so does system (5.26)-(5.28), as the extra modes are designed with no convergence guarantees. We first present the Lyapunov properties in Section 5.4.1, which are used in Section 5.4.2 to prove the desired stability property.

5.4.1 Lyapunov properties

In this section we state the Lyapunov properties, which are employed to prove the stability result in Theorem 5.1 in the next section. Based on Assumption 5.1, we first prove an input/output-to-state stability property [6], whose definition was recalled in Chapter 2, for the generic estimation error system $e := x - \hat{x} \in \mathbb{R}^{n_x}$ associated to (5.1) and (5.8), whose dynamics is defined as

$$\dot{e} = f_p(x,u,v) - f_o(\hat{x}, u, L(y-\hat{y})) \tag{5.31}$$

with $L \in \mathbb{R}^{n_{L_1} \times n_y}$.

Lemma 5.1 (Input/Output-to-State Stability property)**.** *Suppose Assumption 5.1 holds. Then, for any*

$x \in \mathbb{R}^{n_x}$, $u \in \mathscr{U}$, $v \in \mathscr{V}$, $w \in \mathscr{W}$, $\hat{x} \in \mathbb{R}^{n_x}$ and any $L \in \mathbb{R}^{n_{L_1} \times n_y}$,

$$\left\langle \nabla V(e), f_p(x,u,v) - f_o(\hat{x},u,L(y-\hat{y})) \right\rangle \leqslant -\alpha V(e) + \psi_1(|v|) + \psi_2(|w|) + \gamma \left\| L - L_1 \right\|^2 |y-\hat{y}|^2, \tag{5.32}$$

with $\hat{y} = h(\hat{x},0) \in \mathbb{R}^{n_y}$ and $\alpha, \psi_1, \psi_2, \gamma, V$ come from Assumption 5.1. □

Proof. Let $x \in \mathbb{R}^{n_x}$, $u \in \mathscr{U}$, $v \in \mathscr{V}$, $w \in \mathscr{W}$, $\hat{x} \in \mathbb{R}^{n_x}$ and $L \in \mathbb{R}^{n_{L_1} \times n_y}$, we have that

$$\begin{aligned} &\left\langle \nabla V(e), f_p(x,u,v) - f_o\big(\hat{x},u,L(y-\hat{y})\big) \right\rangle \\ &\quad = \left\langle \nabla V(e), f_p(x,u,v) \; - f_o\big(\hat{x},u,L_1(y-\hat{y}) - L_1(y-\hat{y}) + L(y-\hat{y})\big) \right\rangle \\ &\quad = \left\langle \nabla V(e), f_p(x,u,v) \; - f_o\big(\hat{x},u,L_1(y-\hat{y}) + (L-L_1)(y-\hat{y})\big) \right\rangle. \end{aligned} \tag{5.33}$$

Applying Assumption 5.1 with $d = (L-L_1)(y-\hat{y})$ we obtain

$$\begin{aligned} &\left\langle \nabla V(e), f_p(x,u,v) - f_o\big(\hat{x},u,L(y-\hat{y})\big) \right\rangle \\ &\quad \leqslant -\alpha V(e) + \psi_1(|v|) + \psi_2(|w|) + \gamma |(L-L_1)(y-\hat{y})|^2 \\ &\quad \leqslant -\alpha V(e) + \psi_1(|v|) + \psi_2(|w|) + \gamma ||(L-L_1)||^2 |y-\hat{y}|^2. \end{aligned} \tag{5.34}$$

We have obtained the desired result. ■

Lemma 5.1 implies that, for $e_k := x - \hat{x}_k$ for any $k \in \{2,\dots,N+1\}$, the e_k-system, which follows from (5.1) and (5.8), satisfies an input/output-to-state property [6], as defined in Definition 2.6, with the same Lyapunov function as in Assumption 5.1 for any choice for the observer gain $L_k \in \mathbb{R}^{n_{L_1} \times n_y}$. The major difference between (5.5) and (5.32) is the term $\gamma ||(L-L_1)||^2 |y-\hat{y}|^2$ in (5.32), which may have a destabilizing effect and may thus prevent the e_k-system to exhibit input-to-state stability properties similar to (5.6).

In the next proposition, we state Lyapunov properties for system (5.26)-(5.28).

Proposition 5.1 (Lyapunov stability property)**.** *Suppose Assumptions 5.1-5.2 hold. Given any sets of gains $L_k \in \mathbb{R}^{n_{L_1} \times n_y}$, with $k \in \{2,\dots,N+1\}$, any $\nu \in (0,\alpha]$, any $\varepsilon > 0$ and any $\Lambda_1 \in \mathbb{S}^{n_y}_{\geqslant 0}$, $\Lambda_2 \in \mathbb{S}^{n_x}_{\geqslant 0}$ with at least one of them positive definite, there exist $U : \mathscr{Q} \to \mathbb{R}_{\geqslant 0}$ locally Lipschitz, and $\underline{\alpha}_U, \overline{\alpha}_U \in \mathscr{K}_\infty$, $\alpha_0 \in \mathbb{R}_{>0}$, $\phi_1, \phi_2 \in \mathscr{K}_\infty$, such that the following properties hold.*

(i) For any $q \in \mathscr{Q}$,

$$\underline{\alpha}_U(|(e_1,\eta_1,e_\sigma,\eta_\sigma)|) \leqslant U(q) \leqslant \overline{\alpha}_U(|(e,\eta)|), \tag{5.35}$$

with $e := (e_1,\dots,e_{N+1})$ and $\eta := (\eta_1,\dots,\eta_{N+1})$.

(ii) For any $q \in \mathscr{C}$, $u \in \mathscr{U}$, $v \in \mathscr{V}$ and $w \in \mathscr{W}$, such that $F(q,u,v,w) \in T_{\mathscr{C}}(q)$,

$$U^\circ(q; F(q,u,v,w)) \leqslant -\alpha_0 U(q) + \phi_1(|v|) + \phi_2(|w|). \tag{5.36}$$

(iii) For any $q \in \mathscr{D}$ and any $\mathfrak{g} \in G(q)$,

$$U(\mathfrak{g}) \leqslant U(q). \tag{5.37}$$

□

Proof. The Lyapunov function of Proposition 5.1 is defined as

$$U(q) := c_1(aV(e_1)+\eta_1) + c_2 \max_{k\in\{1,\dots,N+1\}}\{bV(e_k)-\eta_k,0\} + c_3\max\{\eta_\sigma-\eta_1,0\}, \tag{5.38}$$

for any $q \in \mathscr{Q}$, where $c_1, c_2, c_3, a, b \in \mathbb{R}_{>0}$ are selected such that $c_2 < c_3 < c_1$, $a > \bar{a}$ where $\bar{a} := \dfrac{\delta_1(\lambda_{\max}(\Lambda_1)+\lambda_{\max}(L_1^\top\Lambda_2 L_1))}{\alpha} \geqslant 0$ and $b \in (0,\bar{b})$ with $\bar{b} := \dfrac{\lambda_{\min}(\Lambda_1)}{\theta}$, with $\theta := \gamma \max_{k\in\{1,\dots,N+1\}} \|(L_k - L_1)\|^2 \in \mathbb{R}_{\geqslant 0}$, where γ comes from Assumption 5.1. Note that U is locally Lipschitz as V is continuously differentiable.

We prove the three items of Proposition 5.1 separately.

Proof of item (i). We first show the upper-bound. Let $q \in \mathscr{Q}$, using (5.4) we have

$$\begin{aligned} U(q) &\leqslant c_1(a\overline{\alpha}(|e_1|)+\eta_1) + c_2 \max_{k\in\{1,\dots,N+1\}}\{b\overline{\alpha}(|e_k|)-\eta_k,0\} + c_3\max\{\eta_\sigma-\eta_1,0\} \\ &\leqslant c_1(a\overline{\alpha}(|e_1|)+\eta_1) + c_2\sum_{k=1}^{N+1}(b\overline{\alpha}(|e_k|)+\eta_k) + c_3(\eta_\sigma+\eta_1) \\ &:= \overline{\alpha}_U(|(e,\eta)|), \end{aligned} \tag{5.39}$$

for some $\overline{\alpha}_U \in \mathscr{K}_\infty$.

We now prove the lower-bound of item (i) of Proposition 5.1. We have that $\max_{k\in\{1,\dots,N+1\}}\{bV(e_k)-\eta_k,0\} \geqslant bV(e_\sigma)-\eta_\sigma$ as $\sigma \in \{1,\dots,N+1\}$. Hence, since $\max(\eta_\sigma-\eta_1,0) \geqslant \eta_\sigma-\eta_1$, in view of (5.4),

$$\begin{aligned} U(q) &\geqslant c_1(a\underline{\alpha}(|e_1|)+\eta_1) + c_2(b\underline{\alpha}(|e_\sigma|)-\eta_\sigma) + c_3(\eta_\sigma-\eta_1) \\ &= c_1a\underline{\alpha}(|e_1|) + (c_1-c_3)\eta_1 + c_2b\underline{\alpha}(|e_\sigma|)) + (c_3-c_2)\eta_\sigma. \end{aligned} \tag{5.40}$$

Since $c_1-c_3>0$ and $c_3-c_2>0$, there exists $\underline{\alpha}_U \in \mathscr{K}_\infty$ such that

$$U(q) \geqslant \underline{\alpha}_U(|(e_1,\eta_1,e_\sigma,\eta_\sigma)|). \tag{5.41}$$

Proof of item (ii). For the sake of convenience we write $U(q) = U_1(q)+U_2(q)+U_3(q)$, for any $q \in \mathscr{C}$, where $U_1(q) = c_1(aV(e_1)+\eta_1)$, $U_2(q) = c_2\max_{k\in\{1,\dots,N+1\}}\{bV(e_k)-\eta_k,0\}$ and $U_3(q) = c_3\max\{\eta_\sigma-\eta_1,0\}$. We introduce here the compact notation $F = F(q,u,v,w)$ for the sake of convenience. Let $q \in \mathscr{C}$, $u \in \mathscr{U}$, $v \in \mathscr{V}$ and $w \in \mathscr{W}$, in view of (5.5) and (5.9),

$$\begin{aligned} &U_1^\circ(q;F) \\ &\leqslant -c_1a\alpha V(e_1) + c_1a\psi_1(|v|) + c_1a\psi_2(|w|) - c_1v\eta_1 + c_1(y-\hat{y}_1)^\top(\Lambda_1 + L_1^\top\Lambda_2L_1)(y-\hat{y}_1) \\ &\leqslant -c_1a\alpha V(e_1) + c_1a\psi_1(|v|) + c_1a\psi_2(|w|) - c_1v\eta_1 + c_1(\lambda_{\max}(\Lambda_1)+\lambda_{\max}(L_1^\top\Lambda_2L_1))|y-\hat{y}_1|^2. \end{aligned} \tag{5.42}$$

Then, using Assumption 5.2 we have $|y-\hat{y}_1|^2 = |h(x,w)-h(\hat{x}_1,0)|^2 \leqslant \delta_1V(e_1)+\delta_2|w|^2$. Thus,

in view of (5.42),

$$U_1^\circ(q;F) \leqslant -c_1(a\alpha - \lambda_{\max}(\Lambda_1)\delta_1 - \lambda_{\max}(L_1^\top \Lambda_2 L_1)\delta_1)V(e_1) - c_1\nu\eta_1 + c_1 a\psi_1(|\nu|) + c_1 a\psi_2(|w|) + c_1(\lambda_{\max}(\Lambda_1) + \lambda_{\max}(L_1^\top \Lambda_2 L_1))\delta_2|w|^2. \tag{5.43}$$

Since $a > \bar{a} = \dfrac{\delta_1(\lambda_{\max}(\Lambda_1) + \lambda_{\max}(L_1^\top \Lambda_2 L_1))}{\alpha} \geqslant 0$ and defining

$$a_1 := \min\left\{\frac{a\alpha - \delta_1\lambda_{\max}(\Lambda_1) - \delta_1\lambda_{\max}(L_1^\top \Lambda_2 L_1)}{a}, \nu\right\} > 0 \tag{5.44}$$

we obtain

$$U_1^\circ(q;F) \leqslant -a_1 U_1(q) + c_1 a\psi_1(|\nu|) + c_1 a\psi_2(|w|) + c_1(\lambda_{\max}(\Lambda_1) + \lambda_{\max}(L_1^\top \Lambda_2 L_1))\delta_2|w|^2. \tag{5.45}$$

We now consider U_2. We need to distinguish four cases.

Case a). Suppose there exists a unique $j \in \{1,\dots,N+1\}$ such that $\max_{k\in\{1,\dots,N+1\}}\{bV(e_k) - \eta_k, 0\} = bV(e_j) - \eta_j$ and $bV(e_j) - \eta_j > 0$. Then, by applying Lemma 5.1 to the j-th dynamics, and by recalling the definition of θ given at the beginning of the proof, we obtain

$$\begin{aligned}
&U_2^\circ(q;F)\\
&= c_2\left(b\left\langle \nabla V(e_j), f_p(x,u,\nu) - f_o\left(\hat{x}_j, u, L_j(y-\hat{y}_j)\right)\right\rangle + \nu\eta_j - (y-\hat{y}_j)^\top(\Lambda_1 + L_j^\top\Lambda_2 L_j)(y-\hat{y}_j)\right)\\
&\leqslant -c_2 b\alpha V(e_j) + c_2 b\psi_1(|\nu|) + c_2 b\psi_2(|w|) + c_2 b\theta|y-\hat{y}_j|^2 + c_2\nu\eta_j - c_2(y-\hat{y}_j)^\top\Lambda_1(y-\hat{y}_j)\\
&\quad - c_2(y-\hat{y}_j)^\top L_j^\top\Lambda_2 L_j(y-\hat{y}_j)\\
&\leqslant -c_2(b\alpha V(e_j) - \nu\eta_j) + c_2 b\psi_1(|\nu|) + c_2 b\psi_2(|w|) - c_2(\lambda_{\min}(\Lambda_1) - b\theta)|y-\hat{y}_j|^2.
\end{aligned} \tag{5.46}$$

Since $\nu \in (0,\alpha]$ and $b \in (0,\bar{b})$ with $\bar{b} = \dfrac{\lambda_{\min}(\Lambda_1)}{\theta}$, $\lambda_{\min}(\Lambda_1) - b\theta > 0$ and thus, defining $a_2 := c_2\alpha$, we have

$$U_2^\circ(q;F) \leqslant -a_2 U_2(q) + c_2 b\psi_1(|\nu|) + c_2 b\psi_2(|w|). \tag{5.47}$$

Case b). If for all $k \in \{1,\dots,N+1\}$, $bV(e_k) - \eta_k < 0$, then $U_2(q) = 0$ and

$$U_2^\circ(q;F) = 0 = -a_2 U_2(q). \tag{5.48}$$

Case c). If there exists a subset $\mathscr{S} \subseteq \{1,\dots,N+1\}$ such that, for all $i \in \mathscr{S}$, $bV(e_i) - \eta_i = 0$ and for all $j \in \{1,\dots,N+1\}\backslash\mathscr{S}$, $bV(e_j) - \eta_j < 0$, then $U_2(q) = 0$. Following similar steps as in

case a), we obtain

$$\begin{aligned} U_2^\circ(q;F) &= \max_{i\in\mathscr{I}}\Big\{-a_2(bV(e_i)-\eta_i)+c_2b\psi_1(|v|)+c_2b\psi_2(|w|),0\Big\} \\ &\leqslant c_2b\psi_1(|v|)+c_2b\psi_2(|w|) \\ &= -a_2U_2(q)+c_2b\psi_1(|v|)+c_2b\psi_2(|w|). \end{aligned} \tag{5.49}$$

Case d). If there exists a subset $\tilde{\mathscr{I}}\subseteq\{1,\dots,N+1\}$ such that, for all $i,j\in\tilde{\mathscr{I}}$, $\max_{k\in\{1,\dots,N+1\}}\{bV(e_k)-\eta_k,0\} = bV(e_i)-\eta_i = bV(e_j)-\eta_j > 0$. Following similar steps as in *case a)*, we obtain $U_2^\circ(q;F)\leqslant\max_{i\in\tilde{\mathscr{I}}}\Big\{-a_2(bV(e_i)-\eta_i)+c_2b\psi_1(|v|)+c_2b\psi_2(|w|)\Big\}$. Then, for any $i\in\tilde{\mathscr{I}}$, by the definition of $\tilde{\mathscr{I}}$, we have

$$\begin{aligned} U_2^\circ(q;F) &\leqslant -a_2(bV(e_i)-\eta_i)+c_2b\psi_1(|v|)+c_2b\psi_2(|w|) \\ &= -a_2U_2(q)+c_2b\psi_1(|v|)+c_2b\psi_2(|w|). \end{aligned} \tag{5.50}$$

Merging (5.47), (5.48), (5.49) and (5.50), we have that, for any $q\in\mathscr{C}$, $u\in\mathscr{U}$, $v\in\mathscr{V}$ and $w\in\mathscr{W}$,

$$U_2^\circ(q;F)\leqslant -a_2U_2(q)+c_2b\psi_1(|v|)+c_2b\psi_2(|w|). \tag{5.51}$$

We now consider U_3. Since $q\in\mathscr{C}$, from (5.26) we have that $\eta_\sigma\leqslant\eta_k$ for all $k\in\{1,\dots,N+1\}$. Therefore, $\eta_\sigma\leqslant\eta_1$. When $\eta_\sigma<\eta_1$ we have that $U_3(q)=0$ and

$$U_3^\circ(q;F)=0=-a_3U_3(q), \tag{5.52}$$

for any $a_3\in\mathbb{R}_{>0}$. When $\eta_\sigma=\eta_1$, since $F(q,u,v,w)\in T_{\mathscr{C}}(q)$ and $T_{\mathscr{C}}(q):=\{q\in\mathscr{Q}:\dot\eta_1\geqslant\dot\eta_\sigma\}$, where we use $\dot\eta_1=-\nu\eta_1+(y-\hat y_1)^\top(\Lambda_1+L_1^\top\Lambda_2L_1)(y-\hat y_1)$ and $\dot\eta_\sigma=-\nu\eta_\sigma+(y-\hat y_\sigma)^\top(\Lambda_1+L_\sigma^\top\Lambda_2L_\sigma)(y-\hat y_\sigma)$ for the sake of convenience, we have

$$U_3^\circ(q;F)\leqslant\max\{\dot\eta_\sigma-\dot\eta_1,0\}=0=-a_3U_3(q), \tag{5.53}$$

for any $a_3\in\mathbb{R}_{>0}$. Consequently, from (5.52) and (5.53), we obtain that,

$$U_3^\circ(q;F)\leqslant 0=-a_3U_3(q), \tag{5.54}$$

for all $a_3\in\mathbb{R}_{>0}$.

From (5.45), (5.51) and (5.54) we have that, for any $q\in\mathscr{C}$, $u\in\mathscr{U}$, $v\in\mathscr{V}$ and $w\in\mathscr{W}$, such

that $F(q,u,v,w) \in T_{\mathscr{C}}(q)$,

$$\begin{aligned} U^{\circ}(q;F) &= U_1^{\circ}(q,F) + U_2^{\circ}(q;F) + U_3^{\circ}(q;F) \\ &\leqslant -a_1 U_1(q) + c_1 a \psi_1(|v|) + c_1 a \psi_2(|w|) + c_1(\lambda_{\max}(\Lambda_1) + \lambda_{\max}(L_1^{\top}\Lambda_2 L_1))\delta_2 |w|^2 \\ &\quad - a_2 U_2(q) + c_2 b \psi_1(|v|) + c_2 b \psi_2(|w|) - a_3 U_3(q). \end{aligned} \tag{5.55}$$

Defining $\alpha_0 := \min\{a_1, a_2, a_3\} \in \mathbb{R}_{>0}$, we obtain

$$U^{\circ}(q;F) \leqslant -\alpha_0 U(q) + \phi_1(|v|) + \phi_2(|w|), \tag{5.56}$$

where $\phi_1(s) := (c_1 a + c_2 b)\psi_1(s)$, $\phi_2(s) := (c_1 a + c_2 b)\psi_2(s) + (c_1(\lambda_{\max}(\Lambda_1) + \lambda_{\max}(L_1^{\top}\Lambda_2 L_1))\delta_2)s^2$, for any $s \geqslant 0$.

Proof of item (iii). As in the proof of item (*ii*), for the sake of convenience we write $U(q) = U_1(q) + U_2(q) + U_3(q)$, for any $q \in \mathscr{D}$, where $U_1(q) = c_1(aV(e_1) + \eta_1)$, $U_2(q) = c_2 \max\limits_{k\in\{1,\ldots,N+1\}}\{bV(e_k) - \eta_k, 0\}$ and $U_3(q) = c_3 \max\{\eta_\sigma - \eta_1, 0\}$. In addition, we use σ^+ to denote the selected mode after a jump, in view of the hybrid system notation in Chapter 2.

Let $q \in \mathscr{D}$ and $\mathfrak{g} \in G(q)$. Then, from (5.16a) and (5.17a) we have

$$U_1(\mathfrak{g}) = c_1(aV(e_1) + \eta_1) = U_1(q). \tag{5.57}$$

We now consider U_2. We need to distinguish the case without resets and the case with resets. We first consider the case without resets. From (5.16a)-(5.17d), we obtain

$$\begin{aligned} U_2(\mathfrak{g}) &= c_2 \max_{k\in\{2,\ldots,N+1\}\setminus\{\sigma^+\}}\{bV(e_1) - \eta_1, bV(e_{\sigma^+}) - \eta_{\sigma^+}, bV(e_k) - \eta_k - \varepsilon, 0\} \\ &\leqslant c_2 \max_{k\in\{2,\ldots,N+1\}\setminus\{\sigma^+\}}\{bV(e_1) - \eta_1, bV(e_{\sigma^+}) - \eta_{\sigma^+}, bV(e_k) - \eta_k, 0\} \\ &= c_2 \max_{k\in\{1,\ldots,N+1\}}\{bV(e_k) - \eta_k, 0\} \\ &= U_2(q). \end{aligned} \tag{5.58}$$

On the other hand, when the resets are implemented, we need to distinguish the case where $\sigma^+ = 1$ and the case when $\sigma^+ \in \{2,\ldots,N+1\}$. Suppose first that $\sigma^+ = 1$. Then, from (5.16a)-(5.17d), we have

$$\begin{aligned} U_2(\mathfrak{g}) &= c_2 \max\{bV(e_1) - \eta_1, bV(e_{k^\star}) - \eta_{\tilde{k}^\star} - \varepsilon, 0\} \\ &\leqslant c_2 \max\{bV(e_1) - \eta_1, bV(e_{k^\star}) - \eta_{\tilde{k}^\star}, 0\} \end{aligned} \tag{5.59}$$

with $k^\star \in \underset{k\in\Pi}{\operatorname{argmin}}\left(-\nu\eta_k + (y - \hat{y}_k)^{\top}(\Lambda_1 + L_k^{\top}\Lambda_2 L_k)(y - \hat{y}_k)\right)\big)$, where $\Pi(q) = \underset{k\in\{1,\ldots,N+1\}\setminus\{\sigma\}}{\operatorname{argmin}} \eta_k$, for all $q \in \mathscr{D}$ and $\eta_{\tilde{k}^\star} = \min\limits_{k\in\{1,\ldots,N+1\}\setminus\{\sigma\}} \eta_k$. Note that, if different observers generate the same minimum η_k, with the same minimum derivative, then $k^\star$ may be different from σ^+. However,

$\eta_{\sigma^+} = \eta_{k^\star} = \tilde{\eta}_{k^\star}$. Consequently, from (5.59) and since $k^\star \in \{1,\dots,N+1\}$,

$$\begin{aligned} U_2(\mathfrak{g}) &\leqslant c_2 \max\{bV(e_1) - \eta_1, bV(e_{k^\star}) - \eta_{k^\star}, 0\} \\ &\leqslant c_2 \max_{k\in\{1,\dots,N+1\}} \{bV(e_k) - \eta_k, 0\} \\ &= U_2(q). \end{aligned} \tag{5.60}$$

On the contrary, when $\sigma^+ \in \{2,\dots,N+1\}$, from (5.16a)-(5.17d), we have

$$\begin{aligned} U_2(\mathfrak{g}) &= c_2 \max\{bV(e_1) - \eta_1, bV(e_{k^\star}) - \eta_{\sigma^+}, bV(e_{k^\star}) - \eta_{\tilde{k}^\star} - \varepsilon, 0\} \\ &\leqslant c_2 \max\{bV(e_1) - \eta_1, bV(e_{k^\star}) - \eta_{\sigma^+}, bV(e_{k^\star}) - \eta_{\tilde{k}^\star}, 0\}, \end{aligned} \tag{5.61}$$

with $k^\star \in \underset{k\in\Pi}{\operatorname{argmin}} \big(-\nu\eta_k + (y-\hat{y}_k)^\top(\Lambda_1 + L_k^\top \Lambda_2 L_k)(y-\hat{y}_k))\big)$, where $\Pi(q) = \underset{k\in\{1,\dots,N+1\}\setminus\{\sigma\}}{\operatorname{argmin}} \eta_k$, for all $q \in \mathscr{D}$ and $\eta_{\tilde{k}^\star} = \min_{k\in\{1,\dots,N+1\}\setminus\{\sigma\}} \eta_k$. Note that, if different observers generate the same minimum η_k, with the same minimum derivative, then $k^\star$ may be different from σ^+. However, $\eta_{\sigma^+} = \eta_{k^\star} = \tilde{\eta}_{k^\star}$. Consequently, from (5.61) and since $k^\star \in \{1,\dots,N+1\}$,

$$\begin{aligned} U_2(\mathfrak{g}) &\leqslant c_2 \max\{bV(e_1) - \eta_1, bV(e_{k^\star}) - \eta_{k^\star}, 0\} \\ &\leqslant c_2 \max_{k\in\{1,\dots,N+1\}} \{bV(e_k) - \eta_k, 0\} \\ &= U_2(q). \end{aligned} \tag{5.62}$$

As a result, from (5.58), (5.60) and (5.62) we have, for any $q \in \mathscr{D}$ and any $\mathfrak{g} \in G(q)$,

$$U_2(\mathfrak{g}) \leqslant U_2(q). \tag{5.63}$$

We now consider U_3. From (5.17a) and (5.17b) we have

$$\begin{aligned} U_3(\mathfrak{g}) &= c_3 \max\{\eta_{\sigma^+} - \eta_1, 0\} \\ &= c_3 \max\{\eta_\sigma - \eta_1, 0\} \\ &= U_3(q). \end{aligned} \tag{5.64}$$

Merging (5.57), (5.63) and (5.64) we obtain, for any $q \in \mathscr{D}$ and any $\mathfrak{g} \in G(q)$,

$$U(\mathfrak{g}) \leqslant U(q), \tag{5.65}$$

which concludes the proof of item (*iii*) of Proposition 5.1. This complete the proof.

■

Proposition 5.1 shows the existence of a Lyapunov function U for system (5.26)-(5.28), which is used to prove the input-to-state stability property in the next section.

5.4.2 Input-to-state stability

In the next theorem we prove that system (5.26)-(5.28) satisfies an input-to-state stability property.

Theorem 5.1 (Two-measure flow input-to-state stability property)**.** *Consider system* (5.26)-(5.28) *and suppose Assumptions 5.1-5.2 hold. Then there exist* $\beta_U \in \mathcal{KL}$ *and* $\gamma_U \in \mathcal{K}_\infty$ *such that for any input* $u \in \mathscr{L}_{\mathscr{U}}$*, disturbance input* $v \in \mathscr{L}_{\mathscr{V}}$ *and measurement noise* $w \in \mathscr{L}_{\mathscr{W}}$*, any solution* q *satisfies*

$$|(e_1(t,j),\eta_1(t,j),e_\sigma(t,j),\eta_\sigma(t,j))| \leqslant \beta_U(|(e(0,0),\eta(0,0))|,t) + \gamma_U(\|v\|_{[0,t]} + \|w\|_{[0,t]}) \tag{5.66}$$

for all $(t,j) \in \operatorname{dom} q$*, with* $e = (e_1,\ldots,e_{N+1})$ *and* $\eta = (\eta_1,\ldots,\eta_{N+1})$. □

Proof. This proof relies on Proposition 5.1. Consider the Lyapunov function U in Proposition 5.1. From item (*ii*) of Proposition 5.1, we have that for any $q \in \mathscr{C}$, $u \in \mathscr{U}$, $v \in \mathscr{V}$ and $w \in \mathscr{W}$ such that $F(q,u,v,w) \in T_{\mathscr{C}}(q)$,

$$U^\circ(q;F(q,u,v,w)) \leqslant -\alpha_0 U(q) + \phi_1(|v|) + \phi_2(|w|). \tag{5.67}$$

We follow similar steps as in [31, proof of Theorem 3.18]. Let $u \in \mathscr{L}_{\mathscr{U}}$, $v \in \mathscr{L}_{\mathscr{V}}$, $w \in \mathscr{L}_{\mathscr{W}}$ and q be a solution to system (5.26)-(5.28). Pick any $(t,j) \in \operatorname{dom} q$ and let $0 = t_0 \leqslant t_1 \leqslant \cdots \leqslant t_{j+1} = t$ satisfy $\operatorname{dom} q \cap ([0,t] \times \{0,1,\ldots,j\}) = \bigcup_{i=0}^{j}[t_i,t_{i+1}] \times \{i\}$. For each $i \in \{0,\ldots,j\}$ and almost all $s \in [t_i,t_{i+1}]$, $q(s,i) \in \mathscr{C}$ and $\dfrac{d}{ds}q(s,i) \in F(q(s,i),u(s,i),v(s,i),w(s,i)) \cap T_{\mathscr{C}}(q(s,i))$, in view of Lemma 2.1 in Chapter 2. Hence, (5.67) implies that, for all $i \in \{0,\ldots,j\}$ and almost all $s \in [t_i,t_{i+1}]$,

$$U^\circ\left(q(s,i);\frac{d}{ds}q(s,i)\right) \leqslant -\alpha_0 U(q(s,i)) + \phi_1(\|v\|_{[0,s]}) + \phi_2(\|w\|_{[0,s]}). \tag{5.68}$$

In view of [139], we have that, for almost all $s \in [t_i,t_{i+1}]$,

$$\frac{d}{ds}U(q(s,i)) \leqslant U^\circ\left(q(s,i);\frac{d}{ds}q(s,i)\right). \tag{5.69}$$

We introduce the compact notation $U(t,j) = U(q(t,j))$. From (5.68) and (5.69), for each $i \in \{0,\ldots,j\}$ and for almost all $s \in [t_i,t_{i+1}]$,

$$\frac{d}{ds}U(s,i) \leqslant -\alpha_0 U(s,i) + \phi_1(\|v\|_{[0,s]}) + \phi_2(\|w\|_{[0,s]}). \tag{5.70}$$

Using [140, Theorem III.16.2], from (5.70) we obtain that for almost all $s \in [t_i, t_{i+1}]$, for all $i \in \{0,\dots,j\}$,

$$\begin{aligned} U(s,i) &\leqslant e^{-\alpha_0(s-t_i)}U(t_i,i) + \int_{t_i}^{s} e^{-\alpha_0(s-\tau)}(\phi_1(\|v\|_{[0,\tau]}) + \phi_2(\|w\|_{[0,\tau]}))d\tau \\ &\leqslant e^{-\alpha_0(s-t_i)}U(t_i,i) + \frac{1}{\alpha_0}(1-e^{-\alpha_0(s-t_i)})(\phi_1(\|v\|_{[0,s]}) + \phi_2(\|w\|_{[0,s]})) \\ &\leqslant e^{-\alpha_0(s-t_i)}U(t_i,i) + (1-e^{-\alpha_0(s-t_i)})\tilde{\gamma}_U(\|v\|_{[0,s]} + \|w\|_{[0,s]}), \end{aligned} \tag{5.71}$$

where $\tilde{\gamma}_U(s) = \dfrac{1}{\alpha_0}(\phi_1(s) + \phi_2(s)) \in \mathcal{K}_\infty$. Thus,

$$U(t_{i+1},i) \leqslant e^{-\alpha_0(t_{i+1}-t_i)}U(t_i,i) + (1-e^{-\alpha_0(t_{i+1}-t_i)})\tilde{\gamma}_U(\|v\|_{[0,t_{i+1}]} + \|w\|_{[0,t_{i+1}]}). \tag{5.72}$$

On the other hand, from item *(iii)* of Proposition 5.1, for each $i \in \{1,\dots,j\}$,

$$U(t_i,i) - U(t_i,i-1) \leqslant 0. \tag{5.73}$$

From (5.72) and (5.73), we deduce that for any $(t,j) \in \operatorname{dom} q$,

$$\begin{aligned} U(t,j) &\leqslant e^{-\alpha_0 t}U(0,0) + (1-e^{-\alpha_0 t})\tilde{\gamma}_U(\|v\|_{[0,t]} + \|w\|_{[0,t]}) \\ &\leqslant e^{-\alpha_0 t}U(0,0) + \tilde{\gamma}_U(\|v\|_{[0,t]} + \|w\|_{[0,t]}). \end{aligned} \tag{5.74}$$

Using item (i) of Proposition 5.1, we obtain, for any $(t,j) \in \operatorname{dom} q$,

$$|(e_1(t,j),\eta_1(t,j),e_\sigma(t,j),\eta_\sigma(t,j))| \leqslant \underline{\alpha}_U^{-1}(e^{-\alpha_0 t}\overline{\alpha}_U(|(e(0,0),\eta(0,0))|)) + \tilde{\gamma}_U(\|v\|_{[0,t]} + \|w\|_{[0,t]})). \tag{5.75}$$

Since for any $\alpha \in \mathcal{K}_\infty$ we have $\alpha(s_1+s_2) \leqslant \alpha(2s_1) + \alpha(2s_2)$ for all $s_1 \geqslant 0, s_2 \geqslant 0$, we obtain

$$|(e_1(t,j),\eta_1(t,j),e_\sigma(t,j),\eta_\sigma(t,j))| \leqslant \beta_U(|(e(0,0),\eta(0,0))|,t) + \gamma_U(\|v\|_{[0,t]} + \|w\|_{[0,t]}) \tag{5.76}$$

where $\beta_U(r,s) := \underline{\alpha}_U^{-1}(2e^{-\alpha_0 s}\overline{\alpha}_U(r)) \in \mathcal{KL}$ and $\gamma_U(r) := \underline{\alpha}_U^{-1}(2\tilde{\gamma}_U(r)) \in \mathcal{K}_\infty$ for all $r,s \geqslant 0$.

■

Theorem 5.1 guarantees a two-measure flow input-to-state stability property [104], see Definition 2.13. In particular, (5.66) ensures that e_1, η_1, e_σ and η_σ converge to a neighborhood of the origin, whose "size" depend on the $\mathcal{L}_\infty$ norm of v and w. Note that we do not guarantee any stability property for the modes $k \neq \sigma$, but this is not needed for the convergence of the hybrid observer estimation error e_σ. Hence, the convergence of the estimated state vector of the selected mode is guaranteed by Theorem 5.1. Equation (5.66) guarantees a two-measure flow input-to-state stability property because we prove a convergence property "only" for the nominal observer estimation error e_1 and monitoring variable η_1 and for the proposed hybrid multi observer estimation error e_σ and monitoring variable η_σ. On the other hand, the function β_U depends on the initial condition of the

estimation errors and monitoring variables of all modes of the multi-observer. This is a consequence of equation (5.35), where the $\mathscr{K}_\infty$ functions $\underline{\alpha}_U$ and $\overline{\alpha}_U$ do not depend on the same arguments, conversely to the "sandwich-bound" in the "classical" Lyapunov characterization of the input-to-state stability property, see e.g., [38, Equation (3)].

5.5 Properties of the solution domains

In this section we concentrate on the completeness and more generally on the properties of the solutions time domains. In Section 5.5.1, we show that maximal solutions are complete, while in Section 5.5.2 we ensure the existence of a uniform semiglobal average dwell-time, as defined in Section 2.3.4, thereby ruling out the Zeno phenomenon.

5.5.1 Completeness of maximal solutions

The goal of this section is to show that maximal solutions to system (5.26)-(5.28) are complete. For this purpose, we need that the system plant (5.1) is complete, as stated in the next assumption.

Assumption 5.3. *Any maximal solution to* (5.1) *with* $u \in \mathscr{L}_{\mathscr{U}}$, $v \in \mathscr{L}_{\mathscr{V}}$ *and* $w \in \mathscr{L}_{\mathscr{W}}$ *is complete.* □

Before proving the main result of this section, we show in the next lemma that maximal solutions to the additional modes (5.8) are complete.

Lemma 5.2 (Additional modes completeness of solutions)**.** *Consider systems* (5.1) *and* (5.8)*. Suppose Assumptions 5.1, 5.2 and 5.3 hold. Then, for any inputs* $u \in \mathscr{L}_{\mathscr{U}}$, $v \in \mathscr{L}_{\mathscr{V}}$, $w \in \mathscr{L}_{\mathscr{W}}$ *and* $y \in \mathscr{L}_{\mathbb{R}^{n_y}}$, *any corresponding maximal solution to* (5.8) *is complete.* □

Proof. Let $k \in \{2, \dots N+1\}$ and let $x \in \mathbb{R}^{n_x}$, $u \in \mathscr{U}$, $v \in \mathscr{V}$, $w \in \mathscr{W}$, $\hat{x}_k \in \mathbb{R}^{n_x}$ and any $L_k \in \mathbb{R}^{n_{L_1} \times n_y}$. From Lemma 5.1, we have, for all $k \in \{2, \dots, N+1\}$,

$$\begin{aligned} &\left\langle \nabla V(e_k), f_p(x,u,v) - f_o\left(\hat{x}_k, u, L_k(y-\hat{y}_k)\right)\right\rangle \\ &\qquad \leqslant -\alpha V(e_k) + \psi_1(|v|) + \psi_2(|w|) + \gamma \left\|L_k - L_1\right\|^2 |y-\hat{y}_k|^2 \\ &\qquad \leqslant -\alpha V(e_k) + \psi_1(|v|) + \psi_2(|w|) + \theta |y-\hat{y}_k|^2, \end{aligned} \tag{5.77}$$

with $\theta = \gamma \max\limits_{k\in\{1,\dots,N+1\}} \left\|L_k - L_1\right\|^2 \in \mathbb{R}_{\geqslant 0}$. Using Assumption 5.2 we have $|y-\hat{y}_k|^2 = |h(x,w) - h(\hat{x}_k, 0)|^2 \leqslant \delta_1 V(e_k) + \delta_2 |w|^2$, for all $k \in \{2, \dots, N+1\}$. Thus, from (5.77) we obtain,

$$\begin{aligned} &\left\langle \nabla V(e_k), f_p(x,u,v) - f_o\left(\hat{x}_k, u, L_k(y-\hat{y}_k)\right)\right\rangle \\ &\qquad \leqslant -\alpha V(e_k) + \psi_1(|v|) + \psi_2(|w|) + \theta\delta_1 V(e_k) + \theta\delta_2 |w|^2 \\ &\qquad = \mathfrak{a} V(e_k) + \psi_1(|v|) + \psi_2^\star(|w|), \end{aligned} \tag{5.78}$$

with $\mathfrak{a} := \theta\delta_1 - \alpha \in \mathbb{R}$ and $\psi_2^\star : s \mapsto \psi_2(|s|) + \theta\delta_2 |s|^2 \in \mathscr{K}_\infty$.

Let $u \in \mathscr{L}_{\mathscr{U}}$, $v \in \mathscr{L}_{\mathscr{V}}$, $w \in \mathscr{L}_{\mathscr{W}}$ and x and $\hat{x}_k$ be solutions to systems (5.1) and (5.8) respectively, for $k \in \{2, \dots, N+1\}$. We have, by definition, $e_k(t) = x(t) - \hat{x}_k(t)$, for all $k \in \{2, \dots, N+1\}$

and all $t \in \mathrm{dom}\,(x, \hat{x}_k)$. Pick any $k \in \{2, \ldots, N+1\}$, for all $t \in [0, +\infty)$, we have from (5.78),

$$\frac{d}{dt}V(e_k(t)) \leqslant \mathfrak{a}V(e_k(t)) + \psi_1(|v(t)|) + \psi_2^\star(|w(t)|). \tag{5.79}$$

Applying the comparison principle [85, Lemma 3.4], we obtain, for all $t \in [0, \infty)$,

$$V(e_k(t)) \leqslant e^{\mathfrak{a}t}V(e_k(0)) + \int_0^t e^{\mathfrak{a}(t-s)}(\psi_1(v(|s|)) + \psi_2^\star(|w(s)|))ds. \tag{5.80}$$

From (5.4) and the last inequality, e_k cannot blow up in finite time as V is positive definite and the right hand side is finite for any $t \geqslant 0$. Moreover, from Assumption 5.3, x cannot blow up in finite time. Consequently, since $\hat{x}_k = x - e_k$ and both x and e_k cannot explode in finite time, $\hat{x}_k$ cannot as well. Thus, for any $k \in \{2, \ldots, N+1\}$, any maximal solution to system (5.8) is complete. ■

We are now ready to prove the completeness of maximal solution of system (5.26)-(5.28).

Proposition 5.2 (Completeness of maximal solutions)**.** *Under Assumptions 5.1-5.3, for any inputs $u \in \mathscr{L}_{\mathscr{U}}$, $v \in \mathscr{L}_{\mathscr{V}}$, $w \in \mathscr{L}_{\mathscr{W}}$, any maximal solution to system* (5.26)-(5.28) *is complete.* □

Proof. We use [37, Proposition 6], which is recalled in Proposition 2.7, to prove Proposition 5.2. Let $u \in \mathscr{L}_{\mathscr{U}}$, $v \in \mathscr{L}_{\mathscr{V}}$, $w \in \mathscr{L}_{\mathscr{W}}$ and q be a maximal solution to (5.26)-(5.28). In view of the definition of the flow and jump sets, $\mathscr{C}$ and $\mathscr{D}$, in (5.26)-(5.27), we have that $q(0,0) \in \mathscr{C} \cup \mathscr{D}$. Suppose $q(0,0) \in \mathscr{C}\backslash\mathscr{D}$, we want to prove that q is not trivial, i.e., its domain contains at least two points. For this purpose we need to show that the viability condition in Proposition 2.7 is satisfied. Since the flow map F is continuous and $u \in \mathscr{L}_{\mathscr{U}}$, $v \in \mathscr{L}_{\mathscr{V}}$ and $w \in \mathscr{L}_{\mathscr{W}}$, from [122, Proposition S1] there exists $\epsilon > 0$ and an absolutely continuous function $z : [0, \epsilon] \to \mathscr{Q}$ such that $z(0) = q(0,0)$ and $\dot{z}(t) = F(z(t), u(t), v(t), w(t))$ for almost all $t \in [0, \epsilon]$. We write $z = (z_x, z_{\hat{x}_1}, \ldots, z_{\hat{x}_{N+1}}, z_{\eta_1}, \ldots, z_{\eta_{N+1}}, z_\sigma)$. Since $q(0,0) \in \mathscr{C}\backslash\mathscr{D}$, with $\mathscr{C}\backslash\mathscr{D}$ open, and z is absolutely continuous, there exists $\epsilon' \in (0, \epsilon]$ such that, for all $k \in \{1, \ldots, N+1\}$, $z_{\eta_k}(t) \geqslant z_{\eta_\sigma}(t)$ for almost all $t \in [0, \epsilon']$. Thus, $z(t) \in \mathscr{C}$ for almost all $t \in [0, \epsilon']$ and the viability condition in Proposition 2.7 holds, which implies that q is a non-trivial solution.

To prove that q is complete we need to exclude items *(b)* and *(c)* in Proposition 2.7. Item *(b)* in Proposition 2.7 occurs when at least one component of q blows up in finite time, and consequently q blows up in finite time. Hence, to exclude *(b)* in Proposition 2.7 we need to show that each component of q must not explode in finite time. Let $q = (x, \hat{x}_1, \ldots \hat{x}_{N+1}, \eta_1, \ldots \eta_{N+1}, \sigma)$. From Assumption 5.3, x cannot blow up in finite time. Moreover, $\hat{x}_1$ cannot do so as well in view of Theorem 5.1 and since x cannot. In addition, $\hat{x}_k$, for all $k \in \{2, \ldots, N+1\}$ cannot blow up in finite time in view of Lemma 5.2 and η_k, with $k \in \{1, \ldots, N+1\}$ cannot as well in view of its dynamics (5.9) and because $y - \hat{y}_k$ does not since both x and $\hat{x}_k$ do not, for all $k \in \{1, \ldots, N+1\}$. Finally, σ is constant in $\mathscr{C}$, consequently, it does not blow up in finite time. Thus, item *(b)* in Proposition 2.7 cannot occur. On the other hand, since $G(\mathscr{D}) \subseteq \mathscr{C} \cup \mathscr{D}$ and the jump set does

not impose conditions on u, v and w, item *(c)* in Proposition 2.7 cannot occur. Consequently, any maximal solution to system (5.26)-(5.28) is complete. This concludes the proof. ■

5.5.2 Average dwell-time

Proposition 5.2 ensures the completeness of maximal solutions under Assumptions 5.1-5.3, still, Zeno phenomenon has not been ruled out yet. In the next proposition, we prove the existence of a uniform semiglobal average dwell-time for the solution to system (5.26)-(5.28), which thus excludes the Zeno phenomenon.

Proposition 5.3 (Average dwell-time)**.** *Suppose Assumptions 5.1, 5.2 hold and the sets $\mathcal{V}$ and $\mathcal{W}$ are compact. Then, system* (5.26)-(5.28) *has a* uniform semiglobal average dwell-time*, i.e., for any $M \in \mathbb{R}_{>0}$ there exists $c > 0$ such that any corresponding solution q with $|q(0,0)| \leqslant M$ and $u \in \mathscr{L}_{\mathscr{U}}$, $v \in \mathscr{L}_{\mathscr{V}}$ and $w \in \mathscr{L}_{\mathscr{W}}$, is such that for any (t,j), $(t',j') \in \operatorname{dom} q$ with $t+j \leqslant t'+j'$, $j'-j \leqslant \frac{1}{\tau}(t'-t)+2$ with $\tau := -\frac{1}{2\nu}\ln\left(\frac{\frac{c}{\nu}}{\varepsilon+\frac{c}{\nu}}\right)$, where ν comes from* (5.9) *and ε is the design parameter in* (5.17c)*.* □

Proof. Let $u \in \mathscr{L}_{\mathscr{U}}$ and $v \in \mathscr{L}_{\mathscr{V}}$, $w \in \mathscr{L}_{\mathscr{W}}$ with $\mathcal{V}$ and $\mathcal{W}$ compact set. Let $\overline{M} \geqslant M$ such that such that $\|v\|_\infty \leqslant \overline{M}$ and $\|w\|_\infty \leqslant \overline{M}$. Let q be a solution to system (5.28) with $|q(0,0)| \leqslant M \leqslant \overline{M}$. Pick any $(t,j) \in \operatorname{dom} q$ and let $0 = t_0 \leqslant t_1 \leqslant \cdots \leqslant t_{j+1} = t$ satisfy $\operatorname{dom} q \cap ([0,t] \times \{0,1,\ldots,j\}) = \bigcup_{i=0}^{j}[t_i, t_{i+1}] \times \{i\}$. For each $i \in \{0,\ldots,j\}$ and almost all $s \in [t_i, t_{i+1}]$, $q(s,i) \in \mathcal{C}$. Then, from (5.9), for all $k \in \{1,\ldots,N+1\}$, for all $s \in (t_i, t_{i+1})$, (we omit the dependency on (s,i) below),

$$\begin{aligned}
&\dot{\eta}_k - \dot{\eta}_\sigma \\
&\quad = -\nu(\eta_k - \eta_\sigma) + (y-\hat{y}_k)^\top(\Lambda_1 + L_k^\top \Lambda_2 L_k)(y-\hat{y}_k) - (y-\hat{y}_\sigma)^\top(\Lambda_1 + L_\sigma^\top \Lambda_2 L_\sigma)(y-\hat{y}_\sigma) \\
&\quad \geqslant -\nu(\eta_k - \eta_\sigma) - (y-\hat{y}_\sigma)^\top(\Lambda_1 + L_\sigma^\top \Lambda_2 L_\sigma)(y-\hat{y}_\sigma) \\
&\quad \geqslant -\nu(\eta_k - \eta_\sigma) - (\lambda_{\max}(\Lambda_1) + \lambda_{\max}(L_\sigma^\top \Lambda_2 L_\sigma))|y-\hat{y}_\sigma|^2.
\end{aligned} \tag{5.81}$$

Then, using Assumption 5.2 we have $|y-\hat{y}_\sigma|^2 = |h(x,w) - h(\hat{x}_\sigma, 0)|^2 \leqslant \delta_1 V(e_\sigma) + \delta_2 |w|^2$. Thus, from (5.81) we obtain, for all $s \in (t_i, t_i+1)$,

$$\dot{\eta}_k - \dot{\eta}_\sigma \geqslant -\nu(\eta_k - \eta_\sigma) - (\lambda_{\max}(\Lambda_1) + \lambda_{\max}(L_\sigma^\top \Lambda_2 L_\sigma))(\delta_1 V(e_\sigma) + \delta_2 |w|^2). \tag{5.82}$$

Using (5.66), from Theorem 5.1, we obtain, for all $(t,j) \in \operatorname{dom} q$,

$$|e_\sigma(t,j)| \leqslant \beta_U(|q(0,0)|, t) + \gamma_U(\|v\|_\infty + \|w\|_\infty), \tag{5.83}$$

with $\beta_U \in \mathcal{KL}$ and $\gamma_U \in \mathcal{K}_\infty$. Then, using $|q(0,0)| \leqslant \overline{M}$, $\|v\|_\infty \leqslant \overline{M}$ and $\|w\|_\infty \leqslant \overline{M}$ we obtain, for all $(t,j) \in \operatorname{dom} q$,

$$\begin{aligned}
|e_\sigma(t,j)| &\leqslant \beta_U(\overline{M}, t) + \gamma_U(2\overline{M}) \\
&\leqslant \beta_U(\overline{M}, 0) + \gamma_U(2\overline{M}).
\end{aligned} \tag{5.84}$$

From Assumption 5.1, for all $e_\sigma \in \mathbb{R}^{n_x}$, $V(e_\sigma) \leqslant \overline{\alpha}(|e_\sigma|)$, where $\overline{\alpha} \in \mathscr{K}_\infty$ comes from Assumption 5.1. From (5.84) and the last inequality we have, for all $(t,j) \in \operatorname{dom} q$,

$$\begin{aligned} V(e_\sigma(t,j)) &\leqslant \overline{\alpha}(\beta_U(\overline{M},t) + \gamma_U(2\overline{M})) \\ &\leqslant \check{\beta}_U(\overline{M},0) + \check{\gamma}_U(2\overline{M}), \end{aligned} \tag{5.85}$$

where $\check{\beta}_U := \overline{\alpha} \circ \beta_U \in \mathscr{KL}$ and $\check{\gamma}_U := \overline{\alpha} \circ \gamma_U \in \mathscr{K}_\infty$. Combining (5.82) with (5.85) we obtain, for all $k \in \{1,\dots,N+1\}$, for all $s \in [t_i, t_{i+1}]$,

$$\begin{aligned} \dot{\eta}_k - \dot{\eta}_\sigma &\geqslant -\nu(\eta_k - \eta_\sigma) - (\lambda_{\max}(\Lambda_1) + \lambda_{\max}(L_\sigma^\top \Lambda_2 L_\sigma))(\delta_1(\check{\beta}_U(\overline{M},0) + \check{\gamma}_U(2\overline{M})) + \delta_2 \overline{M}^2) \\ &\geqslant -\nu(\eta_k - \eta_\sigma) - c, \end{aligned} \tag{5.86}$$

with $c := (\lambda_{\max}(\Lambda_1) + \max\limits_{k\in\{1,\dots,N+1\}} \lambda_{\max}(L_k^\top \Lambda_2 L_k))(\delta_1(\check{\beta}_U(\overline{M},0) + \check{\gamma}_U(2\overline{M})) + \delta_2 \overline{M}^2) \in \mathbb{R}_{>0}$. Integrating (5.86) and applying the comparison principle [85, Lemma 3.4] we obtain, for all $s \in [t_i, t_{i+1}]$, for all $k \in \{1,\dots,N+1\}$,

$$\eta_k(s,i) - \eta_\sigma(s,i) \geqslant e^{-\nu(s-t_i)}(\eta_k(t_i,i) - \eta_\sigma(t_i,i)) - \frac{c}{\nu}(1 - e^{-\nu(s-t_i)}). \tag{5.87}$$

On the other hand, from (5.27), we have

$$t_{i+1} := \inf\{t \geqslant t_i : \min_{k\in\{1,\dots,N+1\}\setminus\{\sigma\}} \eta_k(t,i) = \eta_\sigma(t,i)\}. \tag{5.88}$$

We define $k^\star := \sigma(t_{i+1}, i+1) \in \operatorname{argmin}\limits_{k\in\Pi} (-\nu\eta_k(t_{i+1}, i+1) + (y(t_{i+1}, i+1) - \hat{y}_k(t_{i+1}, i+1))^\top (\Lambda_1 + L_k^\top \Lambda_2 L_k)(y(t_{i+1}, i+1) - \hat{y}_k(t_{i+1}, i+1)))$, where $\Pi(q) = \operatorname{argmin}\limits_{k\in\{1,\dots,N+1\}\setminus\{\sigma\}} \eta_k$. Evaluating (5.87) for $s = t_{i+1}$ and $k = k^\star$, from (5.88), we have

$$\begin{aligned} 0 &= \eta_{k^\star}(t_{i+1}, i) - \eta_\sigma(t_{i+1}, i) \\ &\geqslant e^{-\nu(t_{i+1}-t_i)}(\eta_{k^\star}(t_i,i) - \eta_\sigma(t_i,i)) - \frac{c}{\nu}(1 - e^{-\nu(t_{i+1}-t_i)}). \end{aligned} \tag{5.89}$$

We first consider the case where $k^\star \neq 1$. Note that $\sigma(s,i) \neq k^\star$ by the definition of $k^\star$, for all $s \in [t_i, t_{i+1}]$. We now consider the cases without and with resets separately. From (5.17b), (5.17c) and (5.27) we have in the case without resets, for all $i \in \mathbb{Z}_{>0}$, $\eta_{k^\star}(t_i,i) = \eta_{k^\star}(t_i, i-1) + \varepsilon \geqslant \eta_\sigma(t_i,i) + \varepsilon$, while in the case with resets, $\eta_{k^\star}(t_i,i) = \eta_\sigma(t_i,i) + \varepsilon$. As a result,

$$\eta_{k^\star}(t_i,i) \geqslant \eta_\sigma(t_i,i) + \varepsilon, \tag{5.90}$$

both in the case without and with resets. Thus, $\eta_{k^\star}(t_i,i) - \eta_\sigma(t_i,i) \geqslant \varepsilon$ and from (5.89),

$$0 \geqslant e^{-\nu(t_{i+1}-t_i)}\varepsilon - \frac{c}{\nu}(1 - e^{-\nu(t_{i+1}-t_i)}), \tag{5.91}$$

which can be rewritten as $e^{-\nu(t_{i+1}-t_i)}\left(\varepsilon+\frac{c}{\nu}\right)\leqslant\frac{c}{\nu}$, that implies

$$t_{i+1}-t_i\geqslant-\frac{1}{\nu}\ln\left(\frac{\frac{c}{\nu}}{\varepsilon+\frac{c}{\nu}}\right)\in\mathbb{R}_{>0}. \tag{5.92}$$

On the other hand, when $k^\star=1=\sigma(s,i+1)$, for all $s\in[t_{i+1},t_{i+2}]$, we have that

$$\sigma(t_{i+2},i+2)=\underset{k\in\{2,\dots,N+1\}}{\operatorname{argmin}}\ \eta_k(t_{i+1},i))\neq 1. \tag{5.93}$$

Therefore, from (5.92), we obtain

$$t_{i+2}-t_{i+1}\geqslant-\frac{1}{\nu}\ln\left(\frac{\frac{c}{\nu}}{\varepsilon+\frac{c}{\nu}}\right)\in\mathbb{R}_{>0}. \tag{5.94}$$

Consequently, for all switching times $(t_i,i)\in\operatorname{dom}q$, we have

$$t_{i+2}-t_i\geqslant-\frac{1}{\nu}\ln\left(\frac{\frac{c}{\nu}}{\varepsilon+\frac{c}{\nu}}\right)\in\mathbb{R}_{>0}. \tag{5.95}$$

Pick any $(t,j),(t',j')\in\operatorname{dom}q$ such that $t+j\leqslant t'+j'$, from (5.95) and using $\tau=-\frac{1}{2\nu}\ln\left(\frac{\frac{c}{\nu}}{\varepsilon+\frac{c}{\nu}}\right)$ we obtain

$$j'-j\leqslant\frac{1}{\tau}(t'-t)+2, \tag{5.96}$$

which concludes the proof. ■

We see the importance of the parameter $\varepsilon\in\mathbb{R}_{>0}$, used in the jump map for the monitoring variables (5.17c), in the expression of τ. Indeed, if we would allow ε to be equal to 0 (which we do not), τ would have been equal to 0. In addition, Proposition 5.3 shows that any solution q to (5.26)-(5.28) can exhibit at most two consecutive jumps. Note that to obtain the results of Proposition 5.3 we do not need Assumption 5.3. However, in view of Propositions 5.2 and 5.3 we have that under Assumptions 5.1-5.3, for any inputs $u\in\mathscr{L}_{\mathscr{U}}$, $v\in\mathscr{L}_{\mathscr{V}}$, $w\in\mathscr{L}_{\mathscr{W}}$, any maximal solution q to system (5.26)-(5.28) is t-complete, namely $\sup_t\operatorname{dom}q=+\infty$.

Now that we have established robust stability properties and the properties of the hybrid time domain of the solutions for the hybrid estimation scheme, we focus on its performance in the next section.

5.6 Performance improvement

The goal of this section is to establish the estimation performance improvement given by the proposed hybrid multi-observer. We recall that with the proposed technique we have $\eta_{\sigma(t,j)}(t,j)\leqslant\eta_1(t,j)$ for all $(t,j)\in\operatorname{dom}q$, for any solution q to (5.26)-(5.28) with inputs $u\in\mathscr{L}_{\mathscr{U}}$, $v\in\mathscr{L}_{\mathscr{V}}$ and $w\in\mathscr{L}_{\mathscr{W}}$, both in the case without and with resets. Therefore, the estimation performance of the proposed hybrid multi-observer are always not worse than the performance of the nominal one

according to the monitoring variables we consider.

Variable η_σ defined in Section 5.3.2 is a performance variable that considers the "best" mode among the $N+1$ at any time instant: this is an instantaneous performance, which ignores the past behavior in terms of the monitoring variable. For this reason, to evaluate the performance of the proposed hybrid multi-observer, we also propose the following cost, for any solution q to (5.26)-(5.28) with inputs $u \in \mathscr{L}_{\mathscr{U}}$, $v \in \mathscr{L}_{\mathscr{V}}$ and $w \in \mathscr{L}_{\mathscr{W}}$, for all $(t,j) \in \operatorname{dom} q$,

$$J_{\sigma(t,j)}(t,j) := \sum_{i=0}^{j} \left(\int_{t_i}^{t_{i+1}} \eta_{\sigma(s,i)}(s,i)\, ds \right), \tag{5.97}$$

with $0 = t_0 \leqslant t_1 \leqslant \cdots \leqslant t_{j+1} = t$ satisfying $\operatorname{dom} q \cap ([0,t] \times \{0,1,\ldots,j\}) = \bigcup_{i=0}^{j} [t_i, t_{i+1}] \times \{i\}$.

Similarly, we define the performance cost of the nominal observer, for all $(t,j) \in \operatorname{dom} q$, as

$$J_1(t,j) := \sum_{i=0}^{j} \left(\int_{t_i}^{t_{i+1}} \eta_1(s,i)\, ds \right), \tag{5.98}$$

with $0 = t_0 \leqslant t_1 \leqslant \cdots \leqslant t_{j+1} = t$ satisfying $\operatorname{dom} q \cap ([0,t] \times \{0,1,\ldots,j\}) = \bigcup_{i=0}^{j} [t_i, t_{i+1}] \times \{i\}$.

In the next theorem we prove, that the hybrid scheme in Section 5.3 strictly improves the performance J_1 in (5.98), under some conditions.

Theorem 5.2 (Performance improvement)**.** *Consider system* (5.26)-(5.28) *under Assumptions 5.1-5.3. Let q be a maximal solution with inputs $u \in \mathscr{L}_{\mathscr{U}}$, $v \in \mathscr{L}_{\mathscr{V}}$ and $w \in \mathscr{L}_{\mathscr{W}}$ and for which the initial conditions of the monitoring variables are all the same, namely $\eta_k(0,0) = \eta_0$ for all $k \in \{1,\ldots,N+1\}$ for some $\eta_0 \in \mathbb{R}$. Then, for any $(t,j) \in \operatorname{dom} q$,*

$$J_{\sigma(t,j)}(t,j) \leqslant J_1(t,j), \tag{5.99}$$

with J_σ and J_1 defined in (5.97) *and* (5.98)*, respectively. Moreover, if there exists $(t^\star, j^\star) \in \operatorname{dom} q$ such that*

$$\eta_{\sigma(t^\star,j^\star)}(t^\star,j^\star) < \eta_1(t^\star,j^\star), \tag{5.100}$$

then there exists $j^{\star'} \geqslant j^\star$ such that

$$J_{\sigma(t,j)}(t,j) < J_1(t,j) \tag{5.101}$$

for all $(t,j) \geqslant (t^\star, j^{\star'})$, with $(t,j) \in \operatorname{dom} q$. □

Proof. Consider system (5.26)-(5.28) and let q be a maximal solution to system (5.26)-(5.28) with inputs $u \in \mathscr{L}_{\mathscr{U}}$, $v \in \mathscr{L}_{\mathscr{V}}$ and $w \in \mathscr{L}_{\mathscr{W}}$. From (5.9), (5.17a), (5.17b), (5.26), (5.27) and $\eta_k(0,0) = \eta_0 \in \mathbb{R}$ for all $k \in \{1,\ldots,N+1\}$, we have, for all $(t,j) \in \operatorname{dom} q$,

$$\eta_{\sigma(t,j)}(t,j) \leqslant \eta_1(t,j). \tag{5.102}$$

We then derive from (5.97) and (5.98) that $J_{\sigma(t,j)}(t,j) \leqslant J_1(t,j)$, for all $(t,j) \in \operatorname{dom} q$, which concludes the first part of the proof.

In the second part of the theorem, we have that there exists $(t^\star, j^\star) \in \operatorname{dom} q$ such that

$$\eta_{\sigma(t^\star,j^\star)}(t^\star, j^\star) < \eta_1(t^\star, j^\star). \tag{5.103}$$

We now consider two cases. If $t^\star \in \operatorname{int} I^{j^\star}$, using (5.97), (5.98), (5.102), (5.103), since no jump occurs at $(t^\star, j^\star)$ and η_1 and η_σ are not affected by jumps, by continuity of η_σ and η_1 on $I^{j^\star}$, (5.101) is obtained by integration of (5.102) for all $(t,j) \geqslant (t^\star, j^\star)$, with $(t,j) \in \operatorname{dom} q$. On the other hand, if $I^{j^\star}$ is empty, since q is maximal, it is t-complete by Propositions 5.2 and 5.3 as explained in Section 5.5.2 and thus we have that there exists $j^{\star'} > j^\star$ such that $(t^\star, j^{\star'}) \in \operatorname{dom} q$ and

$$\eta_{\sigma(t^\star,j^{\star'})} \leqslant \eta_{\sigma(t^\star,j^\star)} < \eta_1(t^\star, j^{\star'}) \tag{5.104}$$

with $I^{j^{\star'}}$ non empty. Following similar step as before we have that (5.101) holds for all $(t,j) \geqslant (t^\star, j^{\star'})$, with $(t,j) \in \operatorname{dom} q$. This concludes the proof. ■

Theorem 5.2 shows that, if the condition in (5.100) holds, then the cost of the proposed hybrid multi-observer J_σ is strictly smaller than the one of the nominal observer J_1 and thus, the estimation performance in terms of costs J_σ and J_1 is strictly improved.

In the next proposition, we give the conditions to guarantee that (5.100) is satisfied and consequently, from Theorem 5.2, that the estimation performance is strictly improved with the hybrid multi-observer (5.26)-(5.28).

Proposition 5.4 (Conditions for performance improvement)**.** *Consider system* (5.26)-(5.28) *with* $\Lambda_2 \in \mathbb{S}^{n_x}_{>0}$ *and suppose Assumptions 5.1-5.3 hold. Select the gains* L_k*, with* $k \in \{2,\dots,N+1\}$*, in* (5.8) *such that there exists* $k^\star \in \{2,\dots,N+1\}$ *satisfying* $L_{k^\star}^\top \Lambda_2 L_{k^\star} < L_1^\top \Lambda_2 L_1$*. Let* q *be a maximal solution with inputs* $u \in \mathscr{L}_{\mathscr{U}}$*,* $v \in \mathscr{L}_{\mathscr{V}}$ *and* $w \in \mathscr{L}_{\mathscr{W}}$ *and initial condition* $q(0,0)$ *satisfying the following properties.*

(i) $\hat{x}_k(0,0) = \hat{x}_0$ *for all* $k \in \{1,\dots,N+1\}$ *for some* $\hat{x}_0 \in \mathbb{R}^{n_x}$.

(ii) $\eta_k(0,0) = \eta_0$ *for all* $k \in \{1,\dots,N+1\}$ *for some* $\eta_0 \in \mathbb{R}$.

(iii) $\hat{y}_k(0,0) \neq y(0,0)$ *for all* $k \in \{1,\dots,N+1\}$.

Then, there exists $(t^\star, j^\star) \in \operatorname{dom} q$ *such that*

$$\eta_{\sigma(t^\star,j^\star)}(t^\star, j^\star) < \eta_1(t^\star, j^\star). \tag{5.105}$$

□

Proof. Let q be a maximal solution to system (5.26)-(5.28) with inputs $u \in \mathscr{L}_{\mathscr{U}}$, $v \in \mathscr{L}_{\mathscr{V}}$ and $w \in \mathscr{L}_{\mathscr{W}}$ satisfying items (i)-(iii). We define $\Delta_k := y - \hat{y}_k \in \mathbb{R}^{n_y}$ for all $k \in \{1,\dots,N+1\}$ for the sake of convenience. Note that, thanks to item (i), $\Delta_1(0,0) = y(0,0) - \hat{y}_1(0,0) = y(0,0) - h(\hat{x}_1(0,0),0) = y(0,0) - h(\hat{x}_k(0,0),0) = y(0,0) - \hat{y}_k(0,0) = \Delta_k(0,0)$, for any $k \in \{1,\dots,N+1\}$.

On the other hand, from (5.9) we have, for all $k \in \{1,\dots,N+1\}$,

$$\begin{aligned}\dot{\eta}_k &= -\nu\eta_k + (y-\hat{y}_k)^\top(\Lambda_1 + L_k^\top\Lambda_2 L_k)(y-\hat{y}_k)\\ &= -\nu\eta_k + \Delta_k^\top(\Lambda_1 + L_k^\top\Lambda_2 L_k)\Delta_k.\end{aligned} \tag{5.106}$$

We evaluate (5.106) for $k=1$ at $(t,j)=(0,0)$. As $\Delta_1(0,0)=\Delta_k(0,0)$, from item (*ii*) of Proposition 5.4 and since Λ_2 is positive definite, we obtain

$$\begin{aligned}\dot{\eta}_1(0,0) &= -\nu\eta_1(0,0) + \Delta_1(0,0)^\top(\Lambda_1 + L_1^\top\Lambda_2 L_1)\Delta_1(0,0)\\ &= -\nu\eta_{k^\star}(0,0) + \Delta_{k^\star}(0,0)^\top(\Lambda_1 + L_1^\top\Lambda_2 L_1)\Delta_{k^\star}(0,0)\\ &> -\nu\eta_{k^\star}(0,0) + \Delta_{k^\star}(0,0)^\top(\Lambda_1 + L_{k^\star}^\top\Lambda_2 L_{k^\star})\Delta_{k^\star}(0,0)\\ &= \dot{\eta}_{k^\star}(0,0)\end{aligned} \tag{5.107}$$

for any $k^\star \in \{2,\dots,N+1\}$ such that $L_{k^\star}^\top\Lambda_2 L_{k^\star} < L_1^\top\Lambda_2 L_1$. The strict inequality in (5.107) comes from the condition $L_{k^\star}^\top\Lambda_2 L_{k^\star} < L_1^\top\Lambda_2 L_1$ on the observer gain selection, with $\Lambda_2 \in \mathbb{S}^{n_x}_{>0}$, and $\Delta_{k^\star}(0,0) \neq 0$ by item (*iii*) of Proposition 5.4. Since q is maximal it is t-complete by Propositions 5.2 and 5.3. Moreover, q can exhibit at most two consecutive jumps as explained in Section 5.5.2 and thus there exists $j^\star \in \{0,1\}$ such that $\sigma(0,j^\star)=\tilde{k}$ with $\tilde{k} \in \underset{k\in\Pi}{\operatorname{argmin}}\ \dot{\eta}_k(0,j^\star)$, with $\Pi = \underset{k\in\{1,\dots,N+1\}}{\operatorname{argmin}}\ \eta_k(0,j^\star)$ and $(0,j^\star+1)\notin \operatorname{dom} q$. Note that $L_{\tilde{k}}^\top\Lambda_2 L_{\tilde{k}} < L_1^\top\Lambda_2 L_1$ and

$$\dot{q}(0,j^\star) \in T_{\mathscr{C}}(q) := \{q \in \mathscr{Q} : \dot{\eta}_k \geqslant \dot{\eta}_\sigma, \forall k \in \{1,\dots,N+1\}\}, \tag{5.108}$$

where $\dot{\eta}_k = -\nu\eta_k + (y-\hat{y}_k)^\top(\Lambda_1 + L_k^\top\Lambda_2 L_k)(y-\hat{y}_k)$ and $\dot{\eta}_\sigma = -\nu\eta_\sigma + (y-\hat{y}_\sigma)^\top(\Lambda_1 + L_\sigma^\top\Lambda_2 L_\sigma)(y-\hat{y}_\sigma)$, for all $(t,j)\in\operatorname{dom} q$ with some abuse of notation, in view of Lemma 2.1 in Chapter 2. From (5.17d) and (5.107), we obtain

$$\dot{\eta}_{\sigma(0,j^\star)}(0,j^\star) = \dot{\eta}_{\tilde{k}}(0,j^\star) < \dot{\eta}_1(0,j^\star). \tag{5.109}$$

Moreover, since q is t-complete, we have that there exists $\epsilon > 0$ such that $q(t,j^\star) \in \mathscr{C}$ for all $t \in [0,\epsilon]$. Consequently, $(t^\star,j^\star) \in \operatorname{dom} q^\star$ for all $t^\star \in [0,\epsilon]$. In addition, we have

$$\eta_{\sigma(0,j^\star)}(0,j^\star) = \eta_1(0,j^\star) = \eta_0 \tag{5.110}$$

both when $j^\star=0$ and $j^\star=1$ from (5.17a) and (5.17b). From (5.109) and (5.110) we obtain

$$\eta_{\sigma(t^\star,j^\star)}(t^\star,j^\star) < \eta_1(t^\star,j^\star). \tag{5.111}$$

This concludes the proof. ■

Note that, the conditions in items (*i*) and (*ii*) of Proposition 5.4 can always be ensured by designing the same initial condition for the state estimate and monitoring variables for all the modes.

Moreover, condition in item (*iii*) is verified almost everywhere (it is a set of measure zero). We also acknowledge that we state the performance improvement with respect to costs J_1 and J_σ, and that it would be interesting to state properties for a cost, which involves the state estimation errors e_1 and e_σ. This is a challenging question, which goes beyond the scope of this chapter. Some preliminary results in this direction are presented in Appendix B.

5.7 Numerical case studies

5.7.1 Van der Pol oscillator

We consider

$$\begin{aligned} \dot{x} &= Ax + B\varphi(x) \\ y &= Cx + w \end{aligned} \tag{5.112a}$$

where $x = (x_1, x_2) \in \mathbb{R}^2$ is the system state to be estimated, $y \in \mathbb{R}$ is the measured output and $w \in \mathbb{R}$ is the measurement noise. The system matrices are

$$A = \begin{bmatrix} 0 & 1 \\ 0 & 0 \end{bmatrix},\ B = \begin{bmatrix} 0 \\ 1 \end{bmatrix},\ C = \begin{bmatrix} 1 & 0 \end{bmatrix} \tag{5.112b}$$

and $\varphi(x) = \text{sat}(-x_1 + 0.5(1 - x_1^2)x_2)$ for any $x \in \mathbb{R}^2$, where the saturation level is symmetric and equal to 10. We consider the measurement noise $w(t) = 0.1\cos(\omega(t))$ with $\omega(t) = 10$ when $t \in [0, 20]$, $\omega(t) = 100$ when $t \in (20, 40]$, $\omega(t) = 200$ when $t \in (40, 70]$ and $\omega(t) = 20$ when $t \in (70, 100]$.

We design a nominal high-gain observer [6] for system (5.112a)

$$\begin{aligned} \dot{\hat{x}}_1 &= A\hat{x}_1 + B\varphi(\hat{x}_1) + L_1(y - \hat{y}_1) \\ \hat{y}_1 &= C\hat{x}_1 \end{aligned} \tag{5.113}$$

where $\hat{x}_1$ is the state estimate, $\hat{y}_1$ is the estimated output and $L_1 \in \mathbb{R}^{2\times 1}$ is the output injection gain, which is defined as $L_1 := H_1 D$, where $D \in \mathbb{R}^{2\times 1}$, $H_1 = \text{diag}(h_1, h_1^2) \in \mathbb{R}^{2\times 2}$, with $h_1 \in \mathbb{R}_{>0}$ the high-gain design parameter. To satisfy Assumption 5.1, $D \in \mathbb{R}^{2\times 1}$ is selected such that the matrix $A - DC$ is Hurwitz and the parameter h_1 is taken sufficiently large, i.e., $h_1 \geqslant h_1^\star$, where $h_1^\star$ is equal to $2\lambda_{\max}(P)K$, where $P \in \mathbb{R}^{2\times 2}$ is the solution of the Lyapunov equation $P(A-DC) + (A-DC)^\top P = -I_2$ and $K = 58.25$ is the Lipschitz constant of the function φ. We select D such that the eigenvalues of $A - DC$ are equal to -1 and -2 and we obtain $D = [3, 2]$, while the parameter h_1 is selected equal to $200 > h_1^\star = 152.50$. With this choice of h_1, Assumption 5.1 is satisfied with a quadratic Lyapunov function and $\alpha = 53.28$. Furthermore, since the output is linear, also Assumption 5.2 is satisfied.

We consider $N = 4$ additional modes, with the same structure as the nominal one in (5.113). The only difference is the output injection gain $L_k \in \mathbb{R}^{2\times 1}$, which is defined as $L_k := H_k D$, with $H_k = \text{diag}(h_k, h_k^2) \in \mathbb{R}^{2\times 2}$, with $k \in \{2, \ldots, 5\}$. We select $h_2 = 20$, $h_3 = 1$, $h_4 = 0$ and $h_5 = -1$.

6. High gain observer design is described in Section 2.2.3.

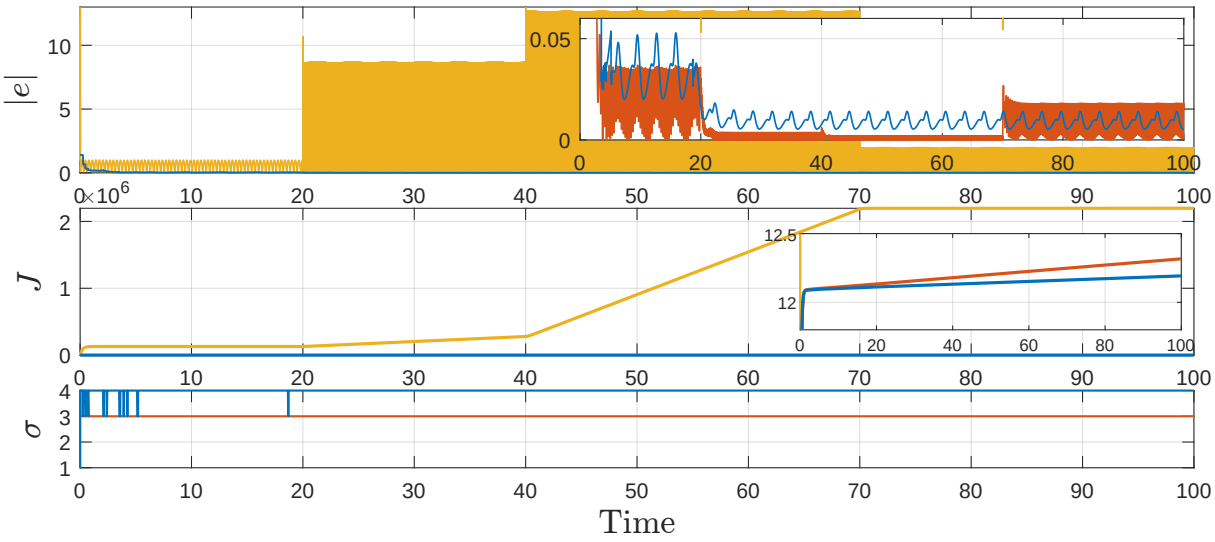

FIGURE 5.2 – Van der Pol oscillator. Norm of the estimation error $|e|$ (top figure), performance cost J (middle figure) and σ (bottom figure). Nominal (yellow), without resets (red), with resets (blue).

TABLE 5.1 – Van der Pol oscillator. Average MAE and RMSE.

	no reset			reset		
	e_1	e_σ	% improv.	e_1	e_σ	% improv.
MAE	4.405	0.025	**99.44**	4.397	0.034	**99.23**
RMSE	4.421	0.026	**99.40**	4.413	0.035	**99.20**

Note that $h_k \leqslant h_1^\star$, for all $k \in \{2,\dots,5\}$. Therefore, we have no guarantees that these modes satisfy Assumption 5.1, and consequently, that they converge. Simulations suggest that the modes with L_2 and L_3 converge, while the ones with L_4 and L_5 do not. Note that, the gain $L_4 = 0_{2\times 1}$ is the best choice to annihilate the effects of the measurement noise.

We simulate the proposed estimation technique considering the initial conditions $x(0,0) = (1,1)$, $\hat{x}_k(0,0) = (0,0)$, $\eta_k(0,0) = 10$ for all $k \in \{1,\dots,5\}$ and $\sigma(0,0) = 1$. Both cases, without and with resets, are simulated with $\nu = 5$, $\Lambda_1 = 1$, $\Lambda_2 = 0.1\cdot I_2$ and $\varepsilon = 10^{-4}$. Note that the condition $\nu \in (0,\alpha]$ is satisfied.

The norm of the nominal estimation error, namely $|e_1|$, as well as $|e_\sigma|$, obtained with or without resets, are shown in Figure 5.2, together with the nominal performance cost J_1 and the costs J_σ obtained both in the case without and with resets. Figure 5.2 shows that both solutions (without resets and with resets) improve the estimation performance compared to the nominal one. The last plot in Figure 5.2 represents σ and indicates which mode is selected at every time instant both in the case without and with resets. Interestingly, when the resets are considered, the fourth mode (with $L_4 = [0,0]^\top$), that is not converging, is selected.

To further evaluate the performance improvement given by the hybrid multi-observer, we run 100 simulations with different initial conditions for the state estimate of all the modes of the multi-observer, both in the case without and with resets. In particular, both components of $\hat{x}_k(0,0) \in \mathbb{R}^2$,

for all $k \in \{1,\dots,5\}$, were selected randomly in the interval $[-2,2]$ and, in each simulation, all modes of the multi-observer were initialized with the same state estimate. The system state, the monitoring variables and the signal σ were always initialized at $x(0,0) = (1,1)$, $\eta_k(0,0) = 10$, for all $k \in \{1,\dots,5\}$, and $\sigma(0,0) = 1$. We considered the same choice of design parameters as before. To quantify the performance improvement, we evaluate the mean absolute error (MAE) and the root mean square error (RMSE), averaged over all the simulations, of the state estimation error obtained with the nominal observer and the hybrid multi-observer both in the case without and with resets. The obtained data are given in Table 5.1. Note that the data for e_1 without and with resets are slightly different because the 100 initial conditions were randomly selected and thus they may be different in the simulations without and with resets. Table 5.1 shows that the proposed technique, both without and with resets, highly improves the estimation performance compared to the nominal one. Indeed, both the MAE and the RMSE are improved by more than 99% both in the case without and with resets. Moreover, in this example, the performance of the hybrid multi-observer without and with resets are very similar, with the case without resets that slightly outperforms the case where the resets are implemented, both in term of MAE and RMSE.

5.7.2 Flexible joint robotic arm

In this second example we consider a flexible joint robotic arm [125]. The system model is described by [7]

$$\begin{aligned} \dot{x} &= Ax + Bu + G\sigma(Hx) + v \\ y &= Cx + w, \end{aligned} \tag{5.114a}$$

where the system state that need to be estimated is $x := (x_1, x_2, x_3, x_4)$, while the measured output y is defined as $y := (y_1, y_2) = (x_1, x_2)$. The system matrices are

$$\begin{aligned} A &= \begin{bmatrix} 0 & 1 & 0 & 0 \\ -48.6 & -1.25 & 48.6 & 0 \\ 0 & 0 & 0 & 1 \\ 19.5 & 0 & -19.5 & 0 \end{bmatrix}, \quad B = \begin{bmatrix} 0 \\ 21.6 \\ 0 \\ 0 \end{bmatrix}, \\ G &= \begin{bmatrix} 0 \\ 0 \\ 0 \\ -1 \end{bmatrix}, \quad H^\top = \begin{bmatrix} 0 \\ 0 \\ 1 \\ 0 \end{bmatrix}, \quad C^\top = \begin{bmatrix} 1 & 0 \\ 0 & 1 \\ 0 & 0 \\ 0 & 0 \end{bmatrix}, \end{aligned} \tag{5.114b}$$

and $\sigma(Hx) = 3.3\sin(x_3)$ for any $x \in \mathbb{R}^4$. As in [125], we assume that the input is $u(t) = \sin(t)$ for all $t \in \mathbb{R}_{\geqslant 0}$. Moreover, we consider the disturbance input $v(t) = 0.01(0,1,0,1)\sin(30t)$ for all $t \in \mathbb{R}_{\geqslant 0}$

7. In Chapter 4 we considered the same example (model and observer) and we implemented the event-triggered observer in the setting where the output measurement are transmitted to the observer via a digital network. In this chapter, we apply the proposed hybrid multi-observer to improve the estimation performance of the observer. Note that, in this case there is no network between the system and the observer. We recall model and nominal observer for completeness.

and the measurement noise $w(t) = 0.1(1,1)\sin(100t)$ for all $t \in \mathbb{R}_{\geqslant 0}$. We design a nominal observer

$$\begin{aligned} \dot{\hat{x}}_1 &= A\hat{x}_1 + Bu + G\sigma(H\hat{x}_1) + L_1(y - \hat{y}_1) \\ \hat{y}_1 &= C\hat{x}_1, \end{aligned} \tag{5.115}$$

where $L_1 \in \mathbb{R}^{4\times 2}$ is the observer gain that is designed following a polytopic approach [8] [95]. To do so, we solve the linear matrix inequalities $PA - WC + PG_i + G_i^\top P + A^\top P - C^\top W^\top \leqslant -Q,\ \ i \in \{1,2\}$, with $P \in \mathbb{R}^{4\times 4}$ symmetric positive definite and $W := PL \in \mathbb{R}^{4\times 2}$, where $G_1 := \begin{bmatrix} 0 & 0 & 0 & 0 \\ 0 & 0 & 0 & 0 \\ 0 & 0 & 0 & 0 \\ 0 & 0 & 3.3 & 0 \end{bmatrix}$, $G_2 := \begin{bmatrix} 0 & 0 & 0 & 0 \\ 0 & 0 & 0 & 0 \\ 0 & 0 & 0 & 0 \\ 0 & 0 & -3.3 & 0 \end{bmatrix}$ and $Q = I_4$. We obtain $L = \begin{bmatrix} 0.58 & -42.96 \\ -4.67 & 2.83 \\ 3.16 & 49.25 \\ 16.34 & 88.46 \end{bmatrix}$. Defining the Lyapunov function $V(\xi) := e_1^\top P e_1$ for any $e_1 \in \mathbb{R}^4$, where $e_1 := x - \hat{x}_1$ is the state estimation error, Assumption 5.1 is satisfied with $\alpha = 0.076$. In addition, since the output is linear, also Assumption 5.2 is satisifed.

We consider $N = 10$ additional modes, with the same structure as the nominal one in (5.115). The only difference is the output injection gain $L_k \in \mathbb{R}^{4\times 2}$. To select the additional gain we consider three possible linearizations of the system dynamics. In particular, we consider $G_i x$ instead of $G\sigma(Hx)$ in (5.114a), with $i \in \{1,2,3\}$ and G_1 and G_2 defined above and $G_3 := 0_{4\times 4}$ and thus, we obtain the linear system

$$\begin{aligned} \dot{x} &= Ax + Bu + G_i x + \nu = A_i x + B_u + \nu \\ y &= Cx + w, \end{aligned} \tag{5.116}$$

with $i \in \{1,2,3\}$ and the matrices A_1, A_2 and A_3 given by $A_1 := A + G_1$, $A_2 := A + G_2$, $A_3 := A$. We then design three Luenberger observers for all the three liner system obtained. In particular, the additional gains L_2, L_3 and L_4 were designed placing the eigenvalues of the matrices $(A_i - L_{i+1}C)$ in -1, -2, -3 and -4, with $i = \{1,2,3\}$, the gains L_5, L_6 and L_7 were designed placing the eigenvalues of the matrices $(A_i - L_{i+4}C)$ in -10, -20, -30 and -40, while the additional gains L_8, L_9 and L_{10} were designed placing the eigenvalues of the matrices $(A_i - L_{i+7}C)$ in -0.1, -0.2, -0.3 and -0.4. Finally, we chose $L_{11} = 0_{4\times 2}$. Note that, the additional gains L_k, $k \in \{2,\ldots,10\}$, where designed considering the linearization of system (5.114a) and the additional gain L_{11} produces an open-loop mode. Therefore, we have no guarantees that these modes satisfy Assumption 5.1 for the nonlinear system (5.114a), and consequently, that their estimation errors converge. Note that, the gain $L_{11} = 0_{4\times 2}$ is the best choice to annihilate the measurement noise.

We simulate the proposed estimation technique considering the initial conditions $x(0,0) = (3,2,3,-2)$, $\hat{x}_k(0,0) = (0,0,0,0)$, $\eta_k(0,0) = 10$ for all $k \in \{1,\ldots,11\}$ and $\sigma(0,0) = 1$. Both cases, without and with resets, are simulated with $\nu = 0.05$, $\Lambda_1 = 1 \cdot I_2$, $\Lambda_2 = 0.01 \cdot I_4$ and $\varepsilon = 10^{-4}$. Note that the

8. Observer design following a polytopic approach is described in Section 2.2.3.

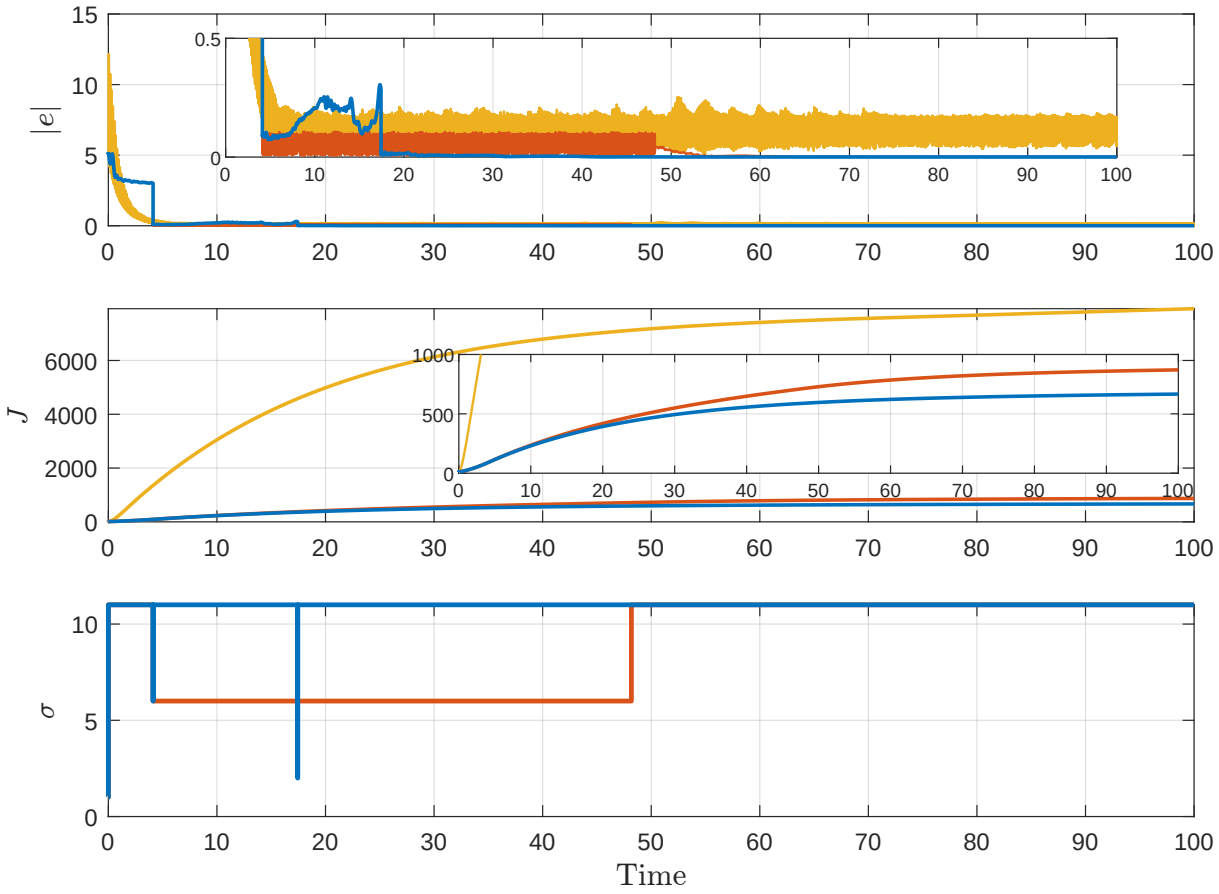

FIGURE 5.3 – Flexible joint robotic arm. Norm of the estimation error $|e|$ (top figure), performance cost J (middle figure) and σ (bottom figure). Nominal (yellow), without resets (red), with resets (blue).

condition $\nu \in (0, \alpha]$ is satisfied.

The norm of the nominal estimation error, namely $|e_1|$, as well as $|e_\sigma|$, obtained with or without resets, are shown in Figure 5.3, together with the nominal performance cost J_1 and the costs J_σ obtained both in the case without and with resets. Figure 5.3 shows that both solutions (without resets and with resets) improve the estimation performance compared to the nominal one, in particular the improvement is relevant after the transients. In addition, the second plot in Figure 5.3 shows that the cost in the case with resets is better than the one obtain in the case without resets and are both smaller than the nominal one. The last plot in Figure 5.3 represents σ and indicates which mode is selected at every time instant both in the case without and with resets. Interestingly, both when the

TABLE 5.2 – Flexible joint robotic arm. Average MAE and RMSE.

	no reset			reset		
	e_1	e_σ	% improv.	e_1	e_σ	% improv.
MAE	0.991	0.718	**27.55**	1.702	1.350	**20.66**
RMSE	3.055	3.027	**0.90**	3.916	4.912	**-25.45**

TABLE 5.3 – Flexible joint robotic arm. Average MAE and RMSE for $t \in [70, 100]$.

	no reset			reset		
	e_1	e_σ	% improv.	e_1	e_σ	% improv.
MAE	0.167	0.012	**92.55**	0.167	0.001	**99.34**
RMSE	0.167	0.013	**91.81**	0.167	0.025	**98.49**

resets are considered and when not, the eleventh mode, which is in open-loop since $L_{11} = 0_{4\times 2}$, is selected.

To further evaluate the performance improvement given by the hybrid multi-observer, we run 100 simulations with different initial conditions for the state estimate of all the modes of the multi-observer, both in the case without and with resets. In particular, the first and third components of $\hat{x}_k(0,0) \in \mathbb{R}^4$, for all $k \in \{1,\dots,11\}$, were selected randomly in the interval $[0, 20]$, while the second and fourth components of $\hat{x}_k(0,0) \in \mathbb{R}^4$, for all $k \in \{1,\dots,11\}$, were selected randomly in the interval $[0, 10]$ and, in each simulation, all modes of the multi-observer were initialized with the same state estimate. The system state, the monitoring variables and the signal σ were always initialized at $x(0,0) = (3,2,3,-2)$, $\eta_k(0,0) = 10$, for all $k \in \{1,\dots,11\}$, and $\sigma(0,0) = 1$. We considered the same choice of design parameters as before. To quantify the performance improvement, we evaluate the mean absolute error (MAE) and the root mean square error (RMSE), averaged over all the simulations, of the state estimation error obtained with the nominal observer and the hybrid multi-observer both in the case without and with resets. The obtained data are given in Table 5.2. Note that the data for e_1 without and with resets are slightly different because the 100 initial conditions were randomly selected (in large intervals) and thus they may be different in the simulations without and with resets. Table 5.2 shows that the proposed technique, both without and with resets, improves the estimation performance compared to the nominal one in almost all the considered MAE and RMSE. However, in the case with resets the RMSE performance are worse. This data does not contradict the theory, since in Section 5.6 we proved the performance improvement in terms of the costs J_1 and J_σ, while Table 5.2 evaluates the improvement in terms of the state estimation error.

We also evaluate the mean absolute error (MAE) and the root mean square error (RMSE), averaged over all the simulations, of the state estimation error obtained with the nominal observer and the hybrid multi-observer both in the case without and with resets only in the time interval $[70, 100]$, in order to evaluate the steady-state performance improvement. The obtained data are given in Table 5.3, which shows that the proposed technique, both without and with resets, highly improves the estimation performance compared to the nominal one when the transient is neglected. Indeed, both the MAE and the RMSE are improved by more than 90% both in the case without and with resets, with the case with resets that slightly outperforms the case without resets, both in term of MAE and RMSE. Thus, from Tables 5.2 and 5.3 we can conclude that, for this example, the proposed hybrid multi-observer techniques is more efficient in improving the estimation performance of the given nominal observer in steady-state, while, during the transient, the performance are similar, or can be even worse, especially in the case with resets. An option to overcome this behaviour and force

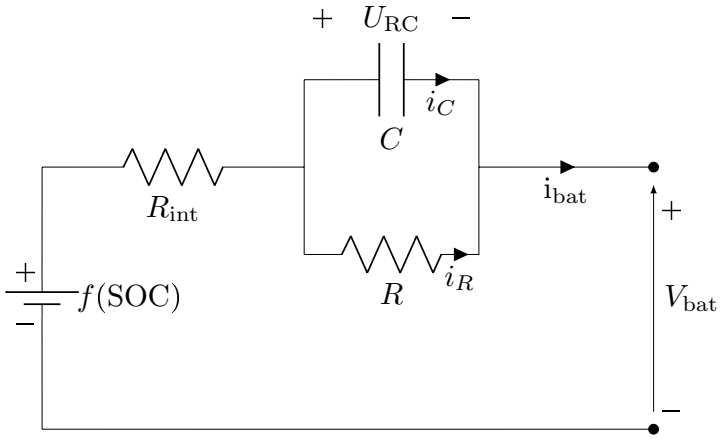

FIGURE 5.4 – Equivalent electrical circuit of a single battery cell.

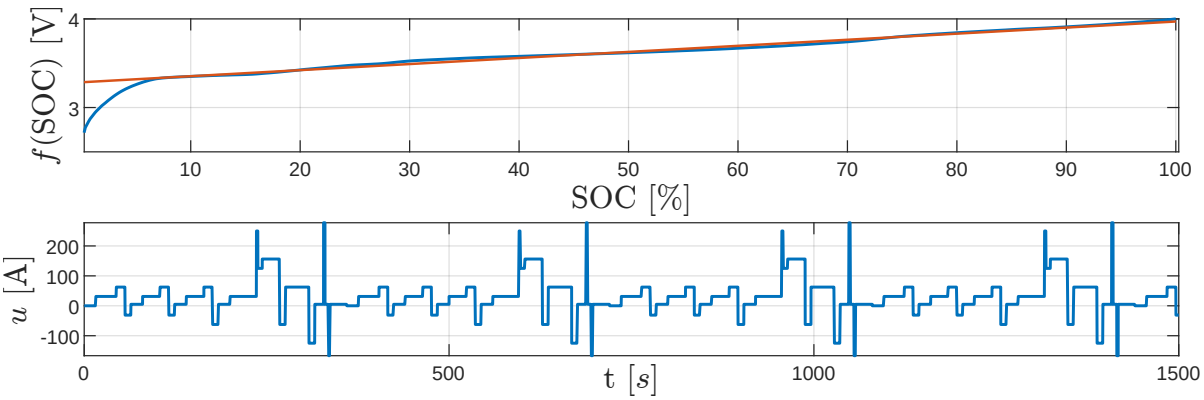

FIGURE 5.5 – $f(\mathrm{SOC})$(blue) with its linearization (red) and PHEV current input.

the selection of the nominal observer for some amount of time at the beginning of the simulation consists in choosing the initial condition of the monitoring variable of the nominal observer, namely, $\eta_1(0,0)$ smaller than the initial condition of the monitoring variables of the other modes, namely, $\eta_k(0,0)$, for all $k \in \{2,\dots,11\}$. This technique is not implemented in this example, but we will use it in Chapter 6 where the hybrid multi-observer approach is applied for the state estimation of an electrochemical model of a lithium-ion battery with standard model and parameters.

5.7.3 Electric circuit model of a lithium-ion battery

We consider an electric circuit model of 1-cell lithium-ion battery shown in Figure 5.4, with a nonlinear output map. Compared to the battery model we considered in the numerical example in Chapter 3, here we do not linearize the function $f(\mathrm{SOC})$ in the output equation. As a result, we are now considering a nonlinear system, compared to the linear time-invariant one used to model the lithium-ion battery in Chapter 3.

From the circuit the following system model is derived

$$\begin{aligned} \dot{x} &= Ax + Bu \\ y &= Cx + f(Hx) + Du + w. \end{aligned} \tag{5.117a}$$

The state is $x := (U_{\text{RC}}, \text{SOC}) \in \mathbb{R}^2$, where U_{RC} is the voltage of the RC circuit and SOC is the state of charge of the battery. The output y is the battery output voltage, the input u is the current and w is the measurement noise. The system matrices are

$$A = \begin{bmatrix} -\frac{1}{\tau} & 0 \\ 0 & 0 \end{bmatrix}, \; B = \begin{bmatrix} \frac{1}{c} \\ -\frac{1}{Q} \end{bmatrix}, \; C = \begin{bmatrix} -1 & 0 \end{bmatrix}, \; H = \begin{bmatrix} 0 & 1 \end{bmatrix}, \; D = \begin{bmatrix} -R_{\text{int}} \end{bmatrix}. \tag{5.117b}$$

Considering the temperature to be constant and equal to 25°C, the parameters values are $\tau = 7$ s, $R = 0.5 \cdot 10^{-3}$ Ω, $c = \frac{\tau}{R}$ F, $Q = 25$ Ah and $R_{\text{int}} = 1$ mΩ. The function f and its linearization are shown in Figure 5.5 on the interval $[0, 100]$ % and we consider a first order approximation outside the interval $[0, 100]$ %. The function f satisfies Assumption 5.2 since it has bounded derivatives. The input u is given by a plug-in hybrid electric vehicle (PHEV) current profile, see Figure 5.5, and the measurement noise is given by $w(t) = 0.01 \sin(10t)$, for all $t \geqslant 0$.

We design the nominal observer

$$\begin{aligned} \dot{\hat{x}}_1 &= A\hat{x}_1 + Bu + L_1(y - \hat{y}_1) \\ \hat{y}_1 &= C\hat{x}_1 + f(H\hat{x}_1) + Du, \end{aligned} \tag{5.118}$$

where $\hat{x}_1$ is the state estimate, $\hat{y}_1$ is the output estimate and $L_1 = [-2.07, 2.48]^\top \in \mathbb{R}^{2\times 1}$ is the observer gain that is designed following a polytopic approach like in [96] as described in Section 2.2.3. Observer (5.118) satisfies Assumption 5.1 with $\alpha = 0.1$.

To improve the estimation performance, we design the hybrid multi-observer considering $N = 3$ additional modes. To select L_2, we linearize the output map and we design a Luenberger observer with eigenvalues in $[-0.2, -0.3]$ and we obtain $L_2 = [0.06, 61.25]^\top$. Note that, since this observer is designed for the linearized system, we have no guarantees that it satisfies an input-to-state stability property for the nonlinear system. Moreover, we chose $L_3 = [0, 0]^\top$ and we designed an extended Kalman filter [98], described in Section 2.2.3, with $R_{\text{EKF}} = 1$, $Q_{\text{EKF}} = 0.1 \cdot I_2$ and $\alpha_{\text{EKF}} = 0.01$, to obtain L_4, which is thus a time-varying gain. Note that, in view of Remark 5.3, the results presented in this chapter hold also in this case.

We simulate the proposed hybrid multi-observer, both without and with resets, considering the initial conditions $x(0,0) = (1, 100)$, $\hat{x}_k(0,0) = (0.5, 50)$, $\eta_k(0,0) = 0$ for all $k \in \{1, \ldots, 4\}$ and $\sigma(0,0) = 1$. The design parameters are selected $\nu = 0.05$, $\Lambda_1 = 1$, $\Lambda_2 = \begin{bmatrix} 1 & 0 \\ 0 & 10^{-4} \end{bmatrix}$ and $\varepsilon = 10^{-2}$. Note that the condition $\nu \in (0, \alpha]$ is satisfied.

Figure 5.6 shows the norm of the nominal estimation error, namely $|e_1|$, as well as $|e_\sigma|$, obtained

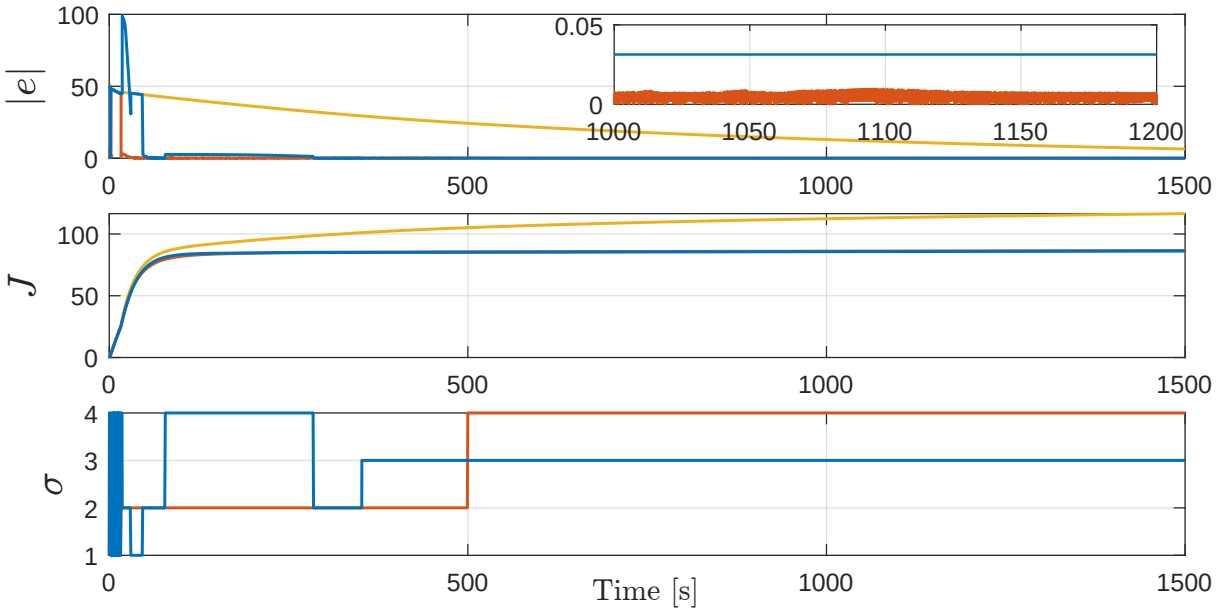

FIGURE 5.6 – Battery example. Norm of the estimation error $|e|$ (top figure), performance cost J (middle figure) and σ (bottom figure). Nominal (yellow), without resets (red), with resets (blue).

TABLE 5.4 – Battery example. Average MAE and RMSE.

	no reset			reset		
	e_1	e_σ	% improv.	e_1	e_σ	% improv.
MAE	28.10	3.37	**87.99**	27.30	1.65	**93.94**
RMSE	30.87	8.66	**71.95**	29.90	5.99	**79.98**

with or without resets. Moreover, the nominal performance cost J_1 and the costs J_σ obtained both in the case without and with resets are shown in Figure 5.6, together with the signal σ, which indicates the selected mode at every time instant. Figure 5.6 shows that both solutions (without resets and with resets) significantly improve the estimation performance compared to the nominal one.

As in the examples in Sections 5.7.1 and 5.7.2, we run 100 simulations with different initial conditions for the state estimate of all modes of the multi-observer. In particular the first component of $\hat{x}_k(0,0)$ was selected randomly in the interval $[0,3]$ [V], while the second component of $\hat{x}_k(0,0)$ was selected randomly in the interval $[1,100]$ [%], for all $k \in \{1,\dots,4\}$. All the other initial conditions and the design parameters were selected as before. We evaluate the MAE and the RMSE as in the examples in Sections 5.7.1 and 5.7.2 and the obtained results, given in Table 5.4, show the estimation performance improvement. In this example, the case with resets outperforms the case without resets, both in term of MAE and RMSE.

5.8 Conclusions

We have presented a novel hybrid multi-observer that improves the state estimation performance of a given nominal nonlinear observer. Each additional mode of the multi-observer differs from the

nominal one only in its output injection gain, that can be freely selected as no convergence property is required for these modes. Inspired by supervisory control/observer approaches, we have designed a switching criterion, based on monitoring variables, that selects one mode at any time instant by evaluating their performance. We have proved an input-to-state stability property of the estimation error and the estimation performance improvement. Finally, numerical examples confirm the efficiency of the proposed approach.

We believe that the flexibility of the presented framework leads to a range of fascinating research questions, which are discussed in Chapter 7. In the next chapter, the proposed hybrid multi-observer is applied for the state estimation of an electrochemical model of a lithium-ion battery.

Chapter 6

Application to lithium-ion batteries

Contents

Abstract - *Effective management and just-in-time maintenance of lithium-ion batteries require the knowledge of unmeasured (internal) variables that need to be estimated. Observers are thus designed for this purpose using a mathematical model of the battery internal dynamics. It appears that it is often*

The results of this chapter are based on [82]. Note that in [82] we consider an earlier version, presented in [83], of the hybrid multi-observer, while results in this chapter consider the final version of the hybrid multi-observer, presented in Chapter 5 and based on [81].

difficult to tune the observers to obtain good estimation performances both in terms of convergence speed and accuracy, while these are essential in practice. In this context, we demonstrate how the hybrid multi-observer presented in Chapter 5 can be used to improve the performance of a given observer designed for an electrochemical model of a lithium-ion battery. Simulation results, obtained with standard parameters values, show the estimation performance improvement using the proposed method.

6.1 Introduction

Lithium-ion batteries are widely used for the many advantages they exhibit in terms of volume capacity, weight, power density and the absence of memory effect, compared to other energy storage technologies. On the other hand, the so-called battery management system (BMS) is required for a safe and efficient usage of the battery. The BMS impacts the battery performance and lifespan and it depends on the actual state of charge (SOC) of the battery, which is directly related to the lithium concentrations in the battery electrodes. An accurate knowledge of the SOC is therefore essential for proper battery management. Unfortunately, the SOC cannot be measured directly and thus needs to be estimated from the measured variables, typically the current and the voltage. To address this challenge, a common approach is to design observers, based on a mathematical model of the internal dynamics, to estimate the unmeasured internal states, see e.g., [116, 141]. This task is non-trivial because of the nonlinear relationships between the internal variables and the measured ones. Several approaches are available in the literature depending on the type of battery model (equivalent circuit model, infinite/finite-dimensional electrochemical models) and the type of observers, see, e.g., [3, 97, 142–148].

In this work, we focus on the finite-dimensional electrochemical model considered in [3,97,149], which is derived from the infinite-dimensional models in [145, 146], as it offers a good compromise between accuracy and computational complexity. The model takes the form of an affine system with a nonlinear output map, where the system states are the lithium concentrations in the electrodes, the input is the current and the measured output is the voltage. A globally convergent observer was designed for this model in [97] based on a polytopic approach. The issue is that to tune this observer to obtain both fast convergence and good robustness properties with respect to measurement noise and model uncertainties is highly non-trivial. The objective of this work is to address this challenge by systematically improving the estimation performance of an observer designed as in [97] using a multi-observer approach (see, e.g., [5, Section 8.3]). In particular, we follow the hybrid methodology presented in Chapter 5. We recall that the proposed technique consists in first designing a nominal observer using [97] that satisfies an input-to-state stability property. Then, a bank of additional observer-like systems, that differ from the nominal one only on their gains, are added in parallel to the nominal observer. The gains of these additional dynamical systems can be arbitrary selected and do not need to be tuned to guarantee a convergence property of their estimation errors. These gains can thus be selected using any analytical or heuristic method to improve the convergence speed or the robustness of the nominal observer. Each of these systems, as well as the nominal observer, is called mode for the sake of convenience. To evaluate the performance of each mode, monitoring

variables are introduced. Based on these monitoring variables, the "best mode" is then selected at any time instant and its state estimate is considered for the battery internal state estimation. Therefore, the state estimate of the hybrid multi-observer switches between the states estimates of the modes and thus it is called hybrid. The observer is modeled as an hybrid system using the formalism of [31]. Note that, due to these switching, the state estimate exhibits discontinuities, which can be a problem for batteries, as this means the SOC estimate would experience jumps. For this reason, in this chapter, we add the filtered version of the hybrid multi-observer state estimate presented in Section 5.3.6. We provide an input-to-state stability property with respect to measurement noise, perturbation and disturbance for the hybrid system representing the lithium-ion battery and the multi-observer implemented for its state estimation. To illustrate the efficiency of the hybrid scheme, we present simulation results where a higher fidelity model of the battery is used to generate the output voltage compared to the one used to design the observers. Using the technique in [97], we first design the nominal observer, which shows good transient performance in terms of speed and small overshoot, but whose accuracy in steady-state may not be satisfactory. To address this issue, we select the gains of the additional modes of the hybrid multi-observer smaller than the nominal one, with the aim of improving the robustness to noises and perturbations. Simulation results show that the estimation performance are significantly improved with the hybrid multi-observer presented in Chapter 5, thereby illustrating the potential of this approach.

6.2 Electrochemical battery model

We recall in this section the single particle electrochemical model of lithium-ion battery in [3].

6.2.1 Model description and assumptions

The lithium-ion battery cell, whose schematic is shown in Figure 6.1, is composed of four elements: two electrodes, one positive and one negative, that are separated by the separator and those three components are immersed in a ionic solution, called electrolyte, which can exchange lithium with the electrodes and provides electrical insulation. Therefore, the electrons cannot be exchanged from one electrode to the other. Due to the electrodes structure, which consists in very small, almost-spherical particles made of porous materials, the electrolyte can penetrate inside the electrode, creating a large contact surface between each electrode and the electrolyte, which produces an electrochemical coupling between the electrode material and the lithium dissolved in the electrolyte. Thus, each electrode has a certain potential and this produces a potential difference between the positive and negative electrode. Since the electrons cannot be exchanged from one electrode to the other within the battery, they will go through an external electrical circuit, if it exists, producing a flow of electrons, that from a macroscopic point of view, corresponds to the current. Note that the charges equilibrium in the electrodes and in the electrolyte is preserved at any time because when lithium is removed from its source electrode, another is inserted in its electrode of destination. The model in [3] relies on the next assumption.

Assumption 6.1. *The following hold.*

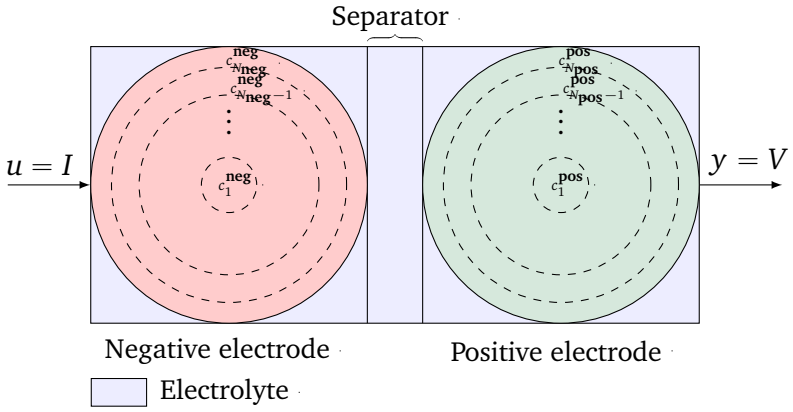

FIGURE 6.1 – Battery model schematic.

(i) Each electrode in the model is composed of a single sphere particle of the average size of the particles that compose the actual electrode.

(ii) The electrolyte dynamics is neglected.

(iii) The temperature is constant. □

Item (*i*) implies that each electrode can be reduced to a single sphere particle of the average size of the particles that compose the actual electrode, which is the single particle model (SPM) as in [3, 97, 147, 150, 151]. In view of item (*ii*) of Assumption 6.1, the electrolyte contribution to the output voltage will be represented by a resistive term. However, we will relax this item in the simulation section to evaluate the estimation scheme robustness, see Section 6.4. On the other hand, it is possible to relax the constant temperature assumption in item (*iii*) of Assumption 6.1 in view of [3, Sections II.A and III.B], this is left for future work.

As explained in [3], in view of item (*i*) of Assumption 6.1, the main physical phenomenon is the lithium diffusion in the electrodes, which can be described using partial differential equations [145, 146]. To simplify the model and obtain a set of ordinary differential equations, each sphere is spatially discretized in N_s samples of uniform volume, corresponding to N_s crowns, where the subscript $s \in \{\text{neg}, \text{pos}\}$ denotes the negative or the positive electrode, see Figure 6.1. We assume for this purpose that the lithium concentration in each crown of the sphere is constant. We denote by c_i^s, with $i \in \{1, \ldots, N_s\}$ and $s \in \{\text{neg}, \text{pos}\}$, the lithium concentration in the i^{th} crown of the electrode, where $i = 1$ corresponds to the one at the center of the electrode, while $i = N_s$ corresponds to the one at the surface of the electrode. As in [3], we obtain the following set of ordinary differential equations for the battery model. For $i \in \{2, \ldots, N_s - 1\}$,

$$\frac{dc_i^s}{dt} = \frac{S_{i-1}^s}{r_i - r_{i-1}} \frac{D_s}{V_i^s} c_{i-1}^s - \left(\frac{S_{i-1}^s}{r_i - r_{i-1}} + \frac{S_i^s}{r_{i+1} - r_i} \right) \frac{D_s}{V_i^s} c_i^s + \frac{S_i^s}{r_{i+1} - r_i} \frac{D_s}{V_i^s} c_{i+1}^s, \tag{6.1a}$$

for $i = 1$,

$$\frac{dc_1^s}{dt} = \frac{S_1^s}{r_2 - r_1} \frac{D_s}{V_1^s} (-c_1^s + c_2^s) \tag{6.1b}$$

and for $i = N_s$,

$$\frac{dc^s_{N_s}}{dt} = \frac{S^s_{N_s-1}}{r_{N_s} - r_{N_s-1}} \frac{D_s}{V^s_{N_s}} (c^s_{N_s-1} + c^s_{N_s}) + \bar{K}^s_I I, \tag{6.1c}$$

where S^s_i is the surface of the i^{th} sample of the electrode s, D_s is the lithium diffusion coefficient, V^s_i is the volume of the sample i of the electrode and r_i is the radius of the i^{th} sample of the electrode, with $i \in \{1, \dots, N_s\}$ and $s \in \{\text{neg}, \text{pos}\}$. In addition, I in (6.1c) is the current and $\bar{K}^s_I := -\dfrac{S^s_{\text{tot}}}{V^s_1 a_s F \mathscr{A}_{\text{cell}} d_s}$, where $a_s := \dfrac{3\varepsilon_s}{R_s}$, S^s_{tot} is the total surface of the electrode, ε_s is the volume fraction, R_s is the radius, F is the Faraday's constant, $\mathscr{A}_{\text{cell}}$ is the cell area, d_s is thickness of the electrode and $s \in \{\text{neg}, \text{pos}\}$.

The quantity of lithium in solid phase is defined as

$$Q_{\text{Li}} := \alpha_{\text{neg}} \sum_{i=0}^{N_{\text{neg}}} c^{\text{neg}}_i V^{\text{neg}}_i + \alpha_{\text{pos}} \sum_{i=0}^{N_{\text{pos}}} c^{\text{pos}}_i V^{\text{pos}}_i, \tag{6.2}$$

where $\alpha_s := \dfrac{F}{3600} \dfrac{\varepsilon_s \mathscr{A}_{\text{cell}} d_s}{V^s_{\text{tot}}}$ and V^s_{tot} is the total volume of the electrode and $s \in \{\text{neg}, \text{pos}\}$. This equation derives from the mass conservation of the lithium in the solid-phase, which holds since the battery does not acquire or leak lithium materials over short time horizons.

Note that, from (6.2), we can express the concentration of lithium at the center of the negative electrode c^{neg}_1 as a linear combination of all other sampled concentration in solid phase,

$$c^{\text{neg}}_1 = \bar{K} + \sum_{i=2}^{N_{\text{neg}}} \beta^{\text{neg}}_i c^{\text{neg}}_i + \sum_{i=1}^{N_{\text{pos}}} \beta^{\text{pos}}_i c^{\text{pos}}_i \tag{6.3}$$

with $\bar{K} := \dfrac{Q_{Li}}{V^{\text{neg}}_1 \alpha_{\text{neg}}}$, $\beta^{\text{neg}}_i := -\dfrac{V^{\text{neg}}_i}{V^{\text{neg}}_1}$ for any $i \in \{1, \dots, N_{\text{neg}}\}$ and $\beta^{\text{pos}}_i := -\dfrac{\alpha_{\text{pos}} V^{\text{pos}}_i}{\alpha_{\text{neg}} V^{\text{neg}}_1}$ for any $i \in \{1, \dots, N_{\text{pos}}\}$. Equation (6.3) allows to reduce the dimension of the system state, which corresponds to the vector of the lithium concentrations in each sample of both electrodes and is defined as

$$x := (c^{\text{neg}}_2, ..., c^{\text{neg}}_{N_{\text{neg}}}, c^{\text{pos}}_1, ..., c^{\text{pos}}_{N_{\text{pos}}}) \in \mathbb{R}^{n_x} \tag{6.4}$$

with $n_x := N_{\text{neg}} - 1 + N_{\text{pos}}$.

We now derive the output voltage equation of the lithium-ion battery model. Its main components are the open circuit voltages (OCVs), which are the potential differences between the electrodes and the electrolyte without current and vary with the lithium concentration at the surface of the electrodes. An example of the OCVs is shown in Figure 6.3.

As in [3], the output voltage is

$$y := OCV_{\text{pos}}(H_{\text{pos}} x) - OCV_{\text{neg}}(H_{\text{neg}} x) + g(u) \in \mathbb{R} \tag{6.5}$$

where u corresponds to the input current I,

$$\begin{aligned} H_{\text{neg}} &:= (0_{1\times(N_{\text{neg}}-2)}, \frac{1}{c_{\text{neg}}^{\max}}, 0_{1\times N_{\text{pos}}}) \in \mathbb{R}^{1\times n_x} \\ H_{\text{pos}} &:= (0_{1\times(N-1)}, \frac{1}{c_{\text{pos}}^{\max}}) \in \mathbb{R}^{1\times n_x} \end{aligned} \tag{6.6}$$

and $g(u) := g_1(u) + g_2(u) + g_3(u)$, with

$$\begin{aligned} g_1(u) &:= 2\frac{RT}{F}\text{Argsh}\Big(\frac{-R_{\text{pos}}}{6\varepsilon_{\text{pos}} j_0^{\text{pos}} \mathscr{A}_{cell} d_{\text{pos}}} u\Big), \\ g_2(u) &:= -2\frac{RT}{F}\text{Argsh}\Big(\frac{R_{\text{neg}}}{6\varepsilon_{\text{neg}} j_0^{\text{neg}} \mathscr{A}_{cell} d_{\text{neg}}} u\Big), \\ g_3(u) &:= -\Big(\frac{1}{2\mathscr{A}_{cell}}\Big(\frac{d_{\text{neg}}}{\sigma_{\text{neg}}} + \frac{d_{\text{pos}}}{\sigma_{\text{pos}}}\Big) + \Omega_{\text{add}}\Big)u, \end{aligned} \tag{6.7}$$

where R is the gas constant, T is the temperature, j_0^s is the exchange current density, σ_s is the electronic conductivity, with $s \in \{\text{neg}, \text{pos}\}$ and Ω_{add} is the additional resistivity. Moreover, $\text{Argsh}(\xi) = \ln(\xi + \sqrt{\xi^2+1})$ for any $\xi \in \mathbb{R}$.

6.2.2 State-space representation

We consider the state-space model of the lithium-ion battery presented in [3], where we recall that the system state corresponds to the vector of the lithium concentrations in each sample of both electrodes $x = (c_2^{\text{neg}}, ..., c_{N_{\text{neg}}}^{\text{neg}}, c_1^{\text{pos}}, ..., c_{N_{\text{pos}}}^{\text{pos}}) \in \mathbb{R}^{n_x}$, with $n_x = N_{\text{neg}} + N_{\text{pos}} - 1$. The system input u is the current I and the system output y is the output voltage. The model is of the form

$$\begin{aligned} \dot{x} &= Ax + Bu + K + Ev \\ y &= h(x) + g(u) + w, \end{aligned} \tag{6.8}$$

where $v \in \mathbb{R}^{n_v}$ is an unknown disturbance input, $w \in \mathbb{R}$ is an unknown exogenous input affecting the output map and $E \in \mathbb{R}^{n_x \times n_v}$. The matrices $A \in \mathbb{R}^{n_x \times n_x}$, $B \in \mathbb{R}^{n_x \times 1}$, $K \in \mathbb{R}^{n_x \times 1}$ are given by

$$A := \begin{pmatrix} A_{2,\text{neg}} \\ A^\star \quad \text{diag}(A_{\text{neg}}, A_{\text{pos}}), \end{pmatrix} \tag{6.9a}$$

with

$$A^\star := \begin{pmatrix} \mu_{3,2}^{\text{neg}} \\ 0_{(n_x-2)\times 1} \end{pmatrix}, \tag{6.9b}$$

and $A_{2,\text{neg}} \in \mathbb{R}^{1\times n_x}$ in (6.9a) is defined as

$$A_{2,\text{neg}} := \begin{pmatrix} \tilde{\nu}_2^{\text{neg}} & \tilde{\tilde{\nu}}_2^{\text{neg}} & \nu_{2,1,4}^{\text{neg,neg}} & \dots & \nu_{2,1,N_{\text{neg}}}^{\text{neg,neg}} & \nu_{2,1,1}^{\text{neg,pos}} & \dots & \nu_{2,1,N_{\text{pos}}}^{\text{neg,pos}} \end{pmatrix}, \tag{6.9c}$$

while $A_{\text{neg}} \in \mathbb{R}^{N_{\text{neg}-2} \times N_{\text{neg}-2}}$, resp. $A_{\text{pos}} \in \mathbb{R}^{N_{\text{pos}} \times N_{\text{pos}}}$, as

$$\begin{aligned} A_{\text{neg}} &:= \underline{\text{diag}}(\mu_{i,i-1}^{\text{neg}}) + \text{diag}(\tilde{\mu_i}^{\text{neg}}) + \overline{\text{diag}}(\mu_{i,i}^{\text{neg}}) \\ A_{\text{pos}} &:= \underline{\text{diag}}(\mu_{i,i-1}^{\text{pos}}) + \text{diag}(\tilde{\mu_i}^{\text{pos}}) + \overline{\text{diag}}(\mu_{i,i}^{\text{pos}}) \end{aligned}$$

for $i \in \{3, \ldots, N_{\text{neg}}\}$, resp., for $i \in \{1, \ldots, N_{\text{pos}}\}$, where $\underline{\text{diag}}$ denotes the lower diagonal, $\overline{\text{diag}}$ denotes the upper diagonal,

$$\begin{aligned} \tilde{\nu}_2^{\text{neg}} &:= \nu_{2,1,2}^{\text{neg,neg}} - \mu_{2,1}^{\text{neg}} - \mu_{2,2}^{\text{neg}}, \\ \tilde{\tilde{\nu}}_2^{\text{neg}} &:= \nu_{2,1,3}^{\text{neg,neg}} + \mu_{2,2}^{\text{neg}}, \\ \mu_{i,j}^{s} &:= \frac{D_s}{V_i^s} \frac{S_j^s}{r_{j+1} - r_j}, \\ \tilde{\mu}_i^{s} &:= -\mu_{i,i-1}^{s} - \mu_{i,i}^{s} \\ \nu_{i,j,z}^{s,s'} &:= \mu_{i,j}^{s} \beta_z^{s'}, \end{aligned} \tag{6.9d}$$

where β_i^{neg} and β_i^{pos} are defined in (6.3), α_{s} is defined in (6.2) and $i, j, z \in \{1, ..., N_s\}, s, s' \in \{\text{neg}, \text{pos}\}$. The matrix B is defined as

$$B := (0_{(N_{\text{neg}-2}) \times 1} \ -\bar{K}_I^{\text{neg}} \ 0_{(N_{\text{pos}-1}) \times 1} \ \bar{K}_I^{\text{pos}} \ )^\top, \tag{6.10}$$

where $\bar{K}_I^s$, $s \in \{\text{neg}, \text{pos}\}$ defined in (6.1c). The matrix K is defined as

$$K := (-\mu_{2,1}^{\text{neg}} \bar{K} \ 0_{(N-1) \times 1})^\top, \tag{6.11}$$

where $\bar{K}$ is defined in (6.3).

The function $h : \mathbb{R}^{n_x} \to \mathbb{R}$ in (6.8) is defined, from (6.5), as, for any $x \in \mathbb{R}^{n_x}$,

$$h(x) := \text{OCV}_{\text{pos}}(H_{\text{pos}} x) - \text{OCV}_{\text{neg}}(H_{\text{neg}} x), \tag{6.12}$$

with H_{neg} and H_{pos} defined in (6.6). We assume that $u : \mathbb{R}_{\geqslant 0} \to \mathbb{R}^{n_u}$, $v : \mathbb{R}_{\geqslant 0} \to \mathbb{R}^{n_v}$ and $w : \mathbb{R}_{\geqslant 0} \to \mathbb{R}$ are such that $u \in \mathscr{L}_{\mathscr{U}}$, $v \in \mathscr{L}_{\mathscr{V}}$ and $w \in \mathscr{L}_{\mathscr{W}}$ for closed sets $\mathscr{U} \subseteq \mathbb{R}^{n_u}$, $\mathscr{V} \subseteq \mathbb{R}^{n_v}$ and $\mathscr{W} \subseteq \mathbb{R}$, which is very reasonable for lithium-ion batteries.

A block diagram representing the system model is shown in Figure 6.2.2. In particular, system (6.8) describes the relation between the current input, the voltage output and the lithium concentrations in the electrodes, which are represented with the system state. As explained in the introduction, for a safe and efficient usage of the battery, the battery management system (BMS) requires the knowledge of the actual state of charge of the battery, which is related to the lithium concentrations, i.e., the system state, as we describe in the next section.

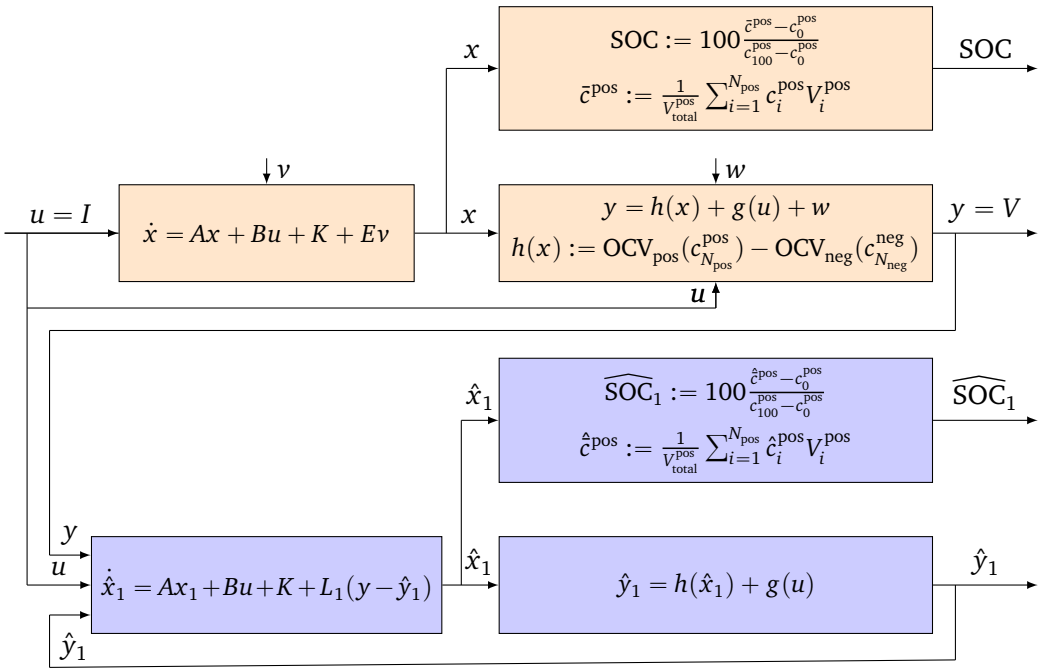

FIGURE 6.2 – Block diagram representing the electrochemical lithium-ion battery model (orange) and nominal observer (blue).

6.2.3 State of charge (SOC)

The lithium concentrations in the electrodes are related to the state of charge (SOC) of the battery (see Figure 6.2.2), which is an essential information. Indeed, the SOC is defined as, for all $t \geqslant 0$,

$$\mathrm{SOC}(t) := 100\frac{\bar{c}^{\mathrm{pos}}(t) - c_0^{\mathrm{pos}}}{c_{100}^{\mathrm{pos}} - c_0^{\mathrm{pos}}} \tag{6.13}$$

with

$$\bar{c}^{\mathrm{pos}}(t) := \frac{1}{V_{\mathrm{tot}}^{\mathrm{pos}}}\sum_{i=1}^{N_{\mathrm{pos}}} c_i^{\mathrm{pos}}(t) V_i^{\mathrm{pos}}, \tag{6.14}$$

where c_0^{pos} and c_{100}^{pos} are the lithium concentrations in the positive electrode at SOC $= 0$ % and at SOC $= 100$ %, respectively, $V_{\mathrm{tot}}^{\mathrm{pos}}$ is the total volume of the positive electrode and $V_{\mathrm{i}}^{\mathrm{pos}}$ is the volume of the i^{th} sample of the positive electrode. The concentrations in the positive electrode are considered in (6.13); the same value for the SOC would be obtained by considering the concentrations in the negative electrode. Hence by estimating the concentrations in the electrodes, we will be able to also estimate the SOC. We now design an estimation scheme for this purpose.

6.3 Hybrid multi-observer design

In this section we recall the hybrid multi-observer presented in Chapter 5. The hybrid multi-observer consists of the following elements:

— *nominal observer*, here we consider the one proposed in [97], which satisfies an input-to-state stability property, as required by Assumption 5.1;

— N additional dynamical systems with the same structure as the nominal observer, but with a different output injection gain, that can be arbitrarily selected. Each of these systems, as well as the nominal observer, is called *mode* for the sake of convenience;

— *monitoring variables* used to evaluate the performance of each mode of the multi-observer;

— *selection criterion*, that selects one mode of the multi-observer at any time instant, based on the performance knowledge given by the monitoring variables;

— *reset rule*, that defines how the estimation scheme may be updated when a switching of the selected mode occurs;

— *filtered version* of the hybrid multi-observer state estimate to produce a continuous state estimate, which is important for the considered application.

6.3.1 Nominal observer

Inspired by [97], we design a nominal observer that satisfies the input-to-state stability property in Assumption 5.1. We make the next assumption for this purpose.

Assumption 6.2. *The parameters of the model are known.* □

The nominal observer has the form

$$\begin{aligned} \dot{\hat{x}}_1 &= A\hat{x}_1 + Bu + K + L_1(y - \hat{y}_1) \\ \hat{y}_1 &= h(\hat{x}_1) + g(u), \end{aligned} \tag{6.15}$$

where $\hat{x}_1 \in \mathbb{R}^{n_x}$ is the state estimate, $\hat{y}_1 \in \mathbb{R}$ is the estimated output and $L_1 \in \mathbb{R}^{n_x \times 1}$ is the output injection gain, that needs to be designed; we use the subscript 1 because the nominal observer in (6.15) is the first element of the multi-observer that we will design in Section 6.3.2. The nominal observer (6.15) estimates the lithium concentrations in the electrodes, represented by $\hat{x}_1$, from which it is possible to obtain an estimate of the state of charge (SOC) of the battery using equation 6.13, see Figure 6.2.2. While (6.15) involves the plant input u, possible mismatches on the input current known by the plant and the observer, which often occur in practice, can be modeled using the disturbance input v and the exogenous input w in (6.8), as we will do in Section 6.4.

We define the state estimation error as

$$e_1 := x - \hat{x}_1. \tag{6.16}$$

As in Assumption 5.1, we define a perturbed version of the e_1-dynamics, which is given by, in view of (6.8) and (6.15),

$$\dot{e}_1 = Ae_1 + Ev - L_1(h(x) - h(\hat{x}_1)) - L_1 w - d, \tag{6.17}$$

where $d \in \mathbb{R}^{n_x}$ represents an additional artificial perturbation on the output injection term $L_1(y - \hat{y}_1)$. We recall that to consider the perturbed dynamics in (6.17) with extra input d is required to check

one of the key assumptions of the hybrid multi-observer presented in Chapter 5, which is needed to establish the main result of the work.

We design the observer gain L_1 to guarantee a convergence property of the estimation error e_1. In particular, L_1 has to be designed such that the origin of (6.17) satisfies an input-to-state stability property with respect to v, w and d. To design the observer gain L_1, we make the next assumption on the OCVs, which is taken from [97, Assumption 5].

Assumption 6.3. *There exist constant matrices $C_1, \dots, C_4 \in \mathbb{R}^{1\times n_x}$ such that, for any x, $x' \in \mathbb{R}^{n_x}$,*

$$h(x) - h(x') = C(x, x')(x - x'), \tag{6.18}$$

where $C(x,x') := \sum_{i=1}^{4} \lambda_i(x,x')C_i$, with $\lambda_i \in [0,1]$, $\sum_{i=1}^{4} \lambda_i(x,x') = 1$ and $i \in \{1,\dots,4\}$. □

Assumption 6.3 means that the output map h lies in a polytope defined by the vertices C_i, with $i \in \{1,\dots,4\}$. This condition is often verified in practice. Indeed, the OCVs are generally defined on the interval $[0,1]$ by experimental data and they are well-approximated by a piecewise continuously differentiable function. Moreover, the OCVs only depend on the surface lithium concentration of the negative and positive electrode. Consequently, the output map h only depends on two states of the system and the set of C_i has only 2^2 elements, which are obtained from the maximum and minimum slopes of the OCVs. Using Assumption 6.3, (6.17) becomes

$$\dot{e}_1 = (A - L_1 C(x, \hat{x}_1))e + Ev - L_1 w - d. \tag{6.19}$$

To design the observer output injection gain L_1 we follow a polytopic approach as described Section 2.2.3 and we propose a modified version of [97, Theorem 1] below.

Theorem 6.1 (Input-to-state stability property of the nominal observer)**.** *Consider system* (6.19)*. If there exist $L_1 \in \mathbb{R}^{n_x\times 1}$, α, μ_v, μ_w and $\mu_d \in \mathbb{R}_{>0}$ and $P \in \mathbb{R}^{n_x\times n_x}$ symmetric positive definite such that*

$$\begin{pmatrix} \mathscr{H}_i + \alpha P & PE & -PL_1 & -P \\ E^\top P & -\mu_v I_{n_v} & 0 & 0 \\ -L_1^\top P & 0 & -\mu_w I_{n_w} & 0 \\ -P & 0 & 0 & -\mu_d I_{n_x} \end{pmatrix} \leqslant 0, \tag{6.20}$$

with $\mathscr{H}_i := (A - L_1 C_i)^\top P + P(A - L_1 C_i)$ for all $i \in \{1,\dots,4\}$. Then $V : e_1 \mapsto e_1^\top P e_1$ satisfies, for any $e_1 \in \mathbb{R}^{n_x}$, $v \in \mathscr{V}$, $w \in \mathscr{W}$ and $d \in \mathbb{R}^{n_x}$,

$$\lambda_{min}(P)|e_1|^2 \leqslant V(e_1) \leqslant \lambda_{max}(P)|e_1|^2, \tag{6.21}$$

$$\langle \nabla V(e_1), (A - L_1 C(x,\hat{x}_1))e_1 + Ev - L_1 w - d \rangle \leqslant -\alpha V(e_1) + \mu_v|v|^2 + \mu_w|w|^2 + \mu_d|d|^2. \tag{6.22}$$

□

Proof. The proof of Theorem 6.1 follows similar steps as [97, proof of Theorem 1].

Let $e_1 \in \mathbb{R}^{n_x}$ and $V(e_1) = e_1^\top P e_1$. Since P is symmetric positive definite, (6.21) is obtain from the definition of V.

Let $v \in \mathcal{V}$, $w \in \mathcal{W}$ and $d \in \mathbb{R}^{n_x}$, using (6.19) and $C(x,\hat{x}_1) = \sum_{i=1}^{4} \lambda_i(x,\hat{x}_1) C_i$, we have

$$\begin{aligned}
&\langle \nabla V(e_1), (A - L_1 C(x,\hat{x}_1))e_1 + Ev - L_1 w - d \rangle \\
&\quad = [(A - L_1 C(x,\hat{x}_1))e_1 + Ev - L_1 w - d]^\top P e_1 + e_1^\top P [(A - L_1 C(x,\hat{x}_1))e_1 + Ev - L_1 w - d] \\
&\quad = \sum_{i=1}^{4} \lambda_i(x,\hat{x}_1) \Big[e_1^\top \big((A - L_1 C_i)^\top P + P(A - L_1 C_i) \big) e_1 + v^\top E^\top P e_1 + e_1^\top P E v - w^\top L_1^\top P e_1 \\
&\qquad - e_1^\top P L_1 D w - d^\top P e_1 - e_1^\top P d \Big].
\end{aligned} \tag{6.23}$$

Defining $\chi := (e_1, v, w, d)$, using $\mathscr{H}_i = (A - L_1 C_i)^\top P + P(A - L_1 C_i)$ for all $i \in \{1,\dots,4\}$, (6.23) becomes

$$\begin{aligned}
&\langle \nabla V(e_1), (A - L_1 C(x,\hat{x}_1))e_1 + Ev - L_1 w - d \rangle \\
&\qquad = \sum_{i=1}^{4} \lambda_i(x,\hat{x}_1) \chi^\top \begin{pmatrix} \mathscr{H}_i & PE & -PL_1 & -P \\ E^\top P & 0 & 0 & 0 \\ -L_1^\top P & 0 & 0 & 0 \\ -P & 0 & 0 & 0 \end{pmatrix} \chi.
\end{aligned} \tag{6.24}$$

Using $\sum_{i=1}^{4} \lambda_i(x,\hat{x}_1) = 1$ and (6.20) for all $i \in \{1,\dots,4\}$, we obtain

$$\begin{aligned}
&\langle \nabla V(e_1), (A - L_1 C(x,\hat{x}_1))e_1 + Ev - L_1 w - d \rangle \\
&\qquad \leqslant \sum_{i=1}^{4} \lambda_i(x,\hat{x}_1) \chi^\top \begin{pmatrix} -\alpha P & 0 & 0 & 0 \\ 0 & +\mu_v I_{n_v} & 0 & 0 \\ 0 & 0 & +\mu_w I_{n_w} & 0 \\ 0 & 0 & 0 & +\mu_d I_{n_x} \end{pmatrix} \chi \\
&\qquad = \chi^\top \begin{pmatrix} -\alpha P & 0 & 0 & 0 \\ 0 & +\mu_v I_{n_v} & 0 & 0 \\ 0 & 0 & +\mu_w I_{n_w} & 0 \\ 0 & 0 & 0 & +\mu_d I_{n_x} \end{pmatrix} \chi \\
&\qquad = -\alpha e_1^\top P e_1 + \mu_v v^\top I_{n_v} v + \mu_w w^\top I_{n_w} w + \mu_d d^\top I_{n_x} d \\
&\qquad = -\alpha V(e_1) + \mu_v |v|^2 + \mu_w |w|^2 + \mu_d |d|^2.
\end{aligned} \tag{6.25}$$

This concludes the proof. ■

Theorem 6.1 guarantees that the nominal observer (6.15) satisfies an input-to-state stability property with respect to the disturbance v, the exogenous perturbation w and the additional perturbation d.

This implies that the estimation error e_1 exponentially converges to a neighborhood of the origin, whose "size" depends on the $\mathscr{L}_\infty$ norm of v, w and d. As a result, Assumption 5.1 is satisfied. The possible drawback of observer (6.15) with L_1 designed as in Theorem 6.1 is that to tune the observer gain L_1 to obtain good estimation performance both in speed of convergence and robustness to measurement noise, exogenous perturbation and disturbance is very difficult in general. For this reason, we apply the hybrid multi-observer presented in Chapter 5 with the aim of improving the estimation performance of (6.15).

6.3.2 Hybrid multi-observer

In this section we recall the hybrid multi-observer we presented in Chapter 5, which is then used to improve the estimation performance of the nominal observer (6.15). For this purpose, we consider N additional dynamical systems with the form of (6.15), where the number $N \in \mathbb{Z}_{>0}$ is freely selected by the user, but with a different output injection gain, i.e., for any $k \in \{2,\dots,N+1\}$, the k^{th} mode of the multi-observer is given by

$$\begin{aligned} \dot{\hat{x}}_k &= A\hat{x}_k + Bu + K + L_k(y - \hat{y}_k) \\ \hat{y}_k &= h(\hat{x}_k) + g(u), \end{aligned} \tag{6.26}$$

where $\hat{x}_k \in \mathbb{R}^{n_x}$ is the mode k state estimate, $\hat{y}_k \in \mathbb{R}$ is the mode k estimated output and $L_k \in \mathbb{R}^{n_x \times 1}$ is its output injection gain. Since there is full freedom on the selection of the gains L_k, with $k \in \{2,\dots,N+1\}$, there are no convergence guarantees on the estimation errors $e_k := x - \hat{x}_k$, with $k \in \{2,\dots,N+1\}$. A recommended approach to select the gains L_k's is to consider the behaviour of the nominal observer in (6.15) in simulation and, based on that, to select the additional gains depending on the property we want to improve. For instance, if the convergence speed of the estimation error e_1 is too slow, we may define the L_k by increasing the values of L_1. On the opposite, if the convergence speed of e_1 is satisfactory but its accuracy for large time is not satisfactory, we may select the gains L_k with small values, as we will do in Section 6.4. As explained in Chapter 5, there are many other approaches that can be followed to select the additional gains. For example, we may pick them in a neighborhood of the nominal one or design one additional gain for each vertex of the polytope. Note that these gain selection criteria may result in diverging estimation errors for some of the modes, still the overall hybrid scheme we present does ensure the (approximate) convergence of the obtained state estimation error to the origin.

To select which state estimate $\hat{x}_k$, $k \in \{1,\dots N+1\}$, we need to consider, we evaluate which mode has the best performance. To define performance, we introduce monitoring variables, denoted $\eta_k \in \mathbb{R}_{\geqslant 0}$, with $k \in \{1,\dots,N+1\}$, whose dynamics are

$$\dot{\eta}_k = -\nu\eta_k + (y - \hat{y}_k)^\top(\Lambda_1 + L_k^\top \Lambda_2 L_k)(y - \hat{y}_k) \tag{6.27}$$

with $\Lambda_1 \in \mathbb{S}^{n_y}_{\geqslant 0}$ and $\Lambda_2 \in \mathbb{S}^{n_x}_{\geqslant 0}$ with at least one of them positive definite and $\nu \in (0, \alpha]$ a design parameter, with α from Theorem 6.1. As explained in Chapter 5, the monitoring variables represent the cost of the modes. Consequently, the idea is to select the mode that produces the minimum

monitoring variable, and thus the minimum cost, at any time instant. Note that, we can freely choose the initial conditions of these monitoring variables, $\eta_k(0) \in \mathbb{R}_{\geqslant 0}$, with $k \in \{1,\dots,N+1\}$. This extra degree of freedom can be used to initially select or penalize one or more modes of the multi-observer, as we do in simulation in Section 6.4. The signal $\sigma : \mathbb{R}_{\geqslant 0} \to \{1,\dots,N+1\}$ is used to indicate the selected mode at any time instant. The corresponding state estimate, monitoring variable and state estimation error are denoted $\hat{x}_\sigma$, η_σ and e_σ, respectively. We denote with $t_0 = 0$ the initial time and with $t_i \in \mathbb{R}_{\geqslant 0}$, $i \in \mathbb{Z}_{>0}$ the times when a switch of the selected mode occurs, i.e.,

$$t_i := \inf\{t \geqslant t_{i-1} : \exists k \in \{1,\dots,N+1\}\backslash\{\sigma(t)\} \text{ such that } \eta_k(t) \leqslant \eta_{\sigma(t)}(t)\}. \tag{6.28}$$

Consequently, for all $i \in \mathbb{Z}_{>0}$, $\dot{\sigma}(t) = 0$ for all $t \in (t_{i-1}, t_i)$ and

$$\sigma(t_i^+) \in \underset{k\in\Pi}{\operatorname{argmin}} \left(-\nu\eta_k(t_i) + (y(t_i) - \hat{y}_k(t_i))^\top (\Lambda_1 + L_k^\top \Lambda_2 L_k)(y(t_i) - \hat{y}_k(t_i))\right), \tag{6.29}$$

where $\Pi(\eta) := \underset{k\in\{1,\dots,N+1\}\backslash\{\sigma\}}{\operatorname{argmin}} \eta_k$ with $\eta := \{\eta_1,\dots,\eta_{N+1}\}$, for all $\eta \in \mathbb{R}_{\geqslant 0}^{N+1}$.

Finally, when switching occur, two possible reset rules are considered. In the first one, called *without resets*, only the signal σ is updated. Conversely, the second option, called *with resets* consists in not only switch the selected mode, but also resetting the state estimates and the monitoring variables of the additional modes to the updated values $\hat{x}_\sigma$ and η_σ. Note that the state estimate and monitoring variable of the nominal observer is never reset. In addition, a regularization parameter $\varepsilon \in \mathbb{R}_{>0}$ is introduced to avoid infinitely fast switching, which guarantees the existence of a semi-global average dwell-time. The detailed equations of the state estimates and monitoring variables updates are given in Section 5.3.4. We do not rewrite them here to avoid repetitions.

The state estimate $\hat{x}_\sigma$ produced by the hybrid multi-observer may be discontinuous, which can be problematic for batteries. For this reason, as explained in Section 5.3.6, we add a filtered version of $\hat{x}_\sigma$, denoted $\hat{x}_f$, whose dynamics between switching is given by

$$\dot{\hat{x}}_f = -\zeta\hat{x}_f + \zeta\hat{x}_\sigma, \tag{6.30}$$

where $\zeta > 0$ is an additional design parameter and, at switching times $t_i \in \mathbb{R}_{>0}$, with $i \in \mathbb{Z}_{>0}$,

$$\hat{x}_f(t_i^+) = \hat{x}_f(t_i). \tag{6.31}$$

6.3.3 Hybrid model and stability guarantees

Including $\hat{x}_f$, we obtain a new hybrid model for the hybrid multi-observer compared to the one presented in Section 5.3.7, whose state is defined as

$$q := (x, \hat{x}_1, \dots, \hat{x}_{N+1}, \eta_1, \dots, \eta_{N+1}, \sigma, \hat{x}_f) \in \mathcal{Q}, \tag{6.32}$$

with

$$\mathcal{Q} := \mathbb{R}^{n_x} \times \mathbb{R}^{(N+1)n_x} \times \mathbb{R}^{N+1}_{\geqslant 0} \times \{1, \ldots, N+1\} \times \mathbb{R}^{n_x}. \tag{6.33}$$

The hybrid system is given by

$$\begin{cases} \dot{q} = F(q,u,v,w), & q \in \mathcal{C} \\ q^+ \in G(q), & q \in \mathcal{D}, \end{cases} \tag{6.34}$$

where the flow map F is obtained from (6.8), (6.15), (6.26), (6.27) and (6.30), the jump map G follows from the above developments, (6.31) and is similar to the jump map in (5.28). The flow and jump sets, $\mathcal{C}$ and $\mathcal{D}$, are defined, similarly to (5.26) and (5.27), as

$$\mathcal{C} := \{q \in \mathcal{Q} : \forall k \in \{1, \ldots, N+1\} \;\; \eta_k \geqslant \eta_\sigma\}, \tag{6.35}$$

$$\mathcal{D} := \{q \in \mathcal{Q} : \exists k \in \{1, \ldots, N+1\} \backslash \{\sigma\} \;\; \eta_k \leqslant \eta_\sigma\}. \tag{6.36}$$

Similarly to Theorem 5.1, the next theorem ensures that system (6.34) satisfies a two-measure input-to-state stability property with respect to the disturbance v and the perturbation w [104], see Definition 2.13.

Theorem 6.2 (Two-measure flow input-to-state stability property)**.** *Consider system* (6.34) *and suppose Assumptions 6.1-6.3 hold and L_1 is selected such that condition* (6.20) *in Theorem 6.1 is satisfied. Then, there exist $\beta_U \in \mathcal{KL}$ and $\gamma_U \in \mathcal{K}_\infty$ such that for any input $u \in \mathcal{L}_\mathcal{U}$, disturbance input $v \in \mathcal{L}_\mathcal{V}$ and exogenous perturbation $w \in \mathcal{L}_\mathcal{W}$, any solution q satisfies*

$$|(e_1(t,j), \eta_1(t,j), e_\sigma(t,j), \eta_\sigma(t,j), e_f(t,j))| \leqslant \beta_U(|(e(0,0), \eta(0,0))|, t) + \gamma_U(\|v\|_{[0,t]} + \|w\|_{[0,t]}) \tag{6.37}$$

for all $(t,j) \in \operatorname{dom} q$, with $e := (e_1, \ldots, e_{N+1})$, $\eta := (\eta_1, \ldots, \eta_{N+1})$, $e_\sigma := x - \hat{x}_\sigma$ and $e_f := x_f - \hat{x}_f$, where x_f is the filtered system state as defined in (5.21)-(5.22). □

Sketch of proof. We first note that all the conditions of Theorem 5.1 are satisfied. Indeed, thanks to Theorem 6.1, Assumption 5.1 holds with $\underline{\alpha}(|e_1|) = \lambda_{\min} P |e_1|^2$, $\overline{\alpha}(|e_1|) = \lambda_{\max} P |e_1|^2$ for all $e_1 \in \mathbb{R}^{n_x}$ and $\psi_1(|v|) = \mu_v |v|^2$, $\psi_2(|w|) = \mu_w |w|^2$ and $\gamma = \mu_d$, for all $v \in \mathcal{V}$ and $w \in \mathcal{W}$. Moreover, Assumption 5.2 is satisfied thanks to Assumption 6.3 and because the Lyapunov function V in Theorem 6.1 is quadratic. We can then follow similar steps as in the proof of Proposition 5.1 and Theorem 5.1 to obtain the desired result. Note that, having $\hat{x}_f$ as part of the hybrid state is not a problem. Indeed, as explained in Section 5.3.6, the filtered estimation error system is an input-to-state stable system in cascade with the hybrid system considered in Theorem 5.1, see [6, Section 4]. ■

Theorem 6.2 ensures that the estimation errors and the monitoring variables of the nominal observer e_1 and η_1 converge to a neighborhood of the origin, whose "size" depends on the $\mathcal{L}_\infty$ norm of v and w, which is not surprising in view of Theorem 6.1. However, Theorem 6.2 also guarantees

that the state estimation error and the monitoring variable of the hybrid multi-observer e_σ and η_σ and also the filtered version of the estimation error, namely e_f, converge to the same neighborhood of the origin. Hence, the convergence of the (filtered) state estimate produced by the hybrid scheme is guaranteed despite the fact that the gains L_k in (6.26) were freely selected.

6.4 Numerical study

In this section, we compare the estimates generated by a nominal observer (6.15) and the associated hybrid multi-observer (6.34) with standard parameter values.

6.4.1 System model

We assume that each electrode is composed of 6 samples with identical volumes. Consequently, $N_{\text{neg}} = N_{\text{pos}} = 6$ and $n_x = N_{\text{neg}} - 1 + N_{\text{pos}} = 11$. We consider the parameters in Table 6.1. We take a measurement noise equal to $0.05\sin(30t)\,V$, which has a reasonable frequency and signal versus noise ratio for embedded battery voltage measurements. The input w in (6.8) is given by

$$w = 0.05\sin(30t) + w_2(t) \tag{6.38}$$

where w_2 is an additional term due to the input mismatch between the battery and its observer as clarified in the sequel. The considered OCV curves for the positive and the negative electrodes are shown in Figure 6.3, which satisfy Assumptions 5.2 and 6.3.

6.4.2 Input current

The input u is given by a Plug-in Hybrid Electrical Vehicles (PHEV) current profile [152]. In practical applications, the observer usually only knows a biased version of the battery current. This bias is due to the precision of the sensor and its conditioning. We therefore introduce I_{biased} to denote the input u known by the observer, which is given by, for all $t \geqslant 0$,

$$I_{\text{biased}}(t) = \begin{cases} 0 & I(t) = 0 \\ I(t) + 0.01 \max\limits_{t^\star \in [0,t]} |I(t^\star)| & I(t) > 0 \\ I(t) - 0.01 \max\limits_{t^\star \in [0,t]} |I(t^\star)| & I(t) < 0. \end{cases} \tag{6.39}$$

We consider a precision of 1% on the full scale for the current bias, which corresponds to a standard sensor. The PHEV current input I and its biased version I_{biased} are shown in Figure 6.4. This mismatch in the current input of system and observer can be modeled using the disturbance input v and the exogenous perturbation w in (6.8). Indeed, the plant input

$$u = I = I_{\text{biased}} + v, \tag{6.40}$$

where v is defined as

$$v := I - I_{\text{biased}}. \tag{6.41}$$

TABLE 6.1 – Physical parameters of the electrochemical model.

$\mathscr{A}_{\text{cell}}$	Cell area $[m^2]$	1.0452
F	Faraday's constant $[C/mol]$	96485
R	Gas constant $[J/K/mol]$	8.3145
T	Temperature $[K]$	298.15
N	Order of the model [-]	7
d_{pos}	Thickness of the positive electrode $[\mu m]$	36
d_{neg}	Thickness of the negative electrode $[\mu m]$	50
D_{pos}	Lithium diffusion coefficient $[m^2/s]$	3.723×10^{-16}
D_{neg}	Lithium diffusion coefficient e $[m^2/s]$	2×10^{-16}
$c_{0,pos}$	Lithium concentration at SOC = 0% $[mol.L^{-1}]$	23.01
$c_{0,neg}$	Lithium concentration at SOC = 0% $[mol.L^{-1}]$	3.167
$c_{100,pos}$	Lithium concentration at SOC = 100% $[mol.L^{-1}]$	9.182
$c_{100,neg}$	Lithium concentration at SOC = 100% $[mol.L^{-1}]$	11.75
$c_{\text{max,pos}}$	Maximum concentration $[mol.L^{-1}]$	23.9
$c_{\text{max,neg}}$	Maximum concentration $[mol.L^{-1}]$	16.1
σ_{pos}	Electronic conductivity $[S/m]$	10
σ_{neg}	Electronic conductivity $[S/m]$	100
R_{pos}	Particle radius $[\mu m]$	1
R_{neg}	Particle radius $[\mu m]$	1
j_0^{pos}	Exchange current density $[A/m^2]$	0.5417
j_0^{neg}	Exchange current density $[A/m^2]$	0.75
ε_{pos}	Volume fraction of the material within the positive electrode [-]	0.5
ε_{neg}	Volume fraction of the material within the negative electrode [-]	0.58
Q_{Li}	Lithium quantity in cell solid phases $[Ah]$	14.8318
Q_{cell}	Cell capacity $[Ah]$	6.9725
Ω_{add}	Additional resistivity $[\Omega]$	0
$\varsigma_{1,\text{pos}}$	Ionic diffusion time constant $[s]$	13.0
$\varsigma_{1,\text{neg}}$	Ionic diffusion time constant $[s]$	17.3
$\varsigma_{1,\text{sep}}$	Ionic diffusion time constant of separator$[s]$	12.3
$\varsigma_{2,\text{pos}}$	Ionic diffusion resistance $[\mu\Omega]$	153.9
$\varsigma_{2,\text{neg}}$	Ionic diffusion resistance $[\mu\Omega]$	209.5
$\varsigma_{2,\text{sep}}$	Ionic diffusion resistance of separator $[\mu\Omega]$	115.1

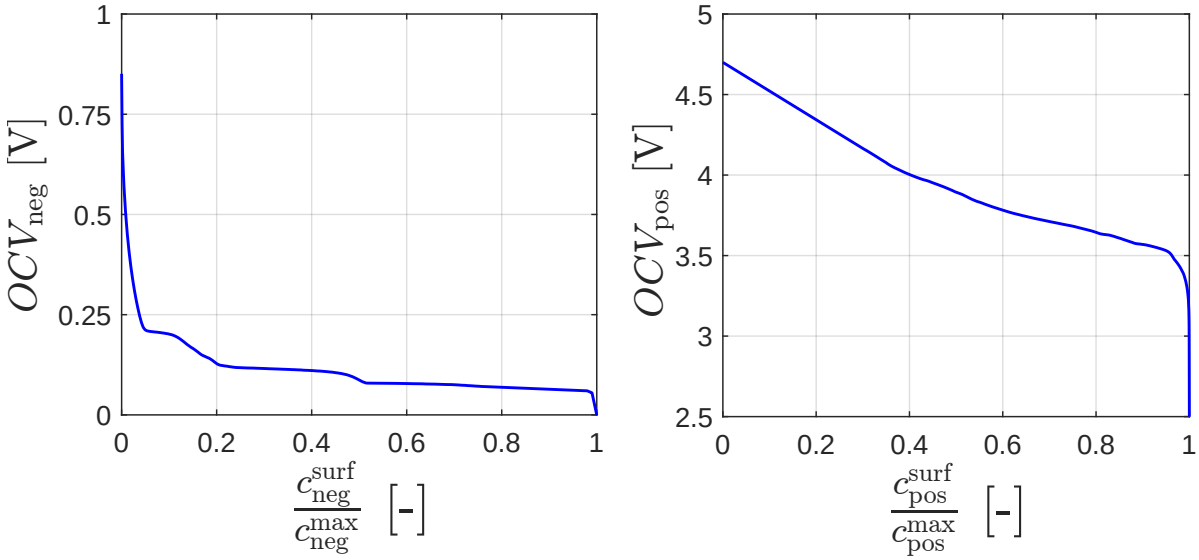

FIGURE 6.3 – OCV curves.

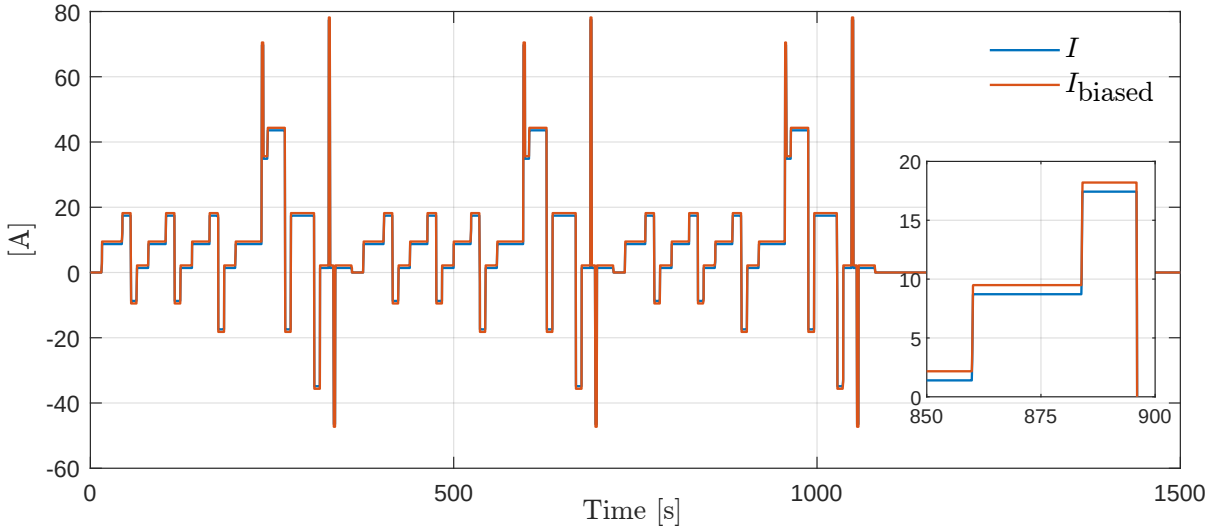

FIGURE 6.4 – Input current profile and its biased version available to the observer.

With the matrix E equal to the matrix B, we obtain

$$\dot{x} = Ax + BI_{\text{biased}} + K + Bv. \tag{6.42}$$

Moreover, to model the input mismatch in the output map, we define

$$w_2 = g(I_{\text{biased}}) - g(I), \tag{6.43}$$

so that w in (6.8) is

$$w = 0.05\sin(30t) + g(I_{\text{biased}}) - g(I). \tag{6.44}$$

High fidelity model for battery	**Low fidelity model for observer**
$N_{\text{pos, sys}} = N_{\text{neg, sys}} = 6$	$N_{\text{pos, obs}} = N_{\text{neg, obs}} = 4$
Electrolyte dynamics	No electrolyte dynamics
System dimension $N_{\mathbf{sys}} = 14$	Observer dimension $N_{\mathbf{obs}} = 7$
PHEV current input	Biased PHEV current input
No measurement noise	Measurement noise $w = 0.05\sin(30t)$

TABLE 6.2 – Different fidelity models for system and observer design.

6.4.3 Electrolyte dynamics

To test the robustness of the estimation scheme, we consider a model of the electrolyte dynamics, as in [148, Section IV.B], thereby relaxing item (*ii*) in Assumption 6.1. Consequently, the battery output voltage becomes

$$y - \varrho_{\text{pos}} - \varrho_{\text{neg}} - \varrho_{\text{sep}}, \tag{6.45}$$

where y is the battery output from (6.8) and ϱ_{r}, with $r \in \{\text{pos, neg or sep}\}$, is the electrolyte diffusional overvoltage in the positive electrode, negative electrode or separator, which dynamics is given by

$$\dot{\varrho}_{\text{r}} = -\varrho_{\text{r}}/\varsigma_{1,\text{r}} + u\varsigma_{2,\text{r}}/\varsigma_{1,\text{r}}, \tag{6.46}$$

where $\varsigma_{1,\text{r}}$ and $\varsigma_{2,\text{r}}$ are the ionic diffusion time constant and ionic diffusion resistance in r. However, these electrolyte dynamics are ignored below when designing the nominal observer and the additional modes.

6.4.4 Nominal observer

We now design the nominal observer in (6.15). To test its efficiency, we design it with a smaller number of samples compared to the system model in (6.8). In this way, a higher fidelity model is used to generate the output voltage. We thus select $N_{\text{neg, obs}} = N_{\text{pos, obs}} = 4$ and $n_{x,\text{obs}} = N_{\text{neg, obs}} - 1 + N_{\text{pos, obs}} = 7$, while the battery model is $11+3$, where the 3 additional dimensions are due to the electrolyte dynamics in Section 6.4.3. All the differences between the system used for the observer design (both nominal observer and hybrid multi-observer) and the one considered in the simulations for the battery system are summarized in Table 6.2 and Figure 6.5.

We then solve (6.20) and we obtain

$$L_1 = (28.03, 27.78, 28.77, -45.54, -45.72, -44.78, -46.28). \tag{6.47}$$

The system is initialized with a state of charge of 100%, which corresponds to

$$x(0,0) = (11.75, 11.75, 11.75, 11.75, 11.75, 9.182, 9.182, 9.182, 9.182, 9.182, 9.182), \tag{6.48}$$

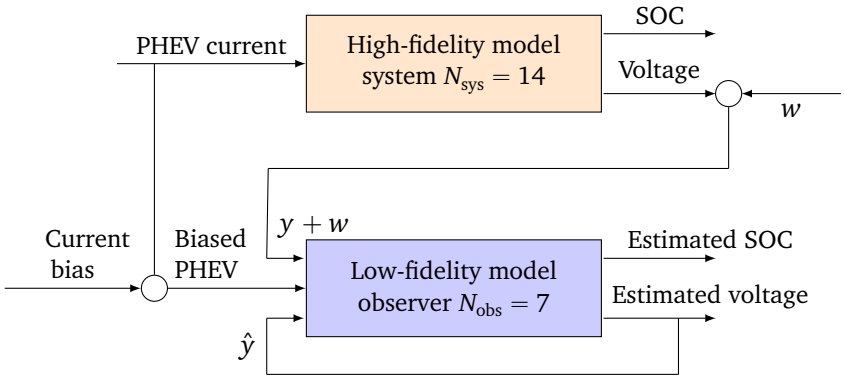

FIGURE 6.5 – Block diagram describing the different fidelity models for system and observer design.

while the nominal observer is initialized with a state of charge of 0%, which corresponds to

$$\hat{x}_1(0,0) = (3.069, 3.069, 3.069, 23.01, 23.01, 23.01, 23.01). \tag{6.49}$$

Therefore, the state of charge estimation error is initialized at 100 %, which is the largest possible initial estimation error. The electrolytes diffusional overvoltages are initialized at $\varrho_r(0,0) = 0$ for any $r \in \{\text{pos}, \text{neg}, \text{sep}\}$. The lithium surface concentrations, and their estimations, of both the negative and positive electrodes are shown in Figure 6.6, together with the state of charge and its estimate.

The nominal observer has good performance in terms of speed of convergence, see Figure 6.6. Indeed, despite the large initial error for the SOC, the nominal observer estimate converges fast to the actual SOC. However, the observer estimates is very sensitive to measurement noise, model mismatch and input bias, which impact the estimation performance especially when the estimation error reaches a neighborhood of the origin. Consequently, the hybrid multi-observer is designed in the next section with the aim of improving the estimation performance in terms of robustness to measurement noise, model mismatch and input bias, while preserving the fast convergence of the nominal observer.

6.4.5 Hybrid multi-observer

We design the multi-observer adding $N = 3$ additional modes (6.26) in parallel to the nominal observer. Since small gains typically help with respect to noise, we chose the additional gains smaller than the nominal one, even though they may not result in converging estimation errors. In particular, we select $L_2 = L_1/10$, $L_3 = L_1/100$ and $L_4 = 0_{7\times1}$. The gain $L_4 = 0_{7\times1}$ does not lead to a "converging mode" but it is the best choice to annihilate the measurement noise. Simulations suggest that the SOC estimation error of the modes with L_2 and L_3 converge, while the one with L_4 does not. Note that, in the choice of the additional gains we exploited the complete freedom given in Section 6.3.

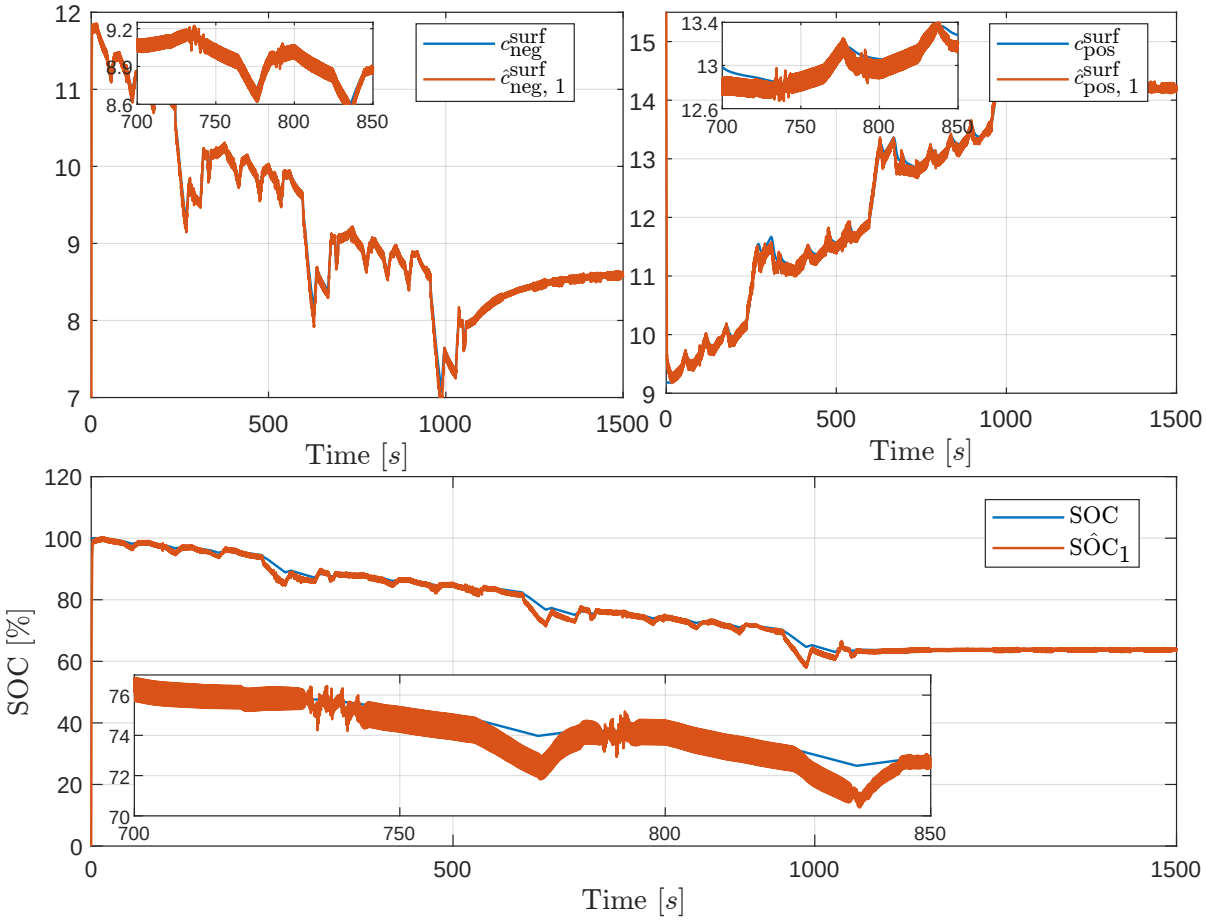

FIGURE 6.6 – Lithium concentrations at the surface of both electrodes c_{neg}^{surf} (top figure left) and c_{pos}^{surf} (top figure right), state of charge (SOC) (bottom figure). Reference system (blue), nominal observer (red).

6.4.6 Initialization and design parameters

The state estimate of the additional modes, $\hat{x}_k$, with $k \in \{2,\dots,4\}$ are initialized at the same value as $\hat{x}_1$ in Section 6.4.4. We select $\eta_1(0,0) = 1$ and $\eta_k(0,0) = 10$ for all $k \in \{2,3,4\}$, $\sigma(0,0) = 1$ and $\hat{x}_f(0,0) = \hat{x}_{\sigma(0,0)}(0,0) = \hat{x}_1(0,0)$. This choice of initializing the nominal monitoring variable η_1 smaller than the monitoring variables of all the additional modes is because the transitory performance of the nominal observer is good and this choice, together with the initialization of σ at the nominal observer, allows to select the nominal observer for some amount of time at the beginning of the simulation. We simulate the proposed hybrid multi-observer with $\nu = 0.005$, $\Lambda_1 = 1$, $\Lambda_2 = 0.005 \cdot I_7$, $\varepsilon = 10^{-4}$ and $\zeta = 3$. Note that, the condition $\nu \in (0, \alpha]$ in Proposition 5.1 is satisfied. Indeed, for the considered lithium-ion battery, we have $\alpha = 0.01$ in Theorem 6.1.

6.4.7 Results

The lithium surface concentrations of both the negative and positive electrodes, namely $c_{\text{neg}}^{\text{surf}}$ and $c_{\text{pos}}^{\text{surf}}$, together with their estimates using the nominal observer, the hybrid multi-observer and its filtered version are shown in Figure 6.7 for the case without resets and in Figure 6.8 when the case with resets is considered. We recall that the lithium surface concentrations are elements of the system state and therefore Figures 6.7 and 6.8 show that the hybrid multi-observer improve the state estimation performance compared to the nominal observer both in the case wihtout and with resets. Moreover, using (6.13), we obtain the state of charge (SOC) and its estimates with the nominal observer and the hybrid multi-observer (filtered and not) and, from these, we evaluate the norm of the state of charge estimation errors. The results are shown in Figures 6.7 and 6.8, where we see that the state of charge estimate is improved, both on the averaged value and on the oscillations, using the hybrid multi-observer both when the resets are implemented and when they are not. The obtained performance improvement is commonly considered to be significant for this application. The last plot in Figures 6.7 and and 6.8 represents the signal σ which indicates the mode that is selected at every time instant. In Figure 6.9 we compare the results obtained in the case without resets with the ones from the case with resets. In particular, the first plot of Figure 6.9 shows the norm of the state of charge estimation errors (filtered and not) both in case without resets and with resets and the second plot of Figure 6.9 represents the signal σ in both cases.

To further evaluate the effectiveness of the proposed hybrid multi-observer, we have run 100 simulations with different initial conditions, both in the case without and with resets. In particular, the initial state of charge estimate of all the modes of the multi-observer $\hat{\text{SOC}}_k(0,0)$, with $k \in \{1,\dots,4\}$, were selected randomly in the interval $[0,100]$%, while the battery state of charge was always initialized at $\text{SOC}(0,0) = 100\%$. We considered the same choice as before for all the design parameters and initial conditions of the monitoring variables η_k, with $k \in \{1,\dots,4\}$, σ and ϱ_{r}, with $r \in \{\text{pos}, \text{neg}, \text{sep}\}$. To quantify the improvement brought by the hybrid multi-observer, we evaluate the mean absolute error (MAE) and the root mean square error (RMSE), averaged over all the simulations, on the SOC estimation error obtained with the nominal observer and the proposed hybrid multi-observer, filtered and not, both in the case without and with resets. The data collec-

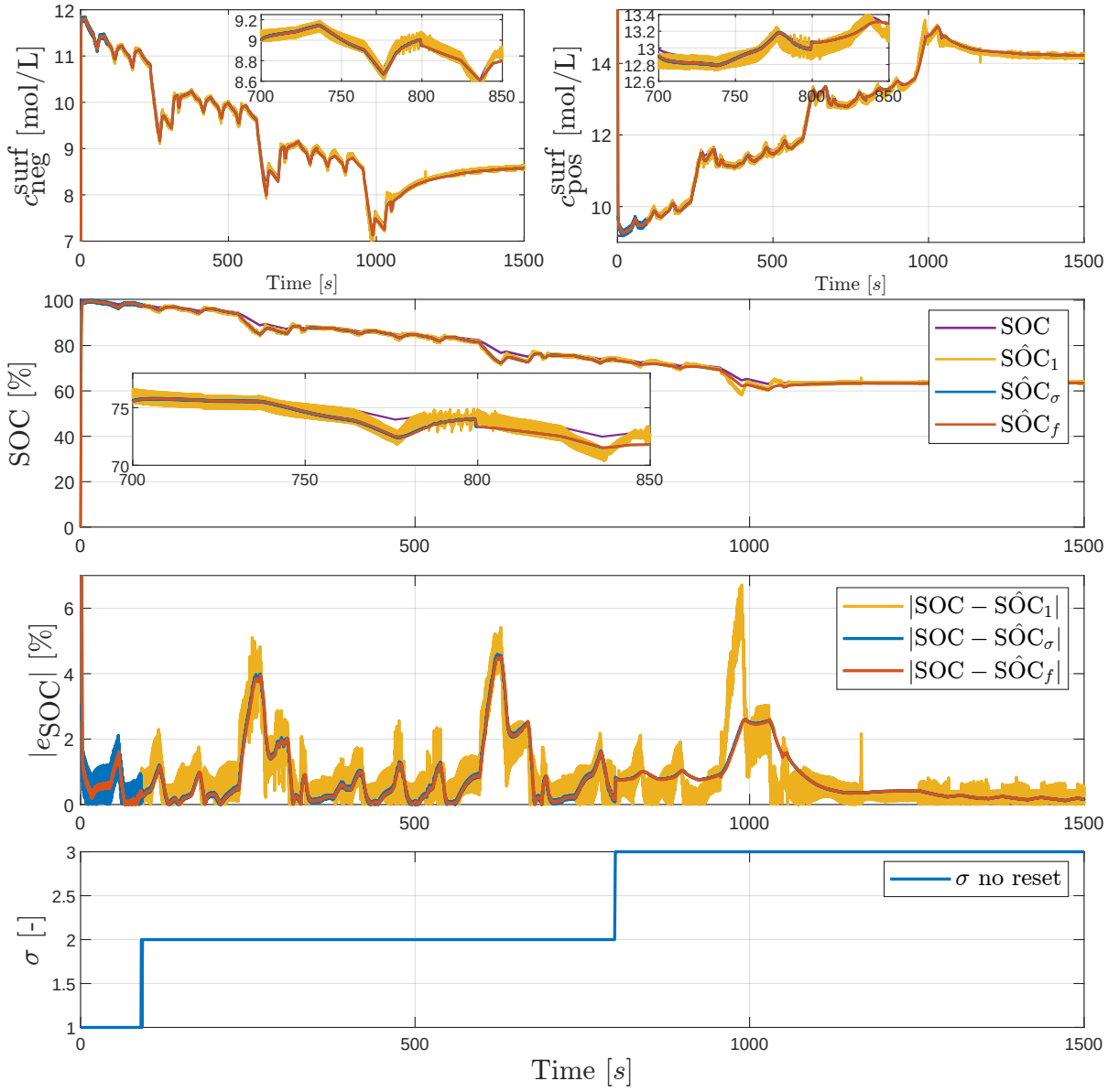

FIGURE 6.7 – No resets case. Lithium concentrations at the surface of both electrodes c_{neg}^{surf} (top figure left) and c_{pos}^{surf} (top figure right), state of charge (SOC) (second figure), norm of the state of charge estimation error (third figure) and σ (bottom figure). Real system (purple), nominal (yellow), σ-estimate (blue), filtered estimate (red).

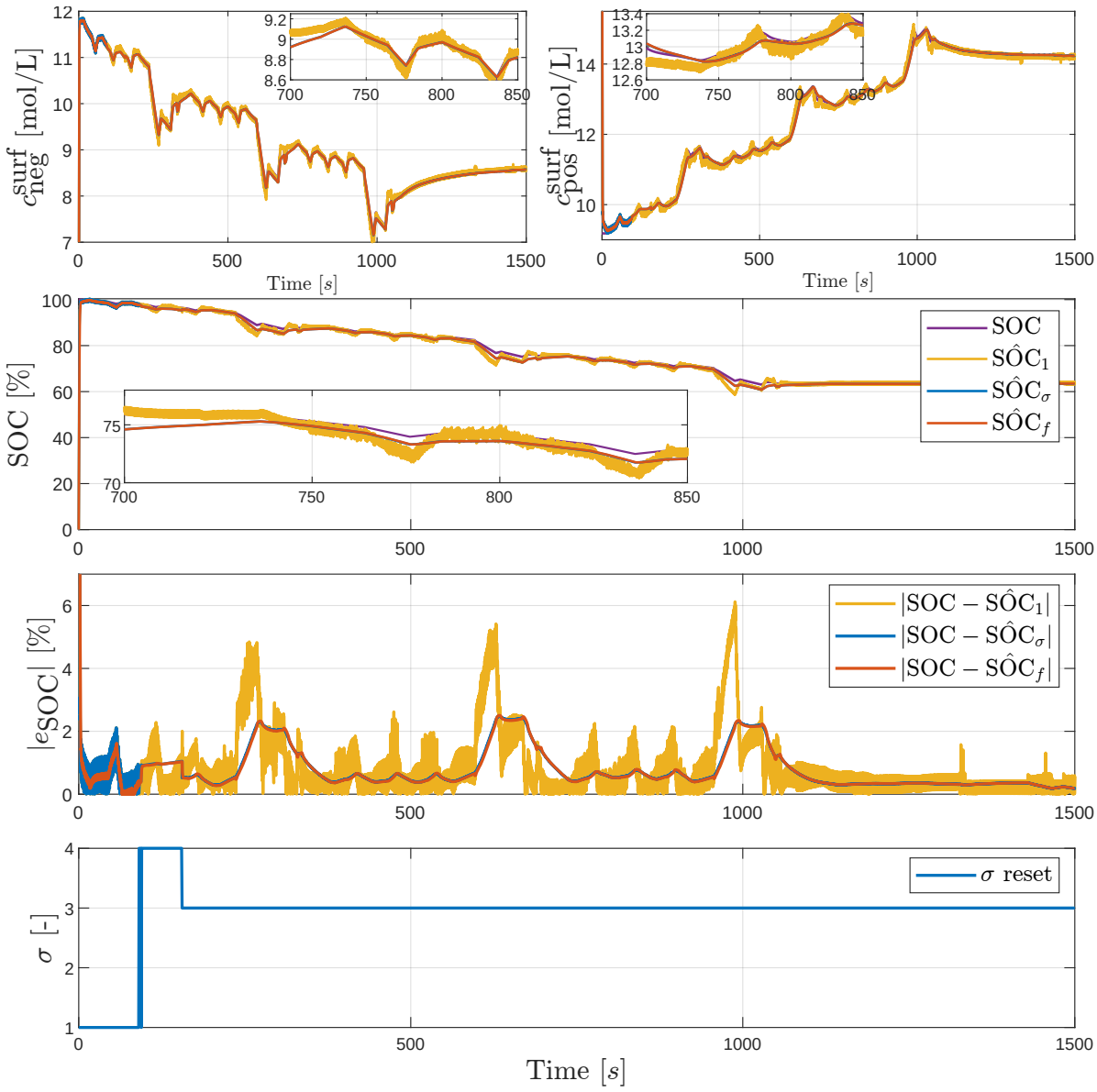

FIGURE 6.8 – Resets case. Lithium concentrations at the surface of both electrodes c_{neg}^{surf} (top figure left) and c_{pos}^{surf} (top figure right), state of charge (SOC) (second figure), norm of the state of charge estimation error (third figure) and σ (bottom figure). Real system (purple), nominal (yellow), σ-estimate (blue), filtered estimate (red).

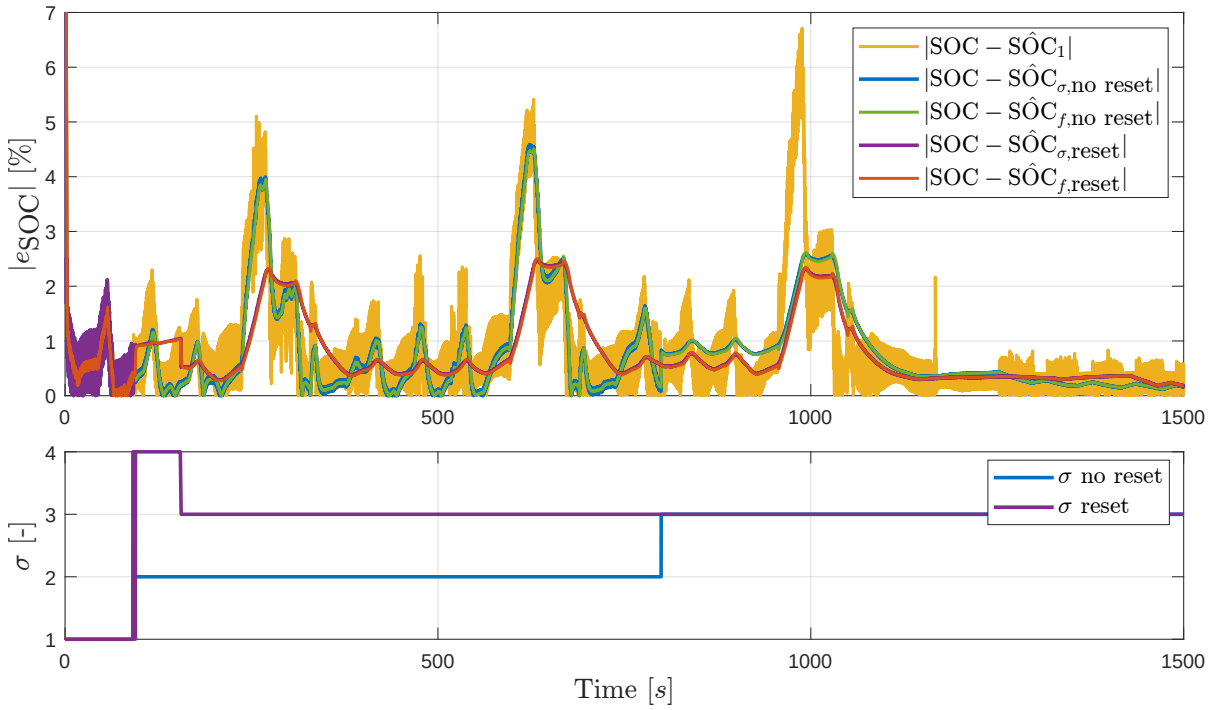

FIGURE 6.9 – Comparison case without reset and with reset. Norm of the state of charge estimation error (first figure) and σ (second figure). Nominal (yellow), σ-estimate no reset (blue), filtered estimate no reset (green), σ-estimate reset (purple), filtered estimate reset (red).

ted are shown in Table 6.3 for the whole simulation time $t \in [0, 1500]$ s, during the transitory for $t \in [0, 150]$ s and after the transitory for $t \in [150, 1500]$ s. Note that the data for e_1 without and with resets are slightly different because the 100 initial conditions were randomly selected and thus they may be different in the simulations without and with resets.

Table 6.3 shows that the hybrid multi-observer unfiltered improves the estimation performance, especially at large times as desired both in the case without and with resets. Indeed, both the MAE and the RMSE are almost always smaller compared to the ones of the nominal observer, except for the transient data in the reset case, where the performance are a bit worse. Moreover, the filtered version, even if during transient has worse performance compared to the nominal observer, after the transient the improvement is clear and, the performance can be also better than the corresponding unfiltered version.

6.5 Conclusions

We have applied the hybrid multi-observer presented in Chapter 5 to improve the estimation performance of the observer based on a polytopic approach designed in [97] to estimate the lithium concentration of the electrodes of an electrochemical battery, which is directly related to the state of charge. Simulations based on standard model parameter values have illustrated the potential of this approach to improve the state of charge estimation performance. Possible future research perspective are given in Chapter 7.

TABLE 6.3 – Average over 100 simulations with different $\hat{\text{SOC}}_k(0,0)$, with $k \in \{1,\dots,4\}$, of the MAE and RMSE of the SOC estimation error (e_{SOC}) for $t \in [0,1500]$ s (tot), $t \in [0,150]$ s (tran) and $t \in [150,1500]$ s (end).

	no reset				reset			
	$e_{\text{SOC},1}$	$e_{\text{SOC},\sigma}$	$e_{\text{SOC},f}$	% improv. σ	$e_{\text{SOC},1}$	$e_{\text{SOC},\sigma}$	$e_{\text{SOC},f}$	% improv. σ
$\text{MAE}_{\text{tot}}[\%]$	0.83	0.78	0.78	**6.16**	0.84	0.80	0.79	**4.13**
$\text{MAE}_{\text{tran}}[\%]$	0.87	0.85	0.90	**2.66**	0.83	0.88	0.93	**-6.53**
$\text{MAE}_{\text{end}}[\%]$	0.83	0.77	0.76	**6.61**	0.84	0.79	0.78	**5.47**
$\text{RMSE}_{\text{tot}}[\%]$	1.73	1.58	1.77	**8.75**	1.67	1.47	1.64	**12.14**
$\text{RMSE}_{\text{tran}}[\%]$	3.41	3.41	4.17	**0**	3.06	3.07	3.74	**0**
$\text{RMSE}_{\text{end}}[\%]$	1.30	1.09	1.08	**15.91**	1.31	1.02	1.01	**22.07**

This chapter concludes the second part of the thesis where we have presented a hybrid multi-observer to improved the estimation performance and we have applied the proposed technique to a electrochemical model of a lithium-ion battery. In the next chapter we will conclude the thesis and we will discuss possible future research directions.

Chapter 7

Conclusions

This thesis focuses on the use of hybrid techniques to solve two important state estimation problems, namely the event-triggered observer design and how to improve the state estimation performance of a given nonlinear continuous-time observer. In Chapter 1 we have introduced the thesis and some preliminaries on observers and hybrid systems were given in Chapter 2. The first part of the thesis focuses on event-triggered estimation. In particular, in Chapter 3 we have presented results for linear time-invariant systems, which were extended in Chapter 4 to general perturbed nonlinear systems in a decentralized scenario. The second part of the thesis focuses on a hybrid multi-observer that aims at improving the state estimation performance. The proposed technique has been described in Chapter 5 and it has been applied for the state estimation of a electrochemical lithium-ion battery model in Chapter 6. Below we summarize the contributions of Chapters 3-6. We then present possible future work directions.

7.1 Summary

7.1.1 Event-triggered estimation

In Chapters 3 and 4, we considered the setting where the output measurements are transmitted from the plant to the observer via a packet-based communication network and we have presented an event-triggered observer design in order to sporadically transmit over the digital network while still obtaining accurate state estimates. In particular, we have proposed a dynamic triggering rule, inspired by [49], implemented by a smart sensor, which decides when the measured output needs to be transmitted to the observer through the digital network. We recall that the proposed triggering rule does not require a copy of the observer in the sensor and thus the sensors are not required to have significant computation capabilities, as they only need to run a local scalar filter. The results are first presented in Chapter 3 for unperturbed linear time-invariant systems and are generalized in Chapter 4 to perturbed nonlinear systems and to a decentralized setting, where the sensors are grouped in N nodes and each node decides when its measured data is transmitted to the observer independently from the others. Both in Chapter 3 and 4 we have modelled the overall system

as a hybrid system using the formalism of [31], where a jump corresponds to an output transmission, and we have established a uniform global practical stability property for the estimation error (Theorems 3.1, 4.1, 4.2 and Proposition 4.2). In addition, we have shown that maximal solutions are complete (Theorem 4.3) and we have guaranteed the existence of a uniform, strictly positive time between any two transmissions of each sensor node under mild conditions on the plant (Theorems 3.2 and 4.4). Moreover, we have shown that the proposed technique stops transmitting when a new output data is not needed to perform a good estimation, which is an advantage against time-triggered strategies (Lemmas 3.1 and 4.1). Finally, in Section 4.6 of Chapter 4 we have also shown how the triggering rule can be generalized and how to cope with measurement noise and/or sampled input. Numerical case studies on a linear lithium-ion battery model (Chapter 3) and on a flexible joint robotic arm (Chapter 4) illustrate the efficiency of the proposed approach.

7.1.2 Improving estimation performance

In the second part of the thesis we focused on the use of hybrid techniques for improving the state estimation performance of a given nominal nonlinear observer. In particular, a novel, flexible and general hybrid multi-observer has been presented in Chapter 5, which can be used to address various trade-offs between speed of convergence and robustness to measurement noise, modelling errors and disturbances. The starting point is a robust nominal nonlinear observer, which ensures that the corresponding state estimation error system satisfies an input-to-state stability property with respect to measurement noise and disturbances. To improve the performance of this nominal observer, we added N additional dynamical systems and we have obtained a multi-observer, where each element is called *mode*. Each additional mode of the multi-observer differs from the nominal one only in its output injection gain, that can be freely selected as no convergence property is required for these modes. Because the gains are different, each mode exhibits different properties in terms of speed of convergence and robustness to measurement noise. We run all modes in parallel and, inspired by supervisory control/observer approaches, we have designed a switching criterion, based on monitoring variables, that selects one mode at any time instant by evaluating their performance. We have proved a two-measure flow input-to-state stability property of the estimation error (Proposition 5.1 and Theorem 5.1), we have shown that maximal solutions are complete (Proposition 5.2) and we have guaranteed the existence of a uniform semiglobal average dwell-time (Proposition 5.3). Moreover, we have shown that the estimation performance of the proposed hybrid multi-observer are always at least as good as the performance of the nominal observer. Furthermore, under some condition on the choice of the additional gains and the initial conditions of modes and monitoring variables, we have proved that the estimation performance in terms of a quadratic output error cost is strictly improved (Theorem 5.2 and Proposition 5.4). To illustrate the efficiency of the proposed technique, three numerical example were presented in Chapter 5. In addition, the proposed technique has been applied for the state estimation of an advanced electrochemical lithium-ion battery model in Chapter 6. There, the estimation performance of the nominal observer based on a polytopic approach designed in [97] to estimate the lithium concentrations of the electrodes of an electrochemical battery model, which are directly related to the state of charge of the battery, has been improved with the proposed

technique.

7.2 Future work perspectives

The results presented in the thesis open the doors to many research directions, some of which are presented next.

7.2.1 Event-triggered estimation

In the first part of the thesis, in Chapters 3 and 4, we considered an the event-triggered observer design for linear time-invariant systems and for general nonlinear systems. In this section we discuss associated possible future research directions.

— **Tailored results for given observers.** It would be interesting in future work to tailor the results of Chapter 4 to other specific classes of systems and observers. Indeed, similarly to Section 4.4.3, where we considered only the observers satisfying an input-to-state stability property with a linear decay rate of the Lyapunov function, and this allowed us to prove an extra property (namely, Theorem 4.2), it may be possible to obtain additional or less restrictive results by considering a specific class of system and observer, such as polytopic based observers, e.g., [95–97] or circle criterion observers, e.g., [3, 153, 154].

— **Generalization to other classes of observers.** Even if many observers designs in the literature can be modeled in the general form (4.1) and satisfy the input-to-state stability property in Assumption 4.2, there are some estimation techniques that escape our theory, see e.g., the Kazantis-Kravaris-Luenberger (KKL) observers in e.g. [155] and the Takagi-Sugeno (TS) observers in e.g., [156, 157]. It would be therefore interesting to adjust the event-triggered observer design presented in this thesis for these classes of nonlinear observers.

— **Tuning of the design parameters.** For the general nonlinear systems considered in Chapter 4 it is challenging to analyze how the design parameters impact the number of transmissions triggered, the speed of convergence of the estimation error and its ultimate bound. However, this can be done in some specific cases, as we did in Chapter 3 for linear time-invariant systems and in Theorem 4.2 where we assumed that the input-to-state stability property in Assumption 4.2 holds with a linear $\alpha \in \mathscr{K}_\infty$. Note that these results give some indication on how to tune the designs parameters to obtained the desired properties, but no optimization criteria is presented. In future work it would be interesting optimizing the tuning of the design parameters using a cost that considers the trade-off between the number of transmissions triggered and the ultimate bound of the estimation error. In the linear time-invariant case presented in Chapter 3 this may result in solving linear matrix inequalities. Note that, optimization problems are exploited in the event-triggered estimation literature to learn the optimal communication policy for discrete-time linear-time invariant systems in the recent work [158].

— **Periodic event-triggered and/or self-triggered estimation.** In this thesis we focused on an event-triggered technique to decide when an output measurement needs to be transmitted to the plant to the observer. Alternatives techniques to trigger transmissions over the network

are present in the literature. For example, in the periodic event-triggered approach, see e.g., [26, 114, 159] the triggering condition is only checked at some specific time instants and, if the triggering rule is satisfied, the data is communicated through the digital network. Another possible option to generate the transmission instants is the self-triggered approach, see e.g., [47, 48, 160, 161]. In this case, the observer decides when to request new information from the sensor based on the last received value only. As a future work perspective, we could adapt the dynamic triggering rule presented in this thesis for an event-triggered observer design to the contexts of periodic event-triggered estimation and/or self-triggered estimation.

— **Analysis of the inter-event times.** In this thesis we proved that the proposed event-triggered observer design can stop the transmissions when the output remains in a small neighborhood of a constant and it guarantees the existence of a minimum time between two consecutive output transmissions of each sensor node over the digital network. This implies that the time between any two transmissions of the same sensor node is lower-bounded by a positive constant. However, the actual inter-event times can be larger than this constant. In this work we have not characterized the actual behaviour of the inter-event time because this technically challenging problem as the work in [162] shows in the context of event-triggered control. A precise analysis of the inter-transmission times and of the number of communications over the network can be an useful and interesting future work direction, which can be inspired by [162, 163].

— **Additional network effects.** In this thesis we did not consider network effects such as quantization and packet losses. Taking into account these network effects is another relevant research direction, that can be inspired by e.g., [111, 164]. In addition, we could also characterize our work for different transmission protocols.

— **Event-triggered multi-observer.** The combination of the results presented in the two parts of the thesis is also a possible and interesting research direction. Indeed, the hybrid multi-observer presented in Chapter 5 requires the knowledge of the whole output both for the modes and for the monitoring variables used to evaluate the performance of the different modes. As a result, an open question is to understand how and if the estimation performance of the hybrid multi-observer is improved in the case the measured output is transmitted from the plant to the multi-observer via a digital network following an event-triggered approach, as the one presented in this thesis.

7.2.2 Improving estimation performance

We believe that the flexibility of the framework presented in Chapter 5 leads to a range of fascinating research questions, some of which are listed below.

Design guidelines and modes gains tuning

The freedom in the design of the additional modes of the hybrid multi-observer described in Chapter 5 can be exploited to further improve the estimation performance. This opens the door to different future work directions, as detailed next.

— **Off-line tuning of the additional modes gains.** We currently do not have a systematic methodology to tune the gains of the additional modes, only some guidelines are given in Section 5.3.5. One possible option for the off-line tuning of the additional mode gains would be to design them using learning based techniques, similarly to [129] in the context of discrete-time KKL observers and thus obtain the “best" possible gains for different classes of inputs or disturbances off-line in simulations. Dynamic programming techniques could be exploited for this purpose, see e.g., [165]. Note that, typically, learning the observer gain produces the best mode for a specific class of input or disturbance, but it often does not provide stability guarantees. Therefore, with the proposed hybrid multi-observer approach we can have both stability properties, thanks to the nominal observer, and good performance, thanks to the additional modes whose gains are designed using learning techniques, for different scenarios.

— **On-line tuning of the number of additional modes and their gains.** In the current framework, N additional observer-like systems are added in parallel to the nominal observer. The number of these modes N and their gains are designed off-line. A possible interesting research perspective would be to adjust the number of additional modes and/or their gains on-line, based on the actual behaviour of the multi-observer. Indeed, to further improve the estimation performance, it may be useful to add additional modes, with new gains. For example, if the multi-observer switches often between two modes, an option can be adding an additional mode with a gain that is the average of the two. Another example is the case where the multi-observer selection ends to only one mode. In this case, we may want to add an extra additional mode taken in a set centered at the selected one. Note that, adding extra modes on-line should not be a problem for the results of Chapter 5 to hold. However, increasing the number of additional modes, increases the required computation capabilities, which may be problematic in some applications. On the other hand, one may be tempted to remove modes that have never been selected, which may for instance be diverging. This may be a good strategy, but care must be taken because a mode not yet selected might be relevant in the future. This can happen, for instance, in the case the mode is a local observer robust to measurement noise and disturbance, which has not yet been selected because its domain of attraction has not yet been reached. Following similar ideas of adding/removing modes, one can also keep the number of additional modes constant, but replace a mode gain that has never been selected with a gain that, looking at the behaviour and the performance of the multi-observer, could be good. This approach, may help to further improve the performance, thanks to the new gain, without requiring additional computational capability compared to the original off-line gain tuning. However, since one or more modes are replaced, there is always the risk of removing a mode with a gain that may be the best in the future and thus worsen the performance of the orginanl multi-observer due to the on-line tuning. As a result, we believe that to design a systematic approach to tune on-line the number of additional modes and the corresponding gains is challenging, but may lead to better estimation performance requiring less computation capabilities. Therefore, we believe this is a future work direction that is worth trying to

explore.

Relationship between a state estimation error cost and an output estimation error cost

The question of the link between the considered cost function, which involves the output estimation error (see (5.10)), and a cost based on the state estimation error is also a relevant challenge to unravel. To start investigating this difficult question, which, to the best of the author knowledge, does not have an answer even in the unperturbed linear time-invariant system case, an approach based on the Lyapunov equation for observability and detectability properties can be envisioned. Some preliminary results in this direction are presented in Appendix B.

Observer-based controller

In the current setting only the estimation problem is considered. It would be also interesting to exploit the proposed scheme to improve the performance of a given observer-based controller. Indeed, an open question is to understand if, providing the controller with a better state estimate, thanks to the hybrid multi-observer, we also obtain better performance for the closed-loop system.

Generalizations

The hybrid multi-observer presented in Chapter 5 can be generalized following different paths, which are detailed below.

— **Generalization to other classes of observers.** The proposed framework considers general nonlinear observers, however, some observer design techniques, like the Kazantis-Kravaris-Luenberger (KKL) observers, see e.g. [155] and the Takagi-Sugeno (TS) observers, see e.g., [156, 157], escape our theory at the moment, just like for part I. Thus, a possible research direction consists in adapting the proposed hybrid multi-observer technique to these classes of nonlinear observers. Moreover, we currently require that the nominal observer state has the same dimension as the system state. Some nonlinear observers in the literature have a state dimension that is bigger than the corresponding system state, see e.g., [5] for a review of nonlinear continuous-time observers. Therefore, it would be interesting to extend the current result enlarging the class of nonlinear observers that can be considered.

— **Discrete-time multi-observer.** The starting point of the proposed hybrid multi-observer design is a nominal continuous-time observer satisfying and input-to-state stability property. It would be interesting to exploit similar multi-observer ideas to improve the estimation performance of a discrete-time nonlinear nominal observer that satisfies a discrete-time input-to-state stability property, see e.g., [166]. In this case we will obtain a discrete-time multi-observer, where a jump can represent both the discrete-time evolution and a switch of the selected mode. A discrete version of the hybrid scheme would be relevant for implementation purposes and could thus be very useful in applications.

— **Multi-observer for hybrid observers.** Going one step further compared to the previous item, we could envision developing a hybrid multi-observer to improve the performance of a nominal hybrid observer, see, e.g, [39, 40], which is used to estimate the state of a possibly hybrid dynamical system.

— **Modes with different structures.** Following similar hybrid multi-observer ideas, a possible relevant future research direction would be to propose a design framework, which allows to consider observers with different structures to further improve the estimation performance. For example, in [43], the authors unite a local and a global observer with different structures (e.g., an extended Kalman filter and a high-gain observer), and thus different behaviours, and switch between them to take the best out of each. We believe that allowing the additional modes of the hybrid multi-observer to have a structure different from the nominal observer, and not only a different gain, may help to further improve the estimation performance. However, to prove stability properties in this case seems challenging. Indeed, even if the additional modes are not required to satisfy a stability property, in Chapter 5 we exploited the structure for the additional mode and the input-to-state stability property of the nominal observer to prove an input/output-to-state stability for the additional modes (Lemma 5.1), which was essential to prove the stability guarantees of the hybrid multi-observer. As a result, allowing the modes to have a different structure than the nominal observer may imply that the additional modes need to guarantee an input-to-state stability property to be able to prove an input-to-state stability property for the multi-observer. Indeed, we believe that, if all the modes of the multi-observer (with the same or different structures) satisfy an input-to-state stability property globally, then, following similar lines as the ones presented in Chapter 5, it should be possible to prove an input-to-state stability property for the hybrid multi-observer state estimate. On the other hand, asking that all modes satisfy an input-to-state stability property might be restrictive, as we saw in the numerical examples, that the performance can be improved thanks to modes that are not converging a priori (see e.g. when the null gain was selected). Therefore, asking all modes to satisfy an input-to-state stability property is a strong assumption compared to the current result, where we have full freedom on the gain selection.

— **Several nominal observers.** Another possible interesting research perspective consists in following similar ideas as in Chapter 5, but with two or more nominal observers, with different structures, satisfying Assumption 5.1 and then add additional modes with the same structure as one of the nominal observers, but with different gains. This should allow to prove an input-to-state stability property for the hybrid multi-observer, which will have modes with different structures and different gains and thus is more general than the one presented in this thesis. However, if we follow the same steps we used for the setting presented in this thesis in this new scenario, the corresponding hybrid system can generate Zeno solutions. As a result, to generalize the hybrid multi-observer presented in Chapter 5 by allowing more than one nominal observer, the hybrid estimation scheme needs to be modified.

Application to lithium-ion battery

Some future work direction for the lithium-ion battery application presented in Chapter 6 are given next.

— **Experimental data and parameters uncertainties.** In Chapter 6 the hybrid multi-observer has been applied in simulations for the state estimation of an electrochemical lithium-ion battery. The next step we plan to pursue is to test the hybrid multi-observer on experimental data.

— **Different system models and thus nominal observers for the specific application.** As described in Chapter 6, lithium-ion batteries can be described using electrochemical models (as the one presented in Chapter 6) or equivalent circuit models (as the ones used in the numerical examples in Chapter 3 and 5). Each model has pros and cons and there is typically a trade-off between accuracy and complexity of model and observer. Using different models for the same physical systems leads to different observer designs. Therefore, we could design a hybrid multi-observer where each mode is represented by an observer designed for one possible system model and satisfying an input-to-state stability property as in Assumption 5.1. Moreover, we could also add additional modes, which are not required to satisfy a stability property, with the same structure as one of the observers designed for one of the possible available models, but with different gains.

Appendix A

Technical lemma - Change of supply rates

The next lemma is invoked in Chapter 4.

Lemma A.1. *Let $f : \mathbb{R}^{n_x} \times \mathbb{R}^{n_{u_1}} \times \cdots \times \mathbb{R}^{n_{u_N}} \to \mathbb{R}^{n_x}$, with $n_x \in \mathbb{Z}_{>0}$ and $n_{u_1}, \ldots, n_{u_N} \in \mathbb{Z}_{\geqslant 0}$. Suppose there exist $V : \mathbb{R}^{n_x} \to \mathbb{R}_{\geqslant 0}$, continuously differentiable, $\underline{\alpha}_V$, $\overline{\alpha}_V$, α, $\gamma_1, \ldots, \gamma_N \in \mathscr{K}_\infty$ such that for all $x \in \mathbb{R}^{n_x}$, $u_i \in \mathbb{R}^{n_{u_i}}$,*

$$\begin{aligned} \underline{\alpha}_V(|x|) \leqslant V(x) \leqslant \overline{\alpha}_V(|x|) \\ \langle \nabla V(x), (f(x, u_1, \ldots u_N)) \rangle \leqslant -\alpha(|x|) + \sum_{i=1}^{N} \gamma_i(|u_i|). \end{aligned} \tag{A.1}$$

Then, for all $i \in \{1, \ldots, N\}$ and any given $\tilde{\gamma}_i \in \mathscr{K}_\infty$ verifying $\gamma_i(r) = O(\tilde{\gamma}_i(r))$ as $r \to +\infty$, there exist $\underline{\alpha}_W$, $\overline{\alpha}_W$, $\tilde{\alpha}$ and $W : \mathbb{R}^{n_x} \to \mathbb{R}_{\geqslant 0}$ continuously differentiable such that for all $x \in \mathbb{R}^{n_x}$, $u_i \in \mathbb{R}^{n_{u_i}}$,

$$\underline{\alpha}_W(|x|) \leqslant W(x) \leqslant \overline{\alpha}_W(|x|) \tag{A.2}$$

$$\langle \nabla W(x), f(x, u_1, \ldots u_N) \rangle \leqslant -\tilde{\alpha}(|x|) + \sum_{i=1}^{N} \tilde{\gamma}_i(|u_i|). \tag{A.3}$$

□

Proof. The proof follows similar steps as the proof of [167, Theorem 1]. Let $W := \rho \circ V$, where ρ is a $\mathscr{K}_\infty$-function defined as

$$\rho(s) := \int_0^s q(t)dt \tag{A.4}$$

where q is a suitably chosen smooth non-decreasing function from $[0, +\infty)$ to $[0, +\infty)$, which satisfies $q(t) > 0$ for $t > 0$. Hence, the function W is smooth and positive definite by properties of ρ and V. As a consequence, there exist $\underline{\alpha}_W \in \mathscr{K}_\infty$ and $\overline{\alpha}_W \in \mathscr{K}_\infty$ such that (A.2) is satisfied.

Let $x \in \mathbb{R}^{n_x}$, $u_i \in \mathbb{R}^{n_{u_i}}$ for any $i \in \{1, \ldots, N\}$ and $\tilde{\gamma}_i \in \mathscr{K}_\infty$ such that $\gamma_i(r) = O(\tilde{\gamma}_i(r))$ as $r \to +\infty$, for all $i \in \{1, \ldots, N\}$. Let $x \in \mathbb{R}^{n_x}$ and $u_i \in \mathbb{R}^{u_i}$. From the definition of W, (A.1) and

(A.4), we have

$$\begin{aligned}\langle \nabla W(x), (f(x,u_1,\dots u_N))\rangle &= \rho'(V(x))\langle \nabla W(x), (f(x,u_1,\dots,u_N))\rangle \\ &\leqslant q(V(x))\left[-\alpha(|x|)+\sum_{i=1}^{N}\gamma_i(|u_i|)\right] \\ &= \sum_{i=1}^{N}\left[q(V(x))\left(-\frac{1}{N}\alpha(|x|)+\gamma_i(|u_i|)\right)\right].\end{aligned} \tag{A.5}$$

We will show that we can upper-bound this last inequality and obtain

$$\langle \nabla W(x), (f(x,u_1,\dots u_N))\rangle \leqslant \sum_{i=1}^{N}\left[q(\vartheta_i(|u_i|))\gamma_i(|u_i|)-\frac{1}{2N}q(V(x))\alpha(|x|)\right] \tag{A.6}$$

with $\vartheta_i := \overline{\alpha}_V \circ \alpha^{-1}(2N\gamma_i) \in \mathscr{K}_\infty$, for any $i \in \{1,\dots,N\}$. To show that (A.6) is satisfied, we have to prove that, for any $i \in \{1,\dots,N\}$,

$$q(V(x))\left(-\frac{1}{N}\alpha(|x|)+\gamma_i(|u_i|)\right) \leqslant q(\vartheta_i(|u_i|))\gamma_i(|u_i|)-\frac{1}{2N}q(V(x))\alpha(|x|). \tag{A.7}$$

To show (A.7) we consider two cases. Let $i \in \{1,\dots,N\}$, when $\gamma_i(|u_i|) \leqslant \frac{1}{2N}\alpha(|x|)$, we have

$$\begin{aligned}-\frac{1}{N}\alpha(|x|)+\gamma_i(|u_i|) &\leqslant -\frac{1}{N}\alpha(|x|)+\frac{1}{2N}\alpha(|x|) \\ &= -\frac{1}{2N}\alpha(|x|),\end{aligned} \tag{A.8}$$

therefore (A.7) is satisfied. Conversely, when $\frac{1}{2N}\alpha(|x|) \leqslant \gamma_i(|u_i|)$, which can be rewritten as $\alpha(|x|) \leqslant 2N\gamma_i(|u_i|)$, we have

$$\begin{aligned}\vartheta_i(|u_i|) &= \overline{\alpha}_V \circ \alpha^{-1}(2N\gamma_i(|u_i|)) \\ &\geqslant \overline{\alpha}_V \circ \alpha^{-1} \circ \alpha(|x|) \\ &= \overline{\alpha}_V(|x|) \\ &\geqslant V(x).\end{aligned} \tag{A.9}$$

As a consequence, we have

$$\begin{aligned}q(V(x))\left(-\frac{1}{N}\alpha(|x|)+\gamma_i(|u_i|)\right) &= -\frac{1}{N}q(V(x))\alpha(|x|)+q(V(x))\gamma_i(|u_i|) \\ &\leqslant -\frac{1}{N}q(V(x))\alpha(|x|)+q(\vartheta_i(|u_i|))\gamma_i(|u_i|) \\ &\leqslant -\frac{1}{2N}q(V(x))\alpha(|x|)+q(\vartheta_i(|u_i|))\gamma_i(|u_i|),\end{aligned} \tag{A.10}$$

thus (A.7) is satisfied. Consequently (A.6) holds. From (A.6), using $V(x) \geqslant \underline{\alpha}_V(|x|)$, which comes from (A.1), we obtain

$$\langle \nabla W(x), (f(x,u_1,\dots u_N))\rangle \leqslant \sum_{i=1}^{N}\left[q(\vartheta_i(|u_i|))\gamma_i(|u_i|) - \frac{1}{2N}q(\underline{\alpha}_V(|x|))\alpha(|x|)\right]. \tag{A.11}$$

Since $\gamma_i(|u_i|) = O(\tilde{\gamma}_i(|u_i|))$ as $|u_i| \to +\infty$, for all $i \in \{1,\dots,N\}$, we can apply [167, Lemma 1] with

$$\begin{aligned}\beta_i &:= \gamma_i \circ \vartheta_i^{-1},\\ \tilde{\beta}_i &:= \tilde{\gamma}_i \circ \vartheta_i^{-1}.\end{aligned} \tag{A.12}$$

Then, there exist q_i smooth non-decreasing functions such that $q_i(0) = 0$ and

$$q_i(r)\beta_i(r) \leqslant \tilde{\beta}_i(r) \tag{A.13}$$

for all $r \in [0,+\infty), i \in \{1,\dots,N\}$. Note that, in [167, Lemma 1] it is not specified that $q_i(0) = 0$. However, the proof applies by adding this extra condition. From (A.12) and (A.13) we have

$$q_i(r)\gamma_i \circ \vartheta_i^{-1}(r) \leqslant \tilde{\gamma}_i \circ \vartheta_i^{-1}(r) \tag{A.14}$$

for all $r \in [0,+\infty)$. As a consequence

$$q_i(\vartheta_i(|u_i|))\gamma_i(|u_i|) \leqslant \tilde{\gamma}_i(|u_i|). \tag{A.15}$$

We define $\tilde{q} := \min\{q_1,\dots,q_N\}$. Note that $\tilde{q}$ is a positive definite, non-decreasing function. Using [168, Lemma 1] we have that there exists a function $q \in \mathscr{K}$, smooth on $\mathbb{R}_{>0}$, so that

$$q(s) \leqslant \tilde{q}(s) \leqslant q_i(s) \tag{A.16}$$

for all $s \geqslant 0$, for all $i \in \{1,\dots,N\}$. Define $\tilde{\alpha} \in \mathscr{K}_\infty$ as

$$\tilde{\alpha}(s) := \frac{1}{2}q(\underline{\alpha}_V(s))\alpha(s) \in \mathscr{K}_\infty. \tag{A.17}$$

From (A.11), (A.15), (A.16) and (A.17), we obtain

$$\begin{aligned}
\langle \nabla W(x), (f(x,u_1,\dots u_N))\rangle &\overset{(A.11)}{\leqslant} \sum_{i=1}^{N}\left[q(\vartheta_i(|u_i|))\gamma_i(|u_i|) - \frac{1}{2N}q(\underline{\alpha}_V(|x|))\alpha(|x|)\right] \\
&\overset{(A.16)}{\leqslant} \sum_{i=1}^{N}\left[q_i(\vartheta_i(|u_i|))\gamma_i(|u_i|) - \frac{1}{2N}q(\underline{\alpha}_V(|x|))\alpha(|x|)\right] \\
&\overset{(A.15),(A.17)}{\leqslant} \sum_{i=1}^{N}\left[\tilde{\gamma}_i(|u_i|) - \frac{1}{N}\tilde{\alpha}(|x|)\right] \\
&= -\tilde{\alpha}(|x|) + \sum_{i=1}^{N}\tilde{\gamma}_i(|u_i|),
\end{aligned} \tag{A.18}$$

which concludes the proof. ■

Appendix B

On the relationship between quadratic state estimation error costs and output estimation error costs

Contents

B.1 Introduction

The objective of this appendix is to unravel relationships between quadratic output estimation costs and state estimation costs. To evaluate online the estimation performance, costs depending on the output estimation error are used in Chapters 5 and 6 and also in e.g., [136, 137]. While the output error can be computed on-line, the state estimation error, which is of primary importance, is unknown since the real state of a dynamical system is unknown in an estimation problem. It would thus be interesting to investigate relationships between a state estimation error cost and an output estimation error one. In particular, given two observers with the same structure but different gains, we would like to know how to design an output error cost, so that if one observer has a smaller output estimation error cost, then it means that an associated state estimation error cost is also smaller.

In this appendix, we consider linear time-invariant systems and we present some preliminary

results on how to compare observer performance online, starting from a quadratic output estimation error cost, which can be evaluated online, to a state estimation error cost, which is the one directly related to the observer performance and thus the cost we are interested on. Contrary to the other contents presented in this thesis, the results of this appendix are preliminary and have not been submitted for pubblication.

B.2 Problem statement

Consider the unperturbed linear time-invariant system

$$\begin{aligned} \dot{x} &= Ax + Bu \\ y &= Cx, \end{aligned} \tag{B.1}$$

where $x \in \mathbb{R}^{n_x}$ is the state, $u \in \mathbb{R}^{n_u}$ is a known input, and $y \in \mathbb{R}^{n_y}$ is the measured output with n_x, $n_y \in \mathbb{Z}_{>0}$ and $n_u \in \mathbb{Z}_{\geqslant 0}$. The pair (A, C) is assumed to be detectable. Hence, by letting $L_1 \in \mathbb{R}^{n_x \times n_y}$ be any matrix such that $A - L_1 C$ is Hurwitz, we can design a Luenberger observer [113] of the form

$$\begin{aligned} \dot{\hat{x}}_1 &= A\hat{x}_1 + Bu + L_1(y - \hat{y}_1) \\ \hat{y}_1 &= C\hat{x}_1, \end{aligned} \tag{B.2}$$

where $\hat{x}_1 \in \mathbb{R}^{n_x}$ is the state estimate. We name this observer *nominal observer* and it is the one for which we compare the estimation performance. We define the state estimation error of the nominal observer as $e_1 := x - \hat{x}_1$. In view of (B.1) and (B.2), the dynamics of the state estimation error e_1 is

$$\dot{e}_1 = (A - L_1 C)e_1. \tag{B.3}$$

Since $A - L_1 C$ is Hurwitz, e_1 globally exponentially converges to the origin. As a consequence, for any $Q \in \mathbb{R}^{n_x \times n_x}$ symmetric positive definite matrix, there exist $\Lambda_1^\star \in \mathbb{R}^{n_y \times n_y}$ and a symmetric positive definite matrix $P \in \mathbb{R}^{n_x \times n_x}$ such that

$$(A - L_1 C)^\top P + P(A - L_1 C) = -Q + C^\top \Lambda_1^\star C. \tag{B.4}$$

Note that there may be more than one possible options for $\Lambda_1^\star$ and P that satisfy (B.4) for the same Q. In particular, since $A - L_1 C$ is Hurwitz, from e.g., [85, Theorem 4.6] we have guarantees that if $\Lambda_1^\star = 0_{n_y \times n_y}$, there exists a unique $P \in \mathbb{R}^{n_x \times n_x}$ symmetric positive definite that satisfies (B.4). In addition, for any $\Lambda_1^\star \in \mathbb{R}^{n_y \times n_y}$ that produces $Q - C^\top \Lambda_1^\star C \in \mathbb{R}^{n_x \times n_x}$ symmetric positive definite, we know that there exists a unique $P \in \mathbb{R}^{n_x \times n_x}$ symmetric positive definite that satisfies (B.4). As a result, a possible option for the design is to chose $Q \in \mathbb{R}^{n_x \times n_x}$ and $\Lambda_1^\star \in \mathbb{R}^{n_y \times n_y}$ such that $Q - C^\top \Lambda_1^\star C$ is symmetric positive definite and then solve the Lyapunov equation (B.4) to find P. However, there are also other possible combinations of $\Lambda_1^\star$, Q and P that satisfy (B.4).

We now consider an additional observer-like system, which has the same structure as (B.2) but with a different output injection gain $L_2 \in \mathbb{R}^{n_x \times n_y}$,

$$\begin{aligned}\dot{\hat{x}}_2 &= A\hat{x}_2 + Bu + L_2(y - \hat{y}_2)\\ \hat{y}_2 &= C\hat{x}_2,\end{aligned} \tag{B.5}$$

where $\hat{x}_2$ is its state estimate. Note that this observer-like system can be an observer or not, as $A - L_2C$ is not necessarily Hurwitz. We denote the corresponding state estimation error $e_2 := x - \hat{x}_2$, whose dynamics is, in view of (B.1) and (B.5),

$$\dot{e}_2 = (A - L_2C)e_2. \tag{B.6}$$

The additional observer-like system (B.5), together with the nominal observer (B.2) are called *modes* for the sake of convenience. We define the output estimation errors for both modes as $e_{y_k} := y - \hat{y}_k = C(x - \hat{x}_k) = Ce_k$, $k \in \{1,2\}$, from (B.1), (B.2), and (B.5).

To evaluate the performance of each mode we should consider a quadratic cost that depends on the state estimation error. Indeed, the smaller is such a cost, the smaller is the estimation error and thus, the better is the performance of the mode. However, in an estimation problem, the system state x is unknown. As a consequence, the state estimation error e_k is unknown and thus it is not possible to evaluate the estimation performance of the modes using a cost that depends on e_k. As a result, in the literature, see e.g. [136, 137], as well as the results in Chapters 5 and 6, the estimation performance is often evaluated using a cost that depends on the output estimation error e_{y_k}, which is accessible since it relies on the knowledge of the measured output y and the estimated output $\hat{y}_k$ of mode k. The quadratic output estimation error cost we can evaluate on-line has the following form, for any $e_{y_k} \in \mathscr{L}_{\mathbb{R}^{n_y}}$, for any $t \in \mathbb{R}_{\geqslant 0}$, $k \in \{1,2\}$,

$$J_k(t, e_{y_k}) := \int_0^t e_{y_k}(s)^\top \Lambda_k^\star e_{y_k}(s) ds, \tag{B.7}$$

with $\Lambda_k^\star \in \mathbb{R}^{n_y \times n_y}$. While cost (B.7) can be evaluated on-line, it does not provide direct information on the performance concerning the state estimation error. A natural question that rises is to understand how and if the output estimation cost (B.7) relates to a cost that considers the state estimation error. In particular, if the two modes are initialized at the same value $e_0 \in \mathbb{R}^{n_x}$, $k \in \{1,2\}$, we want to understand the relationship between the output estimation error cost (B.7), which can be evaluated online, and a quadratic state estimation error cost in the following form, for any $e_k \in \mathscr{L}_{\mathbb{R}^{n_x}}$ initialized at $e_k(0) = e_0$, for any $t \in \mathbb{R}_{\geqslant 0}$, $k \in \{1,2\}$,

$$W_k(t, e_k) := e_k(t)^\top P e_k(t) + \int_0^t e_k(s)^\top Q e_k(s) ds, \tag{B.8}$$

where P and Q come from (B.4).

Note that evaluating the estimation performance based on an cost that depends on the output estimation error does not automatically give information on the estimation performance evaluated using a cost that depends on the whole system state. In particular, it is not guaranteed that if, at time

$t \in \mathbb{R}_{\geqslant 0}$, the additional observer-like system (B.5) has better (worse) performance compared to the nominal observer (B.2) in terms of an output estimation cost, i.e., $W_2(t) \leqslant W_1(t)$ ($W_2(t) \geqslant W_1(t)$), which is the one we can evaluate on-line, then it has better (worse) performance also in terms of a state estimation error cost, i.e., $J_2(t) \leqslant J_1(t)$ ($J_2(t) \geqslant J_1(t)$).

The objective of this work is to identify conditions under which better/worse estimation performance with respect to the output estimation error cost (B.7), implies better/worse estimation performance also with respect to the state estimation error cost (B.8).

B.3 Main result

The goal of this section is to give the conditions under which better performance in terms of the output estimation cost (B.7) implies better performance in terms of a state estimation cost (B.8). In particular, in Section B.3.1 we present a general condition for this purpose and in Section B.3.2 we show, through a counterexample, that this condition is not verified for any choice of the gain $L_2 \in \mathbb{R}^{n_x \times n_y}$ of the additional observer-like system. In Section B.3.3 we provide an extra condition on the gain selection, which guarantees the satisfaction of the condition given in Section B.3.1. Finally, in Section B.3.4, we relax the condition, thereby increasing the applicability of the proposed result.

B.3.1 General condition

In the next theorem, we provide a condition that, if satisfied, allows to compare the observer performance on-line. In particular, by the use of an output estimation error cost, which can be evaluated on-line, when the condition is satisfied, we have information about the estimation performance in terms of a state estimation error cost.

Theorem B.1. *Consider system* (B.1)*, the nominal observer* (B.2) *and the additional observer-like system* (B.5) *with* $e_k(0) = e_0 \in \mathbb{R}^{n_x}$*, for all* $k \in \{1,2\}$*. Given* $L_2 \in \mathbb{R}^{n_x \times n_y}$ *for the additional mode, if there exists* $\Lambda_2^\star \in \mathbb{R}^{n_y \times n_y}$ *such that*

$$(A - L_2C)^\top P + P(A - L_2C) = -Q + C^\top \Lambda_2^\star C \tag{B.9}$$

is satisfied with P *and* Q *from* (B.4)*. Then, for any* $t \in \mathbb{R}_{\geqslant 0}$*,* $J_1(t) - J_2(t) = W_1(t) - W_2(t)$. □

Proof. Let $V(e_k) := e_k^\top P e_k$, for all $e_k \in \mathbb{R}^{n_x}$, $k \in \{1,2\}$, where P comes from (B.4). Then, from (B.3) and (B.6), we have

$$\langle \nabla V(e_k), (A - L_kC)e_k \rangle = e_k^\top \left((A - L_kC)^\top P + P(A - L_kC) \right) e_k. \tag{B.10}$$

Using (B.4), we have

$$\begin{aligned} \langle \nabla V(e_1), (A - L_1C)e_1 \rangle &= e_1^\top \left((A - L_1C)^\top P + P(A - L_1C) \right) e_1 \\ &= -e_1^\top Q e_1 + e_1^\top C^\top \Lambda_1^\star C e_1. \end{aligned} \tag{B.11}$$

Let e_1 be a solution to system (B.3), then (B.11) implies, for any $t \in \mathbb{R}_{\geqslant 0}$,

$$\frac{d}{dt}V(e_1(t)) = -e_1(t)^\top Q e_1(t) + e_1(t)^\top C^\top \Lambda_1^\star C e_1(t). \tag{B.12}$$

Integrating (B.12), we obtain, for all $t \in \mathbb{R}_{\geqslant 0}$,

$$V(e_1(t)) - V(e_1(0)) + \int_0^t e_1(s)^\top Q e_1(s) ds = \int_0^t e_1(s)^\top C^\top \Lambda_1^\star C e_1(s) ds, \tag{B.13}$$

which implies, from the definitions of V and e_{y_1},

$$e_1(t)^\top P e_1(t) - e_1(0)^\top P e_1(0) + \int_0^t e_1(s)^\top Q e_1(s) ds = \int_0^t e_{y_1}(s)^\top \Lambda_1^\star e_{y_1}(s) ds. \tag{B.14}$$

Using (B.8) and (B.7), (B.14) is equivalent to

$$W_1(t) - e_1(0)^\top P e_1(0) = J_1(t). \tag{B.15}$$

Pick $L_2 \in \mathbb{R}^{n_x \times n_y}$ and $\Lambda_2^\star \in \mathbb{R}^{n_y \times n_y}$ such that (B.9) is satisfied with P and Q from (B.4). Then, following similar steps as for the nominal observer, from (B.10) we obtain, for all $t \in \mathbb{R}_{\geqslant 0}$,

$$W_2(t) - e_2(0)^\top P e_2(0) = J_2(t). \tag{B.16}$$

Since $e_1(0) = e_2(0) = e_0 \in \mathbb{R}^{n_x}$, from (B.15) and (B.16) we have $W_1(t) - J_1(t) = W_2(t) - J_2(t)$, for all $t \in \mathbb{R}_{\geqslant 0}$, which is equivalent to

$$J_1(t) - J_2(t) = W_1(t) - W_2(t), \tag{B.17}$$

for all $t \in \mathbb{R}_{\geqslant 0}$. This concludes the proof. ■

Theorem B.1 gives a condition that, if satisfied, provides a relation between a quadratic output estimation error cost and a quadratic state estimation error cost. In particular, it shows that if the output estimation cost related to the observer-like system $J_2(t)$ is smaller than the output estimation cost of the nominal observer $J_1(t)$ at some time $t \in \mathbb{R}_{\geqslant 0}$, then, the corresponding state estimation cost $W_2(t)$ is smaller than the state estimation cost of the nominal observer $W_1(t)$, at the same time t. As a consequence, if the estimation performance are evaluated in terms of output costs and the observer-like system (B.5) has better performance compared to the nominal observer, then, if the condition in Theorem B.1 is satisfied, this mode has better performance also in terms of a state cost. Moreover, also the opposite is true. Indeed, if the observer-like system (B.5) has worse performance compared to the nominal observer (B.2) in terms of an output estimation cost, i.e., $J_2(t) \geqslant J_1(t)$ with $t \in \mathbb{R}_{\geqslant 0}$, then it has worse performance also with respect to a state estimation cost, i.e., $W_2(t) \geqslant W_1(t)$.

Thus, in Theorem B.1 it is shown, under some conditions, that it is possible to evaluate the performance of a mode using an output cost, which can be evaluated since y and $\hat{y}_k$, $k \in \{1, 2\}$

are known, and have guarantees also on the performance of the mode in terms of a state estimation cost, which is the most interesting one. Unfortunately, even if condition (B.9) may look easy to satisfy thanks to the freedom introduced by $\Lambda_2^\star$, we will show in the next section that it is not possible to find $\Lambda_2^\star$ to satisfy condition (B.9) for any choice of the gain L_2 of the additional observer-like system (B.5).

B.3.2 Condition (B.9) is not always satisfied

In this section we show that it is not always possible to guarantee that, for any choice of gain $L_2 \in \mathbb{R}^{n_x \times n_y}$ there exists $\Lambda_2^\star \in \mathbb{R}^{n_y \times n_y}$ such that

$$(A - L_2 C)^\top P + P(A - L_2 C) = -Q + C^\top \Lambda_2^\star C \tag{B.18}$$

is satisfied with P and Q from (B.4). In particular, the freedom we introduce with $\Lambda_2^\star$ is not always enough to allow us to choose any gain L_2 for the additional observer-like system. We now provide an example for which there exists $\Lambda_2^\star \in \mathbb{R}^{n_y \times n_y}$ such that (B.18) is satisfied only for some choices of the output injection gain L_2, while it is not satisfied for some other choices.

Consider system (B.1) with [9]

$$A = \begin{bmatrix} 0 & 1 \\ 0 & 0 \end{bmatrix}, \quad C = \begin{bmatrix} 1 & 0 \end{bmatrix}. \tag{B.19}$$

Note that the pair (A, C) in (B.19) is observable. We design the nominal observer (B.2) with $L_1 = [3\ 2]^\top$. As a result, the matrix $A - L_1 C$ is Hurwitz with eigenvalues -1 and -2. We pick $Q = \begin{bmatrix} 2 & 0 \\ 0 & 1 \end{bmatrix}$ and $\Lambda_1^\star = 1$ in (B.4) so that $Q - C^\top \Lambda_1^\star C = I_2$. As a consequence, $P = \begin{bmatrix} 0.5 & -0.5 \\ -0.5 & 1 \end{bmatrix}$.

We consider the additional observer-like system (B.5) and our objective is to check if, for any choice of the additional gain $L_2 \in \mathbb{R}^{2\times 1}$, there exists $\Lambda_2^\star \in \mathbb{R}$ such that (B.18) is satisfied. For this reason we define $L_2 := [l_1\ l_2]^\top$ and we have

$$A - L_2 C = \begin{bmatrix} -l_1 & 1 \\ -l_2 & 0 \end{bmatrix} \tag{B.20}$$

Using the matrices P and Q from the nominal observer, we write (B.18) for this additional mode and we obtain

$$\begin{bmatrix} -l_1 & -l_2 \\ 1 & 0 \end{bmatrix} \begin{bmatrix} 0.5 & -0.5 \\ -0.5 & 1 \end{bmatrix} + \begin{bmatrix} 0.5 & -0.5 \\ -0.5 & 1 \end{bmatrix} \begin{bmatrix} -l_1 & 1 \\ -l_2 & 0 \end{bmatrix} = \begin{bmatrix} -2 & 0 \\ 0 & -1 \end{bmatrix} + \begin{bmatrix} \Lambda_2^\star & 0 \\ 0 & 0 \end{bmatrix}, \tag{B.21}$$

9. We do not need to provide information for the matrix B in (B.1). Indeed, all the developments in this section are related to the estimation errors e_1 and e_k, which do not depend on the system input, see equations (B.3) and (B.6).

which is equivalent to

$$\begin{bmatrix} -l_1+l_2 & 0.5l_1-l_2+0.5 \\ 0.5l_1-l_2+0.5 & -1 \end{bmatrix} = \begin{bmatrix} -2+\Lambda_2^\star & 0 \\ 0 & -1 \end{bmatrix}. \tag{B.22}$$

For (B.22) to hold, we must have $-l_1+l_2 = -2+\Lambda_2^\star$ and $0.5l_1-l_2+0.5=0$. The first condition can be always satisfied by selecting $\Lambda_2^\star = -l_1+l_2+2$. However, $\Lambda_2^\star$ has no impact on the off-diagonal terms in (B.22) and, as a result, some choices of the gain $L_2 = [l_1\ l_2]^\top$ do not verify this condition. For example, with the gain $L_2 = [2\ 2]^\top$, for any choice of $\Lambda_2^\star \in \mathbb{R}$, $l_1 \neq 2l_2-1$ and thus (B.18) cannot be satisfied.

It is interesting to notice also that, in this example, the necessary condition on the gain L_2 selection to satisfy (B.18) for some $\Lambda_2^\star \in \mathbb{R}$ has no links with the stability of the mode. Indeed, there are gain choices that satisfy $l_1 = 2l_2-1$ that are stable (see e.g., $L_2 = [0\ 0.5]^\top$, $L_2 = [1\ 1]^\top$, $L_2 = [2\ 1.5]^\top$, $L_2 = [5\ 3]^\top$, $L_2 = [10\ 5.5]^\top$) and other that are unstable (see e.g., $L_2 = [-1\ 0]^\top$, $L_2 = [-2\ -0.5]^\top$, $L_2 = [-5\ -2]^\top$, $L_2 = [-0.5\ 0.25]^\top$). On the other hand, selecting the mode gain L_2 such that $A-L_2C$ is Hurwitz does not guarantee that there exists $\Lambda_2^\star \in \mathbb{R}$ such that (B.18) is satisfied. Indeed, $L_2 = [2\ 2]^\top$ produces a converging mode, however, $l_1 \neq 2l_2-1$ and thus (B.18) cannot be satisfied.

This example shows that it is not always possible to satisfy condition (B.9) for any choice of the additional gain $L_2 \in \mathbb{R}^{n_y \times n_x}$ and apply the result of Theorem B.1.

In the next section we prove that, under some conditions on the choice of the additional gain $L_2 \in \mathbb{R}^{n_x \times n_y}$ it is possible to satisfy (B.9) and consequently, from Theorem B.1, show that if the additional observer-like system performs better/worse than the nominal observer in terms of an output estimation error cost, it implies that it is performing better/worse also in terms of a state estimation error cost.

B.3.3 Gains selection to guarantee (B.9)

In the next proposition we prove that if the gain of the additional observer-like system, as well as the one of the nominal observer, are designed as the gains of infinite gain margin observers, then there always exists $\Lambda_2^\star \in \mathbb{R}^{n_y \times n_y}$ such that condition (B.9) in Theorem B.1 is satisfied and thus better performance with respect to an output error cost implies better performance also with respect to a state estimation error cost.

Proposition B.1. *Consider system* (B.1) *and the nominal observer* (B.2) *with* $L_1 := P^{-1}C^\top\Lambda_1$*, with* P *from* (B.4) *and* $\Lambda_1 \in \mathbb{R}^{n_y \times n_y}$ *such that* $A-L_1C = A-P^{-1}C^\top\Lambda_1 C$ *is Hurwitz. Consider the additional observer-like system* (B.5)*. Then, for any* $\Lambda_2 \in \mathbb{R}^{n_y \times n_y}$*, by defining* $L_2 := P^{-1}C^\top\Lambda_2$*, where* P *comes from* (B.4)*, there always exists* $\Lambda_2^\star \in \mathbb{R}^{n_y \times n_y}$ *such that*

$$(A-L_2C)^\top P + P(A-L_2C) = -Q + C^\top\Lambda_2^\star C \tag{B.23}$$

is satisfied with P *and* Q *from* (B.4). □

Proof. Consider system (B.1) and the nominal observer (B.2). Since the pair (A, C) is detectable and the gain L_1 is designed such that the matrix $A - L_1C$ is Hurwitz, from (B.4) we have that for any $Q \in \mathbb{R}^{n_x \times n_x}$ there exist $\Lambda_1^\star \in \mathbb{R}^{n_y \times n_y}$ and a symmetric positive definite matrix $P \in \mathbb{R}^{n_x \times n_x}$ and such that

$$(A - L_1C)^\top P + P(A - L_1C) = -Q + C^\top \Lambda_1^\star C. \tag{B.24}$$

Select $\Lambda_2 \in \mathbb{R}^{n_y \times n_y}$ and design $L_2 = P^{-1}C^\top \Lambda_2$. Then, (B.24) can be rewritten as

$$(A - L_1C + L_2C - L_2C)^\top P + P(A - L_1C + L_2C - L_2C) = -Q + C^\top \Lambda_1^\star C, \tag{B.25}$$

which implies

$$(A - L_2C)^\top P + P(A - L_2C) + C^\top (L_2^\top - L_1^\top)P + P(L_2 - L_1)C = -Q + C^\top \Lambda_1^\star C. \tag{B.26}$$

Using $L_k = P^{-1}C^\top \Lambda_k$, $k \in \{1, 2\}$, from (B.26) we have

$$(A - L_2C)^\top P + P(A - L_2C) + C^\top (\Lambda_2^\top - \Lambda_1^\top)C + C^\top (\Lambda_2 + \Lambda_1)C = -Q + C^\top \Lambda_1^\star C, \tag{B.27}$$

which implies

$$\begin{aligned}(A - L_2C)^\top P + P(A - L_2C) &= -Q + C^\top (\Lambda_1^\star + \Lambda_1 + \Lambda_1^\top - \Lambda_2 - \Lambda_2^\top)C \\ &= -Q + C^\top \Lambda_2^\star C,\end{aligned} \tag{B.28}$$

with $\Lambda_2^\star := \Lambda_1^\star + \Lambda_1 + \Lambda_1^\top - \Lambda_2 - \Lambda_2^\top \in \mathbb{R}^{n_y \times n_y}$. This concludes the proof. ■

Proposition B.1 shows that when the modes are designed as infinite gain margin observers, condition (B.9) is satisfied and the results of Theorem B.1 hold. However, this is not the only possible choice of gains that satisfy condition (B.9). We will now see this on the same example we considered in Section B.3.2. In particular, note that the gain L_1 in the example in Section B.3.2 is not in the form $L_1 := P^{-1}C^\top \Lambda_1$. Indeed, L_1 was selected to place the eigenvalues of $A - L_1C$ in -1 and -2 and we had obtained $L_1 = [3\ 2]^\top$. Solving the Lyapunov equation (B.4) for $Q = I_2$ and $\Lambda_1^\star = 1$ as in Section B.3.2, we obtained $P = \begin{bmatrix} 0.5 & -0.5 \\ -0.5 & 1 \end{bmatrix}$, which implies $P^{-1} = \begin{bmatrix} 4 & 2 \\ 2 & 2 \end{bmatrix}$ and

$$P^{-1}C^\top \Lambda_1 = \begin{bmatrix} 4 & 2 \\ 2 & 2 \end{bmatrix} \begin{bmatrix} 1 \\ 0 \end{bmatrix} \Lambda_1 = \begin{bmatrix} 4 \\ 2 \end{bmatrix} \Lambda_1 \neq L_1 \quad \forall \Lambda_1 \in \mathbb{R}. \tag{B.29}$$

We recall that Λ_1 can be chosen different from $\Lambda_1^\star$ in (B.4). However, in this example, there is no $\Lambda_1 \in \mathbb{R}$ that satisfies $L_1 = P^{-1}C^\top \Lambda_1$.

In addition, for the P obtained from the choices of L_1, Q and $\Lambda_1^\star$, in the example in Section B.3.2 we have showed that condition (B.9) is satisfied if the additional gain L_2 is chosen such that $L_2 = [l_1\ l_2]^\top$ with $l_1 = 2l_2 - 1$, which, from (B.29), is not in the from $P^{-1}C^\top \Lambda_2$.

As a consequence, if the gains are chosen such that $L_k = P^{-1}C^\top \Lambda_k$, $k \in \{1,2\}$, with P from (B.4) and $\Lambda_k \in \mathbb{R}$, from Proposition B.1 we have guarantees that condition (B.9) is satisfied and thus, from Theorem B.1 we can relate a state estimation error cost to an output estimation error cost. However, the example in Section B.3.2 shows that there are other possible choices for the nominal gain L_1 and the observer-like system gain L_2, which are not in the form $L_k = P^{-1}C^\top \Lambda_k$, $k \in \{1,2\}$, but still satisfy condition (B.9). In particular, with the condition $L_1 = P^{-1}C^\top \Lambda_1$, we are only considering the matrix P satisfying

$$\begin{aligned}
&(A - L_1C)^\top P + P(A - L_1C) = -Q + C^\top \Lambda_1^\star C \\
&(A - P^{-1}C^\top \Lambda_1 C)^\top P + P(A - P^{-1}C^\top \Lambda_1 C) = -Q + C^\top \Lambda_1^\star C \\
&A^\top P + PA = -Q + C^\top (\Lambda_1^\star + \Lambda_1 + \Lambda_1^\top) C.
\end{aligned} \tag{B.30}$$

B.3.4 Relaxation of condition (B.9)

In this section we relax the condition on the nominal observer (B.4) and the one for the additional observer-like system (B.9) and we show that, even with less stringent conditions, we can prove that better performance in terms of an output estimation error cost implies better performance with respect to a state estimation error cost.

As explained in Section B.2, since the nominal observer gain L_1 is designed such that $A - L_1C$ is Hurwitz, we have that for any $Q \in \mathbb{R}^{n_x \times n_x}$ symmetric positive definite there exist $\Lambda_1^\star \in \mathbb{R}^{n_y \times n_y}$ and a symmetric positive definite matrix $P \in \mathbb{R}^{n_x \times n_x}$ such that

$$(A - L_1C)^\top P + P(A - L_1C) = -Q + C^\top \Lambda_1^\star C. \tag{B.31}$$

As a consequence,

$$(A - L_1C)^\top P + P(A - L_1C) \geqslant -Q + C^\top \Lambda_1^\star C. \tag{B.32}$$

Theorem B.2. *Consider system* (B.1)*, the nominal observer* (B.2) *and the additional observer-like system* (B.5) *with $e_k(0) = e_0 \in \mathbb{R}^{n_x}$, for all $k \in \{1,2\}$. Given $L_2 \in \mathbb{R}^{n_x \times n_y}$ for the additional mode, if, there exists $\Lambda_2^\star \in \mathbb{R}^{n_y \times n_y}$ such that*

$$(A - L_2C)^\top P + P(A - L_2C) \leqslant -Q + C^\top \Lambda_2^\star C \tag{B.33}$$

is satisfied with P and Q from (B.4)*. Then, for any $t \in \mathbb{R}_{\geqslant 0}$, $J_2(t) \leqslant J_1(t)$ implies $W_2(t) \leqslant W_1(t)$.* □

Proof. Let $V(e_k) := e_k^\top P e_k$, for all $e_k \in \mathbb{R}^{n_x}$, $k \in \{1,2\}$, where P comes from (B.4) as in the proof of Theorem B.1. Similarly to the proof of Theorem B.1 and using condition (B.32) instead of (B.4), from (B.3) we obtain

$$\begin{aligned}
\langle \nabla V(e_1), (A - L_1C)e_1 \rangle &= e_1^\top \left((A - L_1C)^\top P + P(A - L_1C) \right) e_1 \\
&\geqslant -e_1^\top Q e_1 + e_1^\top C^\top \Lambda_1^\star C e_1.
\end{aligned} \tag{B.34}$$

On the other hand, from (B.6), and using (B.33) we have

$$\begin{aligned}\langle \nabla V(e_k), (A - L_k C)e_k \rangle &= e_k^\top \left((A - L_k C)^\top P + P(A - L_k C) \right) e_k \\ &\leqslant -e_k^\top Q e_k + e_k^\top C^\top \Lambda_k^\star C e_k.\end{aligned} \tag{B.35}$$

Following similar steps an in the proof of Theorem B.1, from (B.34) we obtain, for all $t \in \mathbb{R}_{\geqslant 0}$,

$$W_1(t) - e_1(0)^\top P e_1(0) \geqslant J_1(t). \tag{B.36}$$

for the nominal observer, and, from (B.35), for all $t \in \mathbb{R}_{\geqslant 0}$,

$$W_2(t) - e_2(0)^\top P e_2(0) \leqslant J_2(t). \tag{B.37}$$

Since $e_k(0) = e_0 \in \mathbb{R}^{n_x}$, for all $k \in \{1, 2\}$, from (B.36) and (B.37) we have that for all $t \in \mathbb{R}_{\geqslant 0}$ such that $J_k(t) \leqslant J_1(t)$, $W_k(t) \leqslant J_k(t) + e_0^\top P e_0 \leqslant J_1(t) + e_0^\top P e_0 \leqslant W_1(t)$, which concludes the proof. ■

Theorem B.2 provides a relaxed condition compared to the one in Theorem B.1 to guarantee that, if the output estimation error cost of the additional observer-like system (B.5), J_2, is smaller that the output estimation error cost of the nominal observer (B.2), J_1, which means that the observer-like system has better performance in terms of a output estimation error cost, then, it has better performance also in terms of a state estimation error cost. Conversely to Theorem B.1, where we proved also that if the additional mode has worse performance compared to the nominal observer in terms of an output estimation error cost, than it has worse performance also in terms of a state estimation error cost, with the relaxed condition (B.33), we cannot conclude anything in the case the output estimation error cost of the additional mode shows worse performance than the one of the nominal observer.

Even if condition (B.33) in Theorem B.2 is less restrictive than condition (B.9) in Theorem B.1, also in this case it is not always possible to satisfy it for any choice of the gain $L_2 \in \mathbb{R}^{n_x \times n_y}$. In particular, the freedom we introduce with $\Lambda_2^\star$ is not always enough to guarantee that (B.33) holds for any choice of the additional gains. An example to show this is given in the following. We consider system (B.1) with the matrices A and C given in (B.19) and we design the nominal observer with the gain $L_1 = [3\ 2]^\top$ as in Section B.3.2. As before, we chose $Q = \begin{bmatrix} 2 & 0 \\ 0 & 1 \end{bmatrix}$ and $\Lambda_1^\star = 1$, which implies $Q - C^\top \Lambda_1^\star C = I_2$, and, from (B.4), we obtain $P = \begin{bmatrix} 0.5 & -0.5 \\ -0.5 & 1 \end{bmatrix}$. We consider the additional observer-like system (B.5) and our objective is to check if, for any choice of the additional gain $L_2 \in \mathbb{R}^{2\times 1}$, there exists $\Lambda_2^\star \in \mathbb{R}$ such that (B.33) is satisfied. We define $L_2 := [l_1\ l_2]^\top$ and we have

$$A - L_2 C = \begin{bmatrix} -l_1 & 1 \\ -l_2 & 0 \end{bmatrix} \tag{B.38}$$

Following similar steps as in Section B.3.2, for this example (B.33) results

$$\begin{bmatrix} -l_1+l_2 & 0.5l_1-l_2+0.5 \\ 0.5l_1-l_2+0.5 & -1 \end{bmatrix} \leqslant \begin{bmatrix} -2+\Lambda_2^\star & 0 \\ 0 & -1 \end{bmatrix}, \tag{B.39}$$

which is equivalent to

$$\begin{bmatrix} -l_1+l_2+2-\Lambda_2^\star & 0.5l_1-l_2+0.5 \\ 0.5l_1-l_2+0.5 & 0 \end{bmatrix} \leqslant 0. \tag{B.40}$$

The matrix in (B.40) is negative semi-definite if and only if all its eigenvalues are non-positive. From (B.40), we see that this is possible only if $l_2 = 0.5(1+l_1)$ and all different choices of the gain L_2 do not satisfy condition (B.40) no matter the value of $\Lambda_2^\star \in \mathbb{R}$. Thus, in this example, condition (B.33) cannot be satisfied for any choice of the additional mode gain $L_2 \in \mathbb{R}^{2\times 1}$.

B.4 Discounted costs

In this section we generalize the results presented in Section B.3 considering discounted costs. For this reason, we generalize the state estimation error cost (B.8), which is now defined as, for any $e_k \in \mathscr{L}_{\mathbb{R}^{n_x}}$ initialized at $e_k(0) = e_0 \in \mathbb{R}^{n_x}$, for any $t \in \mathbb{R}_{\geqslant 0}$, $k \in \{1,2\}$,

$$\tilde{W}_k(t) := e_k(t)^\top P e_k(t) + \int_0^t e^{-\nu(t-s)} e_k(s)^\top (Q-\nu P) e_k(s) ds, \tag{B.41}$$

where P, Q come from (B.4) and $\nu \in \mathbb{R}_{\geqslant 0}$ is a design parameter selected such that $Q-\nu P$ is positive definite. Note that, when $\nu = 0$, we recover the state estimation error cost in (B.8).

Similarly, we define the discounted output estimation error cost as for any $e_{y_k} \in \mathscr{L}_{\mathbb{R}^{n_y}}$, for any $t \in \mathbb{R}_{\geqslant 0}$, $k \in \{1,2\}$,

$$\tilde{J}_k(t) := \int_0^t e^{-\nu(t-s)} e_{y_k}(s)^\top \Lambda_k^\star e_{y_k}(s) ds, \tag{B.42}$$

with $\Lambda_k^\star \in \mathbb{R}^{n_y \times n_y}$, $k \in \{1,\dots,N+1\}$ and $\nu \in \mathbb{R}_{\geqslant 0}$ from (B.41).

In the next theorem we generalize the result of Theorem B.1 by considering the discounted costs.

Theorem B.3. *Consider system* (B.1)*, the nominal observer* (B.2) *and the observer-like system* (B.5) *with $e_k(0) = e_0 \in \mathbb{R}^{n_x}$, for all $k \in \{1,2\}$. Given $L_2 \in \mathbb{R}^{n_x \times n_y}$ for the additional mode, if there exists $\Lambda_2^\star \in \mathbb{R}^{n_y \times n_y}$ such that*

$$(A-L_2C)^\top P + P(A-L_2C) = -Q + C^\top \Lambda_2^\star C \tag{B.43}$$

is satisfied with P and Q from (B.4)*. Then, for any $t \in \mathbb{R}_{\geqslant 0}$, $\tilde{J}_1(t) - \tilde{J}_2(t) = \tilde{W}_1(t) - \tilde{W}_2(t)$.* □

Proof. Let $U(e_k,t) := e^{\nu t} e_k^\top P e_k$, for all $e_k \in \mathbb{R}^{n_x}$, $k \in \{1,2\}$, where P comes from (B.4) and $\nu \in \mathbb{R}_{\geqslant 0}$ from (B.41). Then, from (B.3) and (B.6), we have

$$\langle \nabla U(e_k,t), ((A-L_kC)e_k, 1)\rangle = \nu e^{\nu t} e_k^\top P e_k + e^{\nu t} e_k^\top \left((A-L_kC)^\top P + P(A-L_kC)\right) e_k. \tag{B.44}$$

Using (B.4), we have

$$\begin{aligned}\langle \nabla U(e_1,t),((A-L_1C)e_1,1)\rangle &= \nu e^{\nu t} e_1^\top P e_1 + e^{\nu t} e_1^\top \left((A-L_1C)^\top P + P(A-L_1C)\right) e_1 \\ &= \nu e^{\nu t} e_1^\top P e_1 - e^{\nu t} e_1^\top Q e_1 + e^{\nu t} e_1^\top C^\top \Lambda_1^\star C e_1.\end{aligned} \tag{B.45}$$

Let e_1 be a solution to system (B.3), then (B.45) implies, for any $t \in \mathbb{R}_{\geqslant 0}$,

$$\frac{d}{dt} U(e_1(t),t) = \nu e^{\nu t} e_1(t)^\top P e_1(t) - e^{\nu t} e_1(t)^\top Q e_1(t) + e^{\nu t} e_1(t)^\top C^\top \Lambda_1^\star C e_1(t). \tag{B.46}$$

Integrating (B.46), we obtain, for all $t \in \mathbb{R}_{\geqslant 0}$,

$$\begin{aligned}&U(e_1(t),t) - U(e_1(0),0) + \int_0^t e^{\nu s} e_1(s)^\top Q e_1(s) ds - \int_0^t \nu e^{\nu s} e_1(s)^\top P e_1(s) ds \\ &\quad = \int_0^t e^{\nu s} e_1(s)^\top C^\top \Lambda_1^\star C e_1(s) ds,\end{aligned} \tag{B.47}$$

which implies, using the definition of U and e_{y_1},

$$\begin{aligned}&e^{\nu t} e_1(t)^\top P e_1(t) - e_1(0)^\top P e_1(0) + \int_0^t e^{\nu s} e_1(s)^\top Q e_1(s) ds - \int_0^t \nu e^{\nu s} e_1(s)^\top P e_1(s) ds \\ &\quad = \int_0^t e^{\nu s} e_{y_1}(s)^\top \Lambda_1^\star e_{y_1}(s) ds.\end{aligned} \tag{B.48}$$

Multiplying (B.48) by $e^{-\nu t}$, we have

$$\begin{aligned}&e_1(t)^\top P e_1(t) - e^{-\nu t} e_1(0)^\top P e_1(0) + \int_0^t e^{-\nu(t-s)} e_1(s)^\top Q e_1(s) ds - \int_0^t \nu e^{-\nu(t-s)} e_1(s)^\top P e_1(s) ds \\ &\quad = \int_0^t e^{-\nu(t-s)} e_{y_1}(s)^\top \Lambda_1^\star e_{y_1}(s) ds,\end{aligned} \tag{B.49}$$

which is equivalent to

$$\begin{aligned}&e_1(t)^\top P e_1(t) - e^{-\nu t} e_1(0)^\top P e_1(0) + \int_0^t e^{-\nu(t-s)} e_1(s)^\top (Q - \nu P) e_1(s) ds \\ &\quad = \int_0^t e^{-\nu(t-s)} e_{y_1}(s)^\top \Lambda_1^\star e_{y_1}(s) ds.\end{aligned} \tag{B.50}$$

Using (B.41) and (B.42), (B.50) is equivalent to

$$\tilde{W}_1(t) - e^{-\nu t} e_1(0)^\top P e_1(0) = \tilde{J}_1(t). \tag{B.51}$$

Pick $L_2 \in \mathbb{R}^{n_x \times n_y}$ and $\Lambda_2^\star \in \mathbb{R}^{n_y \times n_y}$ such that (B.43) is satisfied with P and Q from (B.4). Then, following similar steps as for the nominal observer, from (B.44) we obtain, for all $t \in \mathbb{R}_{\geqslant 0}$,

$$\tilde{W}_2(t) - e^{-\nu t} e_2(0)^\top P e_2(0) = \tilde{J}_2(t). \tag{B.52}$$

Since $e_1(0) = e_2(0) = e_0 \in \mathbb{R}^{n_x}$, from (B.51) and (B.52) we have $\tilde{W}_1(t) - \tilde{J}_1(t) = \tilde{W}_2(t) - \tilde{J}_2(t)$, for all $t \in \mathbb{R}_{\geqslant 0}$, which is equivalent to

$$\tilde{J}_1(t) - \tilde{J}_2(t) = \tilde{W}_1(t) - \tilde{W}_2(t), \tag{B.53}$$

for all $t \in \mathbb{R}_{\geqslant 0}$. This concludes the proof. ■

Theorem B.3 shows that, even when considering discounted estimation error costs (B.41) and (B.42), when condition (B.43) is satisfied, than, better (worse) performance with respect to the discounted output estimation error cost (B.42) implies better (worse) performance also in terms of the discounted state estimation error cost (B.41). Moreover, since conditions (B.43) and (B.9) are equivalent, in view of the developments presented in Section B.3.2, the freedom introduced by $\Lambda_2^\star \in \mathbb{R}^{n_y \times n_y}$ is not always enough to satisfy condition (B.43) for any choice of the gain $L_2 \in \mathbb{R}^{n_y \times n_x}$ for the observer-like system (B.5). However, by applying the results in Proposition B.1, we have that, when both the nominal observer (B.2) and the observer-like system (B.5) are infinite gain margin observers, i.e., $L_k = P^{-1}C^\top \Lambda_k$, for $k \in \{1, 2\}$, then, there always exists $\Lambda_2^\star \in \mathbb{R}^{n_y \times n_y}$ such that condition (B.43) is satisfied and thus we can relate the estimation performance given by the discounted output estimation costs with the estimation performance expressed in terms of the discounted state estimation error costs. Finally, similarly to Section B.3.4, condition (B.43) can be relaxed to enlarge the class of gains satisfying it. However, in this case, if the observer-like system (B.5) has better performance in terms of the output estimation error cost with respect to the nominal observer (B.2), then, it has better performance also in terms of a state estimation error cost, but the opposite is not necessarily true.

B.5 Conclusions and perspectives

In this appendix, we have presented some preliminary results on the relationship between a quadratic output estimation error cost, which can be evaluated on-line, and a quadratic state estimation error cost, which is the one we are interested on when considering the estimation performance of an observer. In particular, we provide a condition that, if satisfied, guarantees that better (worse) performance with respect to a (discounted) output estimation error cost implies better (worse) performance also with respect to a (discounted) state estimation error cost. Moreover, we have shown via a counterexample that this condition is not always satisfied, but it is possible to guarantee it in the case of infinite gain margin observers, which, however, are not the only possible cases satisfying the condition. In addition, for a larger class of observers gains, weaker results, but still insightful, have been proven by relaxing the condition.

We believe that the results presented in this appendix are only the starting point to understand the relationship between output estimation error costs and state estimation error costs. Indeed, in this notes we have considered unperturbed linear time-invariant systems, and it will be interesting including also external unknown disturbances and measurement noise. Moreover, extending the current thoughts to nonlinear systems is definitely a non-trivial interesting future work direction. Finally, to compare the output and the state estimation performance other approaches can be envisioned,

which may depend on the detectability gramian or other detectability properties.

Appendix C

Résumé détaillé

C.1 Estimation d'état

Les systèmes dynamiques sont des objets mathématiques utilisés pour décrire l'évolution de variables dans le temps. En particulier, un système dynamique peut être utilisé pour modéliser une série de systèmes artificiels ou naturels, tels que les circuits électroniques, les structures mécaniques, les systèmes thermodynamiques, les systèmes biologiques, etc. Ces modèles sont généralement représentés par un ensemble d'équations différentielles (on parle alors de *systèmes dynamiques à temps continu*), ou d'équations aux différences (on parle alors de *systèmes dynamiques à temps discret*), qui décrivent l'évolution de ce que l'on appelle les *variables d'état*, représentant le plus souvent des quantités physiques. En général, ces modèles mathématiques dépendent de certains signaux externes, appelés *entrées du système*, qui influencent l'évolution de l'état du système. En outre, des capteurs peuvent être utilisés pour mesurer une combinaison (non linéaire) des états du système, appelée *mesures de sortie*. Le modèle mathématique de la mesure de la sortie est donné par une fonction statique.

La connaissance de l'état interne d'un système dynamique est essentielle dans de nombreuses applications techniques. En effet, elle est très utile, par exemple, pour construire des contrôleurs, qui sont des algorithmes utilisés pour générer des signaux d'entrée afin de contrôler l'évolution des états du système. En outre, la connaissance de l'état du système peut être cruciale pour obtenir des informations en temps réel à des fins de surveillance ou de prise de décision, voir par exemple [1,2] et les références qui y figurent. Une façon d'obtenir ces informations est de mesurer directement ces variables en plaçant des capteurs sur le système physique. Malheureusement, dans de nombreux cas, toutes les variables d'état ne peuvent pas être mesurées directement par des capteurs en raison d'obstacles technologiques, comme l'état de charge d'une batterie dans [3] ou les concentrations d'ammonium, de nitrate et de nitrite dans les processus de boues activées dans [4]. En outre, dans de nombreuses applications, le nombre et le type de capteurs que nous pouvons utiliser sont limités pour des raisons de coût. Par conséquent, l'état interne d'un système dynamique, que nous désignons par x, doit être estimé à partir de la connaissance du modèle mathématique du système et des mesures

disponibles telles que l'entrée u et la sortie y du système. Pour ce faire, nous concevons un algorithme d'estimation, qui prend la forme d'un système dynamique, appelé *observateur*, dont la sortie est une estimation de l'état du système et est désignée par $\hat{x}$. Notez que, puisque ce système dynamique dépend des mesures disponibles, il n'est pas toujours possible de concevoir un observateur pour estimer l'état du système. En effet, un tel algorithme d'estimation n'est pertinent que si les mesures contiennent suffisamment d'informations pour reconstruire de manière unique l'état du système. Cette propriété essentielle est appelée *détectabilité*, voir par exemple [5]. Lorsque le système est détectable, l'objectif est de concevoir ce système dynamique de manière à ce que l'erreur d'estimation, qui correspond à la différence entre l'état inconnu du système et l'estimation de l'état générée par l'observateur, et qui donne donc une indication de la qualité de l'estimation, converge vers l'origine lorsque le temps tends vers l'infini. Cela implique que l'estimation de l'état produite par l'observateur coïncide, après un temps fini ou infini, avec l'état inconnu du système et que l'observateur estime donc correctement l'état du système.

Comme indiqué précédemment, la conception de cet algorithme d'estimation est basée sur un modèle mathématique de la dynamique du système, qui présente pratiquement toujours des incertitudes ou est affecté par des perturbations inconnues. En outre, les mesures de sortie collectées par les capteurs sont généralement affectées par un bruit de mesure. Toutes ces entrées exogènes sont généralement inconnues et ne peuvent donc pas être utilisées pour la conception de l'observateur, qui doit en conséquence être robuste à ces perturbations dans le sens où les perturbations et le bruit de mesure n'affectent pas de manière significative l'estimation de l'état de l'observateur. En particulier, dans ce cas, la conception de l'observateur a pour objectif de garantir que l'erreur d'estimation converge vers un voisinage de l'origine, dont la « taille » dépend de la norme de ces perturbations. En effet, notons qu'en raison des perturbations et du bruit de mesure, il n'est pas possible d'obtenir une estimation (asymptotique) exacte de l'état en général, mais il est souhaitable de générer une estimation avec des garanties de ne pas être trop éloigné de l'état réel du système. En particulier, pour être un observateur, un algorithme d'estimation doit garantir que l'erreur d'estimation de l'état, désignée par $e := x - \hat{x}$, est

— **stable** dans le sens où la trajectoire de l'erreur d'estimation reste « petite » si l'erreur initiale est « petite »,

— **convergeant vers (un voisinage de) l'origine** quand le temps augmente,

— **robuste aux perturbations et au bruit de mesure**.

Une propriété qui englobe toutes ces caractéristiques souhaitées du comportement de l'erreur d'estimation de l'état est la *propriété de stabilité entrée-état* de l'erreur d'estimation par rapport aux perturbations et au bruit chapitre 2.2.2 pour plus de détails.

Dans cette thèse, nous nous concentrons sur les systèmes à temps continu de dimension finie de la forme

$$\begin{aligned} \dot{x} &= f_p(x,u,v) \\ y &= h(x,w), \end{aligned} \tag{C.1}$$

où $x \in \mathbb{R}^{n_x}$ est l'état du système, qui est inconnu et doit être estimé, $u \in \mathbb{R}^{n_u}$ est l'entrée mesurée, $y \in \mathbb{R}^{n_y}$ est la sortie mesurée par les capteurs, $v \in \mathbb{R}^{n_v}$ est une entrée de perturbation non mesurée et $w \in \mathbb{R}^{n_w}$ est un bruit de mesure inconnu avec $n_x, n_y \in \mathbb{Z}_{>0}$, et $n_u, n_v, n_w \in \mathbb{Z}_{\geqslant 0}$. La classe d'observateurs à temps continu pour le système (C.1) étudiée dans cette thèse prend la forme suivante

$$\begin{aligned} \dot{z} &= f_o(z, u, y, \hat{y}), \\ \hat{x} &= \psi(z) \\ \hat{y} &= h(\hat{x}, 0), \end{aligned} \tag{C.2}$$

où $z \in \mathbb{R}^{n_z}$ est l'état de l'observateur, avec $n_z \geqslant n_x$, $\hat{x} \in \mathbb{R}^{n_x}$ est l'estimation de l'état et $\hat{y}$ est l'estimation de la sortie. Notons que, dans cette thèse, nous considérons des observateurs dont la dimension de l'état est au moins aussi grande que l'état du système, à savoir $n_z \geqslant n_x$. Plus de détails et d'informations sur les systèmes (C.1) et (C.2) sont fournis dans le chapitre 2.2.1.

La conception d'observateurs de la forme (C.2) pour estimer l'état du système (C.1) avec les propriétés de stabilité, de convergence et de robustesse souhaitées est un sujet de recherche important en automatique, cf. [5, 8] pour des études sur le sujet. En particulier, selon la structure du système dynamique, différentes techniques de conception peuvent être adoptées. Le point de départ de la plupart des résultats de cette thèse est la connaissance d'un observateur entrée-état stable. Cela implique que son erreur d'estimation est stable et converge vers un voisinage de l'origine, dont la taille dépend de la norme des perturbations. Comme le montre par exemple [5, 9], il existe dans la littérature de nombreuses techniques de conception d'observateurs satisfaisant cette propriété pour les systèmes dynamiques linéaires et non linéaires. Cependant, plusieurs problèmes méthodologiques majeurs restent ouverts. En particulier, l'observateur (C.2) nécessite la connaissance des mesures de sortie en flux continu. Cependant, ce n'est pas toujours le cas dans les applications pratiques, où les données de sortie peuvent être communiquées sporadiquement du système à l'observateur via un réseau numérique, dans le cas où les capteurs du système et l'observateur ne sont pas situés au même endroit. Plusieurs travaux ont abordé ce sujet dans la littérature, voir par exemple, [10–30], mais il reste encore beaucoup à faire, comme nous l'expliquerons plus loin dans ce chapitre, ainsi que dans les chapitres 3 et 4. D'autre part, même si l'observateur a accès à la mesure de sortie en continu, la propriété de stabilité entrée-état garantit une propriété de stabilité robuste de l'erreur d'estimation, mais elle n'est pas toujours satisfaisante en ce qui concerne les performances en termes de vitesse de convergence et de taille de la borne ultime due aux perturbations et au bruit de mesure. Cela pose la question du réglage des observateurs non linéaires afin de garantir une propriété de convergence robuste ainsi que des performances satisfaisantes. Certaines techniques sont évidemment disponibles dans la littérature à cette fin, mais pas pour les systèmes non linéaires généraux, pour autant que nous le sachions. Dans le chapitre 5, ainsi que plus loin dans ce chapitre, nous donnons plus de détails sur la littérature. Dans cette thèse, nous nous concentrons sur ces deux questions ouvertes et nous proposons des solutions en exploitant des techniques hybrides, c'est-à-dire des systèmes qui présentent des dynamiques à la fois à temps continu et à temps discret.

C.2 Systèmes dynamiques hybrides

Dans la théorie classique du contrôle, il est commun de modéliser les systèmes dynamiques soit à l'aide d'équations (ou d'inclusions) différentielles, ce qui permet d'obtenir des « systèmes dynamiques à temps continu », soit à l'aide d'équations (ou d'inclusions) aux différences, ce qui permet d'obtenir des « systèmes dynamiques à temps discret ». Cependant, de nombreux systèmes physiques présentent une combinaison d'évolution en temps continu et de mises à jour en temps discret, tels que les systèmes mécaniques, qui évoluent dans le monde physique en temps continu, mais sont contrôlés par un ordinateur numérique, ou les systèmes mécaniques subissant des impacts, comme pour l'exemple classique de la balle rebondissante [31]. D'autres exemples de systèmes présentant des dynamiques à la fois continues et discrètes sont les systèmes biologiques capables de produire des comportements synchronisés, ce qui implique que leur dynamique en temps continu est affectée par des réinitialisations en temps discret, comme l'exemple des lucioles dans [31, Chapitre 1]. Un autre exemple est celui des circuits électriques avec interrupteurs, où l'activation d'un interrupteur peut être modélisée par des réinitialisations instantanées des variables, qui évoluent continuellement, comme l'onduleur DC/AC [32, Exemple 1.1] ou le contrôle de puissance avec un thyristor [31, Exemple 1.3]. Pour modéliser le comportement riche de ces systèmes, les modèles purement à temps continu ou à temps discret ne sont pas suffisants. Par conséquent, pour obtenir une représentation plus complète des phénomènes du monde réel, une combinaison bien connue de comportements à temps continu et à temps discret est ce que l'on appelle les *systèmes dynamiques hybrides*, ou simplement les *systèmes hybrides*. Plusieurs formalismes de modélisation sont disponibles pour les systèmes dynamiques hybrides, voir par exemple [31, 33–36]. Dans cette thèse, nous adoptons le formalisme présenté dans [31]. En particulier, nous considérons l'extension proposée dans [37] (inspirée par [38]), qui permet d'inclure des entrées à temps continu dans le modèle hybride. Ces entrées sont désignées par u et peuvent être utilisées pour représenter des entrées connues, telles que les entrées de contrôle, mais aussi des perturbations inconnues et des bruits de mesure. Dans ce cadre, étant donné deux ensembles $\mathscr{C}, \mathscr{D} \subseteq \mathbb{R}^{n_x} \times \mathbb{R}^{n_u}$, avec $n_x \in \mathbb{Z}_{>0}$ et $n_u \in \mathbb{Z}_{\geqslant 0}$, et deux fonctions à valeur d'ensemble $F : \mathbb{R}^{n_x} \times \mathbb{R}^{n_u} \rightrightarrows \mathbb{R}^{n_x}$ et $G : \mathbb{R}^{n_x} \times \mathbb{R}^{n_u} \rightrightarrows \mathbb{R}^{n_x}$, la dynamique de l'état hybride $x \in \mathbb{R}^{n_x}$ est décrite par

$$\mathscr{H} \; : \; \begin{cases} \dot{x} & \in & F(x,u), & (x,u) \in \mathscr{C}, \\ x^+ & \in & G(x,u), & (x,u) \in \mathscr{D}. \end{cases} \tag{C.3}$$

L'équation (C.3) signifie que l'état hybride $x \in \mathbb{R}^{n_x}$ peut évoluer selon une dynamique à la fois à temps continu et à temps discret, alternant éventuellement ces comportements en fonction de la région de l'espace d'état où se trouve la paire (x,u). Lorsque l'état x et l'entrée u se trouvent dans l'ensemble de flux $\mathscr{C}$, l'état hybride x évolue en temps continu selon la fonction F. De même, lorsque l'état x et l'entrée u se trouvent dans l'ensemble de sauts $\mathscr{D}$, l'état du système est mis à jour conformément à la fonction G. En outre, lorsque la paire d'état et d'entré se trouve à la fois dans les ensembles de flux et de sauts, à savoir $(x,u) \in \mathscr{C} \cap \mathscr{D}$, si l'évolution en temps continu maintient la paire d'état et d'entré dans l'ensemble $\mathscr{C}$, alors l'état hybride évolue soit selon l'inclusion différentielle, soit selon l'inclusion

différentielle dans (C.3). Par conséquent, l'équation (C.3) décrit une dynamique de système plus riche que les équations (ou inclusions) différentielles ou les équations (ou inclusions) aux différences.

Les techniques hybrides se sont avérées très efficaces pour concevoir des contrôleurs. Par exemple, les contrôleurs sont généralement mis en œuvre par du matériel numérique et des ordinateurs, mais ils sont utilisés pour contrôler des installations physiques, qui sont naturellement décrites par des modèles à temps continu, ce qui conduit à des systèmes dynamiques hybrides. En outre, le comportement plus riche donné par le mélange de dynamiques à temps continu et à temps discret a été exploité dans différents contextes de contrôle, voir par exemple [32] et les références qui y sont citées, où les outils hybrides ont démontré leur pertinence et leur force pour surmonter les limitations des contrôleurs purement à temps continu ou à temps discret et ont ainsi permis de résoudre des problèmes insolubles à l'aide des techniques classiques de l'automatique. De même, il devrait être possible d'exploiter la puissance des outils hybrides dans le contexte de l'estimation d'état, mais cela a été moins exploré dans la littérature. Dans ce cas, nous parlons de la synthèse d'observateurs hybrides, qui consiste donc à concevoir des algorithmes d'estimation décrits par des dynamiques à la fois continues et à temps discret. Notons que nous pouvons également concevoir un observateur hybride pour estimer l'état d'un système dynamique à temps continu si la structure du système, l'objectif d'estimation ou l'approche de conception de l'observateur conduisent à une modélisation hybride. En particulier, nous pouvons classer les observateurs hybrides en trois groupes principaux, comme résumé ci-dessous.

— **Modèle de système hybride.** Comme indiqué précédemment, de nombreux systèmes physiques et techniques présentent un comportement hybride et sont donc bien décrits à l'aide de modèles de systèmes hybrides. Dans ce cas, pour estimer l'état hybride, il convient de concevoir un observateur présentant une dynamique à la fois continue et à temps discret, c'est-à-dire un observateur hybride, voir par exemple [39, 40].

— **Connexion hybride entre le système et l'observateur.** Dans de nombreuses applications, le système et l'observateur ne sont pas situés au même endroit et les mesures de sortie sont transmises de l'usine à l'observateur par l'intermédiaire d'un réseau numérique. Par conséquent, l'observateur ne reçoit les données de sortie qu'à certains moments à temps discret, et le système global peut donc être décrit comme un système hybride, cf. [12, 41].

— **Performance de l'estimation.** Les techniques hybrides peuvent être utilisées pour l'estimation également à des fins de performance. Par exemple, même si le système a une dynamique à temps continu et que le cadre permet de concevoir un observateur à temps continu pour estimer l'état du système, des dynamiques à temps discret peuvent être introduites dans la conception de l'observateur afin d'exploiter la puissance des outils hybrides et la dynamique hybride plus riche pour améliorer les performances de l'estimation, voir par exemple [42, 43].

Les résultats présentés dans cette thèse appartiennent aux deuxième et troisième catégories. Nous expliquons plus en détail dans la suite les deux études de cas considérées dans ce manuscrit.

C.3 Motivation et contributions

Dans cette thèse, nous visons à montrer l'efficacité des techniques hybrides pour résoudre deux problèmes importants d'estimation d'état.

C.3.1 Estimation événementielle

Motivation

Comme indiqué précédemment, dans de nombreuses applications, le système et l'observateur ne sont pas situés au même endroit et, par conséquent, les mesures de sortie sont transmises du système à l'observateur par l'intermédiaire d'un réseau numérique. L'observateur n'a alors pas accès à la sortie mesurée en permanence, mais seulement à certains moments d'échantillonnage. Dans ce cadre, des systèmes hybrides apparaissent naturellement puisque le système et l'observateur évoluent en temps continu, alors que chaque transmission de sortie sur le réseau peut être modélisée comme un événement à temps discret. L'observateur non linéaire général (C.2), pour lequel diverses techniques de conception issues de la littérature peuvent être adoptées afin d'obtenir une propriété de convergence de l'erreur d'estimation, suppose la connaissance de l'ensemble de la sortie mesurée en temps continu. La politique choisie pour déclencher une transmission sur le réseau a un impact sur la vitesse de convergence, la robustesse de l'estimation ainsi que sur la quantité de communications.

Trois approches principales ont été proposées dans la littérature pour générer les instants de transmission. La première, appelée *stratégie à déclenchement temporel*, voir, par exemple, [11, 12, 44–46], consiste à déclencher une nouvelle transmission en fonction du temps écoulé depuis la dernière communication. Un exemple classique simple de la stratégie à déclenchement temporel est l'échantillonnage périodique, où la distance temporelle entre deux transmissions consécutives est constante. L'un des inconvénients potentiels du paradigme du déclenchement en fonction du temps est qu'il peut générer plus de transmissions qu'il n'en faut pour effectuer l'estimation, ce qui entraîne un gaspillage des ressources utilisées. En effet, si la sortie reste à peu près constante, il n'est pas nécessaire de déclencher une nouvelle transmission et donc d'envoyer une nouvelle mesure de sortie à l'observateur, puisqu'il dispose déjà de données de sortie pratiquement identiques. En contrepartie, lorsque la sortie change rapidement, l'observateur a besoin des informations mesurées plus fréquemment. Par conséquent, des approches qui ne sont pas basées sur le temps, mais sur la nécessité d'une nouvelle transmission de données de sortie ont été envisagées dans la littérature. En particulier, en concevant un observateur capable de prédire quand il a besoin de nouvelles données, *stratégies d'auto-déclenchement*, voir par exemple [47, 48], ont été proposées, où l'algorithme d'estimation demande une nouvelle transmission quand il en a besoin. Cette stratégie de communication est très utile dans les applications où la sortie du système ne peut pas être surveillée en continu, puisqu'elle n'est mesurée qu'à certains instants à temps discret. Cependant, la stratégie d'auto-déclenchement nécessite souvent de nombreuses transmissions. En outre, elle ne surveille pas la sortie du système et, par conséquent, elle est généralement plus lente pour détecter les changements rapides sur les mesures ou les perturbations sur les données mesurées dues au bruit. Par conséquent, lorsque la sortie mesurée est surveillée en permanence et que l'objectif consiste à décider quand une transmission

doit être déclenchée sur le réseau, les informations fournies par les mesures de sortie peuvent être exploitées pour générer les instants de transmission. Dans ce contexte, une autre approche puissante pour générer les instants de transmission est la *stratégie événementielle*, voir par exemple, [15–30]. Dans ce cas, une règle de déclenchement basée sur les événements surveille la mesure du système et/ou l'état de l'observateur et décide quand une transmission de sortie doit être déclenchée afin de réduire le nombre de transmissions sur le réseau, tout en garantissant une bonne performance d'estimation. Dans ce contexte, la majorité des travaux sur l'estimation événementielle dans la littérature proposent une règle de déclenchement qui dépend de l'estimation de l'état de l'observateur et, par conséquent, nécessite la mise en œuvre d'une copie locale de l'estimateur dans le capteur, voir par exemple [15–21]. Un inconvénient possible de cette approche est que le capteur doit disposer de capacités de calcul suffisantes, ce qui n'est pas toujours le cas dans la pratique, en particulier pour les systèmes à grande échelle ou les dynamiques hautement non linéaires. Pour pallier cet inconvénient, une solution consiste à concevoir une règle de déclenchement basée sur les événements qui s'appuie uniquement sur les mesures de sortie du capteur. Des solutions suivant cette approche ont été proposées dans la littérature, voir par exemple [22–29], où la stratégie de déclenchement est uniquement basée sur une condition statique impliquant la sortie mesurée et sa (ses) valeur(s) antérieure(s) transmise(s). Toutefois, de telles règles de déclenchement statiques peuvent générer un grand nombre de transmissions. Par conséquent, dans le but de réduire la quantité de transmissions sur le réseau, sans nécessiter une capacité de calcul importante sur le capteur, nous proposons dans cette thèse une approche dynamique déclenchée par un événement, basée uniquement sur la sortie mesurée et la dernière valeur de sortie transmise.

Contributions

L'objectif de la première partie de cette thèse est de concevoir une nouvelle règle dynamique de déclenchement d'événement pour décider quand une donnée de sortie doit être transmise du système à l'observateur via un réseau numérique, afin de réduire le nombre de transmissions, tout en continuant à assurer une bonne performance d'estimation. En particulier, la règle de déclenchement que nous concevons dépend uniquement de la mesure de sortie actuelle et de la dernière valeur de sortie transmise. Elle ne repose donc pas sur une copie de l'observateur, ce qui pourrait s'avérer prohibitif en termes de calcul pour le capteur. Au lieu de cela, inspiré par les règles de déclenchement dynamique utilisées dans la littérature de contrôle événementiel [49–52], nous introduisons une variable scalaire supplémentaire qui aide à réduire le nombre de communications sur le réseau et à garder le calcul requis simple.

Les résultats sont d'abord présentés pour des systèmes linéaires non perturbés invariants dans le temps et sont ensuite généralisés en considérant des systèmes non linéaires perturbés généraux et un cadre décentralisé, où les capteurs sont regroupés en N nœuds et où chaque nœud décide quand ses données mesurées sont transmises à l'observateur indépendamment des autres. Le scénario considéré est donc très général. Dans les deux cas, nous avons modélisé le système global comme un système hybride, où un saut correspond à une transmission de sortie, et nous établissons une propriété de stabilité pour l'erreur d'estimation. Par ailleurs, nous prouvons l'existence d'un temps

positif minimum entre deux transmissions de chaque nœud de capteur, ce qui est essentiel pour la mise en œuvre pratique étant donné que le matériel numérique moderne ne peut pas mettre en œuvre des échantillonnages infiniment rapides. Nous garantissons également l'absence d'échantillonnage lorsque la sortie reste dans un petit voisinage d'une constante et que, par conséquent, l'observateur n'a pas besoin de cette information pour obtenir une bonne estimation, ce qui constitue un avantage par rapport aux stratégies à déclenchement temporel. De plus, nous montrons comment les résultats présentés peuvent être étendus au cas où les mesures de sortie sont affectées par un bruit de mesure additif et au cas où l'entrée du système est également transmise sur un réseau numérique, et donc l'observateur n'a accès à l'entrée qu'à certains instants à temps discret, qui peuvent être différents des instants de transmission de la sortie. Enfin, l'efficacité de la technique proposée est démontrée par des exemples numériques.

C.3.2 Améliorer la performance de l'estimation

Motivation

L'objectif principal lors de la conception d'un observateur pour estimer l'état d'un système dynamique est d'avoir des garanties que l'erreur d'estimation de l'état converge vers l'origine (ou son voisinage) lorsque le temps tend vers l'infini. Comme nous l'avons mentionné précédemment, de nombreuses techniques sont disponibles dans la littérature pour les systèmes linéaires et non linéaires afin de garantir cette propriété, voir [5, 8]. Cependant, lors de la conception d'un observateur, nous aimerions également assurer une bonne performance d'estimation dans le sens où nous souhaitons les propriétés suivantes.

— **Vitesse de convergence rapide** afin que l'observateur soit en mesure de générer rapidement une bonne estimation de l'état et donc de connaître rapidement les variables non mesurées souhaitées.

— **Robustesse aux perturbations et au bruit de mesure** en ce sens que l'estimation est précise même en présence d'incertitudes du modèle et qu'elle n'est pas trop sensible au bruit de mesure, qui est inévitable dans la pratique.

— **Domaine d'attraction global** pour garantir la propriété de convergence indépendamment de l'initialisation de l'observateur et donc de l'erreur d'estimation initiale, qui est inconnue puisque l'état initial est inconnu.

Idéalement, nous aimerions concevoir un observateur qui satisfasse toutes ces propriétés. Malheureusement, cela est très difficile, voire impossible, car des limitations fondamentales apparaissent, voir [53] dans le contexte des systèmes linéaires. En effet, il existe généralement un compromis entre ces propriétés, ce qui rend le réglage de l'observateur très difficile. De nombreuses techniques de conception d'observateurs dans la littérature consistent à concevoir la dynamique de l'observateur en utilisant une copie du système, puis en ajoutant un terme de correction, souvent appelé terme d'injection de sortie. Ce terme dépend d'un gain (linéaire ou non linéaire) qui multiplie l'erreur d'estimation de la sortie, à savoir la différence entre la sortie mesurée et la sortie estimée. La question du réglage de ce gain pour obtenir de bonnes performances d'estimation est extrêmement difficile.

En effet, typiquement, les observateurs avec de « petits » gains dans leurs termes d'injection de sortie produisent une estimation robuste au bruit de mesure, mais la vitesse de convergence est très lente. Au contraire, un observateur avec une « grande » valeur a généralement une convergence rapide, mais est plus sensible au bruit. Il est à noter que des schémas d'estimation optimaux ont été présentés dans la littérature, mais uniquement dans des contextes spécifiques, comme par exemple le filtre de Kalman bien connu [54] pour les systèmes linéaires affectés par des perturbations gaussiennes additives ayant un impact sur la dynamique et les mesures de sortie.

Pour les systèmes non linéaires et perturbations générales, la conception d'un observateur optimal est très difficile, car elle nécessite la résolution d'équations différentielles partielles complexes. Par conséquent, nous pouvons nous concentrer sur les techniques de conception pour améliorer la performance d'estimation d'un observateur donné. À notre connaissance, les solutions dans cette direction se concentrent sur des classes spécifiques de systèmes, voir par exemple [60–62] pour les systèmes linéaires ou par exemple, [63–70] dans le contexte des observateurs à grand gain, ou se concentrent uniquement sur l'une des propriétés spécifiques souhaitées décrites ci-dessus, comme la robustesse au bruit de mesure dans, par exemple, [9, 71]. En outre, des stratégies de commutation, d'estimation adaptative ou de planification des gains ont été étudiées dans la littérature pour l'estimation, voir par exemple [67, 72–74]. La principale limite de ces travaux est qu'ils considèrent des classes spécifiques de systèmes ou d'observateurs. Pour les systèmes non linéaires généraux à temps continu, une solution pour améliorer la performance de l'estimation est présentée dans [43], où les auteurs ont proposé de passer d'un observateur local à un observateur global pour prendre le meilleur des deux. En effet, un observateur local peut typiquement être réglé pour avoir une bonne robustesse au bruit de mesure et aux perturbations, mais son domaine d'attraction peut être très petit. D'autre part, l'observateur global garantit un domaine d'attraction global et souvent une convergence rapide, mais il est sensible au bruit. Malheureusement, la technique présentée dans [43] n'est pas aisée à mettre en œuvre car la connaissance de diverses propriétés des observateurs est nécessaire.

Une difficulté supplémentaire dans le réglage du gain de l'observateur pour obtenir de bonnes performances avec des garanties de stabilité robustes provient du fait qu'il n'est pas facile de prouver la propriété de convergence de l'erreur d'estimation pour tous les gains convergents possibles. En effet, dans la pratique, il peut exister certains choix de gains de l'observateur qui produisent des erreurs d'estimation convergentes, éventuellement avec de bonnes performances transitoires, en régime permanent ou globales, mais malheureusement, nous ne pouvons assurer aucune garantie de stabilité pour ces choix de gains. Par conséquent, il serait très utile de disposer d'un moyen d'exploiter ces gains dans la conception de l'observateur afin d'améliorer éventuellement les performances des observateurs à convergence garantie. Dans ce contexte, nous pensons qu'il y a un véritable besoin de schémas d'estimation pour les systèmes déterministes non linéaires généraux qui assurent une propriété de stabilité robuste de l'erreur d'estimation et garantissent une bonne performance d'estimation. Dans ce travail, nous proposons une solution basée sur un multi-observateur et l'utilisation de techniques hybrides.

Contributions

En se concentrant sur la question difficile liée à la performance d'estimation des observateurs, nous présentons dans cette thèse un nouveau schéma multi-observateurs hybride général et flexible pour améliorer la performance d'estimation d'un observateur nominal robuste donné conçu pour un système non-linéaire général à temps continu. En particulier, l'observateur nominal est supposé être tel que le système d'erreur d'estimation associé satisfait une propriété de stabilité entrée-état vis-à-vis du bruit de mesure et des perturbations. Comme mentionné précédemment, un large éventail d'observateurs non linéaires dans la littérature satisfait cette propriété, voir [5, 9] et les références qui y figurent. Le multi-observateur est alors construit en ajoutant des systèmes dynamiques supplémentaires en parallèle à l'observateur nominal, qui sont collectivement appelés modes. Ces modes supplémentaires ont la même structure que l'observateur nominal, mais avec des gains différents, qui peuvent être arbitrairement choisis. En effet, nous n'exigeons aucune propriété de stabilité pour ces systèmes. Par conséquent, la liberté et la flexibilité que nous introduisons dans le nombre de modes supplémentaires et dans leurs gains peuvent être utilisées pour répondre à une série de compromis de conception très différents entre la robustesse et la vitesse de convergence. En outre, la liberté dans le choix des gains peut donner lieu à des modes de convergence pour lesquels nous n'avons pas de garantie de stabilité. Inspiré par le « supervisory control » et les techniques d'estimation, voir par exemple [75–79], nous exécutons tous les modes en parallèle et nous évaluons leur performance d'estimation en termes de coûts quadratiques à l'aide de variables dites de surveillance. Sur la base de ces variables, nous concevons une règle de commutation qui sélectionne le "meilleur" mode à chaque instant. Les modes qui ne sont pas sélectionnés à un instant donné restent inchangés ou leurs estimations d'état, ainsi que leurs variables de surveillance, sont réinitialisées à celles du mode sélectionné. Il convient de noter que le système global est un système hybride. En effet, le système non linéaire, tous les modes du multi-observateur et les variables de surveillance évoluent en temps continu, tandis que la commutation du mode sélectionné peut être modélisée comme un saut en temps discret.

Nous prouvons que le schéma d'estimation hybride proposé satisfait à une propriété de stabilité entrée-état vis-à-vis des perturbations et du bruit de mesure. De plus, les performances du schéma hybride multi-observateurs sont au moins aussi bonnes que celles de l'observateur nominal et, sous certaines conditions, nous montrons que la technique proposée améliore strictement les performances d'estimation. Enfin, nous illustrons l'efficacité de l'approche hybride multi-observateurs proposée à l'aide d'exemples numériques. La technique d'estimation présentée est appliquée, en simulation, pour améliorer la performance d'estimation d'un observateur conçu selon une approche polytopique, pour l'estimation de l'état d'une batterie électrochimique au lithium-ion avec un modèle et des valeurs de paramètres standard, pour lesquels la performance d'estimation est extrêmement importante.

Bibliography

[1] A. Radke and Z. Gao, "A survey of state and disturbance observers for practitioners," *American Control Conference,* Minneapolis, USA, pp. 6–11, 2006.

[2] W. Kang, A. J. Krener, M. Xiao, and L. Xu, "A survey of observers for nonlinear dynamical systems," *Data Assimilation for Atmospheric, Oceanic and Hydrologic Applications (Vol. II)*, pp. 1–25, Springer, 2013.

[3] P. Blondel, R. Postoyan, S. Raël, S. Benjamin, and P. Desprez, "Nonlinear circle-criterion observer design for an electrochemical battery model," *IEEE Transactions on Control Systems Technology*, vol. 27, no. 2, pp. 889–897, 2018.

[4] I. Queinnec and C.-S. Gómez-Quintero, "Reduced modeling and state observation of an activated sludge process," *Biotechnology progress*, vol. 25, no. 3, pp. 654–666, 2009.

[5] P. Bernard, V. Andrieu, and D. Astolfi, "Observer design for continuous-time dynamical systems," *Annual Reviews in Control*, vol. 53, pp. 224–248, 2022.

[6] E. D. Sontag, "Input to state stability: Basic concepts and results," in *Nonlinear and Optimal Control Theory*, pp. 163–220, Springer, 2008.

[7] H. Shim and D. Liberzon, "Nonlinear observers robust to measurement disturbances in an ISS sense," *IEEE Transactions on Automatic Control*, vol. 61, no. 1, pp. 48–61, 2015.

[8] G. Besançon, *Nonlinear observers and applications*, vol. 363. Springer, 2007.

[9] D. Astolfi, A. Alessandri, and L. Zaccarian, "Stubborn and dead-zone redesign for nonlinear observers and filters," *IEEE Transactions on Automatic Control*, vol. 66, no. 2, pp. 667–682, 2021.

[10] M. Arcak and D. Nešić, "A framework for nonlinear sampled-data observer design via approximate discrete-time models and emulation," *Automatica*, vol. 40, no. 11, pp. 1931–1938, 2004.

[11] D. Dačić and D. Nešić, "Observer design for wired linear networked control systems using matrix inequalities," *Automatica*, vol. 44, no. 11, pp. 2840–2848, 2008.

[12] R. Postoyan and D. Nešić, "A framework for the observer design for networked control systems," *IEEE Transactions on Automatic Control*, vol. 57, no. 5, pp. 1309–1314, 2011.

[13] P. E. Moraal and J. W. Grizzle, "Observer design for nonlinear systems with discrete-time measurements," *IEEE Transactions on automatic control*, vol. 40, no. 3, pp. 395–404, 1995.

[14] E. Bıyık and M. Arcak, "A hybrid redesign of newton observers in the absence of an exact discrete-time model," *Systems & Control Letters*, vol. 55, no. 6, pp. 429–436, 2006.

[15] K. J. A. Scheres, M. S. T. Chong, R. Postoyan, and W. P. M. H. Heemels, "Event-triggered state estimation with multiple noisy sensor nodes," *IEEE Conference on Decision and Control,* Austin, USA, pp. 558–563, 2021.

[16] L. Li, M. Lemmon, and X. Wang, "Event-triggered state estimation in vector linear processes," *American control conference,* Baltimore, USA, pp. 2138–2143, 2010.

[17] D. Shi, T. Chen, and L. Shi, "Event-triggered maximum likelihood state estimation," *Automatica*, vol. 50, no. 1, pp. 247–254, 2014.

[18] L. Li and M. Lemmon, "Performance and average sampling period of sub-optimal triggering event in event triggered state estimation," *IEEE Conference on Decision and Control and European Control Conference,* Orlando, USA, pp. 1656–1661, 2011.

[19] S. Trimpe, "Stability analysis of distributed event-based state estimation," *IEEE Conference on Decision and Control,* Florence, Italy, pp. 2013–2019, 2014.

[20] H. Yu, J. Shang, and T. Chen, "On stochastic and deterministic event-based state estimation," *Automatica*, vol. 123, p. 109314, 2021.

[21] C. Song, H. Wang, Y. Tian, and G. Zheng, "Event-triggered observer design for output-sampled systems," *Nonlinear Analysis: Hybrid Systems*, vol. 43, p. 101112, 2021.

[22] D. Shi, T. Chen, and M. Darouach, "Event-based state estimation of linear dynamic systems with unknown exogenous inputs," *Automatica*, vol. 69, pp. 275–288, 2016.

[23] J. Huang, D. Shi, and T. Chen, "Robust event-triggered state estimation: A risk-sensitive approach," *Automatica*, vol. 99, pp. 253–265, 2019.

[24] J. Sijs and M. Lazar, "Event based state estimation with time synchronous updates," *IEEE Transactions on Automatic Control*, vol. 57, no. 10, pp. 2650–2655, 2012.

[25] J. Hu, Z. Wang, G.-P. Liu, C. Jia, and J. Williams, "Event-triggered recursive state estimation for dynamical networks under randomly switching topologies and multiple missing measurements," *Automatica*, vol. 115, 2020.

[26] L. Etienne, S. Di Gennaro, and J.-P. Barbot, "Periodic event-triggered observation and control for nonlinear Lipschitz systems using impulsive observers," *International Journal of Robust and Nonlinear Control*, vol. 27, no. 18, pp. 4363–4380, 2017.

[27] L. Etienne and S. Di Gennaro, "Event-triggered observation of nonlinear Lipschitz systems via impulsive observers," *IFAC-PapersOnLine*, vol. 49, no. 18, pp. 666–671, 2016.

[28] L. Etienne, Y. Khaled, S. Di Gennaro, and J.-P. Barbot, "Asynchronous event-triggered observation and control of linear systems via impulsive observers," *Journal of the Franklin Institute*, vol. 354, no. 1, pp. 372–391, 2017.

[29] Y. Tong, D. Tong, Q. Chen, and W. Zhou, "Finite-time state estimation for nonlinear systems based on event-triggered mechanism," *Circuits, Systems, and Signal Processing*, pp. 1–21, 2020.

[30] Y. Niu, L. Sheng, M. Gao, and D. Zhou, "Dynamic event-triggered state estimation for continuous-time polynomial nonlinear systems with external disturbances," *IEEE Transactions on Industrial Informatics*, vol. 17, no. 6, pp. 3962–3970, 2020.

[31] R. Goebel, R. G. Sanfelice, and A. R. Teel, *Hybrid Dynamical Systems: Modeling, Stability, and Robustness*. New Jersey, USA, Princeton University Press, 2012.

[32] R. G. Sanfelice, *Hybrid feedback control*. Princeton University Press, 2021.

[33] D. Liberzon, *Switching in systems and control*, vol. 190. Springer, 2003.

[34] W. M. Haddad, V. S. Chellaboina, and S. G. Nersesov, *Impulsive and Hybrid Dynamical Systems: Stability, Dissipativity, and Control*. Princeton University Press, 2014.

[35] J. Lygeros, C. Tomlin, and S. Sastry, *Hybrid systems: modeling, analysis and control*. Electronic Research Laboratory, University of California, Berkeley, CA, Tech. Rep. UCB/ERL M, 99:6, 2008.

[36] B. Brogliato, "Some perspectives on the analysis and control of complementarity systems," *IEEE Transactions on Automatic Control*, vol. 48, no. 6, pp. 918–935, 2003.

[37] W. P. M. H. Heemels, P. Bernard, K. J. A. Scheres, R. Postoyan, and R. G. Sanfelice, "Hybrid systems with continuous-time inputs: Subtleties in solution concepts and existence properties," *IEEE Conference on Decision and Control,* Austin, USA, pp. 5361–5366, 2021.

[38] C. Cai and A. R. Teel, "Characterizations of input-to-state stability for hybrid systems," *Systems & Control Letters*, vol. 58, no. 1, pp. 47–53, 2009.

[39] P. Bernard and R. G. Sanfelice, "Observer design for hybrid dynamical systems with approximately known jump times," *Automatica*, vol. 141, p. 110225, 2022.

[40] P. Bernard and R. G. Sanfelice, "A local hybrid observer for a class of hybrid dynamical systems with linear maps and unknown jump times," *IEEE Conference on Decision and Control,* Austin, USA, pp. 5362–5367, 2021.

[41] F. Ferrante, F. Gouaisbaut, R. G. Sanfelice, and S. Tarbouriech, "$\mathscr{L}_2$ state estimation with guaranteed convergence speed in the presence of sporadic measurements," *IEEE Transactions on Automatic Control*, vol. 64, no. 8, pp. 3362–3369, 2018.

[42] V. Andrieu, C. Prieur, S. Tarbouriech, and L. Zaccarian, "A hybrid scheme for reducing peaking in high-gain observers for a class of nonlinear systems," *Automatica*, vol. 72, pp. 138–146, 2016.

[43] D. Astolfi, R. Postoyan, and D. Nešić, "Uniting observers," *IEEE Transactions on Automatic Control*, vol. 65, no. 7, pp. 2867–2882, 2019.

[44] Y. Li, S. Phillips, and R. G. Sanfelice, "Robust distributed estimation for linear systems under intermittent information," *IEEE Transactions on Automatic Control*, vol. 63, no. 4, pp. 973–988, 2017.

[45] F. Ferrante, F. Gouaisbaut, R. G. Sanfelice, and S. Tarbouriech, "State estimation of linear systems in the presence of sporadic measurements," *Automatica*, vol. 73, pp. 101–109, 2016.

[46] F. Mazenc, V. Andrieu, and M. Malisoff, "Design of continuous–discrete observers for time-varying nonlinear systems," *Automatica*, vol. 57, pp. 135–144, 2015.

[47] V. Andrieu, M. Nadri, U. Serres, and J.-C. Vivalda, "Self-triggered continuous–discrete observer with updated sampling period," *Automatica*, vol. 62, pp. 106–113, 2015.

[48] D. Rabehi, N. Meslem, and N. Ramdani, "Finite-gain event-triggered interval observers design for continuous-time linear systems," *International Journal of Robust and Nonlinear Control*, vol. 31, no. 9, pp. 4131–4153, 2021.

[49] A. Girard, "Dynamic triggering mechanisms for event-triggered control," *IEEE Transactions on Automatic Control*, vol. 60, no. 7, pp. 1992–1997, 2014.

[50] A. Tanwani, A. Teel, and C. Prieur, "On using norm estimators for event-triggered control with dynamic output feedback," *IEEE Conference on Decision and Control,* Osaka, Japan, pp. 5500–5505, 2015.

[51] P. Tabuada, "Event-triggered real-time scheduling of stabilizing control tasks," *IEEE Transactions on Automatic Control*, vol. 52, no. 9, pp. 1680–1685, 2007.

[52] S. Tarbouriech and A. Girard, "LMI-based design of dynamic event-triggering mechanism for linear systems," *IEEE Conference on Decision and Control,* Miami, USA, pp. 121–126, 2018.

[53] M. M. Seron, J. H. Braslavsky, and G. C. Goodwin, *Fundamental limitations in filtering and control*. Springer Science & Business Media, 2012.

[54] R. E. Kalman and R. S. Bucy, "New results in linear filtering and prediction theory," *Journal of Basic Engineering*, vol. 83, no. 1, pp. 95–108, 1961.

[55] J. B. Rawlings and L. Ji, "Optimization-based state estimation: Current status and some new results," *Journal of Process Control*, vol. 22, no. 8, pp. 1439–1444, 2012.

[56] A. Alessandri, M. Baglietto, and G. Battistelli, "Moving-horizon state estimation for nonlinear discrete-time systems: New stability results and approximation schemes," *Automatica*, vol. 44, no. 7, pp. 1753–1765, 2008.

[57] J. D. Schiller, S. Muntwiler, J. Köhler, M. N. Zeilinger, and M. A. Müller, "A Lyapunov function for robust stability of moving horizon estimation," *IEEE Transactions on Automatic Control*, 2023.

[58] J. D. Schiller and M. A. Müller, "Suboptimal nonlinear moving horizon estimation," *IEEE Transactions on Automatic Control*, vol. 68, no. 4, pp. 2199–2214, 2022.

[59] J. W. Helton and M. R. James, *Extending $\mathscr{H}_\infty$ Control to Nonlinear Systems: Control of Nonlinear Systems to Achieve Performance Objectives*. SIAM, 1999.

[60] Y. Li and R. G. Sanfelice, "A finite-time convergent observer with robustness to piecewise-constant measurement noise," *Automatica*, vol. 57, pp. 222–230, 2015.

[61] H. Ríos and A. R. Teel, "A hybrid fixed-time observer for state estimation of linear systems," *Automatica*, vol. 87, pp. 103–112, 2018.

[62] A. Alessandri and R. G. Sanfelice, "Hysteresis-based switching observers for linear systems using quadratic boundedness," *Automatica*, vol. 136, p. 109982, 2022.

[63] D. Astolfi and L. Marconi, "A high-gain nonlinear observer with limited gain power," *IEEE Transactions on Automatic Control*, vol. 60, no. 11, pp. 3059–3064, 2015.

[64] D. Astolfi, L. Marconi, L. Praly, and A. R. Teel, "Low-power peaking-free high-gain observers," *Automatica*, vol. 98, pp. 169–179, 2018.

[65] K. Esfandiari and M. Shakarami, "Bank of high-gain observers in output feedback control: Robustness analysis against measurement noise," *IEEE Transactions on Systems, Man, and Cybernetics: Systems*, vol. 51, no. 4, pp. 2476–2487, 2019.

[66] J. Bernat and S. Stepien, "Multi-modelling as new estimation schema for high-gain observers," *International Journal of Control*, vol. 88, no. 6, pp. 1209–1222, 2015.

[67] J. H. Ahrens and H. K. Khalil, "High-gain observers in the presence of measurement noise: A switched-gain approach," *Automatica*, vol. 45, no. 4, pp. 936–943, 2009.

[68] M. Farza, A. Ragoubi, S. Hadj Saïd, and M. M'Saad, "Improved high gain observer design for a class of disturbed nonlinear systems," *Nonlinear Dynamics*, vol. 106, pp. 631–655, 2021.

[69] C. Prieur, S. Tarbouriech, and L. Zaccarian, "Hybrid high-gain observers without peaking for planar nonlinear systems," *IEEE Conference on Decision and Control,* Maui, USA, pp. 6175–6180, 2012.

[70] G. Besançon, "High-gain observation with disturbance attenuation and application to robust fault detection," *Automatica*, vol. 39, no. 6, pp. 1095–1102, 2003.

[71] S. Battilotti, "Performance optimization via sequential processing for nonlinear state estimation of noisy systems," *IEEE Transactions on Automatic Control*, vol. 67, no. 2, pp. 2957–2972, 2021.

[72] R. G. Sanfelice and L. Praly, "On the performance of high-gain observers with gain adaptation under measurement noise," *Automatica*, vol. 47, no. 10, pp. 2165–2176, 2011.

[73] N. Boizot, E. Busvelle, and J.-P. Gauthier, "An adaptive high-gain observer for nonlinear systems," *Automatica*, vol. 46, no. 9, pp. 1483–1488, 2010.

[74] B. Laurent and P. Massart, "Adaptive estimation of a quadratic functional by model selection," *Annals of statistics*, pp. 1302–1338, 2000.

[75] M. S. Chong, D. Nešić, R. Postoyan, and L. Kuhlmann, "Parameter and state estimation of nonlinear systems using a multi-observer under the supervisory framework," *IEEE Transactions on Automatic Control*, vol. 60, no. 9, pp. 2336–2349, 2015.

[76] J. P. Hespanha, D. Liberzon, and A. S. Morse, "Hysteresis-based switching algorithms for supervisory control of uncertain systems," *Automatica*, vol. 39, no. 2, pp. 263–272, 2003.

[77] A. S. Morse, "Supervisory control of families of linear set-point controllers-part i. exact matching," *IEEE Transactions on Automatic Control*, vol. 41, no. 10, pp. 1413–1431, 1996.

[78] J. Hespanha, D. Liberzon, A. Stephen Morse, B. D. Anderson, T. S. Brinsmead, and F. De Bruyne, "Multiple model adaptive control. part 2: switching," *International Journal of Robust and Nonlinear Control*, vol. 11, no. 5, pp. 479–496, 2001.

[79] J. Peralez, F. Galuppo, P. Dufour, C. Wolf, and M. Nadri, "Data-driven multi-model control for a waste heat recovery system," *IEEE Conference on Decision and Control,* Jeju Island, South Korea, pp. 5501–5506, 2020.

[80] E. Petri, R. Postoyan, D. Astolfi, D. Nešić, and W. P. M. H. Heemels, "Decentralized event-triggered estimation of nonlinear systems," *Automatica, to appear*.

[81] E. Petri, R. Postoyan, D. Astolfi, D. Nešić, and V. Andrieu, "Hybrid multi-observer for improving estimation performance," Submitted to *IEEE Transactions on Automatic Control*.

[82] E. Petri, T. Reynaudo, R. Postoyan, D. Astolfi, D. Nešić, and S. Raël, "State estimation of an electrochemical lithium-ion battery model: improved observer performance by hybrid redesign," *European Control Conference,* Bucharest, Romania, pp. 2151–2156, 2023.

[83] E. Petri, R. Postoyan, D. Astolfi, D. Nešić, and V. Andrieu, "Towards improving the estimation performance of a given nonlinear observer: a multi-observer approach," *IEEE Conference on Decision and Control,* Cancún, Mexico, pp. 583–590, 2022.

[84] E. Petri, R. Postoyan, D. Astolfi, D. Nešić, and W. P. M. H. Heemels, "Event-triggered observer design for linear systems," *IEEE Conference on Decision and Control,* Austin, USA, pp. 546–551, 2021.

[85] H. K. Khalil, *Nonlinear Systems*, vol. 3. Prentice hall Upper Saddle River, NJ, 2002.

[86] F. H. Clarke, *Optimization and Nonsmooth Analysis*. Philadelphia, USA, Classic in Applied Mathematics vol. 5, SIAM, 1990.

[87] A. Levant, "Higher order sliding modes and arbitrary-order exact robust differentiation," *European Control Conference,* Porto, Portugal, pp. 996–1001, 2001.

[88] F. Lopez-Ramirez, A. Polyakov, D. Efimov, and W. Perruquetti, "Finite-time and fixed-time observer design: Implicit Lyapunov function approach," *Automatica*, vol. 87, pp. 52–60, 2018.

[89] J.-L. Gouzé, A. Rapaport, and M. Z. Hadj-Sadok, "Interval observers for uncertain biological systems," *Ecological modelling*, vol. 133, no. 1-2, pp. 45–56, 2000.

[90] A. Khan, W. Xie, B. Zhang, and L.-W. Liu, "A survey of interval observers design methods and implementation for uncertain systems," *Journal of the Franklin Institute*, vol. 358, no. 6, pp. 3077–3126, 2021.

[91] R. Postoyan and D. Nešić, "On emulated nonlinear reduced-order observers for networked control systems," *Automatica*, vol. 48, no. 4, pp. 645–652, 2012.

[92] P. Van Dooren, "Reduced order observers: A new algorithm and proof," *Systems & Control Letters*, vol. 4, no. 5, pp. 243–251, 1984.

[93] C.-T. Chen, *Linear system theory and design*. Saunders college publishing, 1984.

[94] D. Luenberger, "An introduction to observers," *IEEE Transactions on automatic control*, vol. 16, no. 6, pp. 596–602, 1971.

[95] A. Zemouche, M. Boutayeb, and G. I. Bara, "Observers for a class of lipschitz systems with extension to H_∞ performance analysis," *Systems & Control Letters*, vol. 57, no. 1, pp. 18–27, 2008.

[96] H. Dreef, H. Beelen, and M. Donkers, "LMI-based robust observer design for battery state-of-charge estimation," *IEEE Conference on Decision and Control,* Miami, USA, pp. 5716–5721, 2018.

[97] P. G. Blondel, R. Postoyan, S. Raël, S. Benjamin, and P. Desprez, "Observer design for an electrochemical model of lithium ion batteries based on a polytopic approach," *IFAC-PapersOnLine*, vol. 50, no. 1, pp. 8127–8132, 2017.

[98] K. Reif, F. Sonnemann, and R. Unbehauen, "An EKF-based nonlinear observer with a prescribed degree of stability," *Automatica*, vol. 34, no. 9, pp. 1119–1123, 1998.

[99] S. Bonnabel and J.-J. Slotine, "A contraction theory-based analysis of the stability of the deterministic extended kalman filter," *IEEE Transactions on Automatic Control*, vol. 60, no. 2, pp. 565–569, 2014.

[100] A. J. Krener, "The local convergence of the extended Kalman filter," *arXiv, arXiv:math.OC/0212255 v1*, 2004.

[101] M. Krichman, E. D. Sontag, and Y. Wang, "Input-output-to-state stability," *SIAM Journal on Control and Optimization*, vol. 39, no. 6, pp. 1874–1928, 2001.

[102] E. D. Sontag and Y. Wang, "Output-to-state stability and detectability of nonlinear systems," *Systems & Control Letters*, vol. 29, no. 5, pp. 279–290, 1997.

[103] R. Postoyan, P. Tabuada, D. Nešić, and A. Anta, "A framework for the event-triggered stabilization of nonlinear systems," *IEEE Transactions on Automatic Control*, vol. 60, no. 4, pp. 982–996, 2014.

[104] C. Cai, A. R. Teel, and R. Goebel, "Smooth Lyapunov functions for hybrid systems-part I: Existence is equivalent to robustness," *IEEE Transactions on Automatic Control*, vol. 52, no. 7, pp. 1264–1277, 2007.

[105] A. R. Teel and L. Praly, "A smooth Lyapunov function from a class-estimate involving two positive semidefinite functions," *ESAIM: Control, Optimisation and Calculus of Variations*, vol. 5, pp. 313–367, 2000.

[106] C. M. Kellett and F. R. Wirth, "Variants of two-measure input-to-state stability," *IFAC-PapersOnLine*, vol. 56, no. 1, pp. 7–12, 2023.

[107] J. P. Hespanha, P. Naghshtabrizi, and Y. Xu, "A survey of recent results in networked control systems," *Proceedings of the IEEE*, vol. 95, no. 1, pp. 138–162, 2007.

[108] W. P. M. H. Heemels and N. Van De Wouw, "Stability and stabilization of networked control systems," in *Networked Control Systems*, pp. 203–253, Springer, 2010.

[109] W. P. M. H. Heemels, K. H. Johansson, and P. Tabuada, "An introduction to event-triggered and self-triggered control," *IEEE Conference on Decision and Control,* Maui, USA, pp. 3270–3285, 2012.

[110] M. Abdelrahim, R. Postoyan, J. Daafouz, and D. Nešić, "Robust event-triggered output feedback controllers for nonlinear systems," *Automatica*, vol. 75, pp. 96–108, 2017.

[111] V. Dolk, D. P. Borgers, and W. P. M. H. Heemels, "Output-based and decentralized dynamic event-triggered control with guaranteed $\mathscr{L}_p$-gain performance and Zeno-freeness," *IEEE Transactions on Automatic Control*, vol. 62, no. 1, pp. 34–49, 2016.

[112] T. Liu and Z.-P. Jiang, "Event-based control of nonlinear systems with partial state and output feedback," *Automatica*, vol. 53, pp. 10–22, 2015.

[113] D. Luenberger, "Observers for multivariable systems," *IEEE Transactions on Automatic Control*, vol. 11, no. 2, pp. 190–197, 1966.

[114] W. Wang, R. Postoyan, D. Nešić, and W. P. M. H. Heemels, "Periodic event-triggered control for nonlinear networked control systems," *IEEE Transactions on Automatic Control*, vol. 65, no. 2, pp. 620–635, 2019.

[115] D. P. Borgers and W. P. M. H. Heemels, "Event-separation properties of event-triggered control systems," *IEEE Transactions on Automatic Control*, vol. 59, no. 10, pp. 2644–2656, 2014.

[116] H. He, R. Xiong, H. Guo, and S. Li, "Comparison study on the battery models used for the energy management of batteries in electric vehicles," *Energy Conversion and Management*, vol. 64, pp. 113–121, 2012.

[117] J. Lunze and D. Lehmann, "A state-feedback approach to event-based control," *Automatica*, vol. 46, no. 1, pp. 211–215, 2010.

[118] R. Postoyan, "Commande et costruction d'observateur pour des systèmes non linéaires incertains à données échantillonnées et en réseau," *PhD thesis, Paris 11*, 2009.

[119] A. Isidori, *Nonlinear Control Systems II*. Springer-Verlag, 1999.

[120] R. Postoyan, N. Van de Wouw, D. Nešić, and W. P. M. H. Heemels, "Tracking control for nonlinear networked control systems," *IEEE Transactions on Automatic Control*, vol. 59, no. 6, pp. 1539–1554, 2014.

[121] D. Angeli and E. D. Sontag, "Forward completeness, unboundedness observability, and their Lyapunov characterizations," *System & Control Letters*, vol. 38, no. 4-5, pp. 209–217, 1999.

[122] J. Cortes, "Discontinuous dynamical systems," *IEEE Control systems magazine*, vol. 28, no. 3, pp. 36–73, 2008.

[123] K. J. A. Scheres, R. Postoyan, and W. P. M. H. Heemels, "Event-triggered control in presence of measurement noise: A space-regularization approach," *IEEE Conference on Decision and Control,* Jeju Island, Republic of Korea, pp. 6234–6239, 2020.

[124] W. P. M. H. Heemels, A. Teel, N. Van de Wouw, and D. Nešić, "Networked control systems with communication constraints: Tradeoffs between transmission intervals, delays and performance," *IEEE Transactions on Automatic control*, vol. 55, no. 8, pp. 1781–1796, 2010.

[125] T. Raff, M. Kogel, and F. Allgower, "Observer with sample-and-hold updating for Lipschitz nonlinear systems with nonuniformly sampled measurements," *IEEE American Control Conference,* Seattle, USA, pp. 5254–5257, 2008.

[126] D. Astolfi, P. Bernard, R. Postoyan, and L. Marconi, "Constrained state estimation for nonlinear systems: a redesign approach based on convexity," *IEEE Transactions on Automatic Control*, vol. 67, no. 2, pp. 824–839, 2021.

[127] J. D. Schiller, B. Wu, and M. A. Müller, "A simple suboptimal moving horizon estimation scheme with guaranteed robust stability," *IEEE Control Systems Letters*, vol. 7, pp. 19–24, 2022.

[128] N. Barhoumi, F. Msahli, M. Djemaï, and K. Busawon, "Observer design for some classes of uniformly observable nonlinear hybrid systems," *Nonlinear Analysis: Hybrid Systems*, vol. 6, no. 4, pp. 917–929, 2012.

[129] J. Peralez, M. Nadri, and D. Astolfi, "Neural network-based KKL observer for nonlinear discrete-time systems," *IEEE Conference on Decision and Control,* Cancún, Mexico, pp. 2105–2110, 2022.

[130] A. P. Aguiar, V. Hassani, A. M. Pascoal, and M. Athans, "Identification and convergence analysis of a class of continuous-time multiple-model adaptive estimators," *IFAC Proceedings Volumes*, vol. 41, no. 2, pp. 8605–8610, 2008.

[131] A. P. Aguiar, M. Athans, and A. M. Pascoal, "Convergence properties of a continuous-time multiple-model adaptive estimator," *European Control Conference,* Kos, Greece, pp. 1530–1536, 2007.

[132] T. Meijer, V. Dolk, M. S. Chong, R. Postoyan, B. de Jager, D. Nešić, and W. P. M. H. Heemels, "Joint parameter and state estimation of noisy discrete-time nonlinear systems: A supervisory multi-observer approach," *IEEE Conference on Decision and Control,* Austin, USA, pp. 5163–5168, 2021.

[133] W. Han, H. L. Trentelman, Z. Wang, and Y. Shen, "A simple approach to distributed observer design for linear systems," *IEEE Transactions on Automatic Control*, vol. 64, no. 1, pp. 329–336, 2018.

[134] S. Park and N. C. Martins, "Design of distributed lti observers for state omniscience," *IEEE Transactions on Automatic Control*, vol. 62, no. 2, pp. 561–576, 2016.

[135] L. Wang, J. Liu, and A. S. Morse, "A hybrid observer for estimating the state of a distributed linear system," *Automatica*, vol. 146, p. 110633, 2022.

[136] J. C. Willems, "Deterministic least squares filtering," *Journal of Econometrics*, vol. 118, no. 1-2, pp. 341–373, 2004.

[137] J. Na, G. Herrmann, and K. G. Vamvoudakis, "Adaptive optimal observer design via approximate dynamic programming," *American Control Conference,* Seattle, USA, pp. 3288–3293, 2017.

[138] H. K. Khalil and L. Praly, "High-gain observers in nonlinear feedback control," *International Journal of Robust and Nonlinear Control*, vol. 24, no. 6, pp. 993–1015, 2014.

[139] A. R. Teel and L. Praly, "On assigning the derivative of a disturbance attenuation control Lyapunov function," *Mathematics of Control, Signals and Systems*, vol. 13, no. 2, pp. 95–124, 2000.

[140] J. Szarski, *Differential Inequalities*. Polish Scientific Publisher, Warsaw, Poland, 1965.

[141] J. Meng, G. Luo, M. Ricco, M. Swierczynski, D.-I. Stroe, and R. Teodorescu, "Overview of lithium-ion battery modeling methods for state-of-charge estimation in electrical vehicles," *Applied sciences*, vol. 8, no. 5, p. 659, 2018.

[142] S. Lee, J. Kim, J. Lee, and B. H. Cho, "State-of-charge and capacity estimation of lithium-ion battery using a new open-circuit voltage versus state-of-charge," *Journal of Power Sources*, vol. 185, no. 2, pp. 1367–1373, 2008.

[143] J. K. Barillas, J. Li, C. Günther, and M. A. Danzer, "A comparative study and validation of state estimation algorithms for li-ion batteries in battery management systems," *Applied Energy*, vol. 155, pp. 455–462, 2015.

[144] B. Xia, C. Chen, Y. Tian, W. Sun, Z. Xu, and W. Zheng, "A novel method for state of charge estimation of lithium-ion batteries using a nonlinear observer," *Journal of Power Sources*, vol. 270, pp. 359–366, 2014.

[145] M. Doyle, T. F. Fuller, and J. Newman, "Modeling of galvanostatic charge and discharge of the lithium/polymer/insertion cell," *Journal of the Electrochemical Society*, vol. 140, no. 6, p. 1526, 1993.

[146] T. F. Fuller, M. Doyle, and J. Newman, "Simulation and optimization of the dual lithium ion insertion cell," *Journal of the Electrochemical Society*, vol. 141, no. 1, p. 1, 1994.

[147] D. Di Domenico, A. Stefanopoulou, and G. Fiengo, "Lithium-ion battery state of charge and critical surface charge estimation using an electrochemical model-based extended kalman filter," *Journal of Dynamic Systems, Measurement, and Control*, vol. 132, no. 6, 2010.

[148] E. Planté, R. Postoyan, S. Raël, Y. Jebroun, S. Benjamin, and D. M. Reyes, "Multiple active material lithium-ion batteries: finite-dimensional modeling and constrained state estimation," *IEEE Transactions on Control Systems Technology*, 2022.

[149] S. Raël and M. Hinaje, "Using electrical analogy to describe mass and charge transport in lithium-ion batteries," *Journal of Power Sources*, vol. 222, pp. 112–122, 2013.

[150] S. J. Moura, F. B. Argomedo, R. Klein, A. Mirtabatabaei, and M. Krstic, "Battery state estimation for a single particle model with electrolyte dynamics," *IEEE Transactions on Control Systems Technology*, vol. 25, no. 2, pp. 453–468, 2016.

[151] S. Dey, B. Ayalew, and P. Pisu, "Nonlinear robust observers for state-of-charge estimation of lithium-ion cells based on a reduced electrochemical model," *IEEE Transactions on Control Systems Technology*, vol. 23, no. 5, pp. 1935–1942, 2015.

[152] J. R. Belt, "Battery test manual for plug-in hybrid electric vehicles," tech. rep., Idaho National Lab.(INL), Idaho Falls, ID (USA), 2010.

[153] M. Arcak and P. Kokotović, "Nonlinear observers: a circle criterion design and robustness analysis," *Automatica*, vol. 37, no. 12, pp. 1923–1930, 2001.

[154] M. Chong, R. Postoyan, D. Nešić, L. Kuhlmann, and A. Varsavsky, "A robust circle criterion observer with application to neural mass models," *Automatica*, vol. 48, no. 11, pp. 2986–2989, 2012.

[155] V. Andrieu and L. Praly, "On the existence of a kazantzis–kravaris/luenberger observer," *SIAM Journal on Control and Optimization*, vol. 45, no. 2, pp. 432–456, 2006.

[156] Z. Lendek, T. M. Guerra, R. Babuska, and B. De Schutter, *Stability analysis and nonlinear observer design using Takagi-Sugeno fuzzy models*, vol. 262. Springer, 2011.

[157] D. Ichalal, B. Marx, J. Ragot, and D. Maquin, "Advances in observer design for Takagi-Sugeno systems with unmeasurable premise variables," *Mediterranean Conference on Control & Automation*, pp. 848–853, 2012.

[158] M. Marchand, V. Andrieu, S. Bertrand, S. Janny, and H. Piet-Lahanier, "Deep learning of a communication policy for an event-triggered observer for linear systems," *HAL, hal-03945265*, 2023.

[159] C. Song, H. Wang, Y. Tian, and G. Zheng, "Event-triggered observer design for delayed output-sampled systems," *IEEE Transactions on Automatic Control*, vol. 65, no. 11, pp. 4824–4831, 2019.

[160] A. Anta and P. Tabuada, "To sample or not to sample: self-triggered control for nonlinear systems," *IEEE Transactions on Automatic Control*, vol. 55, no. 9, pp. 2030–2042, 2010.

[161] M. Velasco, J. Fuertes, and P. Marti, "The self triggered task model for real-time control systems," *IEEE Real-Time Systems Symposium*, pp. 67–70, 2003.

[162] R. Postoyan, R. G. Sanfelice, and W. P. M. H. Heemels, "Explaining the 'mystery"of periodicity in inter-transmission times in two-dimensional event-triggered controlled system," *IEEE Transactions on Automatic Control*, 2022.

[163] G. d. A. Gleizer and M. Mazo, "Chaos and order in event-triggered control," *IEEE Transactions on Automatic Control*, 2023.

[164] V. S. Dolk and W. P. M. H. Heemels, "Event-triggered control systems under packet losses," *Automatica*, vol. 80, pp. 143–155, 2017.

[165] D. P. Bertsekas, *Dynamic programming and optimal control: Volume I*. Athena scientific, 2012.

[166] Z.-P. Jiang and Y. Wang, "Input-to-state stability for discrete-time nonlinear systems," *Automatica*, vol. 37, no. 6, pp. 857–869, 2001.

[167] E. Sontag and A. Teel, "Changing supply functions in input/state stable systems," *IEEE Transactions on automatic control*, vol. 40, no. 8, pp. 1476–1478, 1995.

[168] C. M. Kellett, "A compendium of comparison function results," *Mathematics of Control, Signals, and Systems*, vol. 26, no. 3, pp. 339–374, 2014.